SALT RESERVE ESTIMATION FOR SOLUTION

MINING IN THE KHORAT BASIN

Hathaichanok Vattanasak

A Thesis Submitted in Partial Fulfillment of the Requirements for the

Degree of Master of Engineering in Geotechnology

Suranaree University of Technology

Academic Year 2006

การประเมินปริมาณเกลือในการทำเหมืองเกลือแบบละลายในแอ่งโคราช

นางสาวหทัยชนก วัฒนศักดิ์

SALT RESERVE ESTIMATION FOR SOLUTION MINING

IN THE KHORAT BASIN

Suranaree University of Technology has approved this thesis submitted in partial fulfillment of the requirements for a Master's Degree.

Thesis Examining Committee

_____

(Asst. Prof. Thara Lekuthai)

Chairperson

_____

(Assoc. Prof. Dr. Kittitep Fuenkajorn)

Member (Thesis Advisor)

_____

(Assoc. Prof. Ladda Wannakao)

Member

_____   _____

(Assoc. Prof. Dr. Saowanee Rattanaphani) (Assoc. Prof. Dr. Vorapot Khompis)

Vice Rector for Academic Affairs   Dean of Institute of Engineering

หทัยชนก วัฒนศักดิ์ : การประเมินปริมาณเกลือในการทำเหมืองเกลือแบบละลายในแอ่งโคราช (SALT RESERVE ESTIMATION FOR SOLUTION MINING IN THE KHORAT BASIN) อาจารย์ที่ปรึกษา : รองศาสตราจารย์ ดร. กิตติเทพ เฟื่องขจร, 191 หน้า.

วัตถุประสงค์ของงานวิจัยคือ เพื่อคำนวณปริมาณสำรองของแร่เกลือหินจากเกลือชั้นล่างใน แอ่งโคราช กิจกรรมหลักในงานวิจัยประกอบด้วย 1) รวบรวมข้อมูลธรณีวิทยาของหมวดหินมหาสาร- คามที่มีการตีพิมพ์เผยแพร่ 2) กำหนดลักษณะการกระจายตัวของเกลือชั้นล่างในรูปของความลึกและ ความหนา 3) ออกแบบโพรงละลายตามหลักการและกฎเกณฑ์ของกระบวนการออกแบบทางวิศวกรรม 4) กำหนดผลกระทบที่เกิดขึ้นจากการทรุดตัวซึ่งส่งผลต่อโครงสร้างทางวิศวกรรมและสิ่งแวดล้อมโดย รอบ และ 5) คำนวณปริมาณสำรองทั้งหมดของเกลือหินจากเกลือชั้นล่างในพื้นที่ที่สามารถทำเหมืองได้

ผลการศึกษาแสดงให้เห็นว่าผิวบนสุดของเกลือชั้นล่างอยู่ที่ความลึกตั้งแต่ 100 เมตร ถึง -700 เมตร จากระดับน้ำทะเลปานกลาง ความหนาของเกลือชั้นล่างผันแปรตั้งแต่ 1 เมตรจนถึง 1,000 เมตร โดมเกลือหินที่พบบริเวณตอนกลางของแอ่งโคราชแสดงความหนามากที่สุดของเกลือชั้นล่าง การออกแบบเบื้องต้นกำหนดให้โพรงมีรูปแบบเป็นทรงกลมเส้นผ่าศูนย์กลาง 60 เมตร ชั้นเกลือหิน ที่สามารถรองรับโพรงได้ต้องมีความหนาอย่างน้อย 150 เมตร โดยมีหลังคาโพรงอยู่ที่ระดับความ ลึกตั้งแต่ 140 เมตร ถึง 340 เมตร ความหนาต่ำสุดของหลังคาโพรงคือ 60 เมตร พื้นโพรงมีความ หนาอย่างน้อย 30 เมตร และมีระยะห่างระหว่างโพรง (จากจุดกึ่งกลางถึงจุดกึ่งกลาง) เท่ากับ 240 เมตร การออกแบบเบื้องต้นได้นำมาวิเคราะห์ด้วยแบบจำลองทางคอมพิวเตอร์ พบว่าโพรงที่ ออกแบบไว้มีเสถียรภาพเชิงกลศาสตร์ตลอดระยะเวลาอย่างน้อย 50 ปี โดยมีการทรุดตัวของผิว ดินสูงสุดสำหรับโพรงที่อยู่ระดับตื้นที่สุดเท่ากับ 2.92 เซนติเมตร และโพรงที่อยู่ลึกสุดมีการทรุด ตัวสูงสุดเท่ากับ 6.45 เซนติเมตร ขนาดการทรุดตัวที่เกิดขึ้นเมื่อเปรียบเทียบกับมาตรฐานข้อปฏิบัติ ทางอุตสาหกรรมสากลแสดงว่าจะไม่ทำให้เกิดผลกระทบต่อโครงสร้างทางวิศวกรรมและ สิ่งแวดล้อมโดยรอบ พื้นที่ที่เหมาะสมสำหรับการทำเหมืองจะพิจารณาจากความลึกและความหนา ของเกลือชั้นล่างแต่ไม่รวมถึงพื้นที่ชุมชนเมือง สิ่งก่อสร้าง ถนนและแหล่งน้ำต่าง ๆ ที่มีอยู่แล้ว บนผิวดิน ปริมาณสำรองทั้งหมดของแร่เกลือหินจากเกลือชั้นล่างในแอ่งโคราชที่สามารถทำเหมือง เกลือแบบละลายได้มีประมาณ 2 หมื่นล้านตัน ซึ่งในแต่ละโพรงที่ออกแบบสามารถผลิตเกลือได้ 201,901 ตัน โดยพิจารณาความบริสุทธิ์ของเกลือเท่ากับ 97% และหลังจากทำการผลิตเรียบร้อยแล้ว ในแต่ละโพรงจะมีเกลือละลายอยู่ในรูปของน้ำเกลือเข้มข้นอยู่ภายในประมาณ 35,060 ตัน และมี สารประกอบที่ไม่ละลายน้ำเท่ากับ 7,329 ตัน

สาขาวิชา <u>เทคโนโลยีธรณี</u>   ลายมือชื่อนักศึกษา _____

ปีการศึกษา 2549   ลายมือชื่ออาจารย์ที่ปรึกษา _____

HATHAICHANOK VATTANASAK : SALT RESERVE ESTIMATION FOR SOLUTION MINING IN THE KHORAT BASIN. THESIS ADVISOR : ASSOC. PROF. KITTITEP FUENKAJORN, Ph.D., P.E. 191 PP.

SALT/RESERVE/KHORAT BASIN/SOLUTION MINING/DESIGN

The objective of this research is to compute the salt reserve estimation for the Lower Salt member in the Khorat Basin. The main tasks include 1) compilation of the published geologic data relevant to the Maha Sarakham Formation, 2) determination of the spatial distribution of the Lower Salt member in terms of depth and thickness, 3) design of solution caverns based on the engineering design methodology and principles, 4) determination of the impacts of surface subsidence on the engineering structures and surrounding environment, and 5) calculation of the total tonnage (reserve) of the salt from the suitable mining area.

Results of the study indicate that depths of the top of the Lower Salt member range from 100 meters to -700 meters from mean sea level. Thickness of the Lower Salt varies from 1 meter to 1000 meters, approximately. Salt domes in the central part of the basin represent the greatest thickness for the Lower Salt. The design results suggest that the cavern should be spherical shaped with a nominal diameter of 60 meters. The salt bed that can host the caverns should have a minimum thickness of 150 meters with the depths of the salt top between 140 meters and 340 meters. Based on this design the minimum salt roof and salt floor thickness should be 60 meters and 30 meters. The spacing (center-to-center) between adjacent caverns should be 240 meters. From these design configurations, the results of finite element analyses

indicate that the cavern will remain mechanically stable for at least the next 50 years. The maximum surface subsidence for the shallowest cavern field is about 2.92 centimeters, and for the deepest cavern field is about 6.45 centimeters. Based on the international industrial standard practice, these magnitudes of the subsidence will not have adverse effect on the engineering structures and on the surrounding environment. The total suitable mining area is defined here as the total area that has appropriate depth and thickness of the Lower Salt, except those areas that are occupied by local communities, highways, all access roads, surface water bodies, reservoirs, rivers, and streams. The total inferred reserve of the salt (halite) from the Lower Salt member for the entire basin mined by solutioning is about 20 billion tons. Each cavern can produce halite about 201,901 tons, considered the purity of rock salt = 97%. After solutioning is complete, there will be halite left in each cavern in form of saturated brine about 35,060 tons with insoluble material about 7,329 tons.

School of Geotechnology   Student's Signature _____

Academic Year 2006   Advisor's Signature _____

ACKNOWLEDGEMENTS

TABLE OF CONTENTS

Page

TABLE OF CONTENTS (Continued)

TABLE OF CONTENTS (Continued)

TABLE OF CONTENTS (Continued)

LIST OF TABLES

LIST OF FIGURES

LIST OF FIGURES (Continued)

LIST OF FIGURES (Continued)

LIST OF FIGURES (Continued)

LIST OF FIGURES (Continued)

LIST OF FIGURES (Continued)

CHAPTER I

INTRODUCTION

1.1 Research objectives

The objective of this research is to determine the rock salt reserve in the Maha Sarakham Formation of the Khorat Basin with respect to the solution mining applications. The mining reserve will be estimated along with the corresponding cavern locations and depths. The final results will be presented by series of contour maps and cross-sections defining the reserve and its variation within the basin.

1.2 Rationale and background

The world demand of salt has increased to an estimate of 190-205 megatons annually. This is primarily due to the rapid growth of the Southeast Asian countries. Rock salt has long been one of the important raw materials for various chemical industries (Roskill, www, 2001). Even though extensive rock salt formations widely distribute in the northeastern region of Thailand (Japakasetr, 1985; Japakasetr and Workman, 1981; Sattayarak, 1983, 1985; Japakasetr, 1992; Japakasetr and Suwanich, 1982), the production from the local salt mining industry is limited, and hence the salt export still can not reach the overseas demands. Such limitation is due to the fact that the necessary geological sequences of the salt formations are not available to the investors, miners and engineers in a readily useful format. In addition, the existing

borehole data and geologic maps in the area have never been systematically interpreted, verified, and compiled for engineering and developing purposes.

1.3 Scope and limitations of the study

This research uses the existing and published data from borehole logs, geology and structural geology of rock salt in the Khorat Basin. The core-logged data are obtained from the Department of Mineral Resources (DMR), which have been acquired mostly for the potash exploration project in the northeast of Thailand. The research will not cover the field investigation. Conventional method of reserve estimation and subsidence calculation will be used. Engineering design methodology will be followed to determine the cavern size and depth. The salt properties are obtained from the reviewed test data. The reserve estimation is carried out based on the solution mining method.

1.4 Research methodology

1.4.1 Literature review

Relevant literatures will be searched, reviewed, summarized and documented. The summary of the literature review will be given in the thesis, which includes geology of the Maha Sarakham Formation in the northeast of Thailand, rock salt properties, solution mining technology, solution mining practices in Thailand, design methodology for solution mining, mechanical constitutive laws of rock salt, computer modeling, subsidence due to solution mining and reserve estimation.

1.4.2 Geologic data compilation

Relevant information of the Maha Sarakham Formation will be systematically compiled. The geologic data compilation will be made from borehole data, seismic survey, geologic maps, topographic maps, mineral potential map, and geologic cross-sections.

1.4.3 Cavern design

Thickness and depth of the salt beds obtained from the data compilation will be used as primary parameters for the design of the solution caverns. The design will give the suitable cavern geometry under various geologic conditions, depths, and thickness. Engineering design methodologies and principles will be used. The design parameters to be determined include depth, volume, shape, and spacing of the caverns. A variety of the designed cavern configurations is expected.

1.4.4 Salt reserve estimation

The salt reserve will be estimated, based on the solution mining method. The parameters considered in the estimation will include depth and thickness of the salt at each location, cavern configuration (depth, diameter, height, roof, and floor), and cavern field arrangement (cavern pattern and spacing). The cavern field area is designated by considering the economical feasibility of the salt reserve within the area and the current regulations for the underground mining practice.

1.4.5 Thesis writing and presentation

Methods and results of the research will be documented and presented in the thesis. It will include comprehensive methodology, results, discussions and conclusions of the findings.

1.5 Expected results

Distribution of the three salt members in Khorat Basin in terms of area, depth, and thickness will be obtained in digital format. A contour map of salt reserve can be constructed. The results will be immediately applicable as a compiled salt sequences to the government agencies, regulators, planners, and geologists. The proposed cavern design configurations will be useful for mining, geological, and civil engineers. Finally, the salt reserve estimation will become the key information for planning and management of the rock salt resources in Thailand.

1.6 Thesis contents

The research objective, rationale, background, scope, limitations, methodology, and expected results are described in Chapter I. Chapter II presents a summary of the literature review on the Maha Sarakham Formation, rock salt properties, solution mining technology, solution mining practices in Thailand, design methodology for solution mining, mechanical constitutive laws of rock salt, computer modeling, surface subsidence due to solution mining, and methods for reserve estimation. Chapter III describes method and results of data compilation. Chapter IV describes the cavern design processes and stability analysis. Chapter V presents the salt reserve estimation. Chapter VI concludes the research results, and provides recommendations for future research studies.

CHAPTER II

LITERATURE REVIEW

2.1 Objectives

Literatures related to the reserve estimation of Maha Sarakham Formation for solution mining in Khorat Basin has been reviewed in this research. The related knowledge is categorized into nine groups: 1) Maha Sarakham Formation in the northeast of Thailand, 2) rock salt properties, 3) solution mining technology, 4) solution mining practices in Thailand, 5) design processes for solution mining, 6) mechanical constitutive laws of rock salt, 7) computer modeling, 8) subsidence due to solution mining, and 9) reserve estimation.

2.2 Maha Sarakham Formation in the northeast of Thailand

The rock salt formation in Thailand is located in the Khorat plateau as shown in Figure 2.1. The Khorat plateau covers 150,000 square kilometers, from 14° to 19° northern latitude and 101° to 106° eastern longitude. It has high escarpment up to 900 meters above mean sea level along the western and southern edges and mesa topography over parts of its area whereas its middle area elevation is about 140 meters above mean sea level. The northern and eastern edges of the plateau lie close to Laos and the southern one close to Cambodia (Utha-aroon, 1993).
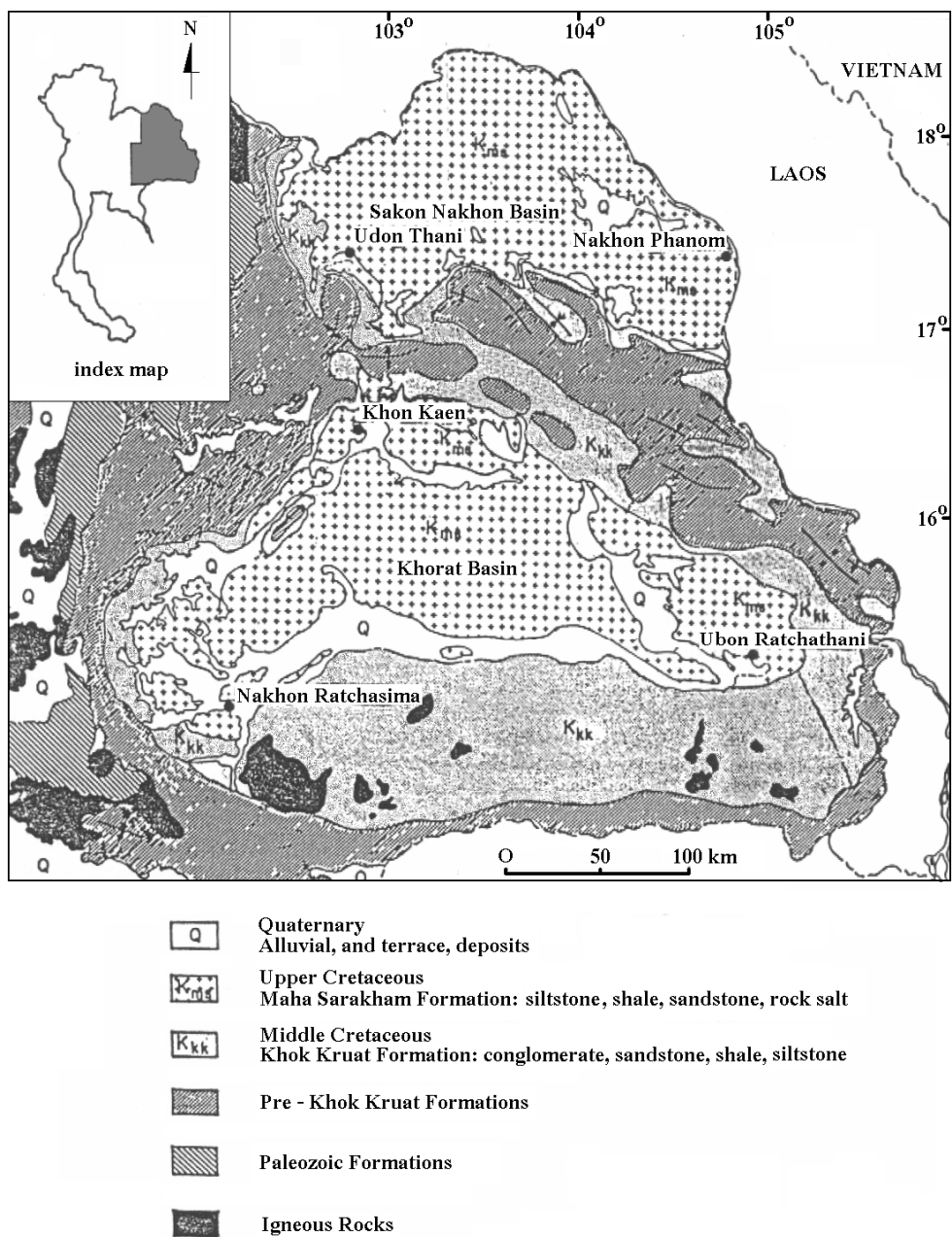
Figure 2.1 Sakon Nakhon and Khorat Basins containing rock salt in the northeast of Thailand (modified from Rattanajarurak, 1990 and Utha-aroon, 1993 adapted from Geological Map of Thailand, scale 1:2,500,000).

Rock salt in the Khorat plateau is separated into 2 basins: Sakon Nakhon Basin and Khorat Basin. The Sakon Nakhon Basin in the north has an area about 17,000 square kilometers. It covers the area of Nong Khai, Udon Thani, Sakon Nakhon, Nakhon Phanom, and Mukdahan provinces and extends to some part of Laos. The Khorat Basin is in the south, which has about 30,000 square kilometers. The basin covers the area of Nakhon Ratchasima, Chaiyaphum, Khon Kaen, Maha Sarakham, Roi Et, Kalasin, Yasothon, Ubon Ratchathani provinces and the north of Burirum, Surin, and Sisaket provinces (Suwanich, 1986).

Both basins contain three cycles of evaporated deposits within the Maha Sarakham salt-bearing strata (Suwanich et al., 1982). Each cycle, defined by intrusion and extrusion of seawater, in-cooperated an evaporation rate that was suitable to form minerals, e.g. halite and potash. All cycles consist of evaporitic strata and sedimentary strata (Hite and Japakasetr, 1979; Suwanich and Rattanajarurak, 1986; Suwanich, 1986; Wongsawat et al., 1992) as given in the following.

1) Lower Cycle consists of the lower sedimentary beds deposited during an intrusion of seawater into the basin and resulted in deposit of ferruginous clastic sediments, calcareous sandstone and the lower evaporite layer formed during an extrusion of seawater from the basin and caused the deposition of anhydrite, potash and sylvite.

2) Middle Cycle consists of the middle sedimentary beds deposited during seawater intrusion and resulted in the deposit of shale and claystone and the middle evaporate layer was formed during an extrusion of seawater that caused higher concentration of seawater and halite and thin layers of anhydrite deposited in consequence.

3) Upper Cycle consists of the upper sedimentary beds deposited during seawater intrusion and resulted in the deposit of reddish-brown claystone and the upper evaporite layer deposited during seawater extrusion.

The Department of Mineral Resources had drilled 194 drilled holes between 1976 and 1977 for the exploration of potash (Japakasetr, 1985; Japakasetr and Workman, 1981; Sattayarak, 1983, 1985; Japakasetr, 1992; Japakasetr and Suwanich, 1982). Some holes were drilled through rock salt layers to the Khok Kruat Formation (Yumuang et al., 1986; Supajanya et al., 1992; Utha-aroon, 1993; Warren, 1999). The sequences of rock layers from the bottom of this formation up to the top of the Maha Sarakham Formation are as follows.

1) Red bed sandstone or dense greenish gray siltstone sometime intercalated with reddish-brown shale.

2) Basal anhydrite with white to gray color, dense, lies beneath the lower rock salt and lies on the underlying Khok Kruat Formation.

3) Lower rock salt, the thickest and cleanest rock salt layer, except in the lower part which contains organic substance. The thickness exceeds 400 meters in some areas and formed salt domes with the thickness up to 1,000 meters, with the average thickness of 134 meters.

4) Potash, 3 types were found; carnallite ($KCl.MgCl_2.6H_2O$) with orange, red and pink color, sylvinite (KCl) rarely found, white and pale orange color, an alteration of carnallite around salt domes, and techydrite ($CaCl_2.2MgCl_2.12H_2O$) often found and mixed with carnallite, orange to yellow color caused by magnesium, the dissolved mineral occurred in place.

5) Rock salt, thin layers with average thickness of 3 meters, red, orange, brown, gray and clear white colors.

6) Lower clastic, clay and shale, relatively pale reddish-brown color and mixed with salt ore and carnallite ore.

7) Middle salt, argillaceous salt, pale brown to smoky color, thicker than the upper salt layer with average thickness of 70 meters, carnallite and sylvite may be found at the bottom part.

8) Middle clastic, clay and shale, relatively pale reddish brown color and intercalated with white gypsum.

9) Upper salt, dirty, mixed with carbon sediment, pale brown to smoky color or orange color when mixed with clay and 3 to 65 meters thick.

10) Upper anhydrite, thin layer and white to gray color.

11) Clay and claystone, reddish brown color, occurrence of siltstone and sandstone in some places, and

12) Upper sediment, brownish gray clay and soil in the upper part, and sandy soil and clay mixed with brown, pink and orange sandy soil in the lower part.

Cross-sections from seismic survey across the Khorat-Ubon and Udon-Sakon Nakhon Basins (Sattayarak and Polachan, 1990) reveal that rock salt can be categorized into 3 types according to their appearances namely, rock salt beds, rock salt fold and salt domes. The Maha Sarakham and Phu Tok Formations fold in harmony with the Khorat megasequence. A part of the cross section through the Khorat Basin is illustrated in Figure 2.2.
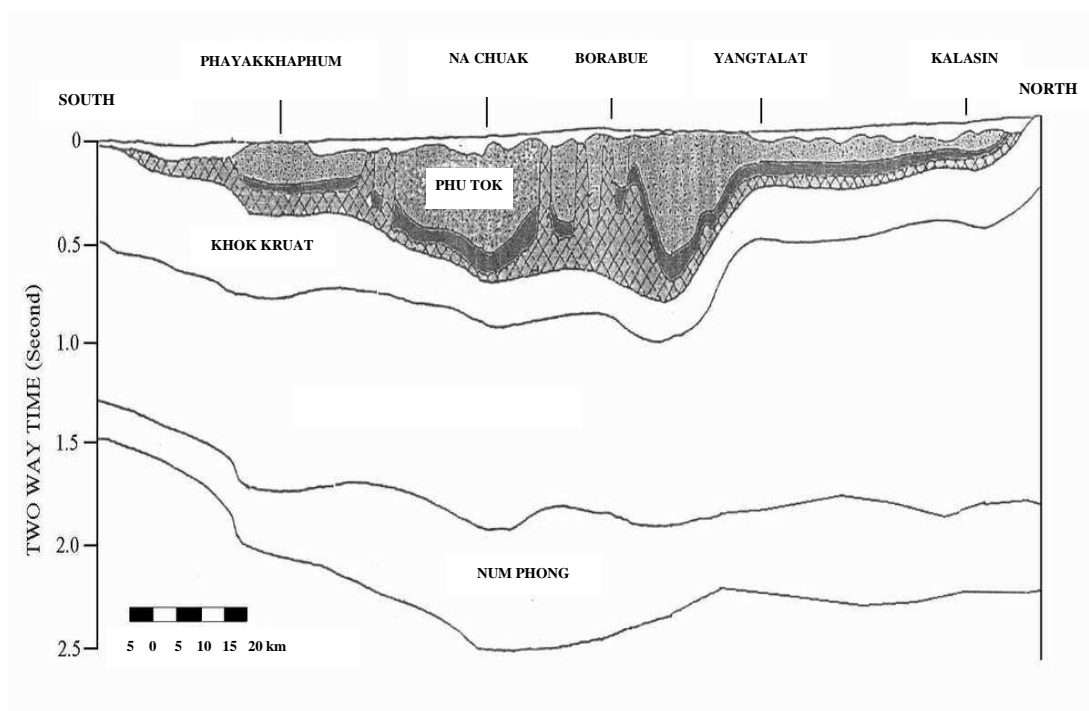
Figure 2.2 Cross-section showing rock salt in the Khorat Basin (from Sattayarak, 1987).

Lateral compression due to collision between the Asian and Indian Plates in Tertiary caused the occurrence of cracks in the Phu Tok Formation. The plastic characteristics of the rock salt made it easy to creep. The rock salt intruded into those cracks. Differences in overburden loads could also cause a deformation of the rock salt and resulted in rock salt folds and domes respectively. Rattanajarurak (1990), Junmaha (1987) and Supajanya et al. (1992) stated that from seismic investigation data around exploration well No. K-66 in Borabue District, Maha Sarakham Province (Figure 2.3), salt domes are different in shape and size. Some had started to form domes. The lower rock salt in the middle of the Khorat and Sakon Nakhon Basins found to be well developed for dome.
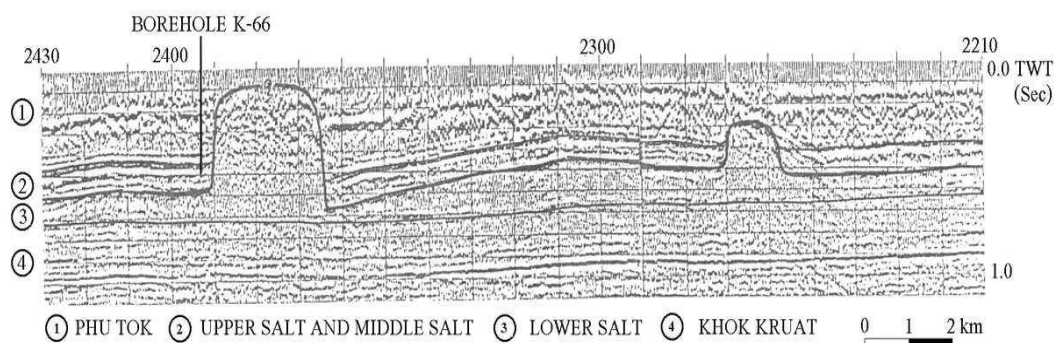
Figure 2.3 Seismic investigation at around the exploration well No. K-66 in Borabue

District, Maha Sarakham province (from Supajanya et al., 1992).

2.3 Rock salt properties

2.3.1 Mechanical properties of rock salt

Researchers from the field of material sciences believe that rock salt behavior shows many similarities with that of various metals and ceramics (Chokski and Langdon, 1991; Munson and Wawersik, 1993). However, because alkali halides are ionic materials, there are some important differences in their behavior. Aubertin et al. (1992a, 1992b, 1993, 1998, and 1999) conclude that the rock salt behavior should be brittle-to-ductile materials or elastic-plastic behavior. This also agrees with the finding by Fuenkajorn and Daemen (1988), Fokker and Kenter (1994), and Fokker (1995, 1998).

Jeremic (1994) discusses the mechanical characteristics of the salt. They are divided into three characteristics: the elastic, the elastic-plastic, and the plastic behavior. The elastic behavior of rock salt is assumed to be linearly elastic with brittle failure. The rock salt is observed as linear elastic only for a low magnitude of loading. The range of linear elastic mainly depends on the content of

elastic strain and can be used to formulate the modulus of elasticity. Normally, the modulus of elasticity of rock salt is relatively low. The elastic and plastic behavior of rock salt can be investigated from the rock salt specimen. The confined rock salt specimen at the beginning of incremental loading shows linear elastic deformation but with further load increases the plastic behavior is induced, which continues until yield failure. Elastic deformation and plastic deformation are considered as separated modes of deformability in the great majority of cases. The salt material simultaneously exhibits both elastic strain and plastic strain. The difference between elastic behavior and plastic behavior is that elastic deformation is temporary (recoverable) and plastic deformation is permanent (irrecoverable). The degree of permanent deformation depends on the ratio of plastic strain to total strain. The elastic and plastic deformation can also be observed by short-term loading, but at higher load magnitude. The plastic behavior of rock salt does not occur if the applied stress is less than the yield stress. The rock salt is deformed continually if the high stress rate is still applied and is more than the yield stress. Increasing the load to exceed the strain limit of the rock salt beyond its strength causes it to fail. The deformation of rock salt by the increase of temperature can also result in the transition of brittle-to-ductile behavior.

The time-dependent deformation (or creep) is the process at which the rock can continue deformation without changing stress. The creep strain seldom can be recovery fully when loads are removed, thus it is largely plastic deformation. Creep deformation occurs in three different phases, as shown in Figure 2.4, which relatively represents a model of salt properties undergoing creep deformation due to the sustained constant load. Upon application of a constant force on the rock salt, an
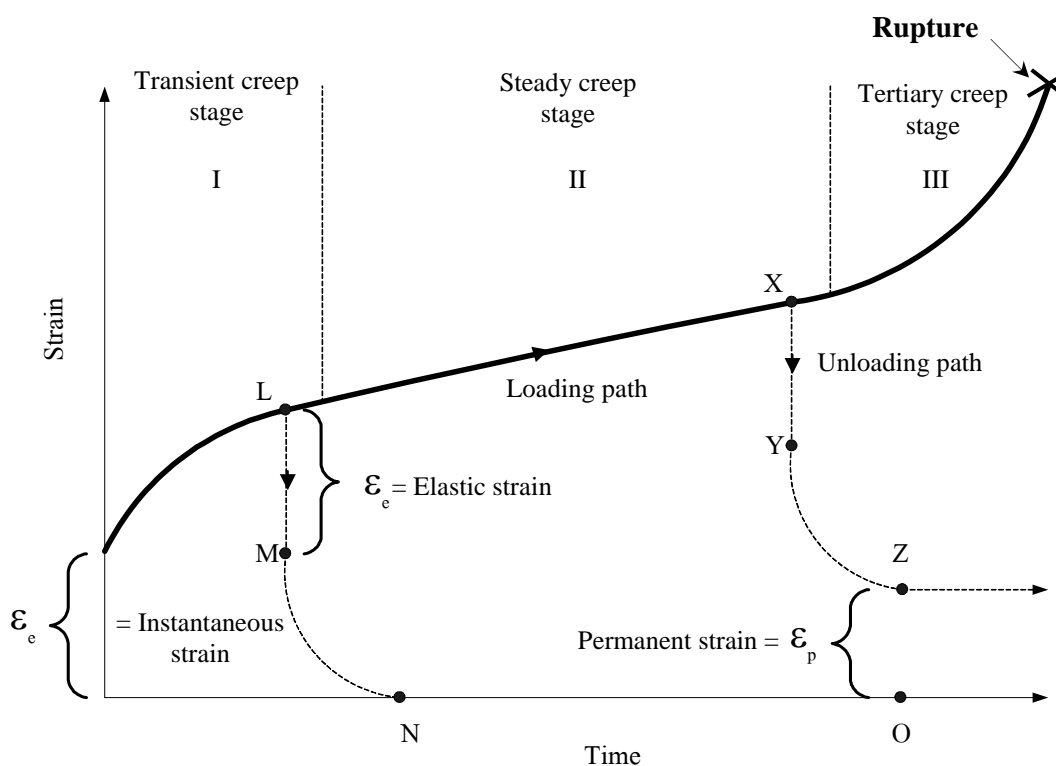
Figure 2.4 The typical deformation as a function of time of creep materials (modified

      from Jeramic, 1994).

instantaneous elastic strain (ε_e) is induced. The elastic strain is followed by a primary

or transient strain, shown as Region I. Region II, characterized by an almost constant

slope in the diagram, corresponds to secondary or steady state creep. Tertiary or

accelerating creep leading to rather sudden failure is shown in Region III. Laboratory

investigations show that removal of applied load in Region I at point L will cause the

strain to fall rapidly to the M level and then asymptotically back to zero at N. The

distance LM is equal to the instantaneous strain ε_e. No permanent strain is induced

here. If the removal of stress takes place in the steady-state phase the permanent

strain (ε_p) will occur. From the stability point of view, salt structure deformations

after constant load removal have only academic significance, since the stresses imposed underground due to mining operations are irreversible. The behavior of the salts with time-dependent deformation under constant load is characterized as a visco-elastic and visco-plastic phenomenon. Under these conditions, the strain criteria are superior to the strength criteria for design purposes, because failure of most salt pillars occurs during accelerated or tertiary phase of creep, due to the almost constant applied load. The dimensions of a pillar in visco-elastic and visco-plastic rock should be established on the basis of a prediction of its long-term strain, to guard against adequate safety factor accelerating creep (Fuenkajorn and Daemen, 1988; Dusseault and Fordham, 1993; Jeremic, 1994; Knowles et al., 1998).

The mechanical behavior of rock salt is complex and is affected by many factors, such as grain size, bonding between grains, time, temperature, humidity, and inclusions, and more. The effects on rock salt characteristics by these factors are normally shown by the differences in deformation and creep properties.

The effects of grain size on the creep behavior and strength of rock salt in laboratory and field conditions are described by Fokker (1998). The average grain size of salt visually observed from the core and post-failure specimens is 5×10×10 millimeters. It is concluded that the large size of the salt crystals increases the effect of the crystallographic features (i.e. cleavage planes) on the mechanics of deformation and failure of the samples. This also agrees with the finding by Aubertin (1996). The dislocations and plastic flows in single crystals of halite are studied by several researchers (Franssen and Spiers, 1990; Raj and Pharr, 1992; Senseny et al., 1992; Wanten et al., 1996). They conclude that the shear strength and deformation of halite crystals are orientation-dependent. The small size of the sample may not provide

good representative test results. This also reflects on the specifications by ASTM (ASTM D2664, D2938, and D3967). The ASTM standard methods specify that to minimize the effect of grain size the sample diameter should be at least ten times the average grain size.

Bonding between grains can affect the creep rate and the strength of salt. Allemandou and Dusseault (1996) observe the post-failure from the Brazilian strength tests and uniaxial compressive strength tests. They report that strength depends on the boundary between grains. This also agrees with the laboratory results obtained by Fuenkajorn and Daemen (1988) who report that weakness or brittleness of the crystal boundary of salt is observed during sample preparation. It is unlikely that a long intact core can drill through the salt formation.

The time-dependent behavior of salt under differential stress raises the question of the significance of time-related test parameters such as loading rate, testing period, and loading sequence. The effects of stress rate and strain rate on the deformation and strength of salt samples have long been recognized (Farmer and Gilbert, 1984; Dusseault and Fordham, 1993). The loading rate must be maintained constant and measured as precisely as possible during the test. The loading sequence and the duration for which each load is sustained by the salt specimens are important since salt tends to behave as a plastic creep material with low yield stress. This situation is found in the triaxial compressive strength test where the confining pressure is applied to the salt cylinder prior to the axial load. Due to the nonlinear behavior of salt, the analysis of stress induced in a salt specimen is complex and the Boltzmann law of superposition cannot be used.

Temperature or heating affects the creep deformation, because they increases the plastic property of salt and long-term deformation (Pudewills et al., 1995). Jeremic (1994) postulates that rock salts lose their brittleness after extension tempering at approximately 600°C and exhibit a critical shear stress up to 1 MPa. Hamami et al. (1996) study the effect of temperature and conclude that the temperature increase, as for the deviatoric stress, results in an increase of the material deformation. Cristescu and Hunsche (1996) study the temperature effect on the strain rate suitable for laboratory testing. They suggest that the appropriate strain rate for testing at 100°C and 200°C is 10^{-8} s^{-1} and 10^{-7} s^{-1} because the temperature can affect the creep deformation and strength of salt under high temperatures.

Humidity affects salt properties by reducing the strength of rock salt (Hunsche and Schulze, 1996; Cleach et al., 1996). Hydrated reaction between water and salt occurs when salt contacts with air humidity. The temperature effects can catalyze the hydration. They find that when subjecting to air humidity, the strength of salt can be decreased by up to 1 MPa (normally, strength of 30 MPa).

Inclusions and impurities in salt have an effect on to the creep deformation and strength of salt. The degree of impurity is varying for different scales of the rock salt. On a small scale, such as for laboratory specimens, the impurities of salt involve ferruginous inclusions and thin clay seams along grain boundaries or bedding planes. The impurities distribute uniformly in the salt may affect the strength of rock salt. This can decrease the creep deformation and strength of rock salt. These phenomena have been reported by Franssen and Spiers (1990), Raj and Pharr (1992) and Senseny et al. (1992).

2.3.2 Experimental research on rock salt

Rock salt has mechanical behavior that differs from most rocks. Basic mechanical laboratory tests that have been carried out on rock salt include uniaxial compressive strength testing, triaxial strength testing, uniaxial creep testing, multi-steps testing, triaxial creep testing, tensile strength testing, cyclic loading testing and permeability measurment testing. The main objective of these tests is to study the strength and the time-dependent deformations of the rock.

The uniaxial compression tests determine the compressive strength of rock salt under unconfined condition. The salt specimens are subjected to the uniaxial load until failure. The compressive strength can be varied with the applied stress and strain rates. Hansen et al. (1984) performs the uniaxial compressive strength tests on rock salt from ten different locations in the United States. The results indicated that compressive strengths vary from 13.3 to 3.6 MPa (see Table 2.1). Fuenkajorn and Daemen (1988) study the compressive strength of rock salt from Permian Basin, New Mexico. The results are 18.44 MPa of compressive strength, 36 degrees of internal friction angle, 3.42 GPa of tangent modulus, and 5.13 GPa of secant modulus. Ratigan and Vogt (1993) summarize the compressive strengths of salt with values ranging from 15 MPa to 30 MPa. Wanten et al. (1996) studies the uniaxial compressive strength under different strain rates. The strain rate ranging from 10^{-4} s^{-1} to 10^{-7} s^{-1} is applied on the crystal (salt grain) at temperature of 20°C to 200°C. The results indicate that the salt samples show work hardening behavior. Microstructure studies revealed high dislocation densities but little or no sub-grain development or cross-slip. Comparison of the results with micro-physical models suggests that obstacle limited dislocation glide is the controlling deformation mechanism.

Table 2.1 The results of uniaxial and triaxial compressive strength tests and Brazilian
tensile strength test on rock salt from the United States (from Hansen et al.,
1984).

Locations	Uniaxial Compressive Strength Test	Brazilian Tensile Strength Test	Triaxial Compressive Strength Test	
	σ_c (MPa)	σ_B (MPa)	C (MPa)	ϕ (degrees)
S. E. New Mexico (1900′ level)	16.9	1.26	2.31	59.5
S. E. New Mexico (2700′ level)	25.7	1.63	3.24	61.7
Lyons	25.2	1.56	3.14	62.1
Permian	22.1	1.72	3.08	58.8
Paradox	33.6	2.61	4.68	58.9
Jefferson Island	24.0	1.54	3.04	61.6
Week's Island	13.9	1.24	2.08	56.7
Cote Blanche	25.2	1.93	3.49	59.1
Avery Island	23.1	1.17	2.60	64.6
Richton	13.3	1.32	2.10	55.0
Vacherie	15.3	1.12	2.07	59.7

Notes: σ_c = Uniaxial Compressive Strength   C = Cohesion Compressive Strength
σ_B = Brazilian Tensile Strength ϕ = Internal Friction Angle

Boontongloan (2000) studies the uniaxial compressive strength with controlled
loading rate on salt cores drilled in Sakon Nakhon Basin in Udon Thani Province,
Thailand. The uniaxial load is applied within 5 to 10 minutes. The results indicate
that the Upper Salt has the uniaxial compressive strength of 18.5 MPa and the Middle
Salt has uniaxial compressive strength of 26 MPa. The tangent and secant elastic
moduli equal 5.6 GPa and 9.9 GPa. The Lower Salt has uniaxial compressive strength
of 25 MPa. The tangent and secant elastic moduli equal 6.4 GPa and 11.4 GPa. The

Poisson's ratio varies between 0.35 and 0.42. Wetchasat (2002) performs the uniaxial compressive strength with controlled loading rates. The loading rate ranging from 0.01 to 1.0 MPa/s are applied on salt specimens from Sakon Nakhon Basin in Udon Thani Province, Thailand. The results indicated that the average compressive strength from thirteen specimens is 27.4 MPa.

The triaxial testing is conducted to determine the compressive strengths of rock salt under confined conditions. The axial load and the confining pressure are increased simultaneously, until the predetermined test level for the confining pressure is reached. Subsequently, the confining pressure shall be maintained to within 2% of the prescribed value. The axial load on the specimen shall then be increased continuously at a constant stress rate such that failure will occur within 5 to 10 minutes of loading. The maximum axial load and the corresponding confining pressure on the specimen are recorded. Hansen et al. (1984) performs the triaxial compressive strength tests on rock salt from ten different locations in the United States. The results indicated that cohesion compressive strengths (C) are varying from 2.07 to 4.68 MPa and 55 to 64.6 degrees of internal friction angle (ϕ), as shown in Table 2.1. Fuenkajorn and Daemen (1988) perform strain rate-controlled triaxial tests on Salado salt samples at confining pressures ranging from 1.54 MPa to 8.18 MPa and constant strain rates ranging from 2.25×10^{-5} to 2.08×10^{-4} s^{-1}. The salt tends to behave as brittle material (strain-softening) when it is subjected to high strain rates and as ductile material (strain-hardening) for lower strain rates. The sample volume tends to decrease at the beginning of loading and it starts increasing shortly before the peak stress has been reached. Therol and Ghoreychi (1996) study the triaxial compressive strength tests on rock salt with measurements of the volumetric strains.

They report that the initiation of damage is supposed to be linked to the change of curvature of volumetric strain from compressibility to dilatancy due to microcracking. Wetchasat (2002) conducts the triaxial compressive strength tests on rock salt from salt cores in Sakon Nakhon Basin in Udon Thani province, Thailand. The results are 8 MPa of cohesion compressive strength and 49 degrees of internal friction angle. The linear equation of Coulomb's criterion is given by $\tau = 8 + \sigma \tan 49°$ MPa.

The cyclic loading test consists of the loading and unloading system, which causes the fatigue in salt specimen and reduces the ultimate compressive strength (Allemandou and Dusseault, 1996). Results of these tests can be shown by the stress, strain, and numerical cycle's graph. The graph shows fatigue concentration of each cycles and ultimate strength at failure. The cyclic loading test can be modified for long-term testing called creep-cyclic loading tests. These results are presented as the relationship between strain and time. Results of all creep-cyclic loading tests show a classical creep response with high strain rates at the beginning, gradually decreasing with time towards an identical asymptotic value from cycle to cycle (Thoms and Gehle, 1984). Wetchasat (2002) performs the uniaxial cyclic loading tests on rock salt from Sakon Nakhon Basin, Thailand to determine the uniaxial compressive strength and the elastic modulus. The average uniaxial compressive strength from eighth specimens is 23.6 MPa and 19.9 GPa for the average elastic modulus.

Uniaxial creep testing is conducted to determine the time-dependent deformation of rock salt. The uniaxial loading is maintained constant during the test while recording the axial strain and time. The results are commonly shown as a strain and time curve. Normally, the curve of creep testing is divided into three stages: 1)

transient or preliminary creep stage, 2) steady or secondary creep stage, and 3) tertiary creep stage (Figure 2.4). Hunsche and Schulze (1996) perform the uniaxial creep testing, and find that different layer formations have different creep properties. The temperature of test varies from 22°C to 630°C. The salt is close to the plastic behavior under a high temperature. Pudewills and Hornberger (1996) study the uniaxial creep testing at different temperatures. The result shows that the creep deformation (strain) at 200°C is higher than the creep deformation at 100°C. A study by Fuenkajorn and Daemen (1988) demonstrated that the strain rate at steady state is 17×10^{-6} hours^{-1} and equal zero when the time of testing is about 300 to 800 hours. Wetchasat (2002) performs uniaxial creep tests to determine time-dependent parameters of rock salt from Sakon Nakhon Basin, Thailand. The results are 1.1 GPa of retarded shear modulus (G_2), 9.1 GPa·day of elasto-viscosity (V_2), and 4.9 GPa of retarded bulk modulus (K_2).

Triaxial creep testing is conducted to determine the time-dependent deformation of rock salt under confined conditions. The triaxial creep test is close to in-situ stress conditions when applying confining pressures. Ong et al. (1998) study creep deformation of salt and potash from Patience Lake Member in the United States. They perform the long-term triaxial creep tests. Adjustment of the desired axial and confining stress levels is quick. The axial and confining stresses are maintained. The test is either a single stage test or multiple stage test which lasts for 90 days. The data storage interval at the start of a test is usually 5 minutes; it is changed to one hour when the creep rate decreased. Upon unloading, the sample is inspected and measured dimensionally. They find that the salt is close to plastic behavior under high confining pressure. Hamami et al. (1996) study the triaxial creep testing on salt

with low deviatoric stress under an axial stress varying between 5.5 and 15 MPa with a step of 2.5 MPa each 3 months. The triaxial creep test with constant deviatoric stress (under an axial stress of 13 MPa) and decreasing (and increasing) the temperature form 20°C to 90°C (and 90°C to 20°C) with a step of 10°C each 1.5 months. They summarize that if the temperature increases, the deviatoric stress results in an increase of the material deformation. A decrease in temperature remarkably reduces the sample deformation, which is subjected to a deformation at higher temperatures in the beginning of test. This phenomenon is called strain hardening. The strain rate depends on the stress, the temperature and the previous strain. This also agrees with the finding by Korthaus (1996).

Hansen et al. (1984) compare the Brazilian tensile strength of rock salt from ten different locations in the United States. The results indicated that tensile strengths are varying from 1.12 to 2.61 MPa (see Table 2.1). Senseny et al. (1992) perform Brazilian tensile strength on rock salt obtained from Permian Basin. During the test, the axial load is applied along diametrical specimen with loading rates of 0.057 to 0.342 MPa/s until the specimen fails. The Brazilian tensile strength is ranging from 1.3 MPa to 1.6 MPa. The high loading rate reduces the tensile strength. Studies by Hunsche (1993) show the suitable loading rates for the tensile strength test which are from 0.017 MPa/s to 0.248 MPa/s. These rates do not affect the tensile strength of rock salt. Hardy (1998) uses fine-grained rock salt for tensile strength tests under conditions of direct-pull, diametric loading (Brazilian tensile strength test), and hoop-stress loading. Acoustic emission is monitored during these tests. The tests use the loading rates ranging from 0.003 MPa/s to 0.059 MPa/s. The results of direct-pull, diametric loading and hoop-stress loading are 1.63 MPa, 3.97 MPa and 0.68

MPa, respectively. Wetchasat (2002) performs Brazilian tensile strength test on the Maha Sarakham Formation in the Sakon Nakhon Basin. The tensile strength averaged from 13 specimens is 1.5 MPa.

In the past decade, many researchers studied the permeability of salt by laboratory and field tests. Gas or brine is pressurized through salt specimen and crushed salt specimen for permeability measurement. The permeability of in-situ and undisturbed salt ranges from 10^{-21} m^2 to 10^{-20} m^2 (Stormont et al., 1992; Fuenkajorn, 2000). The permeability of crushed salt depends on the bulk density. Brodsky et al. (1998) report that the fractional density from 0.85 to 0.90 of the crushed salt, gives permeability ranging from 10^{-15} m^2 to 10^{-12} m^2. The permeability of crushed salt is normally higher than the permeability of salt specimens. The permeability of salt is still very low but salt may increase its permeability with mechanical damages such as induced cracks around openings on caverns in the salt formations. Pueakphum (2003) performs fracture healing tests under uniaxial and radial loading on rock salt from Sakon Nakhon Basin. The results indicated that confining pressure has an advantage over uniaxial loading, in term of the maximum applied pressures on the tested salt fracture. The applied load is limited by the compressive strength of the salt. The maximum axial stress used is therefore limited to 7.8 MPa or about 30% of the strength. For the confined conditions, the specimen can subject to the confining pressure as high as 20 MPa. The results suggest that both applied pressure and time are important factors for fracture healing. The healing effectiveness of salt fractures depends heavily on the origin of the fractures. If a fracture is formed by the separation or splitting of salt crystals, it can be easily healed even under relatively low stress for a short period. The splitting failure of salt crystals occurs by a separation of

cleavage planes. This means that healing is effective if the salt crystals on both sides of the cleavage plane return to their original position. For the fractures formed by separation of inter-crystalline boundaries or by crystals with different orientations on the opposite sides, healing will not be easily achieved. The hydraulic conductivity for all salt fractures decreases with increasing applied confining pressure and time. This implies that the fracture healing is accompanied by the fracture closure. Both processes are time-dependent. The closure involves the visco-plastic deformation for the salt on both sides of the fracture. The healing involves a chemical process. It is permanent and remains even after the load is removed. Owing to the surface smoothness, the polished fractures show a lower permeability than do the tension-induced fractures. This however does not necessarily mean that the polished fractures heal more effective than do the tension-induced fractures. A reduction of fracture permeability does not necessarily mean that the healing has occurred. This is evidenced by that even the polished fracture has been compressed until its hydraulic conductivity becomes lower than 10^{-8} m/s and no healing has taken place in the fracture (Pueakphum, 2003).

2.4 Solution mining technology

Solution mining for salt is a well-established technology that began in the 1860's in the United States. Prior to 1955, most salt in the United States was produced using single well system, where leaching solution is injected and produced through the same well. After 1955, hydraulic fracturing between wells became the prominent system. With hydraulic fracturing, increased efficiency was possible (Nigbor, 1982; Bieniawski and Bieniawski, 1994).

2.4.1 Technology and methods of solution mining

Of engineering interest are the technology and method of controlled solution mining. There are two systems for salt solution and two methods of salt production by solution mining (Jeremic, 1964).

System of indirect circulation (Figure 2.5a), where fresh water is injected between the tubing and the casing. This system is called the 'top injection method', because the water enters the salt deposit at the top of the formation and starts to dissolve the salt near the roof. The salt brine flows downward to the bottom of the tubing where a sump effect has been produced by the pump drawing on the tubing. The brine is pumped from the well and then set to the processing area. For roof control of the cavern, a fluid isolant is applied which does not dissolve salt and does not stick to it.

System of direct circulation (Figure 2.5b), which uses the same type of set-up as an indirect circulation, e.g. the top injection method, except that the flow of water is reversed. The fresh water is pumped down the tubing and dissolves the salt at the bottom of the formation. The brine is then drawn out of the well between the tubing and the casing. This system is also known as the 'bottom injection method'.

Jeramic (1994) states that the difference between the two systems is the rate of decay of the well condition. In the top injection method the roof of the cavity is prone to caving since it is exposed more quickly than in the bottom injection method. The caving of the roof soon caused the tubing to plug or break. This causes reduced production or results in the closing of the well.

The methods of salt production by solution mining are fundamentally represented by the single-well method and by the two-well method (Jeramic, 1964).

1   2   3

Brine

Fresh water

Brine

Brine

Fresh water

Fresh water

(a) Indirect circular   (b) Direct circular
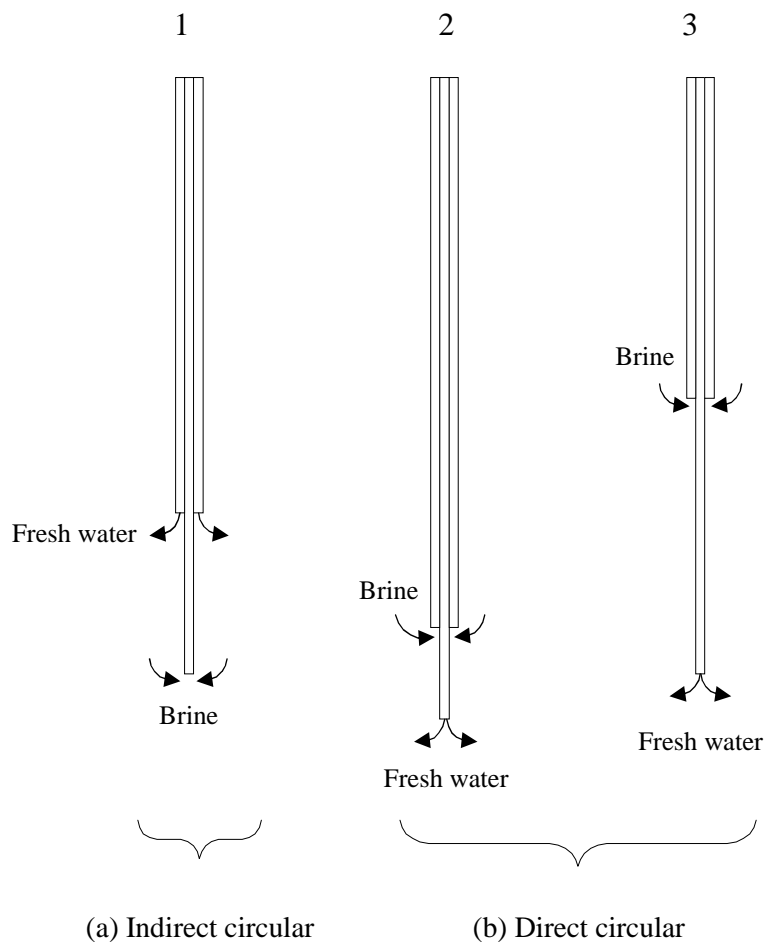
Figure 2.5 Systems for solution mining (modified from Fuenkajorn, 2002).

The single well method of solution mining involves the drilling of a single large diameter drill hole into a salt formation. A casing is used in the hole to stop the walls from caving. A second tubing of smaller diameter is then placed in the cased drill hole. The single well is simultaneously assigned to the production well and the injection well. Under this method the solution mining production is related solely to the individual wells. The single well method is mainly applied for deeper parts of salt deposits.

The two-well method of solution mining of salt deposits is based on drilling two identical wells into a salt body at a distance from several tenths of meters to several hundreds of meters. One well is assigned as the production well and the other as the injection well. Solution mining starts with the individual operation of each well by one of the single-well methods. After completion of the caverns, and in order to get fluids flowing between them, high pressure water is applied at the injection well in order to cause hydraulic fracturing between the wells. The brine is drawn from the production well and, as the flow between the two wells increases, the opening enlarges by dissolving the salt. As the cavity between the two holes enlarges, the volume of water flow between the holes increases, causing damage to the well is less than in the single-well method, because the area where the salt is being removed is far from the wells, where collapses can not cause damage to the well. Figure 2.6 shows a schematic of two-well method.

2.4.2 Solution processes

Adagic (1988) has recommended that the techniques of the solution process to a great extent depend on the geological-structural features of the deposit and its internal structure. This particular technology of solution mining could be characterized by three phases.

First phase: This phase is represented by the formation of the hydro-undercut at the bottom of the future cavern. The height of the undercut is 15 meters. The salt solution flows in a lateral direction, with a protective layer or isolant fluid to control the stability of the cavern back during its formation. The salt solution process ceases when the cavern reaches a diameter of 0.8 D_{max} (D_{max} = maximum
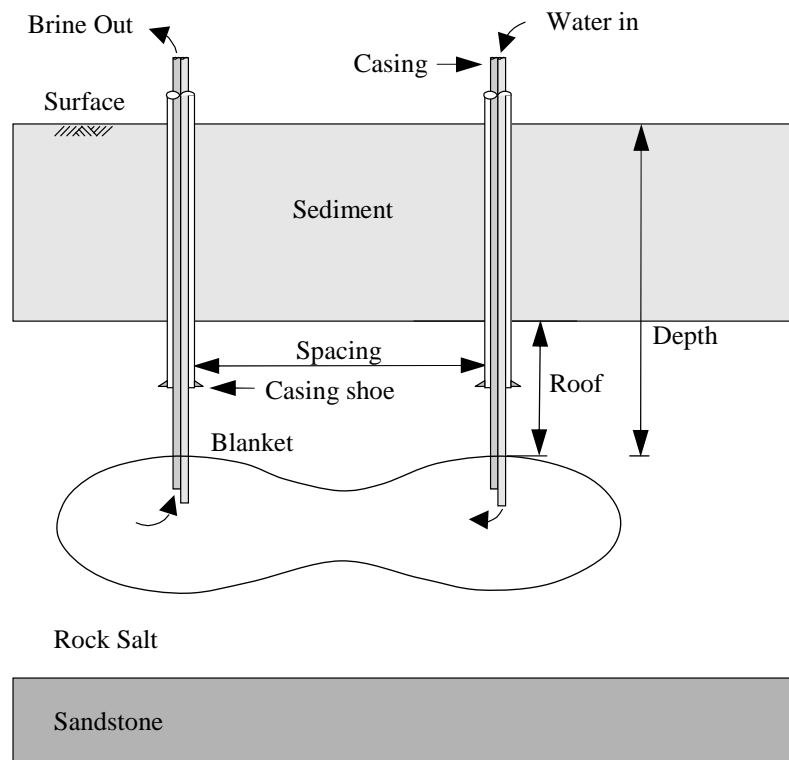
Figure 2.6 Schematic of two-well method (modified from Fuenkajorn, 2002).

design diameter). During this phase the system of indirect circulation is applied. The

capacity of the salt dissolution is 25 m^3/h of unsaturated brine (Figure 2.7).

Second phase: After completion of the hydro-undercut a narrow

cylindrical cavern is dissolved with a diameter of 5 meters and average height of 115

meters, which could be called a hydro-slot. The salt solution of the hydro-slot also

has a protective layer of fluid isolant to control roof stability while reaching the final

height of the exploitation cavern. During this phase a system of direct circulation is

applied with the dissolution capacity of 25 m^3/h of the unsaturated brine (Figure 2.8).

Third phase: The two previous phases should be considered the

development of the solution mining cavern. The third phase is considered the exploitation

Brine

Water

Oil

9 5/8″

Cap Rock

7 5/8″

Salt

5″

Oil isolant

Height of undercut
= 15 m

0.8 D$_{max}$

q = 25 m^3/h
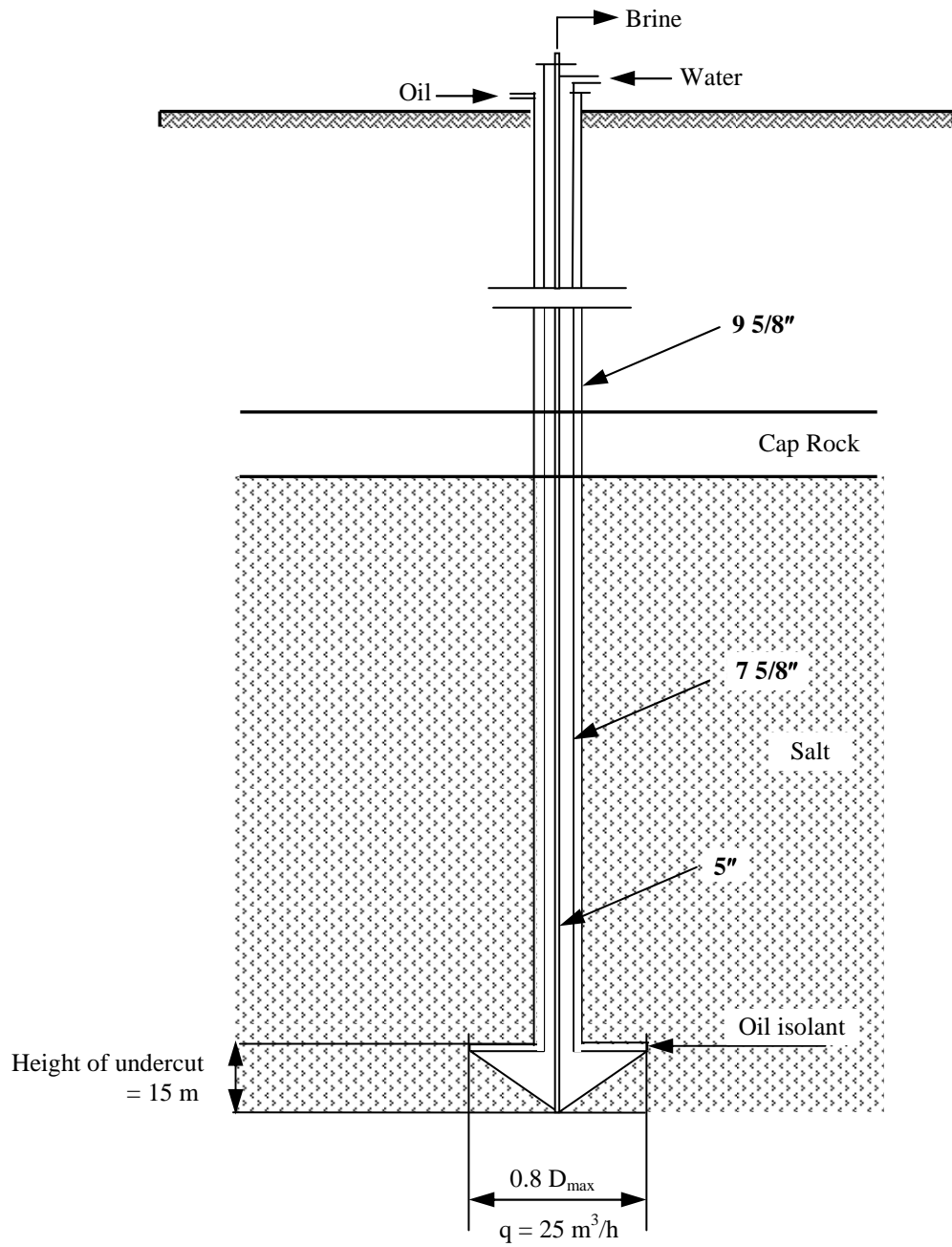
Figure 2.7 First phase: cavern development by hydro-undercut

(modified from Jeramic, 1994).
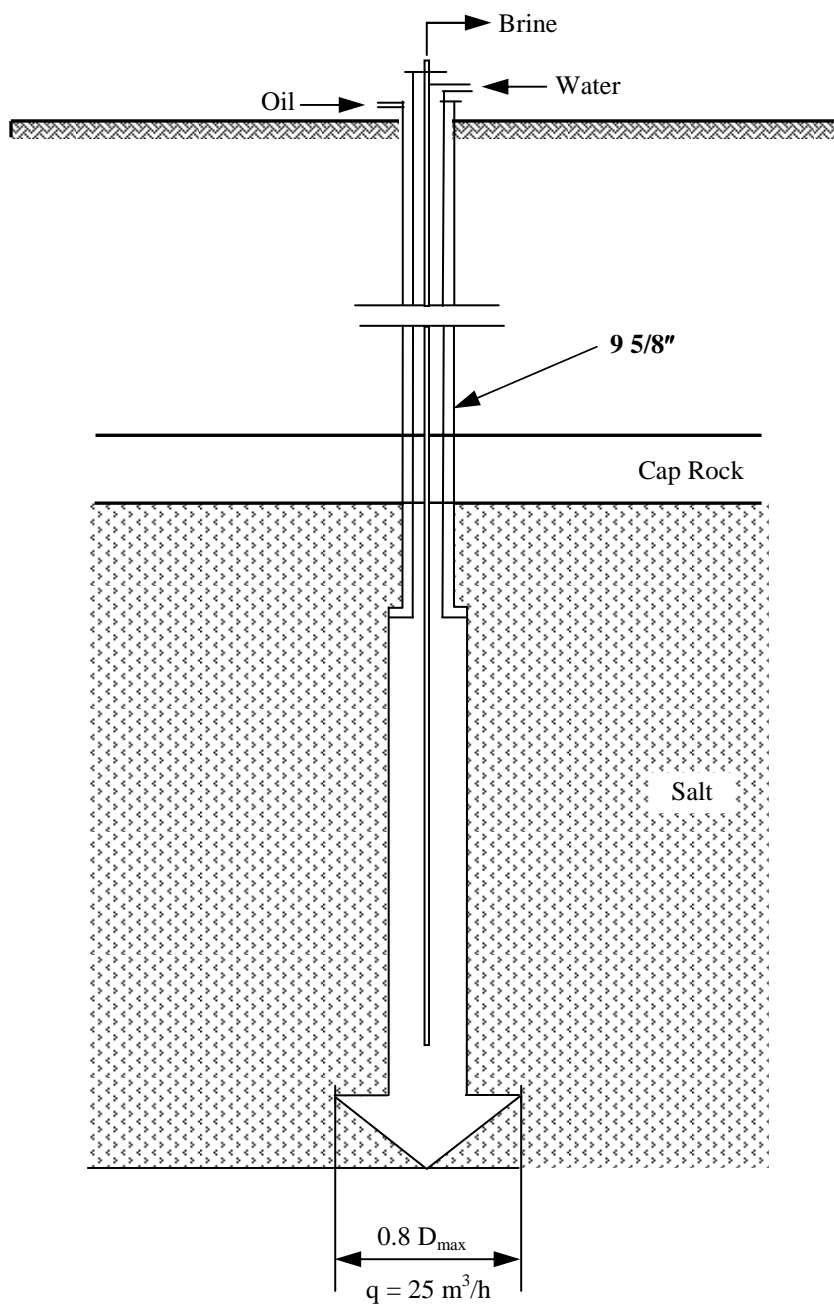
Figure 2.8 Second phase: cavern development by a vertical slot

(modified from Jeramic, 1994).

phase of the cavern, which has and analogy with dry mining stope extraction. The direction of salt dissolution is lateral, by widening the cavern and blocking the roof with isolant fluid on the top of brine. During this phase and indirect circulation is also applied with exploitation tubing installed in the lower part of the cavern. The capacity of salt exploitation in this phase, until cavern completion (D=60 meters) is approximately 50 m^3/h of saturated brine (Figure 2.9).

During solution mining, it is necessary to follow the development of the cylindrical cavern with the following methods.

1) Calculation of the volume increase of the cavern based on the salt mass produced.

2) Checking the level of isolant fluid using gamma density logs and the method of differential pressures.

3) Analysis of the chemical composition of dissolved salt.

4) Surveying the cavern shape by the ultra-sound method, using an echometer.

If the development of the cavern during the solution process is in agreement with the design parameters, then solution exploitation continues. If surveying data record an appreciable deviation to the size and shape of the exploitation cavern, then production has to be stopped. In this case the design parameters must be recalculated and changed, such as the velocity of salt solution, the depth of solution tubing, the level of fluid isolant, and others.

Without cavern control by calculation and instrumentation it is impossible to execute the correct layout of solution mining. Under these circumstances the inter-cavern pillars, sill pillars and finally protective pillars which envelope the
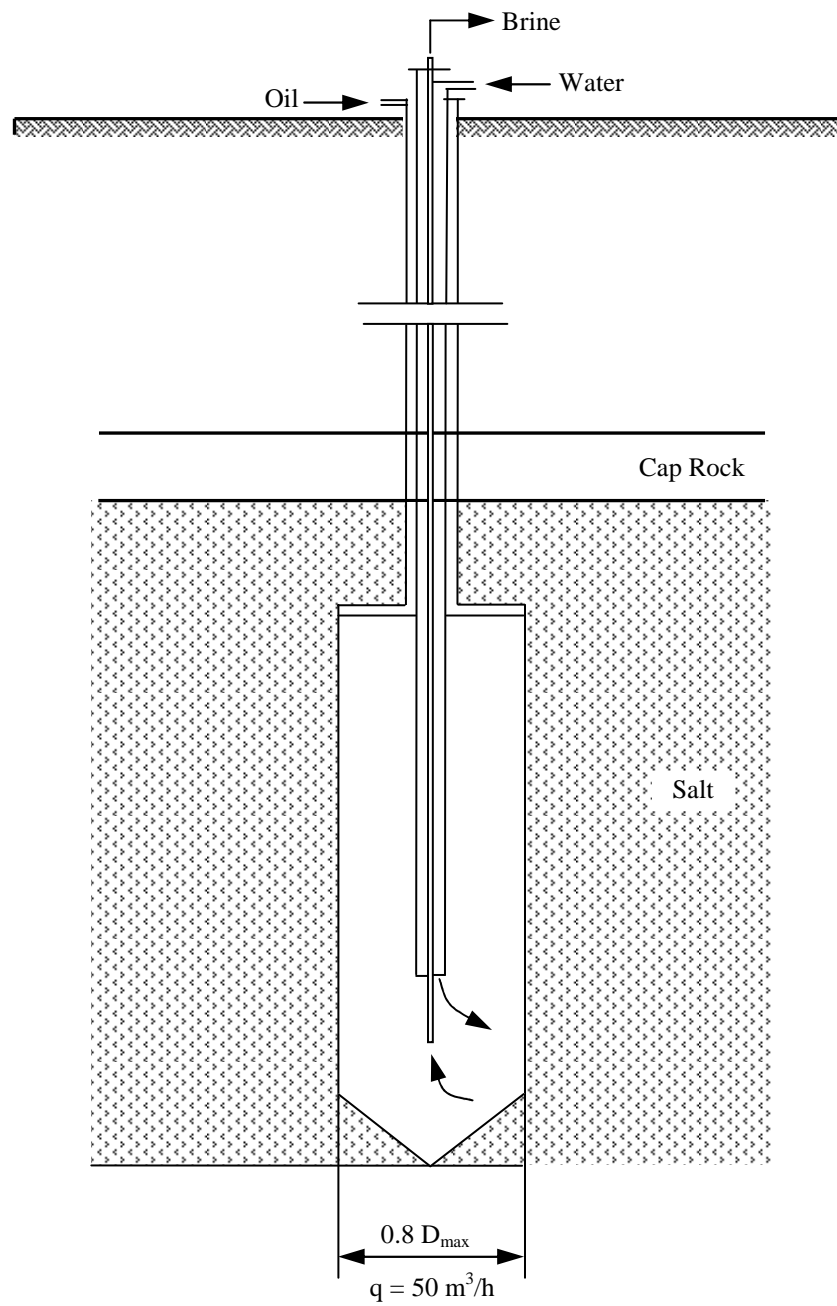
Figure 2.9 Third phase: cavern in exploitation stage (modified from Jeramic, 1994).

solution mining area might become unstable, which could jeopardize not only the stability of the solution mine, but also the stability of the whole salt body.

The spacing ratio, a relationship between the distance of caverns (S) and the diameter of the caverns (D) has been varied. It is obvious that the spacing ratio among caverns is and instrumental factor of interaction stress concentration and cavern deformation (Jeramic, 1964).   There are some opinions that the spacing between caverns should be large enough to prevent coalescing of the respective yield zones surrounding cavities (see Table 2.2).

Table 2.2 Examples of spacing-to-diameter ratio of the storage caverns.

Locations	Storage	Height H (meters)	Diameter D (meters)	Spacing S (meters)	S/D ratio	References
Huntorf, Germany	Compressed-Air	150	60	220	3.7	Crotogino et al., 2001
Alabama, USA	Compressed-Air	305	70	177	2.5	Serata et al., 1989; Serata and Mehta, 1993
Mississippi, USA	Natural Gas	305	30	150	5.0	Katz and Lady, 1976
Pimai, Thailand	Brine	45	80	120	1.5	Gronefeld et at., 1993
Hengelo, Netherlands	Chemical Waste	114	120	600	5.0	Jeramic, 1994

2.5 Solution mining practices in Thailand

Fuenkajorn (2002) derives a generic guideline for the design of solution caverns in rock salt formations in Thailand. A guideline has been developed for the design of salt solution mine caverns in Sakon Nakhon and Khorat Basins. Laboratory testing calibrates the mechanical and rheological properties of the salt formation. Via a series of numerical analyses, conservative configurations of the solution mine

caverns are determined. It is recommended that the caverns be arranged in an array of single well system and should have the maximum diameter and height of 80 and 60 meters, respectively. The minimum spacing is estimated to be 240 meters. The cavern field would yield an extraction ratio of 1.96×10^6 m^3 of rock salt per one square kilometer. The salt roof and floor should be greater than 200 meters to prevent excessive movement of the cavern ground.

Brine production in Thailand has been begun in September 1987 from the dissolution of salt in the lower layer of the Maha Sarakham Formation (Salakshana et al., 1987; Gronefield et al., 1993). The production of brine is achieved by the circulation of fresh water via boreholes. Two freely suspended tubing strings are run into the well, which has been cased and cemented down to the top of the salt bed. This gives three separate surface-to-cavern pipe or annulus connections. Water is pumped through on of the tubing strings into the well. The water dissolves the salt at the exposed well surface, becoming variably saturated. Brine returns to the surface via the second tubing string. A gas or liquid medium, lighter than the brine, which does not dissolve salt, is injected into the well via the third connection. This medium, known as the blanket is designed to prevent dissolution of the salt in an upward direction. The control of brine production process (concentration and volume evolution) is achieved with the time dependent leaching parameters such as leaching string depth, blanket depth, pumping rate as laid down in the leaching plan.

Pimai Salt Co.,Ltd. has modern salt plant is located at Amphoe Pimai in Nakhon Ratchasima province that the only pure vacuum salt plant in Asia with an annual production of over 1,000,000 tons which used the multi-stage with oil blanket technology from Germany. The cavern mined in Lower Salt member of Maha

Sarakham Formation at 200 to 280 meters depths. The cavern diameter and height are 80 and 45 meters with cavern spacing of 120 meters and salt roof of 25 meters. The cavern shape is a modified cylindrical shape with cavern volume of 600,000 cubic meters.

2.6 Design processes for solution mining

Rock mechanics principles are not often applied in the design process. This often leads to failure of the string and cavern. In the past the U.S. industry relied on the 'rules of thumb' for preliminary designs of salt caverns. Typically, the maximum cavern pressure was roughly defined as 0.75-0.85 psi/ft of depth to the casing seat. The minimum pressure depends on the surface facility, pipeline conditions and geological conditions. It was usually unknown. The cavern spacing was normally varied from site to site. Usually the spacing of twice the cavern diameters was used. The height-to-diameter ratio (H/D) usually was taken as 1.0 for bedded salt caverns. It varied for caverns in salt dome (Bieniawski, 1992).

A comprehensive design methodology is not just a sequence of flow charts for step-by-step design, this has been done before (Hoek and Brown, 1980; Bieniawski, 1984). To be comprehensive, a design methodology must incorporate design principles which can be used to evaluate designs and to select the optimum one fulfilling the perceived objectives. A design methodology must indeed recommend and order of design stages but these must be so structured as to assist in effective decision making and promote design innovation in accordance with the design principles (Bieniawski, 1992). The design process for solution mining comprises ten design stages, including 1) identifying the performance objectives, 2) determining the functional requirements

and constraints, 3) collecting relevant information, 4) developing the design solutions, 5) analyzing the design components, 6) synthesizing and defining the specifications, 7) system evaluation, 8) design optimization, 9) design recommendations, and 10) implementations (Figure 2.10).

2.7 Mechanical constitutive laws of rock salt

Several mechanical constitutive laws of rock salt have been developed, which vary from simple visco-elastic models to complex dislocation theory models. Most of the laws emphasize long-term mechanical behavior under a variety of pressures and temperatures. The constitutive models for salt can be divided into three groups: 1) rheological model, 2) empirical model, and 3) physical model.

The rheological models describe the mechanical behavior of salt, but ignore the actual mechanisms of deformation. The deformational characteristics are assumed to be governed by two basic physical elements: spring elasticity and dashpot viscosity. The mechanical behavior of salt is modeled by a combination of these elements. Since the structure of the rheological models is not related to any particular test, the model can be applied to general problems of time-dependent behavior without requiring additional assumptions. The theories of rheological models have been studied by Jin and Cristescu (1998), Cristescu (1993a, 1993b, 1993c, 1996), Serata and Fuenkajorn (1992a), Fuenkajorn and Serata (1992, 1994), Stormont and Fuenkajorn (1994), and Massier (1996).

The empirical models are generally arbitrary functions formulated to fit a set of experimental results. Similar to the rheological approach, the development of the
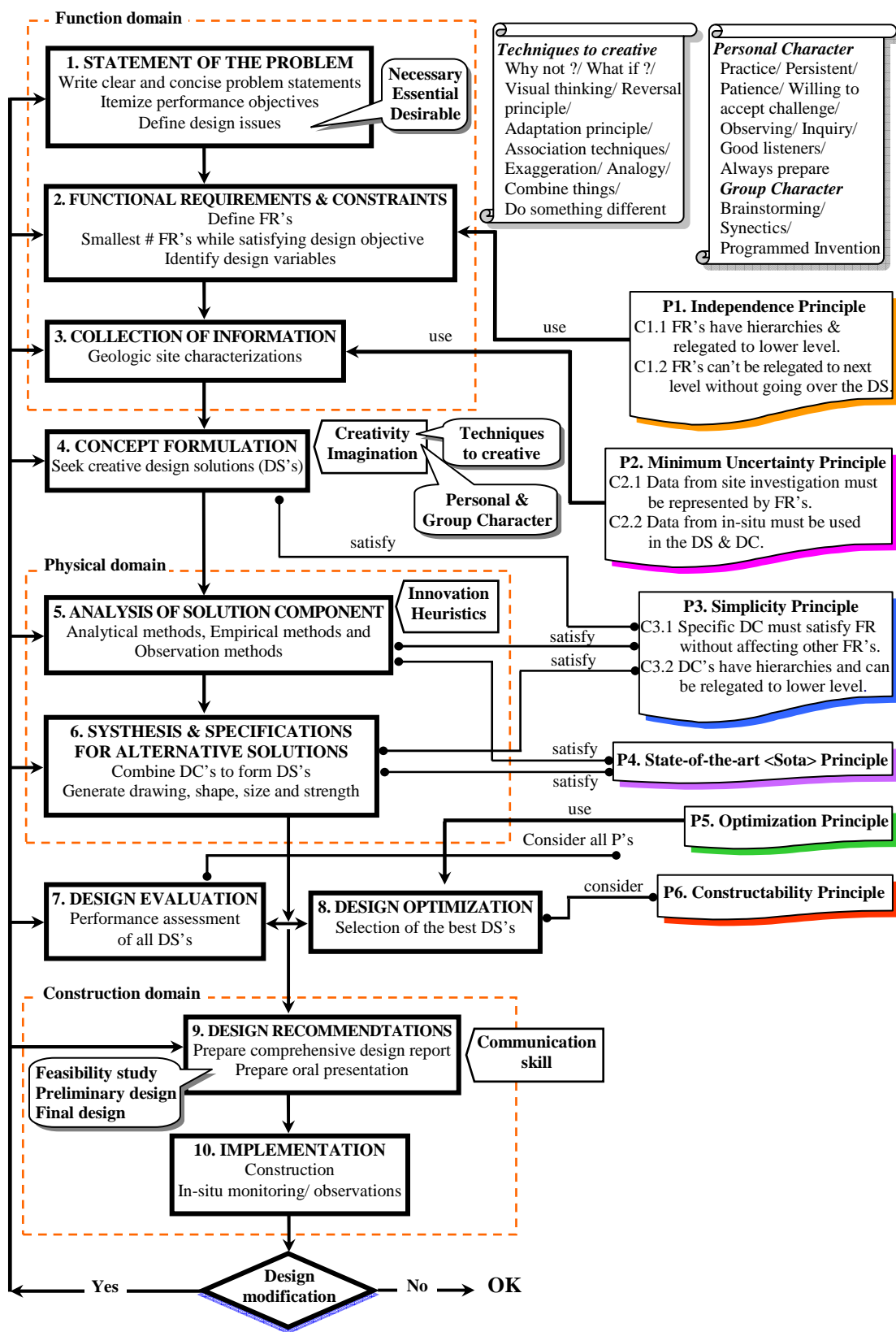
Figure 2.10 Design process for rock engineering (modified from Bieniawski, 1992).

empirical laws ignores the actual mechanism of deformation of salt. By fitting curves to a set of data, certain relationships among the data can be established. The empirical laws can be presented in several forms (power, exponential, polynomial, etc.), depending upon the characteristics of the data. Several forms of empirical model can be studied from Fokker and Kenter (1994), Pudewills and Hornberger (1996), Zhang et al. (1996), Callahan et al. (1998), and Spiers and Carter (1998).

The physical models start from the analysis of the microscopic structural variation of the material observed under loading, and incorporate a theoretical explanation of the basis of time-dependent behavior. The method originated in metallurgy is later introduced into rock mechanics. Rocks are more complex materials than metals. The atomic bonds in natural rocks are always a chemical bond rather than a metallic bond. Furthermore, most rocks are multigranular-structured in contrast to the relatively single phase structure of metals.

The physical models are therefore considered inappropriate for describing the time-dependent behavior of rock salt (Aubertin, 1996; Aubertin et al., 1998, 1999; Korthaus, 1996, 1998; Durup and Xu, 1996; Senseny and Fossum, 1998; Weidinger et al., 1997, 1998; Hampel et al., 1998; Eduardo et al., 1996).

2.8 Computer modeling

There are some computer software in engineering geology that have been used to model mechanical and hydraulic behavior of rock salt, e.g. behavior in terms of stress, strain, permeability, etc. Many software use elasticity, visco-elasticity, visco-plasticity, and plasticity characteristics to predict short-term and long-term behavior as tabulated in Table 2.3. Some software is developed to be used easy, quick, and

Table 2.3 Some computer programs used for describing the rock salt behavior

(modified from Klayvimut, 2003).

Code Names	Methods	References
BEFE	BEM (3D)	Beddoes (1994)
VELMINA	DDM (3D)	Frayne (1998)
VNFOLD	DDM (3D)	Beddoes (1994)
FLAC	FDM (2D)	Itasca (1992)
FLAC	FDM (3D)	Itasca (1994), and Frayne (1996, 1998)
ADINA	FEM (2D)	Pudewills and Hornberger (1996)
ANSALT	FEM (2D)	Heusermann et al. (1998)
ANSPRE	FEM (2D)	Honecker and Wulf (1988)
ANTEMP,ANSPP	FEM (2D)	Honecker and Wulf (1988)
ASTHER	FEM (2D)	Rolnik (1988)
CODE-BRIGHT	FEM (2D)	Olivella et al. (1996, 1998a, 1998b)
COYOTE	FEM (2D)	Gartling (1981a)
DAPROK	FEM (2D)	Harrington et al. (1991)
FAST-BEST	FEM (2D)	Pudewills (1998)
GEO/REM	FEM (2D)	Serata (1991), and Serta and Fuenkajorn (1993)
GEOMEC	FEM (2D)	Nguyen-Minh and Menezes (1996)
GEOROC	FEM (2D)	Rizkalla (1991)
JAC	FEM (2D)	Biffle (1984)
LUBBY-1	FEM (2D)	Rokahr and Staudtmeister (1996)
LUBBY-2	FEM (2D)	Lux and Schmidt (1996)
MARC	FEM (2D)	Van Eekelen (1988)
MERLIN	FEM (2D)	Gartling (1981b)
SANCHO	FEM (2D)	Stone et al. (1985), and Hansen (1996)
SPECTROM-32	FEM (2D)	Callahan et al. (1989)
VIPLEF	FEM (2D)	Vouille et al. (1996)
VISCOT	FEM (2D)	INTERA (1982), and Frayne (1996)
SUVIC-D	FEM (2D/3D)	Julien et al. (1998)
VISAGE	FEM (3D)	Ong (1994)

Note: FEM is finite element method, FDM is finite difference method, DDM is displacement discontinuity method, BEM is boundary element method, and 2D is two-dimension, and 3D is three-dimension.

convenient analysis. Most of them employ finite element methods and the rock salt mechanical behavior role is applied in the main equations to calculate and determine the constants of variable factors derived from laboratory and field testing.

The main objective of this section is to review the computer models (programs) and analytical methods for describing the rock salt behavior. In general, the computer models have been developed to simulate the time-dependent brittle-ductile behavior of rock salt and designed for the analysis of complex material behavior under a variety of loading and thermal conditions (Juliend et al., 1998). It is difficult to obtain an accurate calculation of salt behavior with respect to time by human. Advantages of the computer programs are fast and easy to use. Therefore, the computer programs are widely used for simulating the rock salt behavior. The computer models are divided into two groups: 1) boundary methods and 2) domain methods. The boundary methods include boundary element method (BEM) and displacement discontinuity method (DDM). The domain methods include finite element method (FEM) and finite difference method (FDM).

The boundary element method derives its name from the fact that only the boundaries of the problem geometry are divided into elements. In other word, only the excavation surfaces, the free surface for shallow problems, joint surfaces, where joints are considered explicitly, and material interfaces for multi-material problems are divided into elements. Several types of boundary element methods are collectively referred to as the boundary element method. These models may be grouped as follows: direct method, so named because the displacements are solved directly for the specified boundary conditions. Displacement discontinuity (indirect) method, so named because it represents the result of an elongated slit in an elastic continuum

being pulled apart. Fictitious stress (indirect) method, so named because the first step in the solution is to find a set of fictitious stresses which satisfy pre-described boundary conditions. These stresses are then used in the calculation of actual stresses and displacements in rock mass. The computer programs for the boundary element method have been used by Beddoes (1994) and Frayne (1998).

The finite element method is compatible and appropriate to solving problems involving heterogeneous or non-linear material properties, since each element explicitly models the response of its contained material. However, the finite element method is not well suited to modeling infinite boundaries, such as in underground excavation problems. One technique for handling infinite boundaries is to discrete beyond the zone of influence of the excavation and to apply appropriate boundary conditions to the outer edges. Another approach has been used to develop elements for which one edge extends to infinity (i.e. so-called infinity finite element). Efficient pre and post-processors allow the user to perform parametric analyses and to assess the influence of approximated far-field boundary conditions. The time required for this process is negligible compared to the total analysis time. Joints can be represented explicitly using specific joint element. Once the model has been divided into elements, material properties have been assigned, and loads have been prescribed. Some techniques must be used to redistribute any unbalanced loads and thus determine the solution to the new equilibrium state. Available solution techniques can be broadly divided into two classes, implicit and explicit. Implicit techniques assemble systems of linear equations, which are then solved using standard matrix reduction techniques. Any non-linearity material is taken into account by modifying stiffness coefficients (second approach) and/or by adjusting prescribed variables

(initial stress or initial strain approach). These changes are made in an iterative manner such that all constitutive and equilibrium equations are satisfied for the given load state. Several computer programs for the finite element methods can be studied from Blanquer-Fernandez (1991), Nguyen-Minh and Quintanilha de Menezes (1996), Devries and Callahan (1998), Harrington et al. (1991), Heusermann et al. (1998), Honecker and Wulf (1988), INTERA (1982), Salzer and Scheriner (1998), Julien et al. (1998), Lux and Schmidt (1996), Rokahr and Staudtmeister (1993), Rolnik (1988), Serata and Fuenkajorn (1991), and Vouille et al. (1996).

The finite difference method is compatible and appropriate to solving problems involving inhomogeneous, complicated geometry, and non-linear material properties that are similar to that of the finite element method. The FDM is for approximating derivatives in the equations of motion. Continuous derivatives in differential equations are replaced by finite difference approximations at a discrete set of points in space and time. The resulting set of equations, with appropriate restrictions, can then be solved by algebraic methods. A finite difference model is one, which employs finite difference methods. The resolution of a finite difference model is determined by the spacing of the discrete set of points (grid points) used to approximate the derivatives. The FDM is applied for modeling geomechanical problems that consist of several stages, such as sequential excavation, backfilling, and loading. Several computer programs for describing the rock salt behavior can be studied from Itasca (1992, 1994) and Frayne (1996, 1998).

The distinct element method (DEM) is a domain method, which models each individual block of rock as a unique element (i.e. where the spacing of the joints is of the same order of magnitude as the excavation dimensions). The individual pieces of

rock may be free to rotate and translate, and the deformation that takes place at block contacts may be significantly greater that the deformation of the intact rock, so that individual wedges may be considered rigid. For the rock mass, such as rock salt, the distinct element method is not suitable for the analysis.

2.9 Subsidence due to solution mining

Solution mining subsidence is a complex problem of rock mechanics, particularly in the case of uncontrolled solution mining. Four types of subsidence in regard to solution mining methods are discussed with the type considers subsidence development as a function of time (Jeramic, 1994).

2.9.1 Subsidence from single-well mining

Jeramic (1994) suggests that subsidence from single-well mining can be designed and controlled. This type of subsidence is similar to that in room-and-pillar mining, because the caverns are irregular rooms which are supported by pillars. To control subsidence, it is of paramount importance to design a proper thickness of sill pillar (salt pillar above cavern) and the required thickness of the inter-cavern pillars. The skeleton of the pillars is uniformly deformed, so that subsidence consideration is given as for a block of salt mass in which caverns are located (Figure 2.11). Under this assumption, further consideration of subsidence is a case of room-and-pillar mining, e.g. the case of uniform subsidence of the entire caverns field area. In order to evaluate surface subsidence, the roof subsidence of the caverns is estimated over the volume of convergence. The best control of cavern subsidence is achieved by a trigonal layout of the single-wells, where the contact points are preferred.
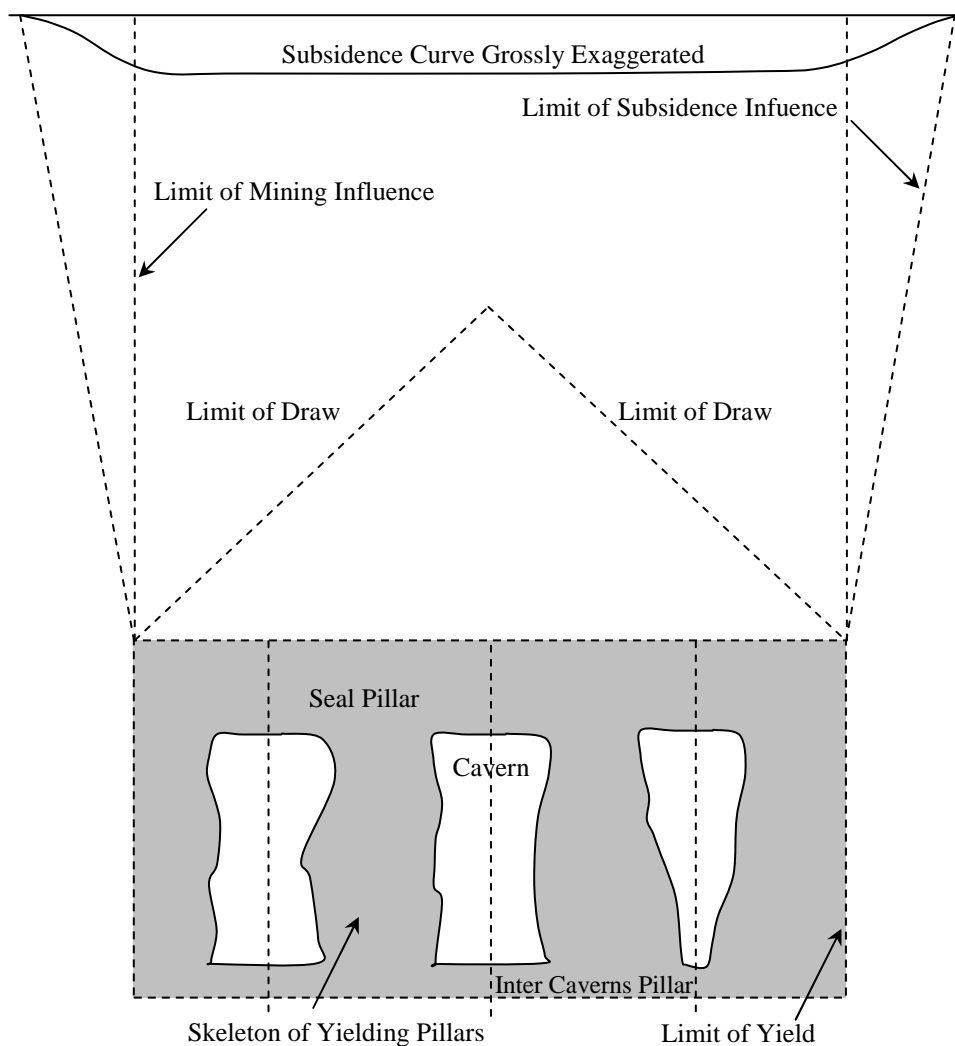
Figure 2.11 Model of subsidence from the single-well solution mining method (modified from Jeramic, 1994).

The cave-in of caverns or collapse of a cavern system leads to damage of the ground surface only in the case of shallow mining. Under these circumstances, damages at the ground surface could be devastating due to the formation of sink holes. At greater depth (over 1,000 meters), regardless of the collapse of the cavern system, destruction at the ground surface is impossible (Dreyer, 1981). This is of paramount importance for storage caverns, which must maintain their stability for a long period

of time. The important requirements for storage caverns are that deformation of the surrounding rock does not fracture to the surface and that the flow of salt maintains small enough deformation that subsidence will also be small.

Several mathematical models have been developed for the analysis of the conditions created in the rock mass surrounding a cavern system with the aim of predicting subsidence, particularly in the case of storage caverns. All of them have some deficiencies because they do not incorporate the discontinuous nature of the salt rock mass.

2.9.2 Subsidence from two-well mining

Solution mining by two or more wells requires a close location of the caverns, that they can be connected without difficulties. Under these circumstances large lateral caverns with irregular shapes are form (called 'galleries'). It is obvious that large caverns/galleries experience a higher stress concentration, surrounded by rocks of deteriorated strength due to high moisture contents induced by the dissolution process. These structures are susceptible to closure and cave-in and could result in the catastrophic collapse of overlying sediments, and significant surface damage through sink hole subsidence (Jeramic, 1994).

2.9.3 Subsidence from uncontrolled solution mining

The most significant subsidence recorded from uncontrolled solution mining, either had been initiated originally or came by conversion from controlled solution mining. To better understand solution mining subsidence, it is necessary to analyze the mechanics of interaction between sub-surface deformation and ground surface damages, as follows (Jeramic, 1975).

Sub-surface subsidence caused by solution mining has no satisfactory mathematical or empirical theories to explain its mechanism due to the fact that it cannot be observed. The quantity and geometry of the rock salt remnants left by solution mining are unknown. It is almost impossible to relate the configuration of one or more caverns in underlying salt beds to the collapse of the rock salt and overlying strata. The general hypothetical model of sub-surface subsidence is based on the assumption that profiles of the caverns in most rock salt deposits exhibit a form similar to loaded thick beam with clamped edges. The caverns of deformation might be in the following order.

a) The postulated thick beam comprised of the roofing strata is subjected to gravitational body forces, whose magnitude depends on the strata thickness (Figure 2.12a). As a result of solution mining, the thick beam will deform. The deformation slowly increases.

b) Slow lateral movement at an approximately constant rate permits gradual bending of the postulated thick beam. During the extraction period, several caverns in the salt formation might be formed, controlled by individual wells. It is assumed that more of less similar sagging takes place in all caverns. As a function of time, creep deformation will be prolonged before rupture occurs (Figure 2.12b)

c) Terzaghi (1969) suggests that sooner or later most salt wells become connected through solution channels to each other and finally to a large gallery. At that moment, the strength of the overlying sediments might be overcome and rupture initiated. The

rupturing will be progressive, and the arch of the overlying rock will be formed (Figure 2.12c).

d) When the rock salt remnants can no longer carry their own weight and the weight of unconsolidated overlying rock in the area of a large gallery, they will collapse. At this moment a large gallery will be totally filled in by fragmented rock and the arch will be extended upwards at the accelerated rate. Probably, when the parabolic slope of the arch of draw intersects the ground surface, a sink hole will be formed with a vertical ground displacement of 1 to 10 meters (Figure 2.12d).
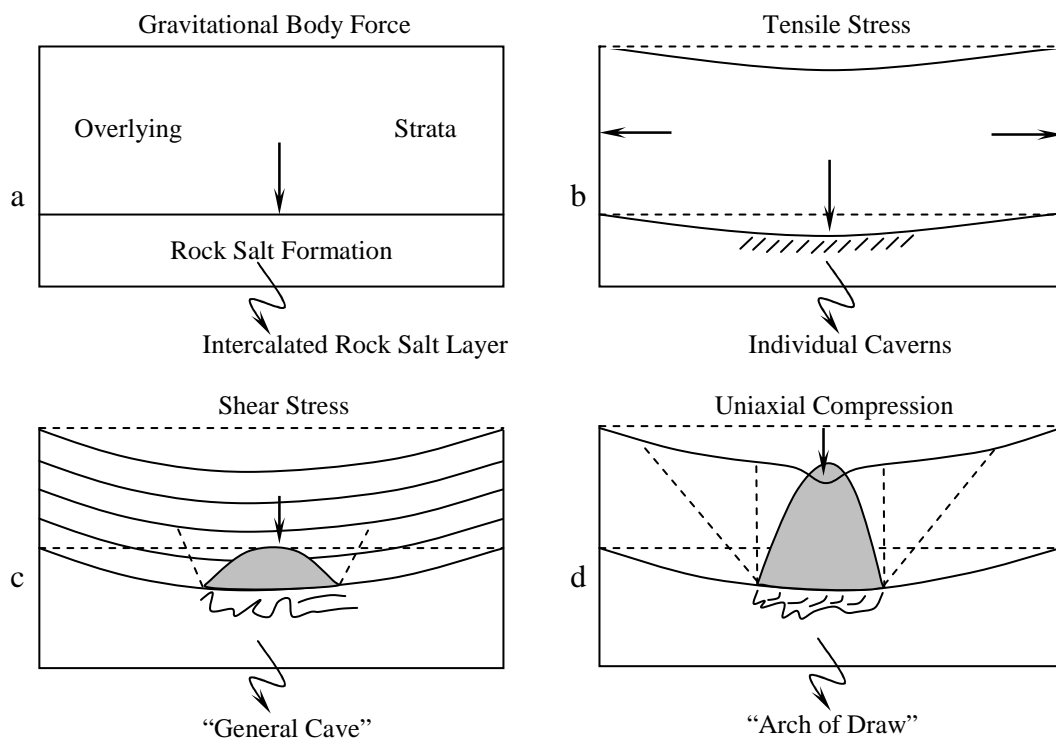
Figure 2.12 Hypothetical model of subsidence development, with stress field delineation (modified from Jeramic, 1994).

Surface subsidence obviously is a product of sub-surface deformations. From many published data of surface subsidence caused by solution mining, several common features of this mechanism can be inferred as suggested here (Jeramic, 1975).

a) The surface effects are associated with vertical and lateral ground movements. Probably all lateral surface displacements are toward the center of the cavern. Vertical surface displacement starts well beyond the lateral limits of the extracted area, with its maximum at the center of the cavern.

b) As a result of this displacement, a curvature of the ground surface results. The curvature in some cases represents Gauss' function. When the subsidence reaches a final settlement. The deformations of the ground surface can be described by three zones (Figure 2.13) (Smailbegovic, 1965).

c) First, the zone of maximal vertical displacement (simple uniaxial compression) which should be above the center of the large gallery in the rock salt formation. This zone of deformation is represented by a sink hole filled in by water. It is located at the middle of the bowl of surface subsidence and it is filled by the broken rock material. The profile of subsidence in this zone caused by solution mining has a convex curvature.

d) The second zone of ground surface deformation surrounds the sink hole. The slope is represented usually by a concave curvature and it is formed by vertical and horizontal ground movements (shear

stresses). It is interesting to note that while the radius of curvature varies, the geometrical shape is always the same.

e) The third zone represents an area of minimal vertical movement, but horizontal extensions occur (tensile stress). The slope of this peripheral part of subsidence could be very gentle with a larger lateral extension (Smailbegovic, 1965).
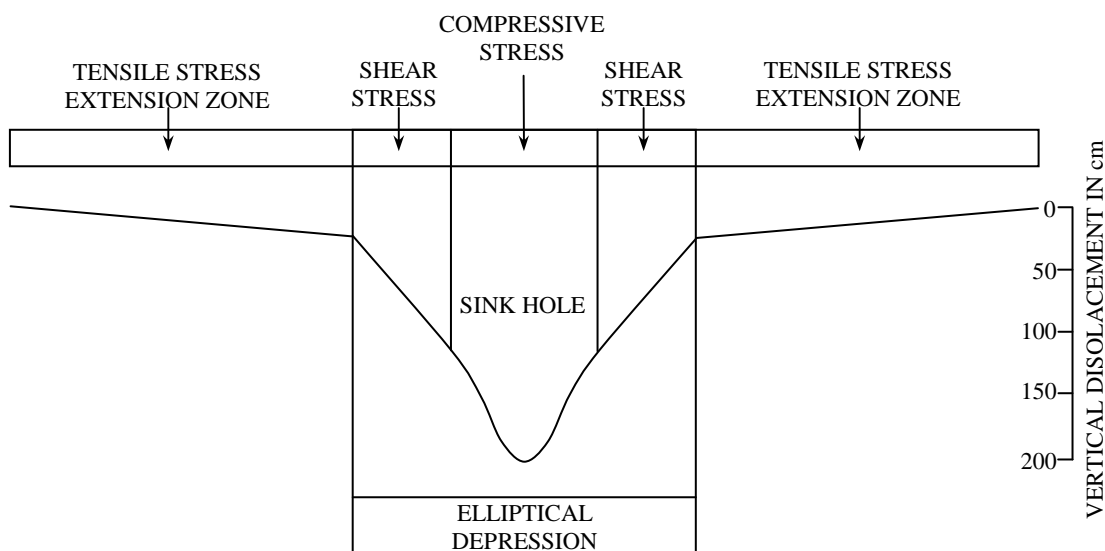
Figure 2.13 Subsidence of the Tuzla brine-field (former Yugoslavia) and the stress fields delineation (modified from Jeramic, 1994).

Theoretical analysis of the deformation on the ground surface caused by mining operations in bedded deposits is very well explained by the trough subsidence. Unfortunately, there is no similar analysis for subsidence caused by the uncontrolled solution mining. From and engineering point of view, it is very difficult to represent the relation between surface ground deformations and the geometry of the extraction area. However, in a general sense, subsidence curvature of deformation might

sometimes be used as a parameter for an approximate estimation of the extension of the large cavern and the tip of the parabolic slope of the arch of draw (Jeramic, 1994).

2.9.4 Subsidence as a function of time

Surface and sub-surface subsidence are time-dependent deformations. For example, the surface subsidence of most rock salt deposits excavated by the room-and-pillar method is very shallow and regular without rupture of the ground surface. In this case, subsidence is not manifested immediately after excavation and it can only be measured after several years.

Usually a couple of year after underground excavation ceases, the surface comes to rest. However, on the contrary subsidence caused by solution mining may cause an erratic and unpredictable surface deformation. An instructive example of the subsidence progress is published by Terzaghi (1969) in a paper entitled 'Brine-field subsidenceat Windsor, Ontario'. The rate of subsidence at Windsor had many features in common with that of other surface deformations caused by solution mining in many parts of the world (Figure 2.14). At Windsor, the salt formation is about 180 meters thick and consists of shale, dolomite, gypsum, anhydrite and rock salt. The thickness of the overlying sediments is about 270 meters. The subsidence deformation as a function of time can be summarized as follows.

a) The period interval before subsidence is evident, is much longer for solution mining that for and excavation formed by underground mining methods. Usually subsidence above an excavation due to mining is noticeable after two or three years. However, this period is much greater for solution mining of rock salt deposits and subsidence may perhaps be only noticeable after decades, and in

some cases after centuries depending on the intensity of solution mining. For example, at Windsor solution mining began in 1902, but the first noticeable surface deformation was in the late 1940's.

b) The first phase settlement of subsidence for solution mining progresses at a very slow rate and it can last for several decades. At Windsor, the first phase of surface subsidence was from 1940 to 1952 forming a convex shaped depression.
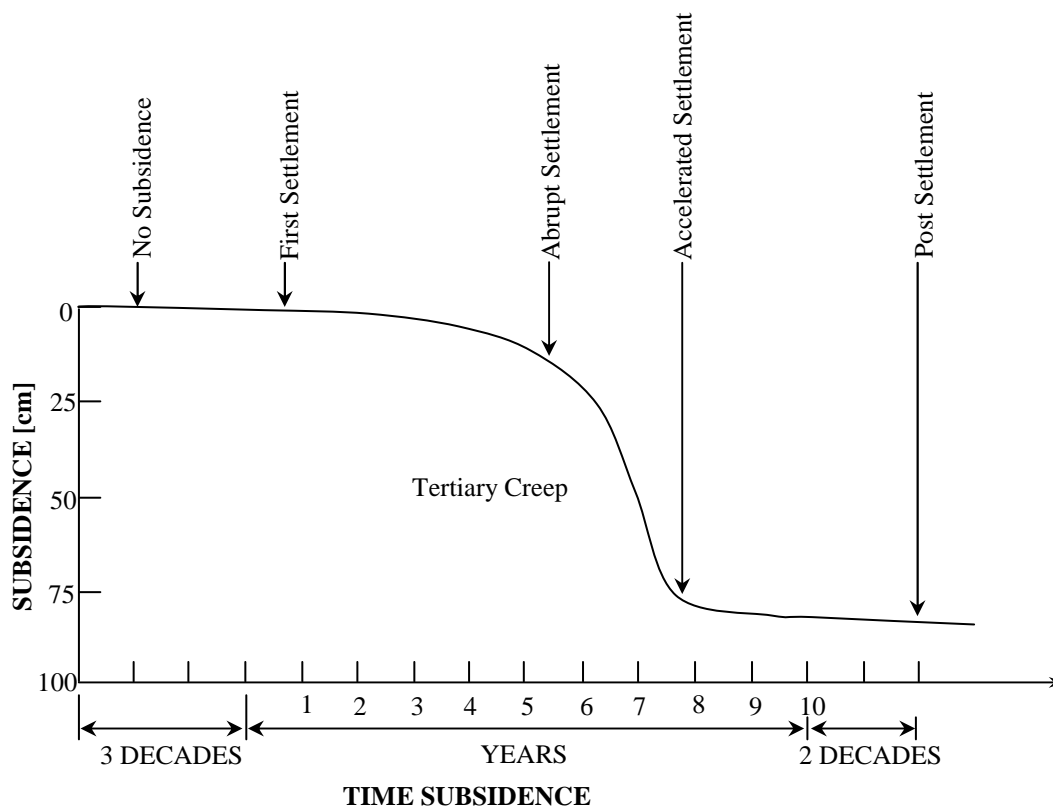
Figure 2.14 Diagram of subsidence as a function of time at the Windsor brine-field, Ontario (from Jeramic, 1994, modified after Terzaghi, 1969).

c) However, the phase of accelerated subsidence takes place within a period of a couple of years. During this time, the ground surface deformation forms a bowl-shaped depression which might subside up to 40 centimeters. Accelerated subsidence at Windsor occurred during the years 1953-1954.

d) Abrupt subsidence can occur within several days or hours. For example, at Windsor the catastrophic subsidence happened with an interval of only several hours. The bowl-shaped depression began to fill with water and rapid subsidence formed a sinkhole. The sinkhole appeared along one side of the rim of the bowl-shaped depression and it was up to 75 centimeters deep. By mid-afternoon, movement had virtually ceased. In a similar manner, the sinkhole at Tuzla (former Yugoslavia) was formed, but the process of abrupt subsidence lasted through several days.

e) Post subsidence settlement was immediately followed by irregular movements of small magnitude. At Windsor, the average annual rate of settlement over the fourteen-year period following the sinkhole was up to 1.25 centimeters per year.

If the curve of the subsidence deformation as a function of time is analyzed, many similarities with a generalized creep curve can be noticed. A typical three-stage creep is developed in which the deformation rate accelerates with time. In time (decades and years), a rock salt formation with some ductile properties may be deformed by the creep mechanism with three distinct component processes. In

accordance with this suggestion, the ground surface subsidence is rather the product of the creep deformation than of elastic yielding deformation (Jeramic, 1994).

2.9.5 Subsidence prediction

Existing subsidence prediction techniques fall under two basic categories: empirical and phenomenological (Voight and Pariseau, 1970; Brauner, 1973; Singh, 1978). The empirical theories are principally based on observations and experience from field subsidence studies (Hartman, 1992). Some of the empirical methods have proved sufficiently reliable for subsidence prediction, at least for a given region. Many of these have been successfully applied in a number of countries, especially in Europe. Phenomenological techniques are based on equivalent material modeling principles where the subsiding strata are mathematically represented as idealized materials that obey the law of continuum mechanics. Unlike empirical methods, the procedures used in the latter category have not achieved much success to date mainly due to the difficulty of representing complex geologic properties of the strata in simple mathematical terms.

Promising empirical methods for prediction of subsidence over underground mines consists of the following.

1) Graphical method: This simply involves displaying subsidence data in the form of graphical charts or monographs whereby subsidence magnitude and the associated parameters may be directly obtained for a specified set of mine parameters. This method is adaptable in areas where considerable subsidence data exist, and its applicability is generally restricted to relatively few

geologically similar regions. This technique has seen considerable use in the United Kingdom (Anon, 1975).

2) Profile function: This involves the derivation of a mathematical function that can be used to plot a complete profile of the subsidence trough at the surface. It differs from a phenomenological approach in that the constraints employed in the profile function are empirically derived from observed data. This method can be readily applied to geologically dissimilar conditions by modifying the constant values. Profile functions have been successfully applied in several countries abroad such as Poland, Hungary, the Soviet Union, and currently in the United States. Selected profile functions are given in Table 2.4.

3) Influence function: This principle for subsidence prediction is based on the extraction of infinitesimal elements of area. Subsidence at any point on the surface is obtained from the sum of the influence of each extracted element using the principle of superposition. Unlike profile functions, influence functions can not be found directly by measurement. In addition, this method assumes a homogeneous, isotropic overburden material and therefore, has limited accuracy. In general, influence functions have been found to be especially suitable for subsidence prediction over underground workings with irregular of complex geometries. This method has received considerable attention in Europe, and to limited extent in the United States.

Table 2.4 Profile Functions (modified from Hartman, 1992).

Name	Functions
Critical Extraction:	
Hyperbolic	$S(x) = \dfrac{1}{2} S_{max} \left[1 - \tanh\left(\dfrac{cx}{B} \right) \right]$
Error	$S(x) = \dfrac{1}{2} S_{max} \left\{ 1 - \left[\dfrac{2}{(\pi)^{\frac{1}{2}}} \int_0^{\pi/x} \exp(-u^2) du \right] \right\}$
Exponential	$S(x) = \dfrac{1}{2} S_{max} \exp\left[-\left(\dfrac{1}{2} \right) \dfrac{(x+B)^2}{B^2} \right]$
	$S(x) = \dfrac{1}{2} S_{max} \exp\left[-\left(\dfrac{cx}{B} \right)^d \right]$
Trignometric	$S(x) = \dfrac{1}{2} S_{max} \left[1 - \left(\dfrac{x}{B} \right) - \left(\dfrac{1}{\pi} \right) \sin\left(\dfrac{\pi x}{B} \right) \right]$
	$S(x) = S_{max} \sin^2 \left[\left(\dfrac{\pi}{4} \right) \left(\dfrac{x}{B} \right) - 1 \right]$
Subcritical Extraction:	
Trignometric	$S(x) = S_{max} (n_1, n_2)^{1/2} \left[n^2 \left(1 - x + \dfrac{\sin 2\pi x}{2\pi} \right) + \dfrac{1-n^2}{4} (1 + \cos 2\pi x)^2 \right]$
hyperbolic	$S(x) = \dfrac{1}{2} S_{max} \left[\tanh \dfrac{2(x+w)}{B} - \tanh \dfrac{2x}{B} \right]$

Where

x	=	horizontal distance	
c	=	arbitrary constant	
B	=	radius of critical area of excavation	
u	=	integration variable	
w	=	panel width	
$S(x)$	=	profile function	
S_{max}	=	maximum possible subsidence	
n_1, n_2	=	coefficients related to width/depth	
n	=	n_1 or n_2 depending of side of panel	

Phenomenological methods are primarily based on the principles of continuum mechanics and assume the media to be elastic, visco-plastic, plastic, and elastic-elastoplastic. Only the elastic-plastic model has been used with success in the United States. Recently an elastic, frictionless, and laminated model has been proposed (Salamon, 1989).

2.10 Reserve estimation

Leigh et al. (1998) suggest that reserves will be classified with respect to the confidence level of the estimate. Traditionally, ore reserves have been classified as proven (measured), probable (indicated), and possible (inferred). An ore reserve estimate contains two important parameters, including the amount of ore and the average grade or value of that ore. The calculation of the tonnage and grade of a deposit requires the collection and documentation of a considerable amount of data. These data include accurate assay information, plans and sections, details of ore controls, the tonnage factor, applicable cutoff grade to be used, potential mineral recovery, and engineering details.

Some European countries group ore reserves into three classes in terms of cost and mineability (Jeramic, 1964).

Mineral reserves correspond to total ore reserves in place, calculated, and assumed. These reserves belong to underground geological-structural environments. Mineral reserves are divided into three sub-classes.

a) Mineable reserves with a grade, tonnage, and shape which are adequate for profitable mining operations.

b) Conditionally mineable reserves are represented by parts of deposits which have not been sufficiently explored so that their mineability can be identified. If further exploration gives positive results, then they could become mineable. In addition, if mining of the ore at the present time is not profitable but with technological changes or market price improvement their exploitation could become profitable, then they can be reclassified as mineable reserves.

c) Unmineable reserves are represented by complex shapes and low quality of ore. Ore left in safety pillars and in some cases where hydrogeological conditions do not permit mining operation also falls into this classification.

Industrial reserves represent only the ore which is recovered and brought to surface as defined below.

Industrial reserves = mineable reserves – unrecovered reserves

Only recoverable reserves can be identified with the industrial reserves. The tonnage of industrial reserves depends on the coefficient of ore recovery.

Commercial reserves correspond to the tonnage of the ore which is delivered to the market. To obtain commercial reserves it is necessary to subtract from industrial reserves a loss of ore due to beneficiation and transportation processes. The beneficiation loss in related to the amount of waste partings and other impurities which have to be removed from the ore in order that it becomes commercially valuable. The transportation loss is due mainly to loading and unloading operations of the mineral commodity.

Hartman (1987) suggests that mineral reserve estimation or ore estimation involves the calculation of extent (units: tons, tonnes, yd^3, etc.) and average grade or tenor (units: percent, oz/ton, g/tonne, \$/ton, \$/million Btu, etc.) of reserves in a deposit. Ore estimation is a process that begins during exploration with continuing refinement during the life of the mine. Data derived from ore estimation are the basic input for the feasibility study the outcome of which determines if a mine is to be developed. Two general methods are in use for ore estimation: 1) the classical, employing two-dimensional maps and hand calculation and 2) the geostatistical, a more sophisticated approach requiring a digital computer to prepare statistically derived estimates. The classical method is entirely satisfactory for small, uncomplicated ore bodies (Leigh et al., 1998).

CHAPTER III

GEOLOGIC DATA COMPILATION

3.1 Objectives

The objective of this chapter is to compile all existing information relevant to the Maha Sarakham Formation in Khorat Basin in order to construct three-dimensional distribution of the salt units. The published conference papers, journals and reports of Maha Sarakham Formation are reviewed to understand the characteristics of the rock sequence. These and other published materials include as follows.

1) Borehole logs, scale 1:500,000 from Department of Mineral Resources, DMR (Japakasetr and Suwanich, 1982, 1984).

2) Geologic map of Thailand, scale 1:500,000 (DMR, 1983).

3) Topographic map of Thailand, scale 1:50,000 (Royal Thai Survey Department, 1991).

4) Geologic cross-sections and seismic surveys in the northeast of Thailand (Wongsawat et al., 1992; Sattayarak and Polachan, 1990).

5) Mineral potential map of Thailand, scale 1:2,500,000 (DMR, 1997)

6) Geological and mineral occurrence map of Lao People's Democratic Republic, scale 1:1,000,000 (Department of Geology and Mines, 1990).

3.2 Formation identification

The sequences of rock salt in Thailand have been compiled by many investigators (Suwanapal, 1992; Japan International Coorperation Agency, 1981; Suwanich and Ratanajarurak, 1982; Suwanich, et al., 1982; Yumuang, et al., 1986; Japakasetr and Suwanich, 1982, 1983, 1984). They are mostly obtained from the borehole logging conducted as part of the potash exploration project in the northeast of Thailand. The locations of the boreholes are shown in Figure 3.1.

The borehole logs data were previously classified by grain size, color, inclusions, and associated rocks. The sequence of rock layers was classified into eight 8 layers from the top to the bottom as follows (Japakasetr, 1985; Japakasetr and Workman, 1981; Sattayarak, 1983, 1985; Japakasetr, 1992; Japakasetr and Suwanich, 1982).

1) Top soil is the unconsolidated to semi-consolidated covering the top of bed rock till to the surface.

2) Sedimentary rocks above Upper Salt consist of sandstone, siltstone, and claystone. Sandstone is usually on the top of all, siltstone in the middle and claystone at the bottom. They compose of quartz with calcareous and silica cementing.

3) Upper Salt is the uppermost salt bed.

4) Middle Clasitc is dark reddish brown clay or claystone that mostly sticky, soft, plastic, and damp or always wet.

5) Middle Salt is a salt bed stratified between the Middle Clastic and Lower Clastic which locally present of anhydrite.

6) Lower Clastic may has a thin anhydrite layer between Lower Clastic and Lower Salt. Clay in Lower Clastic is sticky, plastic, always dank and unconsolidate to semi-consolidated.

7) Lower Salt and potash are at the bottommost of salt beds.

8) Sandstone and/or Siltstone (Khok Kruat Formation) are downwards from the basal anhydrite. The base rock is dark reddish brown.

This research will focus on identifying the salt units in each borehole log by using the mineralogical characteristics of rock salt. The rock salt is divided here into three units, the Upper Salt, Middle Salt, and Lower Salt.

1) The Upper Salt is between the Upper and Middle Clastic units. It consists mainly of moderate to dark yellowish brown or honey halite, minor of anhydrite stringers, smoky dark halite bands, milky white grained halite, few orange grained halite near the bottom contact, and locally large crystals of colorless halite (about 1-2 centimeters in diameter). Anhydrite may present between the Upper Salt and the Middle Clastic.

2) The Middle Salt in the uppermost portion is found as white and clear salt, rather pure. The crystals and grains are interlocked tightly. When the depth increases, the white clear halite changes gradually to pale, medium and dark honey halite. Milky white halite occurs as small grains ranging from 0.1 to 0.3 centimeters in diameter. Milky white halite, smoky dark halite and anhydrite stringers increase in volume along the depth. Near the bottom contact with the Lower Clastic, the Middle Salt appears in moderate to dark orange color or may be interbedded with smoky dark halite bands. Accessory minerals include locally occurrences of sylvite and carnallite.

3) The Lower Salt is the bottommost salt bed overlying basal anhydrite and overlain by strata of potash zone. Below the potash zone is glassy white, clear or translucent, colorless or white halite with little or no impurity of carbonaceous matter. The grain size is usually 0.2 to 0.5 centimeters diameter but locally occurs as large crystals in the range of 2.0 to 5.0 centimeters diameter. When the depth increases, the color of halite changes gradually from white to grey with 1% to 2% of milky white halite grain. The density of anhydrite stringers and contents of milky white halite increase with depth. Locally, anhydrite stringers are mostly fractured appearing like breccias. There are a lot of differences in the bottom part, anhydrite stringers or fragments are less than the uppermost. Gypsum spots and clusters are decreased and consisted mostly of smoky dark halite interbedded with transparent halite to the base of salt bed.

Results from the above rock identification allow correlating the salt units between adjacent boreholes, and hence permit construction of three-dimentional view of the salt units. The results of the salt identification in each borehole are shown in Appendix A.

3.3 Three-dimensional rock sequences

The depth of Sandstone/Siltstone or Khok Kruat Formation, Upper Salt, Middle Salt, and Lower Salt units and thickness of Lower Salt between boreholes are estimated using the above results combined with seismic data, where available. Tables 3.1 through 3.5 show the salt thickness and depth that identify from borehole logging data (Japakasetr and Suwanich, 1982, 1984).

Table 3.1 Thickness of rock beds with 3 salt layers in Khorat Basin (RS-1.2, RS-1.4, RS-1.5, RS-2.0, RS-2.1, RS-2.4, RS-2.11, RS-2.14, RS-2.17, RS-2.18, PQ-1, PQ-4, KB-9, KB-10, KB-11, KB-15, KB-16, KB-17, KB-18, KB-19, KB-20, KB-21, KB-24, KB-25, KB-30, KB-31, KB-34, KB-35, K-021, K-025, K-036, K-040, K-041, K-056, K-076, K-079, and K-095).

Units	Thickness (meters)	Depth (meters)
Top Soil	0 – 18.3	0
Upper Clastic	23.47 – 316.08	0 – 18.36
Upper Salt	0.91 – 52.78	15.24 – 320.65
Middle Clastic	8.97 – 83.72	21.94 – 346.05
Middle Salt	3.45 – 121.73	53.59 – 361.87
Lower Clastic	0 – 61.35	71.42 – 469.94
Lower Salt	5.25 – 167.34	86.9 – 528.52

Table 3.2 Thickness of rock beds with 2 salt layers in Khorat Basin, Upper Salt and Middle Salt (K-062, K-090, and K-096).

Units	Thickness (meters)	Depth (meters)
Top Soil	2.0 – 34.0	0
Upper Clastic	256.37 – 650.0	2.0 – 34.0
Upper Salt	25.3 – 60.06	258.37 – 684.0
Middle Clastic	23.9 – 30.2	309.26 – 744.06
Middle Salt	16.04 – 56.99	339.46 – 774.18
Lower Clastic	0 – 16.53	355.5 – 821.82
Lower Salt	–	355.5 – 838.35

Table 3.3 Thickness of rock beds with 2 salt layers in Khorat Basin, Middle Salt and Lower Salt (RS-1.1, RS-1.6, RS-2.2, RS-2.3, RS-2.6, RS-2.7, RS-2.10, RS-2.12, RS-2.13, RS-2.15, RS-2.19, RS-2.22, RS-2.23, PQ-3, PQ-5, PQ-6, PQ-9, KB-1, KB-2, KB-3, KB-4, KB-5, KB-6, KB-7, KB-8, KB-12, KB-14, KB-22, KB-23, KB-26, KB-27, KB-28, KB-29, KB-32, KB-33, K-010, K-014, K-017, K-018, K-022, K-024, K-030, K-034, K-042, K-053, K-059, K-068, K-072, K-075, K-078, K-084, K-087, K-092, K-093, K-098, K-100, K-102, K-104, K-107, K-108, K-114, K-115, K-117, and K-118).

Units	Thickness (meters)	Depth (meters)
Top Soil	0 – 140.21	0
Upper Clastic	0 – 222.15	0 – 140.21
Upper Salt	–	–
Middle Clastic	0 – 117.04	0 – 225.15
Middle Salt	0.17 – 171.95	26.52 – 275.83
Lower Clastic	0 – 185.05	31.93 – 387.37
Lower Salt	1.37 – 521.06	51.88 – 416.19

Table 3.4 Thickness of rock beds with only 1 salt layers in Khorat Basin, Middle Salt (K-069, K-071, K-082 and K-099).

Units	Thickness (meters)	Depth (meters)
Top Soil	2.56 – 30.48	0
Upper Clastic	0 – 5.54	0 – 30.48
Upper Salt	–	–
Middle Clastic	0 – 41.15	2.56 – 34.19
Middle Salt	45.41 – 316.33	50.04 – 71.63
Lower Clastic	0 – 417.8	97.52 – 350.52
Lower Salt	–	–

Table 3.5 Thickness of rock beds with only 1 salt layers in Khorat Basin, Lower Salt

(RS-1.3, RS-2.5, RS-2.8, RS-2.9, RS-2.16, RS-2.20, RS-2.21, PQ-2, PQ-7,

PQ-11, KB-13, K-011, K-012, K-013, K-015, K-016, K-019, K-020, K-023,

K-026, K-027, K-028, K-029, K-031, K-033, K-037, K-047, K-049, K-050,

K-051, K-052, K-054, K-057, K-058, K-060, K-061, K-063, K-064, K-066,

K-070, K-073, K-077, K-080, K-089, K-091, K-094, K-097, K-101, K-103,

K-105, K-106, K-109, K-110, K-111, K-112, K-113, and K-116).

Units	Thickness (meters)	Depth (meters)
Top Soil	0 – 167.64	0
Upper Clastic	0 – 687.02	0 – 167.64
Upper Salt	–	–
Middle Clastic	0 – 84.21	3.0 – 167.64
Middle Salt	–	–
Lower Clastic	0 – 132.89	9.38 – 325.34
Lower Salt	4.378 – 1,080.0	33.53 – 517.52

From the results, the Upper Salt is the thinnest unit, with maximum thickness less than 60 meters. The depth of the top surface is at about 40 meters (measured from ground surface). The Middle Salt is less than 233 meters thick with the top located at 120 meters depth. The Lower Salt and potash zone is about 4 to 1,080 meters thick. The top of this unit is located at about 200 meters depth.

In this study, borehole logs number PQ-8, PQ-10, K-032, K-035, K-038, K-039, K-065, K-067, K-074, and K-088 show no salt unit. The depth reported here is estimated by using data from borehole logs (Japakasetr and Suwanich, 1982, 1984). In the area between the borehole logs, the salt distribution determination is assisted by

using data from geologic map of Thailand, topographic map of Thailand (Royal Thai Survey Department, 1991), geologic cross-sections, and seismic surveys in the northeast of Thailand (Wongsawat et al., 1992; Sattayarak and Polachan, 1990), mineral potential map of Thailand, and geological and mineral occurrence map of Lao People's Democratic Republic (Department of Geology and Mines, 1990). The results show that thickness of the Lower Salt unit in Khorat Basin tends to be uniform and continuous, particularly at distance from the edges of the basin. For the preliminary study to be performed here the Lower Salt unit is suitable and therefore concentrated for solution mine design and reserve estimation.

The distribution of boreholes in Khorat Basin is irregular. For example, it is dense in Bamnet Narong district, Chaiyaphum province, but in most areas they are far apart especially in the central of the basin. Geologic cross-sections and seismic surveys are available in the central of the basin.

The depth distribution of Khok Kruat Formation shows that the study area is a basin. The bottom is deeper than 1,250 meters below mean sea level. The basin center is at Borabue, Muang and Wapi Prathum districts, Maha Sarakham province. The top is about 150 to 250 meters high from mean sea level at the edge of the basin (Figure 3.2).

Top of the Lower Salt unit has rough surface. The bottom is deeper than 700 meters below mean sea level in the middle of the basin at Borabue district, Maha Sarakham province. The top is located at about 100 meters above mean sea level at the west in Manjakiri district of Khon Kaen province, Khon Sawan, Muang, and Chaturat districts of Chaiyaphum province (Figure 3.3).

The thickness of the Lower Salt is estimated from the difference between contours of the Lower Salt and the Khok Kruat Formation. The thickness contour of the Lower Salt in Khorat Basin is show in Figure 3.4. The Lower Salt contains several salt domes. The largest dome is more than 1,000 meters thick near the center of the basin (near by borehole No.K-089) at Borabue district, Maha Sarakham province. The thickness decreases as approaching the edge of the basin, e.g. at Manjakiri district, Khon Kaen province and Khon Sawan district, Chaiyaphum province. It exhibits the decrease thickness of the unit toward the edge of the basin.

The thickness of the Middle Salt is estimated from the difference between contours of the Middle Salt and the Lower Clastic units. The Middle Salt can found in some area which completely erode and disappear near the edge of the basin.

The thickness of the Upper Salt is estimated from the difference between contours of the Upper Salt and the Upper Clastic/Sedimentary rocks above Upper Salt that contained very thin salt bed. The Upper Salt is occurred as a small area which decreases and disappears close to the edge of the basin.

CHAPTER IV

CAVERN DESIGN

4.1 Objectives

The objective of this chapter is to design the solution cavern in the Lower Salt member of the Khorat Basin. The design methodology and process suggested by Bieniawski and Bieniawski (1994) are used here. Described in this chapter are the step-by-step design process and the required data input and design principles used in each step.

4.2 Design process

Bieniawski and Bieniawski (1994) have proposed ten engineering design stages to develop solution cavern in rock salt. The principles of these design stages have been derived of the systematic approach proposed by Pahl and Beitz (1984) and the heuristics approach proposed by Koen (1984). In accordance with the Bieniawski and Bieniawski's design stages, the design of solution caverns in the Khorat Basin can be described as follows.

4.2.1 Stage 1: Statements of the problem

The performance objectives identified for this study are 1) to economically extract the halite from the Lower Salt member of the Maha Sarakham formation in the Khorat basin, 2) to maintain mechanical stability of the geologic

formation in the mining area, and 3) to apply the lastest technology and state-of-the-art approach to accomplish this task.

4.2.2 Stage 2: Identification of functional requirements and constraints

In this stage, a set of specific functional requirements (FR's) and all constraints (C's) are identified. The functional requirements are independent, i.e. the independent principle (Bieniawski and Bieniawski, 1994) is applied. To extract the salt from underground, three FR's are defined as follows.

FR#1: To provide access connecting between the salt unit and the surface facility.

FR#2: To extract or excavate the in-situ salt.

FR#3: To transport the salt from underground and collect it on the ground surface.

Suh (1990) classifies the engineer's constraints into two categories: system constraints and input constraints. For salt mining, the system constraints are identified here as follows.

C#1: Maintaining the mechanical stability of the underground area where the salt is excavated.

C#2: Minimizing and preventing any damage to the engineering structures, topography, farmlands, and surface and underground water resources.

The input constraints for salt mining include the availability of the local resources normally identified in terms of budget, equipment, and personal experience. These types of constraint are considered in the design evaluation.

4.2.3 Stage 3: Collection of information

The design proposed here is made such that the design solutions (results) are traceable to the site-specific conditions as much as possible. As a result, all geological information relevant to the Lower Salt member and the nearby rock units in the Maha Sarakham Formation are considered in the design analysis. The analysis also considers the mechanical, chemical, and physical properties of the rocks specifically, the depth, thickness, and orientation of the Lower Salt member in the Khorat Basin as complied and described in Chapter three are considered in the design. Jandakaew (2003), Klayvimut (2003), Pueakphum (2003), and Wetchasat (2002) studied experimentally the Maha Sarakham salt properties and published the results. These properties will be used here. Since the test results are limited, only few locations have been test, it is assumed here that these published salt properties represent all the in-situ salt properties in the Maha Sarakham Formation. It is recognized that such assumption may not be strictly valid, as the natural salt has intrinsic variability in terms of its physical, chemical, mineralogical, and mechanical properties. Nevertheless, the design process used here will employ the minimum uncertainty principle (Bieniawski, 1992) and hence minimizes the effect of the intrinsic variability of the salt. Table 4.1 summarizes the physical and mechanical properties of the Maha Sarakham salt.

4.2.4 Stage 4: Concept formulation

The concept formulation in this stage basically involves determination of alternative design solutions. It is recognized that there are more than one method (solution) to mine or excavate the salt from its in-situ condition. These include, for example, solution mining and dry mining. The scope in this research is concentrated

Table 4.1 Summary of the physical and mechanical properties of some rock units in Maha Sarakham Formation (modified from Pueakphum, 2003; Jandakaew, 2003, and Fuenkajorn, 2006).

Rock Types	Sandstone/Siltstone	Middle Salt	Lower Salt
Density (g/cc)	2.61	2.24	2.14
Uniaxial Compressive Strength (MPa)	32.5$\pm$5.2	27.5$\pm$4.2	31.0$\pm$2.3
Brazilian Tensile Strength (MPa)	0.19$\pm$0.04	1.98$\pm$0.33	1.62$\pm$0.22
Point Load Index (MPa)			
L/D=1.0	1.45$\pm$0.24	-	-
L/D=0.5	2.56$\pm$0.95	-	-
L/D=2.5-3		1.0	0.6$\pm$0.05
Cohesion (MPa)	-	6.0	-
Friction Angle (Degree)	-	56	-
Viscoplastic Parameter (GPa·Day)	-	4.82$\pm$6.39	1.62$\pm$1.06
Poisson's Ratio	0.32$\pm$0.08	0.37$\pm$0.05	0.35$\pm$0.03
Elastic Modulus (GPa)	-	24.7$\pm$5.4	25.2$\pm$9.5

the study on the solution mining method. The solution mining method is, therefore, selected as only design solution here. Pros and cons of this method as compared with the dry mining method will be described later in stage 8 (design optimization). The design components (DC's) or parameters for the solution mining method are identified here to satisfy the functional requirements (FR's) defined earlier.

DC#1: A vertical borehole drilled to the depth of the salt to be mined to provide an access between surface and underground.

DC#2: Use fresh water to dissolve the underground salt to obtain brine and collect it inside the cavern.

DC#3: Use system of steel tubes (string) to pump the brine from underground to surface facility.

DC#4: Use spherical shaped cavern to collect the brine underground.

DC#5: Use sufficient thickness of salt (cavern) roof with sufficient ratio of spacing-to-diameter (S/D) to minimize the movement of overburden formations and the subsidence of the ground surface.

The DC's#1, #2, and #3 are proposed to satisfy the FR's#1, #2, and #3. And DC's#4 and #5 satisfy the constraints C's#1 and #2. All the design components proposed here are based on the simplicity principle given by Bieniawski (1992).

4.2.5 Stage 5: Analysis of solution components

This stage specifically involves calculation and computation to obtain the safe, practical, and economic design parameters. The main parameters include diameter and depth of the salt cavern, salt roof, salt floor, and spacing between adjacent caverns. In this research, series of numerical analysis is performed. A time-dependent finite element code (GEO: Fuenkajorn and Serata (1992, 1994); Serata and Fuenkajorn (1992a); Stormont and Fuenkajorn (1994)) is used to determine the stress, strain, and closure of the salt around the cavern and to predict the time-dependent subsidence over the cavern ground. This approach satisfies the state-of-the-art principle given by Bieniawski (1992). Detailed methods and results are described in Appendix B. Previous case studies and guideline (Fuenkajorn, 2002) of the salt solution mining are also used where applicable.

The geologic information compiled in Chapter three are reclassified in terms of depth and thickness of the Lower Salt member where the solution caverns

will be excavated. This classification is made to simplify and minimize the sets of design parameters. The results indicate that there are 11 depth ranges to be designed with the maximum at 400 meters and minimum at 200 meters. The minimum thickness of the Lower Salt should be 150 meters. Under the above limitations, the results of the finite element analysis can be summarized in terms of the design parameters as follows.

Cavern shape : sphere

Cavern diameter = 60 meters

Minimum cavern depth (at roof top) = 200 meters

Maximum cavern depth (at roof top) = 400 meters

Minimum salt roof = 60 meters

Minimum salt floor = 30 meters

Minimum cavern spacing = 240 meters

The single well system proposed by Fuenkajorn (2002) for the Maha Sarakham salt are adopted here. The single well system (an array of individual caverns) is appropriate for the relatively thin and shallow salt beds because the salt roof and inter-cavern pillars can provide mechanical support to the excavations (Jeramic, 1994). This research therefore concentrates effort on the design of the single well system. Figure 4.1 shows a schematic of the essentials of the single well method. In this system, a hole is drilled into the salt, cased and cemented back to the surface. A string of tubing is run inside the cemented casing into the salt. Dissolution is made by injecting fresh water into either the annulus of the casing or into the suspended tubing. When the fresh water is injected in the annulus and brine produced through the suspended tubing. This is called direct (forward) circulation. When the fresh water is injected in
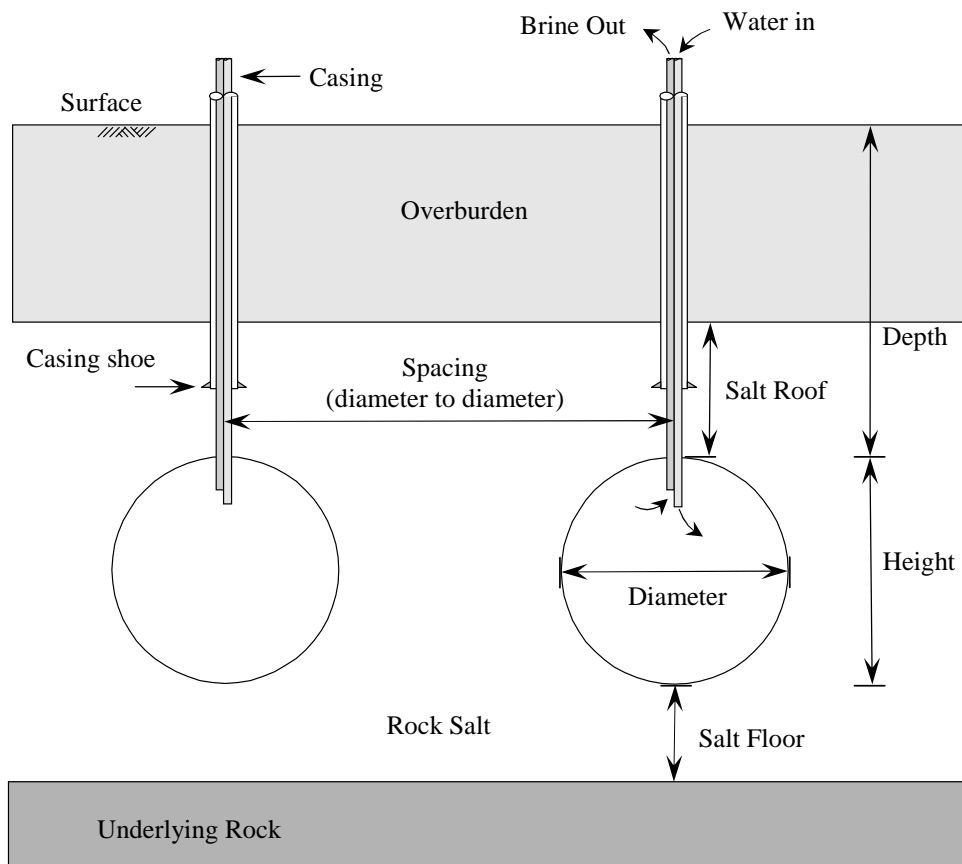
Figure 4.1 Design parameters for solution-mined caverns (modified from

Fuenkajorn, 2002).

the hanging pipe and brine produced in the annulus. It is called reverse circulation. Figure 4.2 illustrates the difference between direct and reverse circulation. A second annular hanging string can be installed. The technique is called intermediate injection because the injection point can be varied throughout the height of the cavern. Figure 4.2 illustrates the various combinations possible between direct and reverse circulation using intermediate injection.
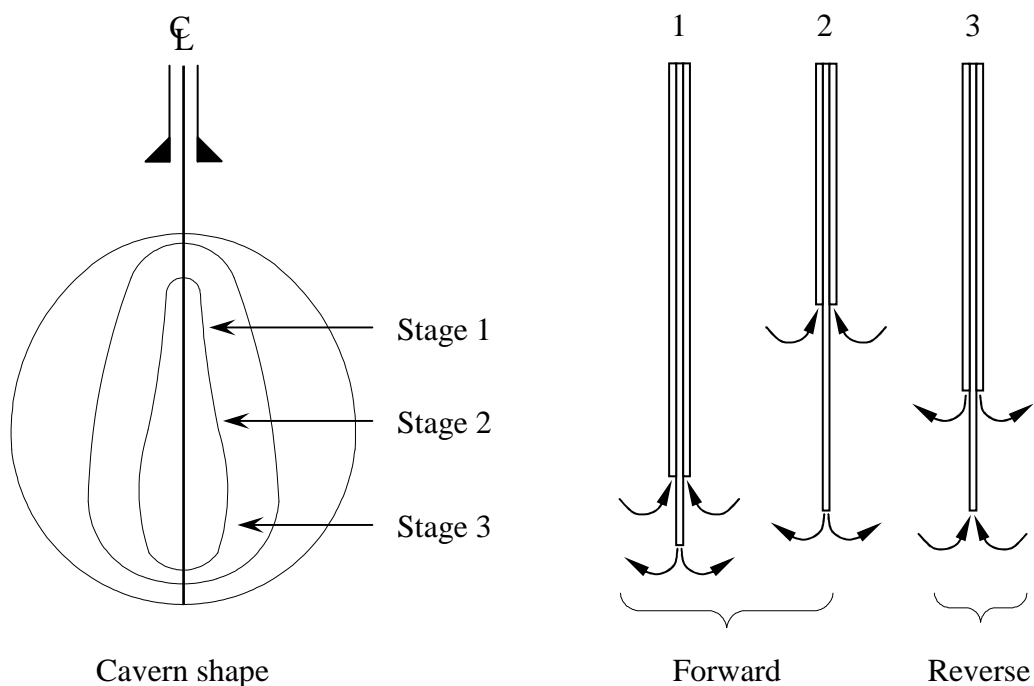
Figure 4.2 Cavern development stages. (modified from Fuenkajorn, 2002).

A method has been developed to increase the shape control for the solution caverns. The method became known as the "Trump method". It uses a gas or hydrocarbon "pad" placed at the top of the cavern to prevent the upper portion of salt from dissolving. Without the pad at the top, the lower density fresh water tends to dissolve along the roof. As the solution become more concentrated, it gains density and flows down the walls of the cavern. Figure 4.3a shows the shape of cavern that results from such process, often called a "morning glory". Dissolution continues upward until the top of the salt is reached. After the roof is reached, dissolving continues horizontally away from the well. This results in a large and unstable roof and leads to low recovery. The intermediate injection technique along with the use of isolating blanket of air or hydrocarbons could control where the most active

dissolution taken place. Figure 4.3b shows the shape of cavern controlled by using the

Trump method. The Trump method became the standard method of salt solution

mining in the U.S. since 1940.
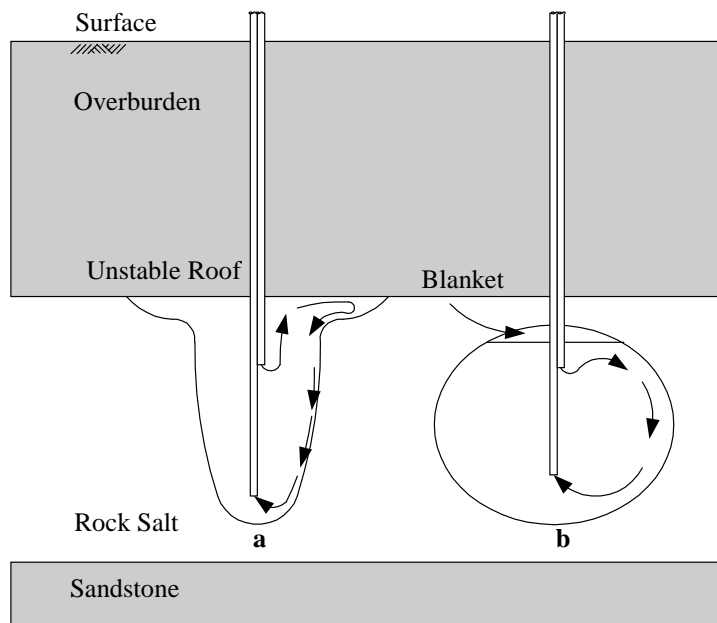
Figure 4.3 Effect of blanket on cavern shape (a) without pad (b) with pad (modified

from Fuenkajorn, 2002).

4.2.6 Stage 6: Synthesis of design components

This stage involves the formulation of the individual design components

to obtain a complete system of the design solution. Here, the synthesis will basically

include the formulation of the access borehole (with all tubing installed) and the

cavern in the salt. The location of the casing shoe and the depths of salt roof are

determined.

Prior to mining the salt, a well (production hole) must be developed. The size of the final or production casing depends on the capacity desired for the well. All other casing is then sized to accommodate it. The numbers of other casings that have to be run depend on the local requirements and subsurface conditions. Well design for solution mining is more closely allied with oil well design than it is with wells used for other types of in-situ extraction, like groundwater, uranium or copper. Figure 4.4 shows typical well construction that might be used. Typically, the diameter of the final cemented string might be 8 5/8 inches and the diameter of the first casing might be 15-18 inches. Characteristics and functions for each casing are described below.

Casing One (Conductor Casing): In many locations the first feet of drilling are in unconsolidated sediments that are not self-supporting therefore an initial casing is driven to the top of the first competent zone. This casing is called the conductor casing. Alternately, if the sediments will stay open for a short time, the hole can be drilled to bedrock and casing set and cemented back to the surface. Occasionally, the sediments are thin or stable enough to permit drilling further into the formation. In this case, the first casing is omitted. The conductor casing also protects shallow fresh water aquifers.

Casing Two (Surface Casing): Casing two is often called the surface casing. The primary function is to protect or seal off any potable or fresh water aquifers. Cement is usually returned all the way back to the surface. Cementing is usually accomplished by injecting the cement into the casing, chasing it out the bottom and up the annulus with drilling mud.

Surface

(1) Conductor casing:
24″ Casing, 26″ Hole

Overburden

(2) Surface casing:
20″ Casing

(3) Production casing:
17″ Casing

Rock Salt

(4) Optional (for lost
circulation): 13″ Casing

(5) Liner: 10″ Casing

(6) Tubing: 7″ Casing

Cavern
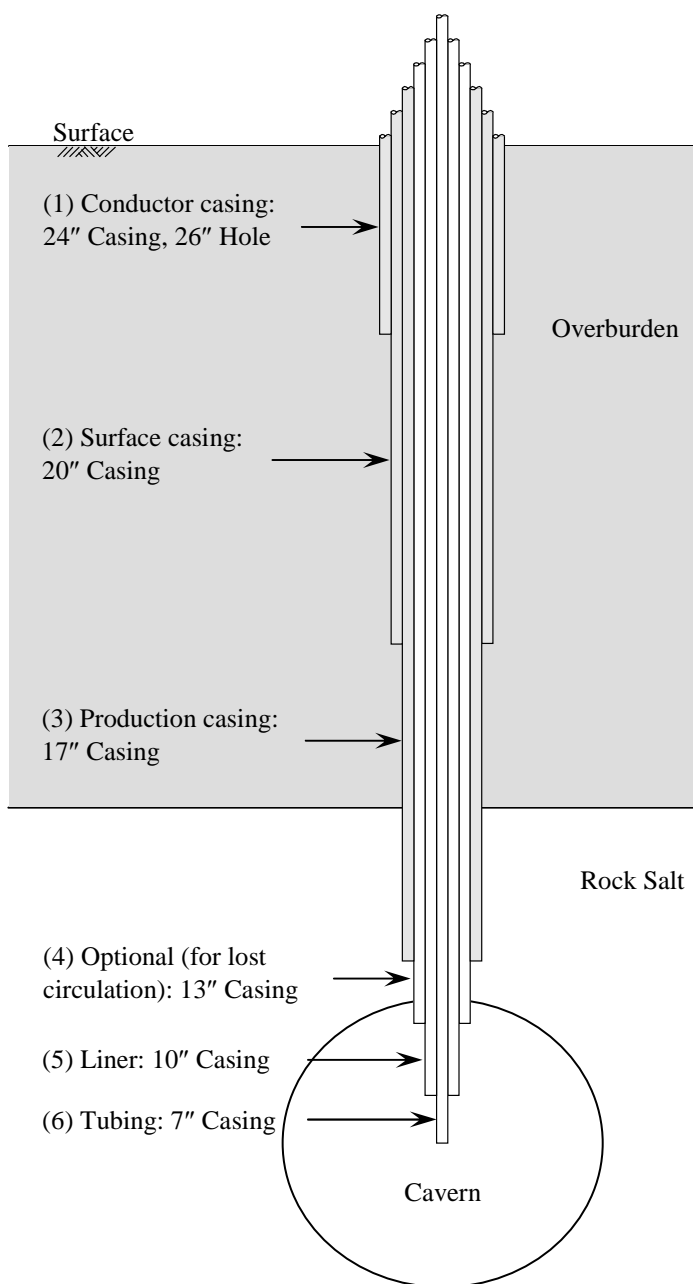
Figure 4.4 Typical casing scheme in solution mining (modified from

Fuenkajorn, 2002).

Casing Three (Intermediate Casing): If highly porous or fractured formations are encountered, a condition known as lost circulation may occur. That may be suggested by that the drilling mud used to move cuttings up the hole did not return to the surface. In the event of lost circulation, an additional casing, called intermediate casing, may be required to isolate further drilling from these zones.

Casing Four (Production Casing): If intermediate casing is set to seal off lost circulation, a second intermediate casing, called the production casing, is usually set into the salt. In bedded salt this casing is set commonly 5 to 15 feet into the salt. In a very thick salt bed the casing may be set more than 100 feet. into the salt. If the intermediate casing is successfully set into the salt, it becomes the production casing and further casing would be unnecessary. This casing is cemented to the surface.

Casing Five (Liner): Casing is often hung inside the production casing. It provides an annulus for access between casing and tubing. A liner may be used for intermediate injection or pad control. Liners are not cemented.

Casing Six (Tubing): One or two hanging tubes are the last casings hung in the well. These casings are the conduits used during dissolution for the injection and recovery of fluids. They are not cemented and are suspended from the well head. Occasionally, these suspended casings may be raised or lowered to control shape of the cavern.

4.2.7 Stage 7: Design evaluation

This stage involve the development of procedure and performance requirements of the proposed design. The field methods commonly-used to test the system prior to mining are proposed here. Pressure testing is a common method of

testing for casing leaks. It is accomplished by setting a packer at the bottom of the hole and pressurizing the casing with air or water. The well is then shut in and the pressure drop over a period of time is measured. Advantages are that it is a relatively cheap and effective way of testing for leaks. Disadvantages are that it provides no information on the location or type of leak, should one be identified.

Caliper logs of casings can be run quickly and for nominal cost. Calipers can identify and locate large casing failures. However, small or vertical imperfections may go unnoticed. An impression packer is an inflatable packer with a compliant element that takes on the characteristics of the casing when inflated. Impression packers can be used to map the exact nature of failed well casing. Impressions can be taken only over about 6 feet. Television logs (TV) can be used to visually inspect the condition of well casing provided the water is relatively clear. TV logs are relatively expensive to run and yield very limited information if the water is cloudy. TV logs are also depth limited.

Radiation logs use emitted gamma rays to measure the density and thickness of the casing, the formation and the cement around a hole. A properly interpreted log can locate corroded casing the gaps between the cement, formation and casing where fluid might travel. Sonic logs use sound pulse transit time to measure density around the hold in the same manner as radiation logs. Both types are relatively expensive and subject to interpretative error. The methods proposed in this stage have considered the state-of-the-art principle and the constructability principle as suggested by Bieniawski (1992).

4.2.8 Stage 8: Design optimization

This research is concentrated only on the solution mining method. The design optimization or comparison with other methods are therefore not applicable here. Salt can be mined in two different ways, as a solution mining and dry mining. In solution mining, fresh water is injected through a pipe into deep shafts that end in the salt beds and salty water (brine) is drawn upward. The salt or salty brine found in shallow wells can simply be pumped to the surface. In dry mining, the salt is mined in large underground caverns, much like one would mine coal or iron ore. An advantage of solution mining is that surface facilities and disturbances are significantly less extensive than open pit or other surface mining methods. The cost of bringing salts to the surface by solution mining is cheaper than extracting ore by conventional mining, but this advantage is offset by greater costs in the refining process, which uses natural gas to evaporate the water. The comparison between solution mining and dry mining shows in Table 4.2.

Table 4.2 Comparison methods to mined the salt (modified from Klayvimut, 2003).

Criterias	Solution Mining	Dry Salt Mining
Construction cost	Less than 500 MM Baht	3,000 – 5,000 MM Baht
Stability monitoring	Indirect measurement	Direct measurement
Backfill installation	Simple and low cost	Complicated and high cost
Mechanical stability	Fairly high	high
Surface subsidence	Low	Relatively high
Construction duration	Short	Long

4.2.9 Stage 9: Design recommendation

The design recommendations involve the preparation of a comprehensive design report. It includes the geological conditions, site characteristics, performance requirements, reserve, and subsidence impact on the engineering structures and natural process directly above and near by the solution mined area. The methods and results of analysis and synthesis for the design are provided. Figure 4.5 shows the results of the design for various salt depths and thickness. The design parameters are show in Figure 4.6.

4.2.10 Stage 10: Implementation

The last stage of the design process is the implementation of the solution cavern design. Due to the uncertainty of the geological characteristics and complexity of the salt unit, the lastest design may be adjusted or modified to satisfy the actual geological conditions and to minimizing environmental impact.

4.3 Discussions

The design results show that the cavern should be spherical shaped with a nominal diameter of 60 meters. The salt bed that can host the caverns should have a minimum thickness of 150 meters with the depths of the top salt between 140 meters and 340 meters. Based on this design the minimum salt roof and salt floor thickness should be 60 meters and 30 meters. The spacing (center-to-center) between adjacent caverns should be 240 meters. From these design configurations, the results of finite element analyses indicate that the cavern will remain mechanically stable. The maximum surface subsidence for the shallowest cavern field (D200) is about 2.92 centimeters, and for the deepest cavern field (D400) is about 6.45 centimeters.
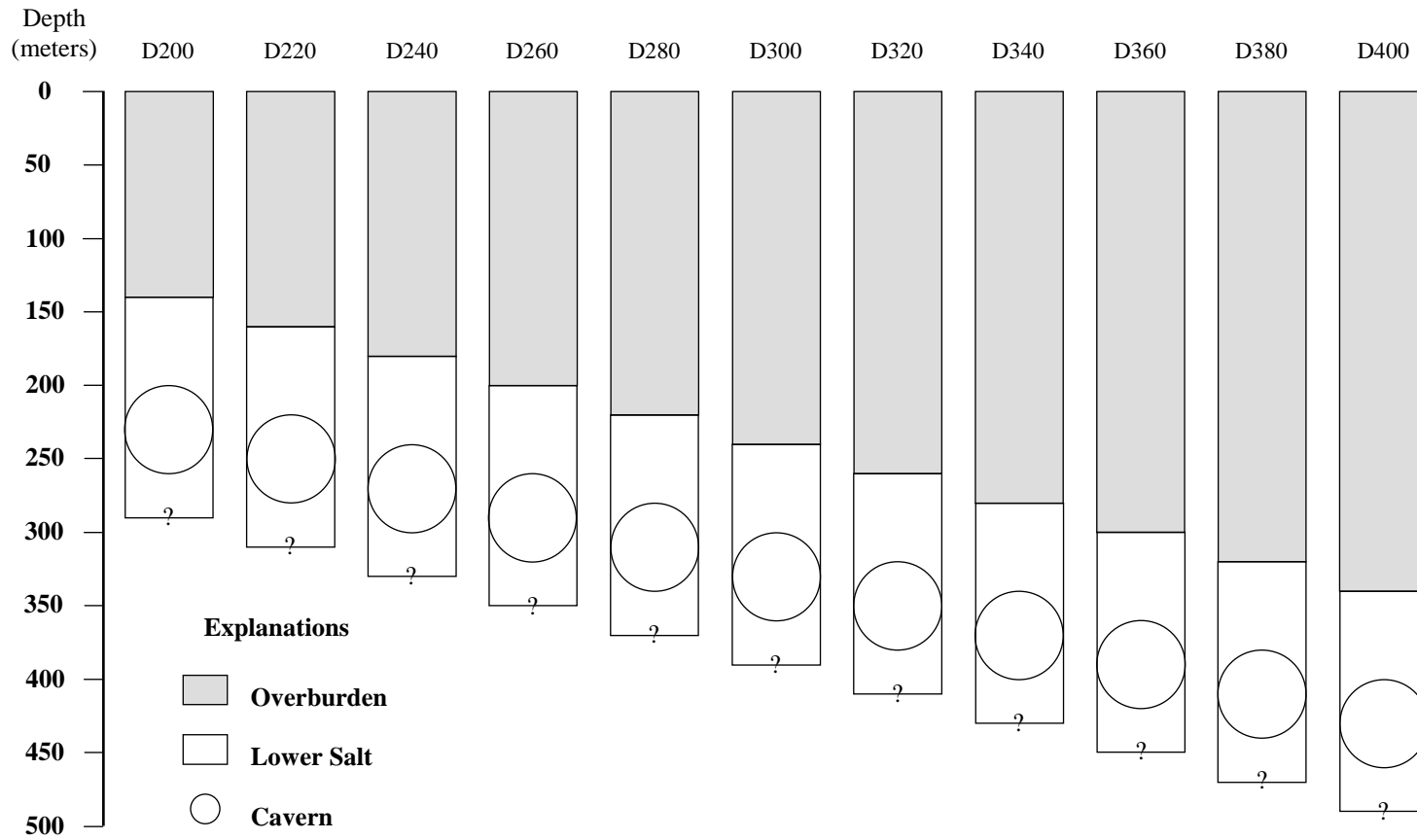
Figure 4.5 The results of the design for various depths and thickness.
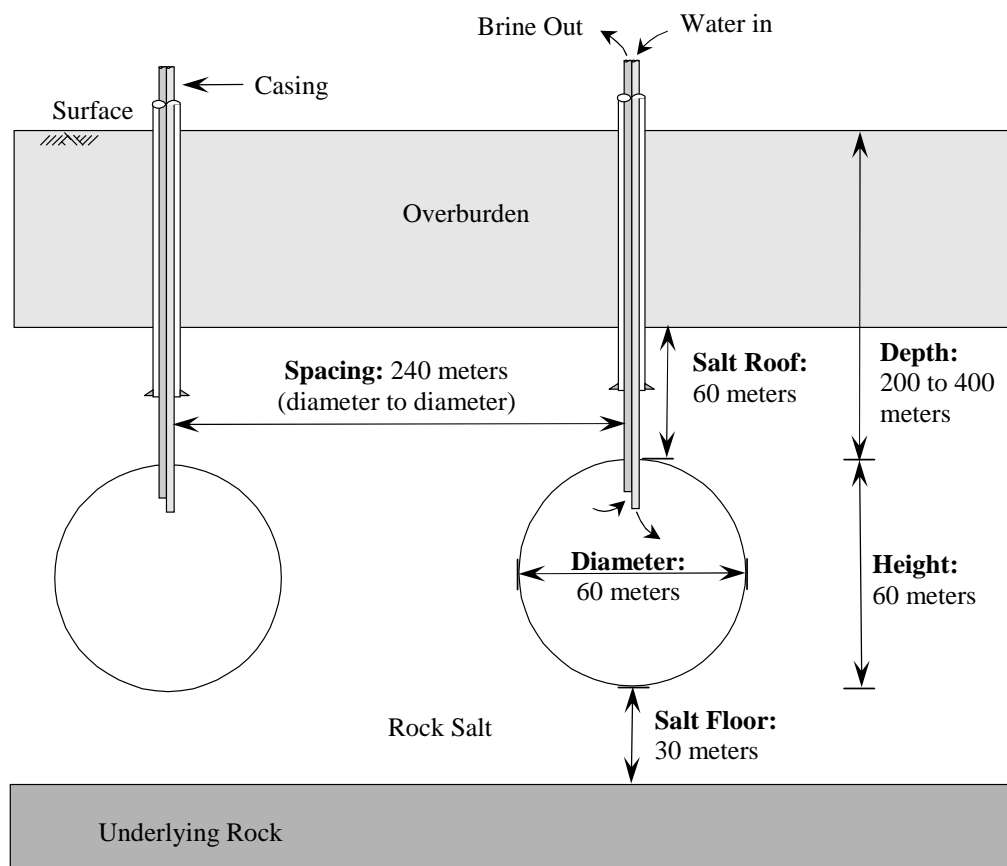
Figure 4.6 The design results for solution mined caverns.

The subsidence increases during the first year and remains constant through the 50 years. The maximum vertical closure for the shallowest cavern field is 9.84 centimeters (0.33%) and maximum horizontal closure is about 3.71 centimeters. The maximum vertical closure for the deepest cavern field is 20.08 centimeters and maximum horizontal closure is about 7.47 centimeters. Based on the international industrial practice standards, these magnitudes of the subsidence will not have adverse impact on the engineering structures and the surrounding environment.

CHAPTER V

SALT RESERVE ESTIMATION

5.1 Objectives

The objective of this chapter is to perform the salt reserve estimation for the Lower Salt member for the suitable mining area in the Khorat Basin. The computation considers the proposed solution mining method, thickness, and depth of the Lower Salt member, land uses, and water resources.

5.2 Determination of suitable area

Lower Salt reserve is estimated as a function of area, depth and thickness that are suitable for solution mining. Such area excludes the local communities, highways, all access roads, surface water bodies, reservoirs, rivers, and streams (based on Royal Thai Survey Department, 1991). The proposed solution mining cavern shape is sphere with 60 meters diameter. The salt roof is 60 meters, and salt floor is 30 meters. The cavern spacing from center-to-center is 240 meters. The minimum thickness of the Lower Salt to be mined is defined here as 150 meters with the depths of the salt top between 140 meters and 340 meters. Figure 5.1 shows areas that are suitable in terms of the Lower Salt depth and thickness. These areas are located in the central part of the Khorat Basin, and cover Nakhon Ratchasima, Khon Kaen, Maha Sarakham, Roi Et, and Kalasin provinces. The outer areas are not suitable for

solution mining in terms of depths or thickness or both. The salt in the inner of the basin is too deep; the depth of the salt top is greater than 340 meters.

5.3 Salt reserve calculation

The evaluation of the salt reserve is based on several parameters. The density of the Lower Salt is 2.16 gram/cubic centimeter with 97% halite and 3% impurity (Suwanich, 1986). The salt left in each cavern in form of saturated brine after mining is 0.31 gram/cubic centimeter (Fuenkajorn, 2006). The suitable areas are classified into 11 models, in terms of depths of salt top (Figure 5.2).

The tonnage of salt each cavern is calculated as follows.

Cavern volume	$=$	$(4/3)\pi \times$ (cavern radius)^3
Weight of salt	$=$	salt density $\times$ cavern volume
Weight of pure salt (halite)	$=$	(% halite/100) $\times$ weight of salt
Inclusions (insoluble materials)	$=$	{(100 – (% halite)/100} $\times$ weight of salt
Salt left in cavern	$=$	brine density $\times$ cavern volume
Total salt reserve	$=$	weight of pure salt – salt left in cavern

There are approximately 17 caverns in one square kilometer (one cavern used 5.76×10^{-2} square kilometers). Table 5.1 shows the summary of salt reserve calculation in the Khorat basin. The total suitable area is about 5,741 square kilometers. In each cavern, the pure salt is about 236,960 tons with inclusions and insoluble materials about 7,329 tons. The total salt reserve from each cavern is about 201,900 tons. There will be salt left inside the cavern (in form of saturated brine) about 35,060 tons. In the entire basin, total pure salt is about 24 billion tons. The salt reserve from the Lower Salt mined by solutioning is about 20 billion tons (Table 5.1).

Table 5.1 Summary of salt reserved in Khorat Basin.

Cavern Diameter:	60 meters
Cavern Volume	113,097.3 cubic meters
Weight of Salt in 1 Cavern:	244,290.2 tons
Weight of Pure Salt in the 1 Cavern:	236,961.5 tons
Inclusions and Insoluble Materials in 1 Cavern:	7,328.7 tons
Salt Left in 1 Cavern:	35,060.2 tons
Salt Reserve in 1 Cavern:	201,901.4 tons
In 1 Square kilometer	17.4 caverns
Salt Reserve in 1 Square kilometer	3,505,210 tons

Models	Depth of Salt Top (m)	Minable Areas (km^2)	Number of Caverns	Total Salt Reserves (tons)
D200	140	1,833	31,823	6,425,090,263
D220	160	1,303	22,622	4,567,317,301
D240	180	1,286	22,326	4,507,728,357
D260	200	175	3,038	613,415,601
D280	220	177	3,073	620,426,065
D300	240	171	2,969	599,394,673
D320	260	188	3,264	658,983,617
D340	280	202	3,507	708,056,865
D360	300	120	2,083	420,627,840
D380	320	153	2,656	536,300,497
D400	340	133	2,309	466,195,856
Total		**5,741**	**99,670**	**20,122,249,027**

It should be noted that the total reserve calculated here is much less than those computed by Suwanich (1986). This is because Suwanich (1986) considers all salt members (Upper Salt, Middle Salt, and Lower Salt) and all areas in the basin, and hence his calculated reserve is considered as "geologic reserve" for the Maha Sarakham salt. The reserve calculated in this research is considered as "mining reserve".

CHAPTER VI

CONCLUSIONS AND RECOMMENDATIONS

6.1 Conclusions

The objective of this research is to determine the reserve of the Lower Salt in the Maha Sarakham Formation of the Khorat Basin with respect to the solution mining application. The mining reserve is estimated along with the corresponding cavern locations and depths.

Results of the geological study on the published information indicate that depths of the top of the Lower Salt member range from 100 meters to -700 meters from mean sea level. Thickness of the Lower Salt varies from 1 meter to over 1,000 meters. Salt domes in the central part represent the greatest thickness. The design results suggest that the cavern should be spherical shaped with a nominal diameter of 60 meters. The salt bed that can host the caverns should have a minimum thickness of 150 meters with the depths of the salt top between 140 meters and 340 meters. The minimum salt roof and salt floor thickness should be 60 meters and 30 meters. The spacing (center-to-center) between adjacent caverns should be 240 meters. The design configurations show the results of finite element analyses indicate that the cavern will remain mechanically stable for at least the next 50 years. The maximum surface subsidence for the shallowest cavern field is about 2.92 centimeters, and for the deepest cavern field is about 6.45 centimeters. Based on the international industrial

standard practice, these magnitudes of the subsidence will not have adverse effect on the engineering structures and on the surrounding environment.

The total suitable mining area is defined here as the total area that has appropriate depth and thickness of the Lower Salt, and excludes the areas that are occupied by local communities, highways, all access roads, surface water bodies, reservoirs, rivers, and streams. The total suitable area is about 5,741 square kilometers. The total inferred reserve of the salt (halite) from the Lower Salt member for the entire basin mined by solutioning is about 20 billion tons per square kilometer. Each cavern can produce halite about 201,901 tons, considered the purity of rock salt = 97%. After solutioning is complete, there will be halite left in each cavern in form of saturated brine about 35,060 tons with insoluble material about 7,329 tons.

6.2 Recommendations

The main difficulty encountered during the evaluation of the thickness and depth of the Lower Salt member is the inadequacy of the published geologic data. Even though over two hundreds of exploration boreholes were drilled, they were concentrated in small areas, such as Bamnet Narong district, Chaiyaphum province. In addition most of the existing geophysical data produced as part of oil exploration have not been published, and hence can not be used in this research. The results of reserve estimation obtained here are therefore classified as "inferred level". Additional core drilling exploration is required if one wants to determine the reserve in any area at a higher confidence level.

The configurations of the designed caverns (diameter, depth, spacing, etc.) are relatively conservative as they are derived from conservative set of material properties

of the salt and surrounding rock formations. The design can be more refined by performing additional mechanical testing on the salt in any area of interest.

The areas that suitable for the development of solution mining are determined based on the current topographic map scale 1:50,000 (Royal Thai Survey Department, 1991). These maps may lack some important detailed information that have been recently developed. The scope of this research does not cover the site survey and field investigation. The accuracy of the determined suitable areas is therefore made at best to the nearest 1 square kilometer. Prior to developing an actual mining operation in any area, detailed site mapping and survey are necessary to ensure that the selected areas are environmentally feasible and do not conflict with the local and state regulations.

REFERENCES

Adagic, M. (1988). Basic information of salt cavern solution in salt deposits. **Mineral and Metallurgical Journal.** 39(4): 1-7.

Allemandou, X. and Dusseault, M.B. (1996). Procedures for cyclic creep testing of salt rock, results and discussions. In **Proceedings of the Third Conference on the Mechanical Behavior of Salt** (pp. 207-218). Clausthal-Zellerfeld, Germany: Trans Tech Publications.

Anon, (1975). **Subsidence Engineer's Handbook.** National Coal Board Mining Department. London. 111p.

Aubertin, M. (1996). On the physical origin and modeling of kinematics and isotropic hardening of salt. In **Proceedings of the Third Conference on the Mechanical Behavior of Salt** (pp. 1-18). Clausthal-Zellerfeld, Germany: Trans Tech Publications.

Aubertin, M., Gill, D.E., and Ladanyi, B. (1991). A unified visco-plastic model for the inelastic flow of alkali halides. **Mechanics of Materials.** 11: 63-82.

Aubertin, M., Gill, D.E., and Ladanyi, B. (1992). Modeling the transient inelastic flow of rocksalt. In **the Seventh Symposuim on Salt** (vol. 1, pp. 93-104). Amsterdam: Elsevier Science Publishers.

Aubertin, M., Sgaoula, J., and Gill, D.E. (1992). A damage model for rock salt: Application to tertiary creep. In **the Seventh Symposuim on Salt** (vol. 1, pp. 117-125). Amsterdam: Elsevier Science Publishers.

Aubertin, M., Sgaoula, J., and Gill, D.E. (1993). Constitutive modeling of rock salt: Basic considerations for semi-brittle behavior. In **Proceedings of the Fourth International Symposuim on Plasticity and It's Current Applications** (pp. 92). Baltimore.

Aubertin, M., Sgaoulla, J., Servant, S., Julien, M.R., Gill, D.E., and Ladanyi, B. (1998). An up-to-date version of SUVIC-D for modeling the behavior of salt. In **Proceedings of the Fourth Conference on the Mechanical Behavior of Salt** (pp. 205-220). Clausthal-Zellerfeld, Germany: Trans Tech Publications.

Aubertin, M., Julien M.R., Servant, S., and Gill, D.E. (1999). A rate-dependent model for the ductile behavior of salt rocks. **Canadian Geotechnical Journal.** 36(4): 660-674.

Barber, D.J. (1990). Regimes of plastic deformation processes and microstructure. In **An Overview, Deformation Processes in Minerals, Ceramics and Rocks** (pp. 138-178). Unwin Hyman.

Barbour, A.K. (1994). Mining non-ferous metals. In R. E. Hester and R. M. Harrison (eds). **Mining and its Environmental Impact** (pp. 1-16). Cambridge: The Royal Society of Chemistry.

Beddoes, R.J. (1994). **Analyses of bench test area at Goderich mine**. Internal Report for Sifto Canada Inc., Prepared by Golder Associate Ltd., Calgary, AB, Canada.

Berest, P. (1993). General report: Mining and civil engineering in rock salt. In **Proceedings of the Seventh International Congress on Rock Mechanics.** (Vol. 3, pp. 1847-1851). A.A. Balkema: Rotterdam.

Berest, P., Brouard, B., and Durup, G. (1998). Behavior of sealed solution-mined caverns. In **Proceedings of the Fourth Conference on the Mechanical Behavior of Salt** (pp. 511-524). Clausthal-Zellerfeld, Germany: Trans Tech Publications.

Bieniawski, P.W. and Bieniawski, Z.T. (1994). **Design principles and methodology applied to solution mined salt caverns.** Presented at the 1994 Spring Meeting in Houston, April 24-27. Texas.

Bieniawski, Z.T. (1992). Design Methodology in Rock Engineering. A.A. Balkema: Rotterdam.

Billiotte, J., Guen, L.C., Deveughele, M and Brulhet, J. (1996). On laboratory measurements of porosity and permeability of salt rocks (Bressa basis-France). In **Proceedings of the Third Conference on the Mechanical Behavior of Salt** (pp. 221-230). Clausthal-Zellerfeld, Germany: Trans Tech Publications.

Blanquer-Fernandez, S. (1991). **Interaction des cavities souterraines**. Project de Fin d'Etudes, EPF, LMS. French Ecole: Polytechnique.

Boontongloan, C. (2000). **Engineering Pproperties of The Evaporitic and Clastic Rocks of Maha Sarakam Formation, Sakon Nakhon Evaporite Basin**. M.S. thesis, Asian Institute of Technology, Thailand.

Booth, J. (2000). Petroleum geology of the Khorat Plateau Basin N.E. Thailand. Amerada Hess Thailand.

Brauner, G. (1973). Subsidence due to Underground Mining. 2 parts, US Bureau of Mines, Information Circular 8571, 56 pp., and 8572, 53 pp.

Brodsky, N.S., Hansen, F.D., and Pfeifle, T.W. (1998). Properties of dynamically compacted WIPP salt. In **Proceedings of the Fourth Conference on the Mechanical Behavior of Salt** (pp. 303-316). Clausthal-Zellerfeld, Germany: Trans Tech Publications.

Broek, W.M. G.T. and Heilbron, H.C. (1997). Influence of salt behavior on the retrievability of radioactive waste. In **Proceedings of the Fourth Conference on the Mechanical Behavior of Salt** (pp. 561-573). Clausthal-Zellerfeld, Germany: Trans Tech Publications.

Callahan, G.D., Loken, M.C., Hurtads, L.D., and Hansen, F.D. (1998). Evaluation of constitutive models for crushed salt. In **Proceedings of the Fourth Conference on the Mechanical Behavior of Salt** (pp. 317-330). Clausthal-Zellerfeld, Germany: Trans Tech Publications.

Canter L.W. (1996). **Environmental Impact Assessment** (2nd). Singapore: McGraw-Hill, Inc.

Carter, N.L., Horseman, S.T., Russell, J.E., and Handin, J. (1993). Rheology of rocksalt. **Structural Geology** 15(10): 1257-1272.

Chokski, A.H. and Langdon, T.G. (1991). Characteristics of creep deformation in ceramics. **Materails Science and Technology** 7: 577-584.

Cleach, J.M.L., Ghazali, A., Deveughele, H., and Brulhet, J. (1996). Experimental study of the role of humidity on the thermomechanical behavior of various halitic rocks. In **Proceedings of the Third Conference on the Mechanical Behavior of Salt** (pp. 231-236). Clausthal-Zellerfeld, Germany: Trans Tech Publications.

Cristescu, N.D. (1993a). Constitutive equation for rock salt and mining applications. In **Proceedings of the Seventh Symposium on Salt** (Vol. 1, pp. 105-115). Amsterdam: Elserier Science Publishers.

Cristescu, N.D. (1993b). Constitutive equation for rock salt and mining applications. In **Proceedings of the Seventh Symposium on Salt** (Vol. 1, pp. 105-115). Amsterdam: Elsevier Science Publishers.

Cristescu, N.D. (1993c). A general constitutive equation for transient and stationary creep of rock salt. **International Journal of Rock Mechanics, Sciences and Geomechanics Abstracts.** 30 (2): 125-140.

Cristescu, N. (1996). Stability of large underground caverns in rock salt. In **Proceedings of the Second North American Rock Mechanics Symposium on Rock Mechanics Tools and Technique** (NARNS'96, pp. 101-107). A.A. Balkema: Rotterdam.

Cristescu, N. and Hunsche, U. (1996). A comprehensive constitutive equation for rock salt determination and application. In **Proceedings of the Third Conference on the Mechanical Behavior of Salt** (pp. 191-205). Clausthal-Zellerfeld, Germany: Trans Tech Publications.

Crotogino, F., Mohmeyer, W.U., and Scharf, R. (2001). **Huntorf CAES: More than 20 years of successful operation**. Presented at the 2001 Spring Meeting, Orlando, Florida, USA.

Department of Geology and Mines (DGM). (1990). **Geological and Mineral Occurrence Map scale 1:1,000,000**. Vientiane, Lao: Ministry of Industry and Handicraft.

Department of Mineral Resources. (1983). **Geologic Map of Thailand, scale 1:500,000.** Bangkok, Thailand: Geological Survey Division.

Department of Mineral Resources. (1997). **Mineral potential Map of Thailand, scale 1:2,500,000.** Bangkok, Thailand: Geological Survey Division.

DeVries, K.L. and Callahan, G.D. (1998). WIPP panel simulations with gas generation. In **Proceedings of the Fourth Conference on the Mechanical Behavior of Salt** (pp. 537-550). Clausthal-Zellerfeld, Germany: Trans Tech Publications.

Diane, E.L., Alex, D., Craig, F.B., and Nancy, A.S. (1999). Digital geologic map production and database development in the central publications group of the geologic division. In **Digital Mapping Techniques on Workshop Proceedings of the US Geological Survey.** United State: US Geological Survey.

Dreyer, W. (1982). **Underground storage in salt deposits and other non-hard rocks** (pp. 147-176). New York: Halsted Press.

Dreyer, W.E. (1981). Crude oil storage caverns in a system of salt caverns. In **Proceedings of the First Conference on Mechanics behaviour of Salt** (pp. 629-660). Penn. State University. Clausthal-Zellerfeld, Germany: Trans Techn. Publ.

Durup, G. and Xu, J. (1996). Comparative study of certain constitutive laws used to describe the rheological deformation of salts. In **Proceedings of the Third Conference on the Mechanical Behavior of Salt** (pp. 75-84). Clausthal-Zellerfeld, Germany: Trans Tech Publications.

Dusseault, M.B. and Fordham, C.J. (1993). Time-dependent behavior of rocks. **Comprehensive Rock Engineering Principles, Practice and Project: Rock Testing and Site Characterization** (Vol. 3, pp. 119-149). London, Pergamon.

Eduardo, J., Menezes, Q.D., and Ngugen-Minh, D. (1996). **Numerical modeling of leached cavern fields using mixed BEM-FEM method** (pp. 417-426). ESRI (1992-1996). **Introduction to Arcview GIS, Redlands.** California: Environmental Systems Research Institute.

Farmer, I.W. and Gilbert, M.J. (1984). Time dependent strength reduction of rock salt. In **Proceedings of the First Conference on the Mechanical Behavior of Salt** (pp. 3-18). Clausthal-Zellerfeld, Germany: Trans Tech Publications.

Fokker, P.A. (1995). **The Behavior of Salt and Salt Caverns.** Ph. D. Thesis, Delft University of Technology.

Fokker, P.A. (1998). The micro-mechanics of creep in rock salt. In **Proceedings of the Fourth Conference on the Mechanical Behavior of Salt** (pp. 49-61). Clausthal-Zellerfeld, Germany: Trans Tech Publications.

Fokker, P.A. and Kenter, C.J. (1994). The micro mechanical description of rock salt plasticity. In **Eurock'94** (pp. 705-713). A.A. Balkema: Rotterdam.

Franssen, R.C.M. (1998). Mechanical anisotropy of synthetic polycrystalline rock salt. In **Proceedings of the Fourth Conference on the Mechanical Behavior of Salt** (pp. 63-75). Clausthal-Zellerfeld, Germany: Trans Tech Publications.

Franssen, R.C.M. and Spiers, C.J. (1990). Deformation of polycrystalline salt in compression and in shear at 250-350°C. **Deformation Mechanisms, Rheology and Tectonics, Geological Society Special Publication** 45: 201-213.

Frayne, M.A. (1996). Four cases study in salt rock: Determination of material parameters for numerical modeling. In **Proceedings of the Third Conference on the Mechanical Behavior of Salt** (pp. 471-482). Clausthal-Zellerfeld, Germany: Trans Tech Publications.

Frayne, M.A. (1998). The goderich salt mine: past, present & future. In **Proceedings of the Fourth Conference on the Mechanical Behavior of Salt** (pp. 445-458). Clausthal-Zellerfeld, Germany: Trans Tech Publications.

Fuenkajorn, K. (2000). Geohydrological integrity of storage caverns in salt formation. In **Symposium on Mineral, Energy, and Water Resources of Thailand: Towards the year 2000**, October 28-29, 1999 (pp. 270-275). Bangkok, Thailand.

Fuenkajorn, K. (2002). Design guideline for salt solution mining in Thailand. **Research and Development Journal of the Engineering Institute of Thailand**, 13(1): 1-8.

Fuenkajorn, K. (2006). **Study on Mechanical Properties of rock salt from Siamsubmanee, Nakhon Ratchasima**. Institute of Engineering, Suranaree University of Technology. (Unpublished manuscript).

Fuenkajorn, K. and Daemen, J.J.K. (1992a). Borehole Sealing. In **Compressed-Air Energy Storage Proceedings of the Second International Conference**, Electric Power Research Institute, July 7-9, San Francisco, CA (pp. 5.1-5.21).

Fuenkajorn, K. and Daemen, J.J.K. (1992b). Drilling-Induced Fractures in Borehole Walls. **Journal of Petroleum Technology** 44(2): 210-216.

Fuenkajorn, K. and Serata, S. (1992). Geohydrological integrity of CAES in rock salt. In **Proceedings of the Second International Conference on Compressed-Air Energy Storage** (pp. 4.1-4.21). San Francisco, CA: Electric Power Research Institute.

Fuenkajorn, K. and Serata, S. (1994). Dilation-induced permeability increase around caverns in rock salt. In **Proceedings of the First North American Rock Mechanics Symposium** (pp. 648-656). A.A. Balkema: Rotterdam.

Fuenkajorn, K. and Daemen, J.J.K. (1996). **Sealing of Boreholes and Underground Excavations in Rock**. London: Chapman & Hall.

Fuenkajorn, K. and Stormont, J.C. (1997). **Geomechanics and geohydrological issues in mine sealing**. Presentation at the SME Annual Meeting, February 24-27, 1997, Denver, Colorado.

Fuenkajorn, K. and Daemen, J.J.K. (1988). **Boreholes closure in salt**. Technical Report Prepared for The U.S. Nuclear Regulatory Commission. Report No. NUREG/CR-5243 RW. University of Arizona.

Fuenkajorn, K and Wetchasat, K. (2001). **Rock salt formations as potential nuclear waste repository**. The 6th Mining, Metallurgical, and Petroleum Engineering Conference: Resources Exploration and Utilization for Sustainable Environment (REUSE). Bangkok, Thailand.

Gronefeld, P., Yoshida, Y., Koder, M., and Bunpapong, T. (1993). Four years of brine production by solution mining: The Pimai project in Thailand. In **Proceedings of the Seventh Symposium on Salt** (Vol. I, pp. 315-320). Amsterdam: Elsevier Science Publishers B.V.

Hamami, M., Tijani, S.M., and Vouille, G. (1996). A methodology for the identification of rock salt behavior using multi-step creep tests. In **Proceedings of the Third Conference on the Mechanical Behavior of Salt** (pp. 53-66). Clausthal-Zellerfeld, Germany: Trans Tech Publications.

Hampel, A., Hunsche, U., Weidinger, P., and Blum, W. (1998). Description of the creep of rock salt with the composite model – II: Steady-state creep. In **Proceedings of the Forth Conference on the Mechanical Behavior of Salt** (pp. 287-300). Montreal, Canada: Trans Tech Publications.

Hansen, F.D. Mellegard, K.D., and Senseny, P.E. (1984). Elasticity and strength of ten natural rock salts. In **Proceedings of the First Conference on the Mechanical Behavior of Salt**, The Pennsylvania State University, November 9-11, 1981 (pp. 71-83). Clausthal-Zellerfeld, Federal Republic of Germany: Trans Tech Publications.

Hardy, H.R. (1996). Application of the Kaiser effect for the evaluation of in-situ stress in salt. In **Proceedings of the Third Conference on the Mechanical Behavior of Salt**, (pp. 85-100). Clausthal-Zellerfeld, Germany: Trans Tech Publications.

Harold, W.B. (1999). Arcview a geologic mapping tool, geological survey, In **Digital Mapping Techniques on Workshop Proceedings of the U.S. Geological Survey.** United State: US Geological Survey.

Harrington, T.J., Chabannes, C.R., and Shukla, K. (1991). Rock mechanics consolidations in the WIPP room design. In **Proceedings of the First Conference on the Mechanical Behavior of Rock Salt** (pp. 681-696). Clausthal-Zellerfeld, Germany: Trans Tech Publications.

Harris, Jr., R.W. (1977). **Palynological analyses of outcrop and well samples from the Khorat Basin, Central Thailand.** Bangkok, Thailand: Mineral Fuels Division.

Hartman, H.L. (1987). **Introductory Mining Engineering.** New York: John Wiley & Sons.

Hartman, H.L. (1992). SME Mining Engineering Handbook. Society for Mining Metallurgy and Exploration, Inc. Littleton, Colorado. 2260 p.

Heusermann, S., Kob, S., and Sonnke, J. (1998). Analysis of stress measurements in the TSDE at the Asse salt mine. In **Proceedings of the Fourth Conference on the Mechanical Behavior of Salt** (pp. 17-29). Clausthal-Zellerfeld, Germany: Trans Tech Publications.

Hite, R.J. and Japakasetr, T. (1979). Potash deposits of the Khorat Plateau, Thailand and Laos (pp. 448-458). In Economic Geology Division (ed). Bangkok, Thailand: Department of Mineral Resources, Economic Geology Division.

Hoek, E. and Brown, E.T. (1980). Empirical strength criterion for rock masses. **Journal of Geotechnical Engineering Division**, A.S.C.E., pp. 1013-1035 (Vol. 106, No. GT9).

Honecker, A. and Wulf, A. (1988). The FE-system ANSALT a dedicated tool for rock and salt-mechanics. In **Proceedings of the Second Conference on the Mechanical Behavior of Rock Salt** (pp. 4409-4520). Clausthal-Zellerfeld, Germany: Trans Tech Publications.

Hunsche, U.E. (1993). Failure behaviour of rock salt around underground cavities. In **Proceedings of the Seventh Symposium on Salt** (Vol. I, pp. 59-65). Amsterdam: Elsevier Science Publishers B.V.

Hunsche, U. and Schulze, O. (1996). Effect of humidity and confining pressure on creep of rock salt. In **Mechanical Behavior of salt, Series on Soil and Rock Mechanics** (Vol. 20, pp. 237-248). Trans Tech Publications.

INTERA. (1982). **VISCO Maual**, Technical Report, Houston, TX.

Itasca. (1992). **User manual for FLAC–fast Langrangian analysis of continua, version 3.0**. Itasca Consulting Group Inc., Minneapolis, MN.

Itasca. (1994). **User manual for FLAC–fast Langrangian analysis of continua in 3 dimensions, version 1.0**. Itasca Consulting Group Inc., Minneapolis, MN.

Jaeger, J.C. and Cook, N.G.W. (1979). **Fundamentals of Rock Mechanics.** London: Chapman and Hall.

Jandakaew, M. (2003). **Experimental assessment of stress path effects on rock salt deformation**, M.S. thesis, Suranaree University of Technology, Thailand.

Japakasetr, T. (1985). Review on rock salt and potash exploration in Northeast Thailand. In **Conference on Geology and Mineral Resources Development of the Northeast of Thailand** (pp. 135-147). Khon Kaen, Thailand: Khon Kaen University.

Japakasetr, T. (1992). Thailand's mineral potential and investment opportunity In **National Conference on Geologic Resources of Thailand: Potential for Future Development** (pp. 641-652). Bangkok, Thailand: Department of Mineral Resources.

Japakasetr, T. and Workman, D.R. (1981). Evaporite deposits of Northeast Thailand. In **Proceedings of the Circum-Pacific Conference** (pp. 179-187). New York: American Associate of Petroleum Geologist.

Japakasetr, T. and Suwanich, P. (1982). Potash and rock salt in Thailand (pp. A1-A252). In Economic Geology Division (ed). Bangkok, Thailand: Department of Mineral Resources, Economic Geology Division.

Japakasetr, T. and Suwanich, P. (1983). Potash and Rock Salt in Thailand: Appendix F Showing Locations Maps of Drilled Holes. Nonmetallic Minerals Bulletin No.2, Economic Geology Division, Department of Mineral Resources. Bangkok, Thailand.

Japakasetr, T. and Suwanich, P. (1984). Potash and Rock Salt in Thailand: Appendix C Core log of Bamnet Narong Area. Nonmetallic Minerals Bulletin No.2, Economic Geology Division, Department of Mineral Resources. Bangkok, Thailand.

Japan International Cooperation Agency. (1981). **Evaluation study report for ASEAN rock salt-soda ash project in the kingdom of Thailand**. Tokyo, Japan.

Jeremic, M.L. (1964). Dry mining and solution mining of rock salt in Romania. **Mineral and Metallurgical Journal.** 12: 265-274.

Jeremic, M.L. (1964). Exploitation methods for rock salt deposits in Poland. **Min. & Metall. Bulletin (Belgrade)**. 2: 264-274. Yugoslav.

Jeremic, M.L. (1975). Subsidence problems caused by solution mining of the rock salt deposits. In **Proceedings of the Tenth Canadian Rock Mechanics Sysmposium** (Vol. I, pp. 203-223). Kingston, Department of Mining Engineering, Queen's University.

Jeremic, M.L. (1985). Mining subsidence. In Strata mechanics in coal mining (pp. 343-353). A.A. Balkema: Rotterdam/Boston.

Jeremic, M.L. (1994). **Rock Mechanics in Salt Mining**. A.A. Balkema: Rotterdam. 530 pp.

Jin, J. and Cristescu, N.D. (1998). An elastic/visco-plastic model for transient creep of rock salt. **International Journal of Plasticity** 14 (1-3): 85.

Jin, J., Cristescu, N.D., and Hunche, U. (1998). A new elastic/visco-plastic model for rock salt. In **Proceedings of the Fourth Conference on the Mechanical Behavior of Salt** (pp. 249-262). Clausthal-Zellerfeld, Germany: Trans Tech Publications.

Julien, M.R., Foerch, R., Aubertin, M., and Cailletaud, G. (1998). Some aspects of numerical implementation of SUVIC-D. In **Proceedings of the Fourth Conference on the Mechanical Behavior of Salt** (pp. 389-402). Clausthal-Zellerfeld, Germany: Trans Tech Publications.

Junmaha, S. (1987). Salt dome in Khorat Plateau (in Thai). In **Proceedings of the Conference on Geology and Mineral Resources of Thailand** (pp. 301-317). Bangkok, Thailand: Department of Mineral Resources.

Katz, D.L. and Lady, E.R. (1976). **Compressed Air Storage for Electric Power Generation**. Department of Energy, Pacific Northwest: Richland, Washington.

Klayvimut, K. (2003). **Mechanical performance of underground excavation in rock salt formation for nuclear waste repository in northeastern Thaialnd**, M.S. thesis, Suranaree University of Technology, Thailand.

Knowles, M.K., Borns, D., Fredrich, J., Holcomb, D., Price, R., and Zeuch, D. (1998). Testing the disturbed zone aroud a rigid inclusion in salt. In **Proceedings of the Fourth Conference on the Mechanical Behavior of Salt** (pp. 175-188). Clausthal-Zellerfeld, Germany: Trans Tech Publications.

Koen, B.V. (1984). Toward a definition of the engineering method. **Engineering Education 75**, pp. 150-155.

Korthaus, E. (1996). Measurement of crushed salt consolidation under hydrostatic and deviatoric stress conditions. **In Proceedings of the Third Conference on the Mechanical Behavior of Salt** (pp. 311-322). Clausthal-Zellerfeld, Germany: Trans Tech Publications.

Korthaus, E. (1998). Consolidation and deviatoric deformation behavior of dry crushed salt at temperatures up to 150°C. **In Proceedings of the Fourth Conference on the Mechanical Behavior of Salt** (pp. 365-378). Clausthal-Zellerfeld, Germany: Trans Tech Publications.

Leigh, A.R., David, S.B., and Graham, A.M. (1998). Ore reserve calculation. In R.E. Gertsch and R.L. Bullock (eds.). **Techniques in underground mining** (pp. 3-44). Colorado.

Lux, K.H. and Schmidt, T. (1996). Optimizing underground gas storage operations in salt caverns, with special reference to the rock mechanics and thermodynamics involved. In **Proceedings of the Third Conference on the Mechanical Behavior of Salt** (pp. 445-458). Clausthal-Zellerfeld, Germany: Trans Tech Publications.

Maranate, S. (1982). **Paleomagnetism of the Khorat Group in Northeast Thailand** (71 p.). In Geology Survey Division (ed). Bangkok, Thailand, Geology Survey Division: Department of Mineral Resources.

Massier, D. (1996). Rate type constitutive equations with applications to the calculus of the stress state and of the displacement field around cavities in rock salt. In **Proceedings of the Third Conference on the Mechanical Behavior of Salt** (pp. 545-558). Clausthal-Zellerfeld, Germany: Trans Tech Publications.

Munson, D.E. and Wawersik, W. R. (1993). Constitutive modeling of salt behavior-State of the technology. In **Proceedings of the Seventh International Congess on Rock Mechanics** (vol. 3, pp. 1797-1810). A.A. Balkema: Rotterdam.

Nguyen-Minh, D. and Quintanilha de Menezes, E. (1996). Incompressible numerical modeling for long term convergence evaluation of underground works in salt. In **Proceedings of the Third Conference on the Mechanical Behavior of Salt** (pp. 523-531). Clausthal-Zellerfeld, Germany: Trans Tech Publications.

Nguyen-Minh, D., Braham, S., and Durup, J.G. (1996). Modelling subsidence of the tersanne underground gas storage field. In **Proceedings of the Third Conference on the Mechanical Behavior of Salt** (pp. 405-416). Clausthal-Zellerfeld, Germany: Trans Tech Publications.

Nigbor, M.T. (1982). State of the art of solution mining for salt, potash and soda ash. In **Research Project Report No. 82-0002-SMRI.** Illinois, U.S.A: Solution Mining Research Institute.

Ong, V., Unrau, J., Jones, J. Coode, A., and Mackintosh, D. (1998). Triaxial creep testing of saskatchewan potash samples. In **Proceedings of the Fourth Conference on the Mechanical Behavior of Salt** (pp. 469-480). Clausthal-Zellerfeld, Germany: Trans Tech Publications.

Pahl, G. and Beitz, W. (1984). **Engineering Design**. Springer-Verlag, New York. 450 pp.

Pueakphum, D. (2003). **Compressed-air energy storage in rock salt of the Maha Sarakham formation**, M.S. thesis, Suranaree University of Technology, Thailand.

Pudewills, A. and Hornberger, K. (1996). A unified visco-plastic model for rock salt. In **Proceedings of the Third Conference on the Mechanical Behavior of Salt** (pp. 45-52). Clausthal-Zellerfeld, Germany: Trans Tech Publications.

Pudewills, A., Muller-Hoeppe, N. and Papp, R. (1995). Thermal and thermo-mechanical analyses for disposal in drifts of a repository in rock salt. **Nuclear Technology** 1: 79-88.

Radomski, A. (1981). Exploitation of the salt deposits by borehole solution mining. **Gornictwo.** 8: 38-49.

Raj, S.V. and Pharr, G.M. (1992). Effect of temperature on the formation of creep substructure in sodium chloride single crystal. **American Ceramic Society** 75 (2): 347-352.

Ratigan, J.L. (1991). **Ground subsidence at Mont Belvieu**. Presented at the 1991 SMRI meeting, Atlanta, Georgia, April 29. Texas.

Ratigan, J.L. and Vogt, T.J. (1993). LPG storage at Mont Belvieu, Texas: A case history. **SPE Advanced Technologies Series** 1 (1): 204-211.

Rattanajarurak, P. (1990). **Formation of The Potash Deposits, Khorat Plateau, Thailand.** M.S. Thesis, School of Mine, Kensington, Australia.

Rokahr, R. and Staudtmeister, K. (1996). The assessment of the stability of a cavern field in bedded salt with the help of the new hannover dimensioning concept. In **Proceedings of the Third Conference on the Mechanical Behavior of Salt** (pp. 533-544). Clausthal-Zellerfeld, Germany: Trans Tech Publications.

Rolnik, H. (1988). High-level waste repository in rock salt: Suitable rheological forms. In **Proceedings of the Second Conference on the Mechanical Behavior of Rock Salt** (pp. 625-643). Clausthal-Zellerfeld, Germany:Trans Tech Publications.

Roskill. (2001). **The economics of salt** [On-line]. Available: http://www.roskill. com/report/salt.html

Royal Thai Survey Department. (1991). **Topographic map scale 1:50,000**: map sheets 5238, 5239, 5240, 5337, 5338, 5339, 5340, 5437, 5438, 5439, 5440, 5441, 5442, 5443, 5537, 5538, 5539, 5540, 5541, 5542, 5543, 5637, 5638, 5639, 5640, 5641, 5642, 5643, 5737, 5738, 5739, 5740, 5741, 5742, 5743, 5837, 5838, 5839, 5840, 5841, 5842, 5937, 5938, 5939, 5940, 5941, 5942, 6037, 6038, 6039, 6040, 6041, 6137, 6138, 6139 and 6140. Bangkok, Thailand: Royal Thai Survey Department.

Salakshana, D., Quast, P., Lux, K.H., and Rokahr, R.B. (1987). Salt production by solution mining, the Pimai project. In **Proceedings of the Ninths Southeast Asian Geotechnical Conference.** Bangkok, Thailand.

Salamon, M.D.G., (1963/644). Elastic Analysis of displacements and stress induced by mining of seam or reef deposit. Journal of south African Institute of Mining and Metallurgy. Vol.64. pp. 128-149, 197-218, 468-500.

Salzer, K. and Scheriner, W. (1998). Long-term safety of salt mines in flat bedding. In **Proceedings of the Fourth Conference on the Mechanical Behavior of Salt** (pp. 481-494). Clausthal-Zellerfeld, Germany: Trans Tech Publications.

Sattayarak, N. (1983). Review of continental Mesozoic stratigraphy of Thailand. In **Proceedings of the Stratigraphic correlation of Thailand and Malaysia** (Vol. 1, pp. 127-148). Bangkok, Thailand: Geological Society.

Sattayarak, N. (1985). Review on geology of Khorat Plateau. In **Conference on Geology and Mineral Resources Development of the Northeast, Thailand** (pp. 23-30). Khon Kaen, Thailand: Khon Kaen University.

Sattayarak, N. and Polachan, S. (1990). Rock salt beneath the Khorat Plateau (in Thai). In **Proceedings of the Conference on Geology and Mineral Resources of Thailand** (pp. 1-14). Bangkok, Thailand: Department of Mineral Resources.

Sattayarak, N., Chaisilboon, B., Srikulwong, S., Charusirisawat, R., Mahattanachai, T., and Chantong, W. (1998). Tectonic evolution and basin development of the Northeast Thailand. In **Seminar on Mesozoic redbeds in the Northeastern Thailand** (pp. 43-58). Bangkok, Thailand: Department of Mineral Resources.

Schneefub, J., Droste, J. (1996). **Thermo-mechanical effects in back-filled drifts.** In **Proceedings of the Third Conference on the Mechanical Behavior of Salt** (pp. 373-380). Clausthal-Zellerfeld, Germany: Trans Tech Publications.

Senseny, P.E. and Fussum, A.F. (1998). Testing to estimate the Munson-Dawson parameters. In **Proceedings of the Fourth Conference on the Mechanical Behavior of Salt** (pp. 263-272). Clausthal-Zellerfeld, Germany: Trans Tech Publications.

Senseny, P.E., Handin, J.W., Hansen, F.D., and Russell, J.E. (1992). Mechanical behavior of rock salt: phenomenology and micro-mechanisms. **International Journal of Rock Mechanics and Mining Sciences** 29 (4): 363-378.

Serata, S. and Fuenkajorn, K. (1991). **Permeability studies in relation to stress state and cavern design, Phase I**. Research Project Report, Contract 1-91, prepared for Solution Mining Research Institute by Serata Geomechanics, Inc., Richmond, CA.

Serata, S. and Fuenkajorn, K. (1992a). Formulation of a constitutive equation for salt. In **Proceedings of the Seventh International Symposium on Salt** (Vol. 1, pp. 483-488). Amsterdam: Eisevier Science.

Serata, S. and Fuenkajorn, K. (1992b). **Finite element program "GEO" for modeling brittle-ductile deterioration of aging earth structures**. SMRI Paper, presented at the Solution Mining Research Institute, Fall Meeting, October 19-22, Houston, Texas. (24 pp.).

Serata, S. and Mehta, B. (1993). Design and stability of salt cavern for compressed air energy storage (CAES). In **the Seventh Symposuim on Salt** (vol. 1, pp. 395-403). Amsterdam: Elsevier Science Publishers.

Serata, S., Mehta, B., and Hiremath, M. (1989). **Geomechanical stability analysis for CAES cavern operation**. In Nilsen and Olsen (eds.). (pp. 129-135). Storage of Gases in Rock Caverns. A.A. Balkema: Rotterdam.

Singh, M.M. (1992). Mine Subsidence. **SME Mining Engineering Handbook**. Hartman, H. L. (ed). (pp.938-971). Society for mining metallurgy and exploration, Inc. Colorado.

Singh, M.M. (1978). Experience with Subsidence due to Mining. Proceedings of the International Conference on Evaluation and Prediction of Subsidence. ASCE, New York. pp.92-112.

Smailbegovic, F. (1965). The results of surveying vertical and horizontal displacement at Tuzla town area. **Fond for Subsidence Tuzla town**, former Yugoslavia.

Spiers, C.J. and Carter, N.L. (1998). Microphysics of rock salt flow in nature. In **Proceedings of the Fourth Conference on the Mechanical Behavior of Salt** (pp. 115-128). Clausthal-Zellerfeld, Germany: Trans Tech Publications.

Stormont, J.C. and Fuenkajorn, K. (1994). Dilation-induced permeability changes in rock salt. In **Proceedings of the Eight International Conf, Computer Methods and Advances in Geomechanics** (pp. 1296-1273). Morgantown, West Virginia.

Stormont, J.C., Daemen J.J.K., and Desai, C.S. (1992). Prediction of dilation and permeability changes in rock salt. **International Journal for Numerical and Analytical Methods in Geomechanics** 16 (8): 545-569.

Suh, N.P. (1990). The Principles of Design. Oxford University Press. New York. 401 pp.

Supajanya, T., Vichapan, K., and Sri-issaporn, S. (1992). Surface expression of shallow salt dome in Northeast Thailand, In National Conference on Geologic Resources of Thailand: Potential for Future Development (pp. 89-95). Bangkok, Thailand: Department of Mineral Resources.

Suwanapal, A. (1992). Potash mine: A co-operative project among ASEAN countries and private sectors. In **National Conference on Geologic Resources of Thailand: Potential for Future Development**. Bangkok, Thailand: Department of Mineral Resources.

Suwanich, P. (1986). Potash and rock salt in Thailand. In **Nonmetallic minerals Bulletin No.2.** Bangkok, Thailand: Economic Geology Division, Department of Mineral Resources.

Suwanich, P. and Rattanajarurak, P. (1982). Sequences of rock salt and potash in Thailand. **Nonmetallic Minerals Bulletin No. 1**. Bangkok: Economic Geology, Division, Department of Mineral Resources.

Suwanich, P. and Rattanajarurak, P. (1986). Potash and rock salt in Thailand, Appendix A: core log of K-holes. In Nonmetallic minerals bulletin no.2. Bangkok, Thailand: Economic Geology Division, Department of Mineral Resources.

Suwanich, P., Rattanajarurak, P., and Kunawat, P. (1982). **Core Log Bamnet Narong Area Chaiyaphum Province**. Bangkok, Thailand: Economic Geology Division, Department of Mineral Resources.

Suwanich, P., Rattanajarurak, P., and Kunawat, P. (1982). Sequences of rock salt and potash in Thailand. In **Nonmetallic Minerals Bulletin No. 1.** Bangkok, Thailand: Economic Geology Division, Department of Mineral Resources.

Terzaghi, R.D. (1969). Brine-field subsidence at Windsor, Ontario. In **Proceedings of the Third Symposium on Salt** (Vol. I, pp. 298-307).

Therol, L. and Ghoreychi, M. (1996). Rock salt damage experimental results and interpretation. In **Proceedings of the Third Conference on the Mechanical Behavior of Salt** (pp. 175-189). Clausthal-Zellerfeld, Germany: Trans Tech Publications.

Thoms, R.L. and Gehle, R. (1994). **Analysis of a solidified waste disposal cavern in gulf coast salt dome.** SMRI Fall Meeting (p. 637).

Utha-aroon, C. (1993). Continental origin of the Maha Sarakham evaporates, Northeastern Thailand. Journal of Southeast Asian Earth Sciences. 8(1-4): 193-203.

Voight, B., and Pariseau, W. (1970). State of Predictive Art in Subsidence Engineering. ASCE Journal of Soil Mechanics Foundation Division. Vol.96 No.SM2, paper 7187. pp. 721-750.

Vouille, G., Bergues, J., Durup, J.G., and You, T. (1996). Study of the stability of caverns in rock salt created by solution mining proposal for a new design criterion. In **Proceedings of the Third Conference on the Mechanical Behavior of Salt** (pp. 427-444). Clausthal-Zellerfeld, Germany: Trans Tech Publications.

Wanten, P.H., Spiers, C.J., and Peach, C.J. (1996). Deformation of NaCl single crystals at $0.27Tm < T < 0.44Tm$. In **Proceedings of the Third Conference on the Mechanical Behavior of Salt** (pp. 117-128). Clausthal-Zellerfeld, Germany: Trans Tech Publications.

Warren, J. (1999). **Evaporites: Their evolution and economics** (pp. 235-239). Philadelphia: Blackwell Science.

Weidinger, P., Blum, W., Hampel, A., and Hunsche, U. (1998). Description of the Creep of Rock Salt with the Composite Model - I. Transient Creep. In **Proceedings of the Fourth Conference on the Mechanical behavior of salt** (pp. 277-286): Clausthal-Zellerfeld, Germany: Trans Tech Publications.

Wetchasat, K. (2002). Assessment of mechanical performance of rock salt formations for nuclear waste repository in northeastern Thailand. **The 3rd National Symposium on Graduate Research: Extended Abstracts**, 18-19 July 2002 (pp. 427-428). Nakhon Ratchasima, Thailand: Suranaree University of Technology.

Wetchasat, K. (2002). **Assessment of mechanical performance of rock salt formations for nuclear waste repository in northeastern Thailand**, M.S. thesis, Suranaree University of Technology, Thailand.

Wongsawat, S., Dhanesvanich, O., and Panjasutaros, S. (1992). Groundwater resources of Northeastern Thailand. In National Conference on Geologic Resources of Thailand: Potential for Future Development (pp. 507-521). Bangkok, Thailand: Department of Mineral Resources.

Yumuang, S. (1983). On the origin of evaporate deposits in the Mahasarakham Formation in Bamnet Narong area, Changwat Chaiyaphum. M.S. Thesis, Chulalongkorn University, Thailand.

Yumuang, S. (1995). **Potash ore reserve evaluation of Bamnet Narong area, Northeast Thailand.** Department of Geology, Faculty of Science: Chulalongkorn University.

Yumuang, S., Khantapab, C., and Taiyagupt, M. (1986). The evaporate deposits in Bamnet Narong area, Northeastern Thailand. In **Proceedings of the GEOSEA V** (Bulletin 20, Vol. 2, pp. 249-267). Geological Society of Malasia.

Zhang, C., Schmidt, M.M., and Staupendahl, G. (1996). Experimental and modeling results for compaction of crushed salt. In **Proceedings of the Third Conference on the Mechanical Behavior of Salt** (pp. 391-402). Clausthal-Zellerfeld, Germany: Trans Tech Publications.

APPENDIX A

IDENTIFICATION OF SALT UNITS FROM

BOREHOLE LOGS
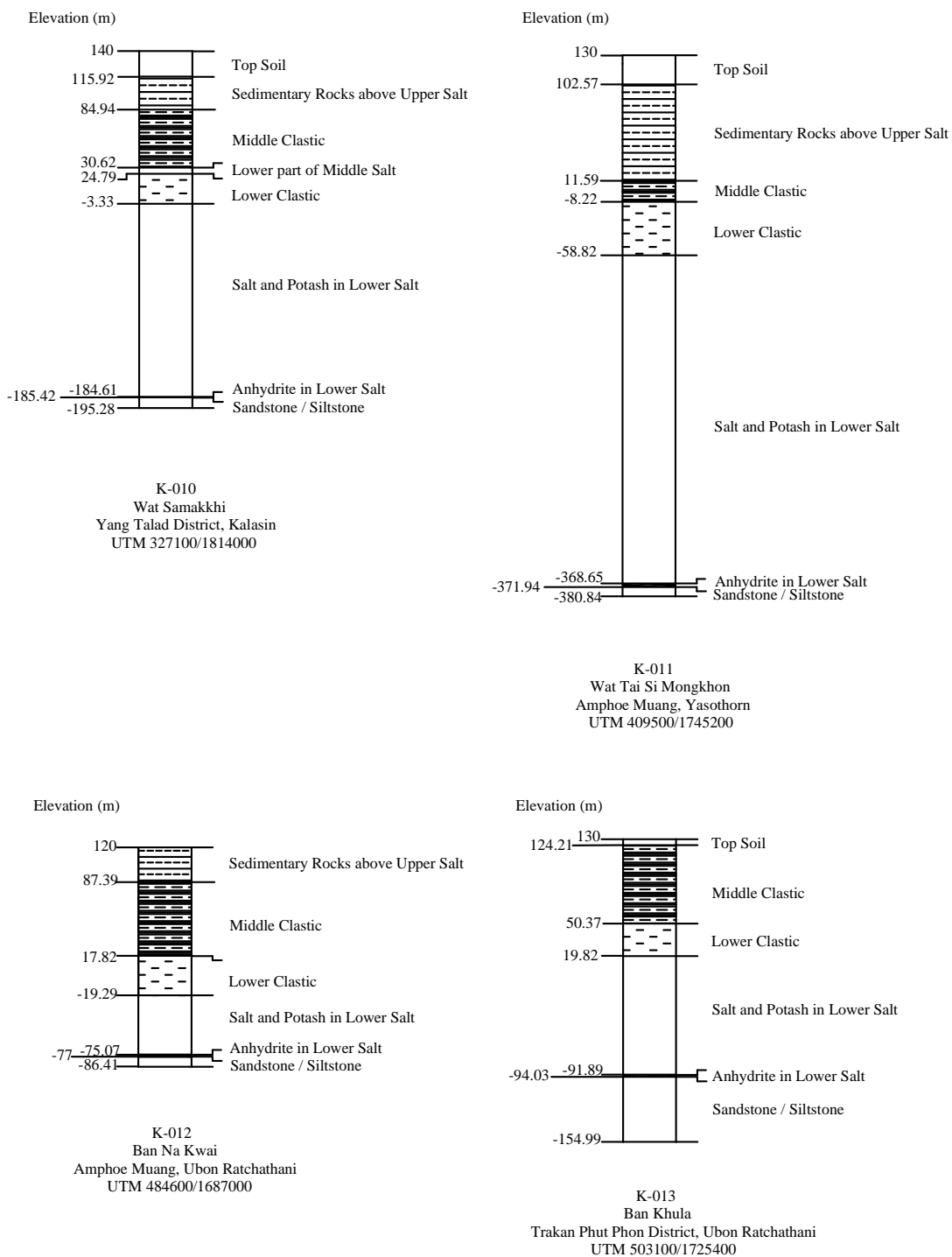
Figure A.1 Identification of stratigraphic units for borehole Nos. K-010 to K-013.

123
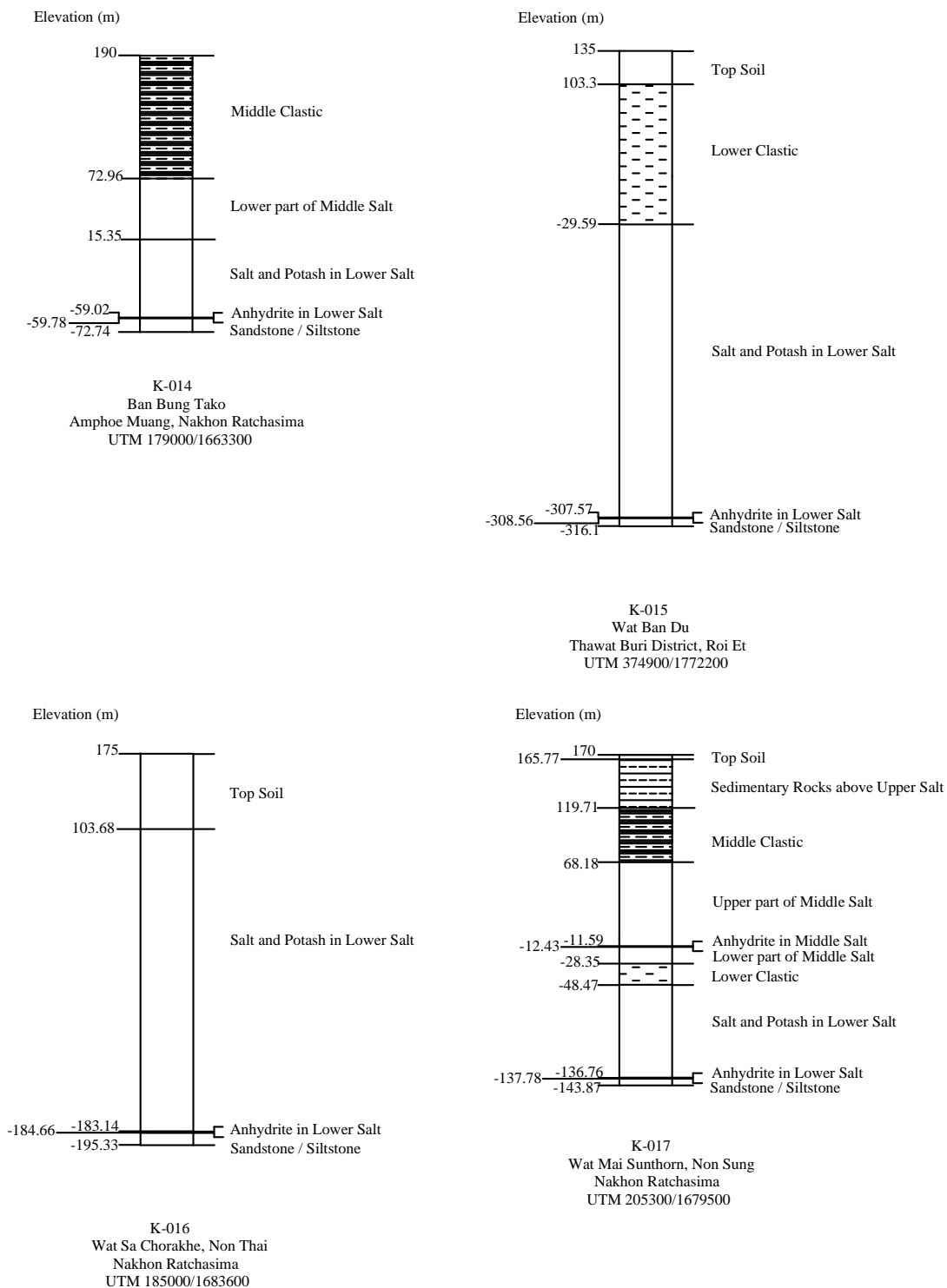
Figure A.2 Identification of stratigraphic units for borehole Nos. K-015 to K-017.
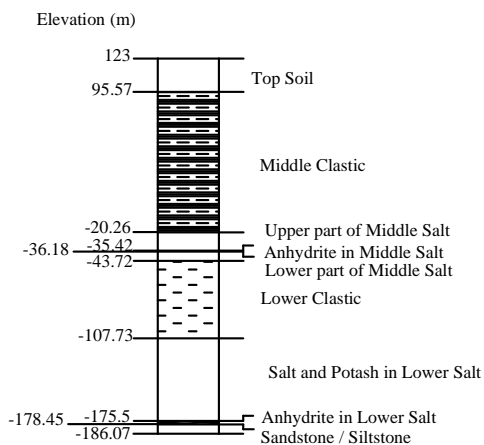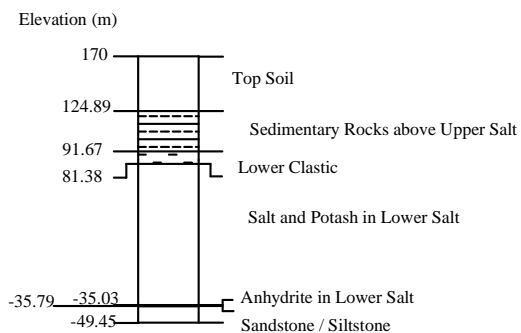
Figure A.3 Identification of stratigraphic units for borehole Nos. K-018 to K-021.

Figure A.4 Identification of stratigraphic units for borehole Nos. K-022 to K-025.

Elevation (m)

160 — Top Soil

114.28 — Lower Clastic
93.86 —

Salt and Potash in Lower Salt

-136.57 — Anhydrite in Lower Salt
-137.86 — Sandstone / Siltstone
-139.92 —

K-026
Ban Pha Lai
Non Sung District, Nakhon Ratchasima
UTM 214200/1682600

Elevation (m)

165 — Middle Clastic

107.09 — Lower Clastic
71.98 —

Salt and Potash in Lower Salt

-27.3 -26.34 — Anhydrite in Lower Salt
-31.6 — Sandstone / Siltstone

K-027
Ban Fai
Amphoe Muang, Nakhon Ratchasima
UTM 185800/1663500

Elevation (m)

170 — Top Soil

138 — Lower Clastic

71.55 —

Salt and Potash in Lower Salt

-5.26 -3.13 -2.01 — Anhydrite in Lower Salt
Sandstone / Siltstone

K-028
Wat Nong Chok
Amphoe Muang, Nakhon Ratchasima
UTM 200500/1664300

Elevation (m)

193.9 200 — Top Soil

Lower Clastic

117.2 —

Salt and Potash in Lower Salt

-24.33 — Anhydrite in Lower Salt
-25.22 — Sandstone / Siltstone
-27.08 —

K-029
Ban Don Ta Baeng
Dan Khun Thot District, Nakhon Ratchasima
UTM 803000/1678700

Figure A.5 Identification of stratigraphic units for borehole Nos. K-026 to K-029.
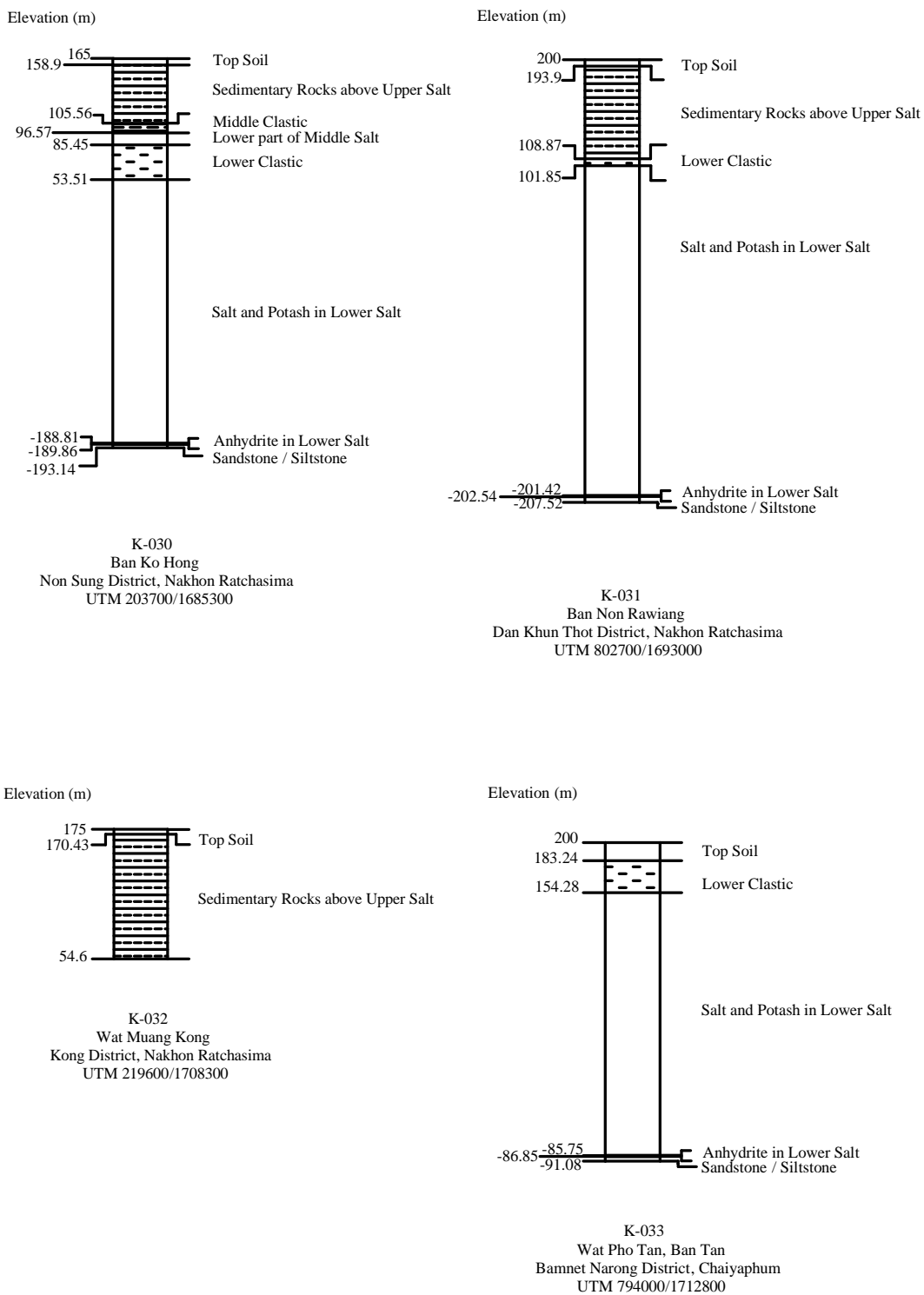
Figure A.6 Identification of stratigraphic units for borehole Nos. K-030 to K-033.

Elevation (m)

K-034
Wat Tam Yae
Pimai District, Nakhon Ratchasima
UTM 227300/1685800

156.95 — 160 — Top Soil
Middle Clastic
71 — Lower part of Middle Salt
54.84 — 63.38 — Lower Clastic
Salt and Potash in Lower Salt
-81.89 — -80.26 — Anhydrite in Lower Salt
-85.36 — Sandstone / Siltstone

Elevation (m)

160 — Top Soil
124.95 — Sedimentary Rocks above Upper Salt
-53.36 —

K-035
Ban Don Ta Nin
Phra Thai District, Nakhon Ratchasima
UTM 245800/1720300

Elevation (m)

150 — Top Soil
148.48 — Sedimentary Rocks above Upper Salt
-22.13 — Upper Salt
-33.37 — Middle Clastic
-78.87 — Upper part of Middle Salt
-161.38 — -160.62 — Anhydrite in Middle Salt
-173.33 — Lower part of Middle Salt
-199.3 — Lower Clastic
Salt and Potash in Lower Salt
-284.64 —

K-036
Ban Nong Hai
Chieng Yun District, Maha Sarakham
UTM 301700/1810600

Elevation (m)

145 — Top Soil
121.84 — Lower Clastic
37.56 —
Salt and Potash in Lower Salt
-304.35 — -302.93 — Anhydrite in Lower Salt
-306.41 — Sandstone / Siltstone

K-037
Ban Hua Khua
Kantharawichai District, Maha Sarakham
UTM 317300/1798700

Figure A.7 Identification of stratigraphic units for borehole Nos. K-034 to K-037.

Elevation (m)

150
143.9 ⟶ Top Soil

Sedimentary Rocks above Upper Salt

-63.36

K-038
Ban Sok Chuak
Amphoe Muang, Roi Et
UTM 338700/1782200

Elevation (m)

180
173.9 ⟶ Top Soil

Sedimentary Rocks above Upper Salt

-119.72

K-039
Ban Waeng Ton
Wapi Pathum District, Mahasarakham
UTM 322200/1765300

Elevation (m)

140
129.94 ⟶ Top Soil

Sedimentary Rocks above Upper Salt

-76.41 ⟶ Upper Salt
-90.38

Middle Clastic

-167.69

Upper part of Middle Salt

-267.39 -266.48 ⟶ Anhydrite in Middle Salt
-282.6 ⟶ Lower part of Middle Salt

Lower Clastic

-349.20 -343.95 ⟶ Salt and Potash in Lower Salt

K-041
Ban Na Srinuan
Phayakaphumphisai District, Maha sarakham
UTM 312200/1728300

Figure A.8 Identification of stratigraphic units for borehole Nos. K-038 to K-039 and

K-041.

Figure A.9 Identification of stratigraphic units for borehole Nos. K-040 and K-042.

Elevation (m)

160
144.76
Top soil
Sedimentary Rocks above Upper Salt
79.23
Middle Clastic
53.32
33.41
Lower Clastic

Salt and Potash in Lower Salt

-125.66 -124.61
-130.47
Anhydrite in Lower Salt
Sandstone / Siltstone

K-047
Wat Pa Chaiwan
Amphoe Muang, Khon Kaen
UTM 267900/1818500

Elevation (m)

165.43 170
Top soil
Sedimentary Rocks above Upper Salt
112.09
Middle Clastic
88.70
Lower Clastic

35.89

Salt and Potash in Lower Salt

-168.39 -167.17
-171.38
Anhydrite in Lower Salt
Sandstone / Siltstone

K-049
Wat Sra Kaeo, Ban Sra Kaeo
Amphoe Muang, Khon Kaen
UTM 250600/1818200

Elevation (m)

160
149.33
Top soil
Sedimentary Rocks above Upper Salt

92.94
Middle Clastic
54.24
34.73
Lower Clastic

Salt and Potash in Lower Salt

-131.89 -130.57
-133.52
Anhydrite in Lower Salt
Sandstone / Siltstone

K-050
Wat Sai Thong, Ban Kham Hai
Amphoe Muang, Khon Kaen
UTM 265800/1818300

Elevation (m)

205
Middle Clastic
156.23
Lower Clastic
141.07

Salt and Potash in Lower Salt

71.99 73.33
66.32
Anhydrite in Lower Salt
Sandstone / Siltstone

K-051
Wat Bung Chuan
Bamnet Narong District, Chaiyaphum
UTM 788500/1714900

Figure A.10 Identification of stratigraphic units for borehole Nos. K-047 and K-049 to K-050.

Elevation (m)

210 — Top Soil
189.88 — Sedimentary Rocks above Upper Salt
165.8 — Lower Clastic
127.7 —

Salt and Potash in Lower Salt

53.7 — 54.93 — Anhydrite in Lower Salt
49.98 — Sandstone / Siltstone

K-052
Wat Phet Phum Suwan
Bamnet Narong District, Chaiyaphum
UTM 788300/1710700

Elevation (m)

160
152.38 — Top soil

Sedimentary Rocks above Upper Salt

9.43 — Middle Clastic
-19.22 —

Upper part of Middle Salt

-86.28 — Anhydrite in Middle Salt
-86.78 — Lower part of Middle Salt
-98.67 — Lower Clastic
-123.54 —

Salt and Potash in Lower Salt

-333.84 — Anhydrite in Lower Salt
-334.89 — Sandstone / Siltstone
-338.04 —

K-053
Wat Pa Aranyawasri, Ban Lao Nadee
Amphoe Muang, Khon Kaen
UTM 255500/1812300

Elevation (m)

195 —
Top soil
179.76 —
Sedimentary Rocks above Upper Salt
123.37 — Upper Salt
114.11 — Middle Clastic
81.3 —

Upper part of Middle Salt

8.04 — 8.95 — Anhydrite in Middle Salt
-7.72 — Lower part of Middle Salt
-19.04 — Lower Clastic

Salt and Potash in Lower Salt

-132.2 — -130.93 — Anhydrite in Lower Salt
-140.28 — Sandstone / Siltstone

K-056
Chaturat Town Hall
Chaturat District, Chaiyaphum
UTM 805500/1722700

Elevation (m)

180 —

Top soil

12.36 — Lower Clastic
-3.49 —

Salt and Potash in Lower Salt

-114.92 — Anhydrite in Lower Salt
-115.69 — Sandstone / Siltstone
-117.18 —

K-054
Wat Chaisri, Ban Sawathi
Amphoe Muang, Khon Kaen
UTM 254600/1825400

Figure A.11 Identification of stratigraphic units for borehole Nos. K-052 to K-054 and K-056.

Elevation (m)

155
145.86 — Top soil

Sedimentary Rocks above Upper Salt

70.27 —
Middle Clastic
39.33 —
19.36 — Lower Clastic

Salt and Potash in Lower Salt

-14.16 —

K-057
Wat Wutharam, Ban Non Nong Wat
Amphoe Muang, Khon Kaen
UTM 268300/18164000

Elevation (m)

160
Top soil

105.14 —
Lower Clastic

51.9 —
Salt and Potash in Lower Salt

-15.26 —

K-058
Infront of Khon Kaen University
Amphoe Muang, Khon Kaen
UTM 267500/1818700

Elevation (m)

160
150.86 — Top soil

Sedimentary Rocks above Upper Salt

112.76 —
Middle Clastic

64.9 —

Upper part of Middle Salt

-0.35 — Anhydrite in Middle Salt
-1.09 — Lower part of Middle Salt
-17.76 — Lower Clastic

-45.51 —

Salt and Potash in Lower Salt

-200.87 -197.35 -195.78 — Anhydrite in Lower Salt
Sandstone / Siltstone

K-059
Wat Sri Bunruang, Ban Thum
Amphoe Muang, Khon Kaen
UTM 257000/1819300

Elevation (m)

170
165.43 — Top soil

Sedimentary Rocks above Upper Salt

75.51 —
Middle Clastic

28.27 —
Lower Clastic
2.85 —

Salt and Potash in Lower Salt

-63.17 —

K-060
Ban Daeng Noi
Amphoe Muang, Khon Kaen
UTM 251000/1818900

Figure A.12 Identification of stratigraphic units for borehole Nos. K-057 to K-060.

Elevation (m)

170 — Top soil
151.7 —
Lower Clastic
81.61 — Salt and Potash in Lower Salt
79.17 — Anhydrite in Lower Salt
77.24 —
Sandstone / Siltstone
19.12 —

K-061
Wat Mong Kon Luang, Ban Muang Pear
Ban Phai District, Khon Kaen
UTM 250000/1779000

Elevation (m)

170 — Top soil
165.43 —

Sedimentary Rocks above Upper Salt

-187.50 —
Upper Salt
-212.83 — Middle Clastic
-236.73 —
Upper part of Middle Salt
-283.75 — Anhydrite in Middle Salt
-284.25 — Lower part of Middle Salt
-293.72 — Lower Clastic
-297.56 —

K-062
Wat Sra Chanthrawat
Phon District, Khon Kaen
UTM 843300/1748800

Elevation (m)

180 — Top soil
149.52 —
Sedimentary Rocks above Upper Salt
135.80 —
Lower Clastic
76.17 —
Salt and Potash in Lower Salt
21.63 —
Anhydrite in Middle Salt
20.53 — Sandstone / Siltstone
16.93 —

K-063
Wat Pho Chai, Ban Na Kha
Mancha Kiri District, Khon Kaen
UTM 233500/1788400

Elevation (m)

123 —

Top soil

14.8 —
Middle Clastic
-17.51 —
Lower Clastic
-47.89 —

Salt and Potash in Lower Salt

-166.81 —
Anhydrite in Lower Salt
-173.01 —
Sandstone / Siltstone
-174.18 —

K-064
Wat Plap Pla Chai, Ban Ta Yuak
Amphoe Suwanna Phum, Roi Et
UTM 363700/1708100

Figure A.13 Identification of stratigraphic units for borehole Nos. K-061 to K-064.

Elevation (m)

130 ⎯

Top soil

-5.64 ⎯
-29.72 ⎯

Sedimentary Rocks above Upper Salt

K-065
Wat Suchit Thammaram, Ban Nikom
Amphoe Satuk, Burirum
UTM 316600/1691600

Elevation (m)

172 ⎯

Top soil

65.32 ⎯

Sedimentary Rocks above Upper Salt

-621.70 ⎯

Upper Salt

-646.08 ⎯

K-066
Town Hall Area
Amphoe Borabou, Maha Sarakham
UTM 299200/1773800

Figure A.14 Identification of stratigraphic units for borehole Nos. K-065 to K-066.

Figure A.15 Identification of stratigraphic units for borehole Nos. K-067 to K-070.

Figure A.16 Identification of stratigraphic units for borehole Nos. K-071 to K-074.

Figure A.17 Identification of stratigraphic units for borehole Nos. K-075 to K-076.

Figure A.18 Identification of stratigraphic units for borehole Nos. K-077 to K-078.

Elevation (m)

200 — Top soil
188 —
162.82 — Sedimentary Rocks above Upper Salt
158.85 — Upper Salt
131.12 — Middle Clastic

Lower part of Middle Salt

47.61 —
36.88 — Lower Clastic

Salt and Potash in Lower Salt

-21 —

K-079
Ban Khok
Amphoe Jaturat, Chaiyaphum
UTM 805500/1723300

Elevation (m)

210 — Top soil
197.81 —
Middle Clastic

160.5 —
Lower Clastic
129.56 —

Salt and Potash in Lower Salt

-308.49 — -307.52 — Anhydrite in Lower Salt
-311.82 — Sandstone / Siltstone

K-080
Wat Ban Pra Kam
Amphoe Kong, Nakhon Ratchasima
UTM 192200/1712900

Elevation (m)

211.95 — 215 — Top soil

Sedimentary Rocks above Upper Salt

104.84 —

Middle Clastic

59 —

Upper part of Middle Salt

-41.15 — -40 — Anhydrite in Middle Salt
-54.66 — Lower part of Middle Salt
-86.78 — Lower Clastic

Salt and Potash in Lower Salt

-163 —

K-084
1 Km W of K 080, Ban Prakam
Amphoe Kong, Nakhon Ratchasima
UTM 191200/1712300

Elevation (m)

210 —
179.52 — Top soil
Middle Clastic
138.37 —
Lower part of Middle Salt
92.96 —

K-082
Ban Prakam (800 m E of K 080)
Amphoe Kong, Nakhon Ratchasima
UTM 192800/1712800

Figure A.19 Identification of stratigraphic units for borehole Nos. K-079 to K-080,

K-082 and K-084.

Figure A.20 Identification of stratigraphic units for borehole Nos. K-087 to K-088.

Figure A.21 Identification of stratigraphic units for borehole Nos. K-089 to K-090.

Figure A.22 Identification of stratigraphic units for borehole Nos. K-091 to K-094.

Elevation (m)

Top soil

Sedimentary Rocks above Upper Salt

Upper Salt

Middle Clastic

Upper part of Middle Salt

Anhydrite in Middle Salt
Lower part of Middle Salt
Lower Clastic

Salt and Potash in Lower Salt
Anhydrite in Lower Salt
Sandstone / Siltstone

154 — 157
-124.6
-162.65
-204.87
-282.72 — -277.22
-292.94
-310.87
-344.75 — -343.72
-349

K-095
Wat Ban Nong Kho
Amphoe Chieng Yuen, Maha Sarakham
UTM 301700/1814000

Elevation (m)

Top soil

Sedimentary Rocks above Upper Salt

Upper Salt

Middle Clastic
Lower part of Middle Salt

210
208
-48.37
-99.26
-129.46
-145.5

K-096
100 m S of K 080, Ban Prakam
Amphoe Kong, Nakhon Ratchasima
UTM 192300/1712500

Elevation (m)

Top soil

Lower Clastic

Salt and Potash in Lower Salt

210
175
139.5
125

K-097
420 m NE of K 080, Ban Prakam
Amphoe Kong, Nakhon Ratchasima
UTM 192200/1713100

Elevation (m)

Top soil

Sedimentary Rocks above Upper Salt

Middle Clastic

Upper part of Middle Salt

Anhydrite in Middle Salt
Lower part of Middle Salt
Lower Clastic

Salt and Potash in Lower Salt

205 — 210
106.75
58.47
-89.23
-90.23
-113.48
-141.60
-206.03

K-098
Ban Prakam, Tambon Ban Prang
Amphoe Kong, Nakhon Ratchasima
UTM 192300/1712700

Figure A.23 Identification of stratigraphic units for borehole Nos. K-095 to K-098.

Figure A.24 Identification of stratigraphic units for borehole Nos. K-099 to K-102.

Elevation (m)

170
157.81

115.75

83.13

-12.88

Top soil

Middle Clastic

Lower Clastic

Salt and Potash in Lower Salt

K-103 (RS-3.3)
About 2 km N of RS -3.1
Amphoe Chakarat, Nakhon Ratchasima
UTM 200500/1670000

Elevation (m)

170
159.33
151.71

73.28
65.61

30.98

-48.6
-49.66
-52.81

Top soil
Sedimentary Rocks above Upper Salt

Middle Clastic

Lower part of Middle Salt
Lower Clastic

Salt and Potash in Lower Salt

Anhydrite in Lower Salt
Sandstone / Siltstone

K-104 (RS-3.4)
About 1.5 km E of K 019
Amphoe Chakarat, Nakhon Ratchasima
UTM 203400/1669400

Elevation (m)

170
160.86

134.34

83.36

45.92

-47.93

Top Soil
Sedimentary Rocks above Upper Salt

Middle Clastic

Lower Clastic

Salt and Potash in Lower Salt

K-105 (RS -3.5)
About 2 km N of RS -3.4, Ban Krao
Amphoe Chakarat, Nakhon Ratchasima
UTM 202700/1671400

Elevation (m)

170
168.48
151.71

83.16

59.97

-34.52

Top soil
Sedimentary Rocks above Upper Salt

Middle Clastic

Lower Clastic

Salt and Potash in Lower Salt

K-106 (RS -3.6)
About 1 km N of RS -3.4, Ban Krao
Amphoe Chakarat, Nakhon Ratchasima
UTM 202900/1670500

Figure A.25 Identification of stratigraphic units for borehole Nos. K-103 to K-106.

Elevation (m)

160
109
39.06
30.63 30.8
12.92
-60

Top soil

Sedimentary Rocks above Upper Salt

Middle Clastic
Lower part of Middle Salt
Lower Clastic

Salt and Potash in Lower Salt

K-107 (KK - 1)
Near Raiway line
Amphoe Kong, Khon Kaen
UTM 268600/1818400

Elevation (m)

151 160
48.35 47.8
26.1
-62.7

Top soil

Middle Clastic

Lower part of Middle Salt
Lower Clastic

Salt and Potash in Lower Salt

K-108 (KK - 2)
1 km S of K 047
Amphoe Muang, Khon Kaen
UTM 267900/1817700

Elevation (m)

160
146
61.79
39.64
-126.97
-128.48
-135

Top soil

Middle Clastic

Lower Clastic

Salt and Potash in Lower Salt

Anhydrite in Middle Salt

Sandstone / Siltstone

K-109 (KK - 3)
Infront of City Hall
Amphoe Muang, Khon Kaen
UTM 269300/1818400

Elevation (m)

160
93
64.74
51.94
-101.2
-102.3
-103

Top soil

Sedimentary Rocks above Upper Salt
Lower Clastic

Salt and Potash in Lower Salt

Anhydrite in Middle Salt
Sandstone / Siltstone

K-110 (KK - 4)
600 m N of KK - 3
Amphoe Muang, Khon Kaen
UTM 269300/1819000

Figure A.26 Identification of stratigraphic units for borehole Nos. K-107 to K-110.

Elevation (m)

160 ⎯

Top soil

82 ⎯
47.11 ⎯

Lower Clastic

Salt and Potash in Lower Salt

-37.76 ⎯

K-111 (KK - 5)
700 m N of K 047
Amphoe Muang, Khon Kaen
UTM 268300/1819100

Elevation (m)

157 ⎯ 160 ⎯

Top soil

Sedimentary Rocks above Upper Salt

53.12 ⎯ 58.14 ⎯
50.4 ⎯

Middle Clastic
Lower Clastic

Salt and Potash in Lower Salt

5.3 ⎯

K-112 (KK - 6)
600 m S of KK - 1
Amphoe Muang, Khon Kaen
UTM 268600/1818100

Elevation (m)

160 ⎯

Top soil

61.5 ⎯
43.7 ⎯

Lower Clastic

Salt and Potash in Lower Salt

-40 ⎯

K-113 (KK - 7)
500 m N of KK - 1
Amphoe Muang, Khon Kaen
UTM 268700/1818900

Elevation (m)

160 ⎯
152 ⎯

Top soil

Middle Clastic

63.68 ⎯

Upper part of Middle Salt

-10.45 ⎯
-11 ⎯

Anhydrite in Middle Salt
Lower part of Middle Salt

-27.56 ⎯

Lower Clastic

-56 ⎯

Salt and Potash in Lower Salt

-117.5 ⎯

K-114 (KK - 8)
600 m N of K 059, Ban Thum
Amphoe Muang, Khon Kaen
UTM 257400/1819900

Figure A.27 Identification of stratigraphic units for borehole Nos. K-111 to K-114.

Elevation (m)

160 — 165
Top soil

Middle Clastic

46.7 —
Upper part of Middle Salt

-46.38 — Anhydrite in Middle Salt
-47.03 — Lower part of Middle Salt
-63.64 — Lower Clastic
-90.2 —
Salt and Potash in Lower Salt

-136.8 —

K-115 (KK - 9)
1 m W of K 059, Ban Thum
Amphoe Muang, Khon Kaen
UTM 256400/1819500

Elevation (m)

160 —
Top soil
136 —
Lower Clastic

53.32 —
Salt and Potash in Lower Salt

-25 —

K-116 (KK - 10)
Wat Chom Sri, Ban Yai Tan
Amphoe Muang, Khon Kaen
UTM 267500/1817900

Elevation (m)

150 —
139 — Top soil

Middle Clastic

56.54 —
Upper part of Middle Salt
24.24 — Anhydrite in Middle Salt
23.37 — Lower part of Middle Salt
6.31 — Lower Clastic
-17.57 —

Salt and Potash in Lower Salt

-97.5 —

K-117 (KK - 11)
700 m E of K 059, Ban Thum
Amphoe Muang, Khon Kaen
UTM 258000/1819000

Elevation (m)

155 —
153 — Top soil

Sedimentary Rocks above Upper Salt

59.9 —
Middle Clastic

17.84 —

Upper part of Middle Salt

-73.27 — Anhydrite in Middle Salt
-73.90 — Lower part of Middle Salt
-89.35 — Lower Clastic
-114.5 —

Salt and Potash in Lower Salt

-170 —

K-118 (KK - 12)
Ban Lao Kwaen Hak
Amphoe Muang, Khon Kaen
UTM 257400/1817700

Figure A.28 Identification of stratigraphic units for borehole Nos. K-115 to K-118.

Elevation (m)

205.69 — Top Soil
190.69 — Middle Clastic
155.49 — Anhydrite in Middle Salt
149.34 — Lower part of Middle Salt
140.61 — Lower Clastic
122.14 —

Salt and Potash in Lower Salt

-109.51 — Anhydrite in Lower Salt
-110.87 — Sandstone/Siltstone
-114.31 —

KB-1
Ban Nong Pradu, Amphoe
Bamnet Narong, Chaiyaphum
UTM 793900/1710300

Elevation (m)

204.01 —

Top Soil

152.20 —

Upper part of Middle Salt
103.86 — Anhydrite in Middle Salt
103.01 — Lower part of Middle Salt
81.74 — Lower Clastic
63.91 —

Salt and Potash in Lower Salt

-149.34 — Anhydrite in Lower Salt
-150.32 — Sandstone/Siltstone
-152.39 —

KB-2
Ban Hua Sa, Tambon Hua Thale,
Amphoe Bamnet Narong,
Chaiyaphum
UTM 795200/1709900

Elevation (m)

204.79 —
Top Soil
169.79 — Middle Clastic
149.84 — Upper part of Middle Salt
130.08 — Anhydrite in Middle Salt
129.46 — Lower part of Middle Salt
109.71 — Lower Clastic
91.41 —
Salt and Potash in Lower Salt

28.79 —

KB-3
Ban Nong Pradu, Amphoe
Bamnet Narong, Chaiyaphum
UTM 793500/1711100

Elevation (m)

203.96 — Top Soil
179.96 — Middle Clastic
152.96 — Upper part of Middle Salt
150.06 — Anhydrite in Middle Salt
149.40 — Lower part of Middle Salt
127.41 — Lower Clastic
107.91 —
Salt and Potash in Lower Salt

39.96 —

KB-4
Ban Hua Thale, Amphoe Bamnet
Narong, Chaiyaphum
UTM 794700/1711000

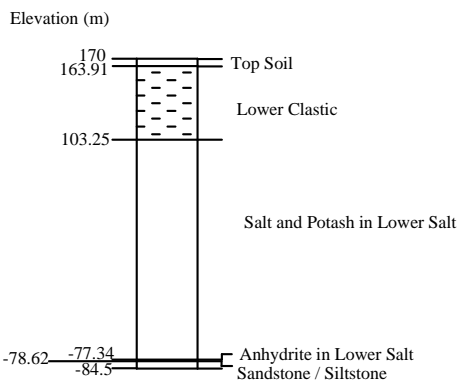**Figure A.29** Identification of stratigraphic units for borehole Nos. KB-1 to KB-4.

Elevation (m)

208.50 — Top Soil
190.50 —
                Middle Clastic
152.88 — Anhydrite in Middle Salt
148.96 — Lower part of Middle Salt
138.89 —
120.70 — Lower Clastic

                Salt and Potash in Lower Salt

42.75 —

KB-5
Ban Nong Pradu, Amphoe
Bamnet Narong, Chaiyaphum
UTM 793500/1710300

Elevation (m)

207.89 — Top Soil
187.89 —
                Middle Clastic
155.47 — Lower part of Middle Salt
149.98 —
133.52 — Lower Clastic

                Salt and Potash in Lower Salt

65.89 —

KB-6
Ban Nong Pradu, Amphoe
Bamnet Narong, Chaiyaphum
UTM 794500/1710300

Elevation (m)

206.25 — Top Soil
195.25 —
                Middle Clastic
151.95 —
134.30 — Lower Clastic

                Salt and Potash in Lower Salt

-118.93 — Anhydrite in Lower Salt
-119.91 —
-121.55 — Sandstone/Siltstone

KB-7
Ban Hua Sa, Amphoe Bamnet
Narong, Chaiyaphum
UTM 793800/1709300

Elevation (m)

204.83 — Top Soil
183.83 —
                Middle Clastic
149.69 —
                Upper part of Middle Salt
123.43 —
                Anhydrite in Middle Salt
122.44 — Lower part of Middle Salt
102.83 —
84.26 — Lower Clastic

                Salt and Potash in Lower Salt

10.83 —

KB-8
Ban Hua Sapan, Amphoe Bamnet
Narong, Chaiyaphum
UTM 794600/1709100

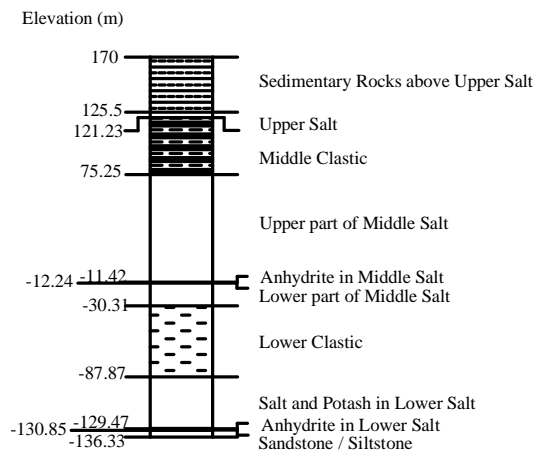**Figure A.30** Identification of stratigraphic units for borehole Nos. KB-5 to KB-8.

Elevation (m)

205.20
201.20 — Top Soil
Sedimentary rocks above Upper Salt
104.25 — Middle Clastic
64.33 —
Upper part of Middle Salt
-26.13 — Anhydrite in Middle Salt
-26.97 — Lower part of Middle Salt
-46.80 — Lower Clastic
-65.59 —
Salt and Potash in Lower Salt
-113.80 —

KB-9
Ban Hua Thale, Amphoe Bamnet
Narong, Chaiyaphum
UTM 796900/1709900

Elevation (m)

209.11
207.11 — Top Soil
Sedimentary rocks above Upper Salt
134.11 — Middle Clastic
81.11 —
Upper part of Middle Salt
-14.22 — Anhydrite in Middle Salt
-14.81 — Lower part of Middle Salt
-34.86 — Lower Clastic
-54.19 —
Salt and Potash in Lower Salt
-113.89 —

KB-10
Ban Hua Sa, Amphoe Bamnet
Narong, Chaiyaphum
UTM 796900/1709100

Elevation (m)

206.70 — Top Soil
202.70 — Sedimentary rocks above Upper Salt
177.70 — Middle Clastic
139.55 —
Upper part of Middle Salt
84.98 — Anhydrite in Middle Salt
84.09 — Lower part of Middle Salt
62.58 — Lower Clastic
44.64 —
Salt and Potash in Lower Salt
-26.30 —

KB-11
Ban Hua Sa, Amphoe Bamnet
Narong, Chaiyaphum
UTM 795000/1708200

Elevation (m)

204.79 — Top Soil
171.79 — Middle Clastic
150.08 — Upper part of Middle Salt
145.15 — Anhydrite in Middle Salt
144.29 — Lower part of Middle Salt
122.86 — Lower Clastic
104.59 —
Salt and Potash in Lower Salt
35.79 —

KB-12
Ban Nong Pradu, Amphoe
Bamnet Narong, Chaiyaphum
UTM 793900/1710900

Figure A.31 Identification of stratigraphic units for borehole Nos. KB-9 to KB-12.

Elevation (m)

201.48 — Top Soil
192.48 — Sedimentary rocks above Upper Salt
155.48 — Lower Clastic
122.23 —
Salt and Potash in Lower Salt
25.98 —

KB-13
Ban Hua Thale, Amphoe Bamnet
Narong, Chaiyaphum
UTM 796500/1711400

Elevation (m)

203.95 — Top Soil
199.95 — Sedimentary rocks above Upper Salt
178.95 — Middle Clastic
144.21 —
Upper part of Middle Salt
67.73 — Anhydrite in Middle Salt
67.11 — Lower part of Middle Salt
49.34 — Lower Clastic
27.10 —
Salt and Potash in Lower Salt
-27.05 —

KB-14
In paddy field of Ban Hua Thale,
Amphoe Bamnet Narong,
Chaiyaphum
UTM 795900/1709900

Elevation (m)

205.69 — Top Soil
203.69 — Sedimentary rocks above Upper Salt
183.75 — Middle Clastic
143.82 —
Upper part of Middle Salt
65.02 — Anhydrite in Middle Salt
64.29 — Lower part of Middle Salt
43.43 — Lower Clastic
26.29 —
Salt and Potash in Lower Salt
-14.81 —

KB-15
In paddy field of Ban Hua Sa,
Amphoe Bamnet Narong,
Chaiyaphum
UTM 795500/1709100

Elevation (m)

214.00 — Top Soil
209.00 —
Sedimentary rocks above Upper Salt
45.14 —
Upper Salt
0.85 — Middle Clastic
-24.91 —
Upper part of Middle Salt
-86.19 — Anhydrite in Middle Salt
-86.80 — Lower part of Middle Salt
-104.34 — Lower Clastic
-112.22 —
Salt and Potash in Lower Salt
-141.50 —

KB-16
Ban Nong Yai But, Amphoe
Bamnet Narong, Chaiyaphum
UTM 799000/1709000

Figure A.32 Identification of stratigraphic units for borehole Nos. KB-13 to KB-16.

Elevation (m)

217.00
211.00 — Top Soil

Sedimentary rocks above Upper Salt

75.57
71.31 — Upper Salt

Middle Clastic

31.07

Upper part of Middle Salt

-48.47 — Anhydrite in Middle Salt
-49.08 — Lower part of Middle Salt
-65.65 — Lower Clastic

-90.85

Salt and Potash in Lower Salt

-133.00

KB-17
Ban Nong Yai But, Amphoe
Bamnet Narong, Chaiyaphum
UTM 799000/1707000

Elevation (m)

220.00
219.00 — Top Soil

Sedimentary rocks above Upper Salt

115.14
110.27 — Upper Salt
Middle Clastic

70.95

Upper part of Middle Salt

-17.32 — Anhydrite in Middle Salt
-18.08 — Lower part of Middle Salt
-38.87 — Lower Clastic
-56.00

Salt and Potash in Lower Salt

-100.00

KB-18
Ban Hua Sa, Amphoe Bamnet
Narong, Chaiyaphum
UTM 797000/1707000

Elevation (m)

200.00
195.43 — Top Soil

Sedimentary rocks above Upper Salt

118.92
115.27 — Upper Salt
Middle Clastic

77.47

Upper part of Middle Salt

-13.97 — Anhydrite in Middle Salt
-15.04 — Lower part of Middle Salt
-35.30 — Lower Clastic
-54.58

Salt and Potash in Lower Salt

-90.78

KB-19
Wat Tha Sala, Ban Tha Sala,
Amphoe Bamnet Narong,
Chaiyaphum
UTM 797000/1712800

Elevation (m)

200.00
195.43 — Top Soil

Sedimentary rocks above Upper Salt

79.91
72.90 — Upper Salt

Middle Clastic

34.70

Upper part of Middle Salt

-50.65 — Anhydrite in Middle Salt
-52.00 — Lower part of Middle Salt
-71.48 — Lower Clastic
-90.48

Salt and Potash in Lower Salt

-124.92

KB-20
Ban Na, Amphoe Jaturat,
Chaiyaphum
UTM 797300/1714200

Figure A.33 Identification of stratigraphic units for borehole Nos. KB-17 to KB-20.

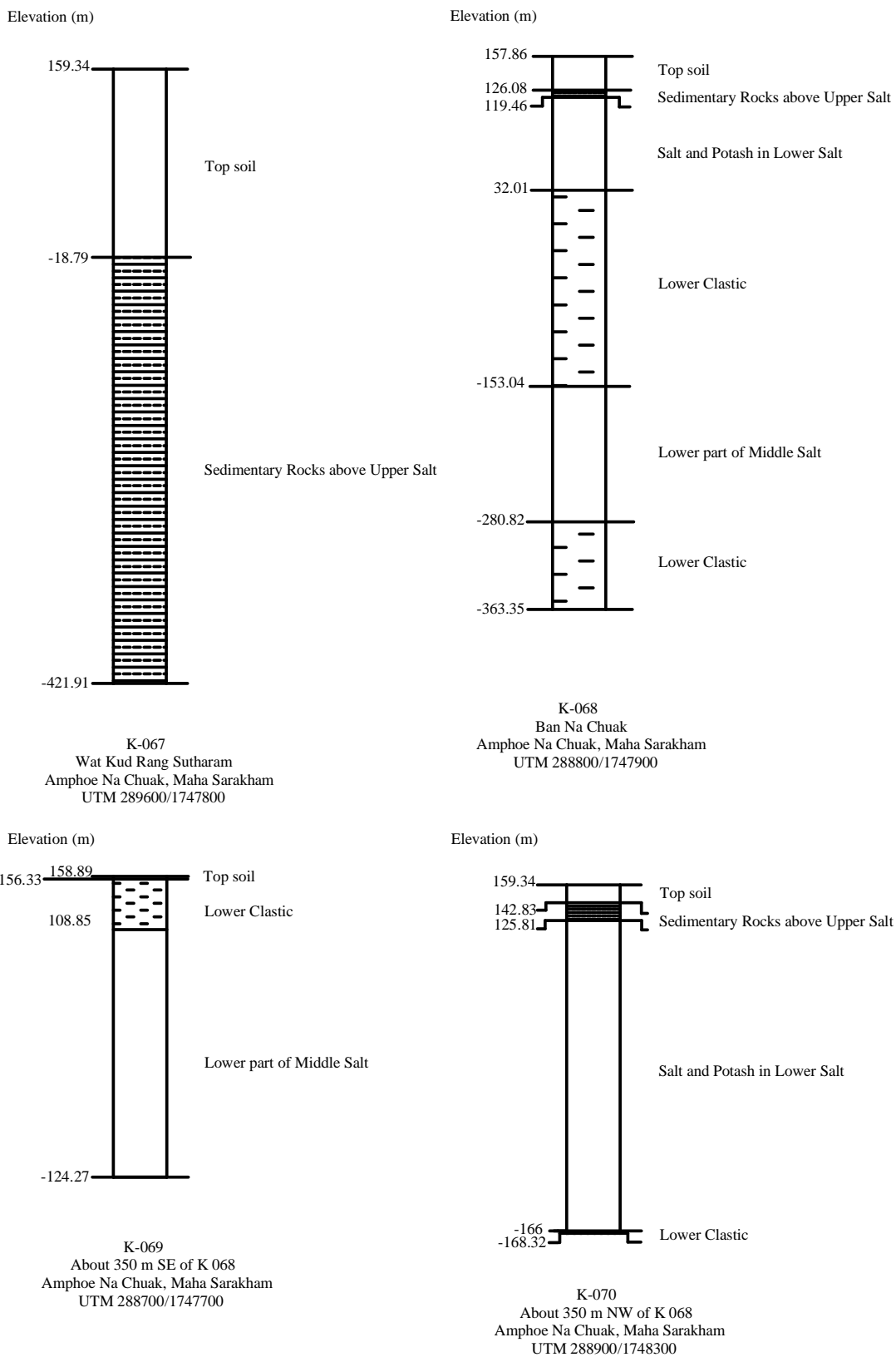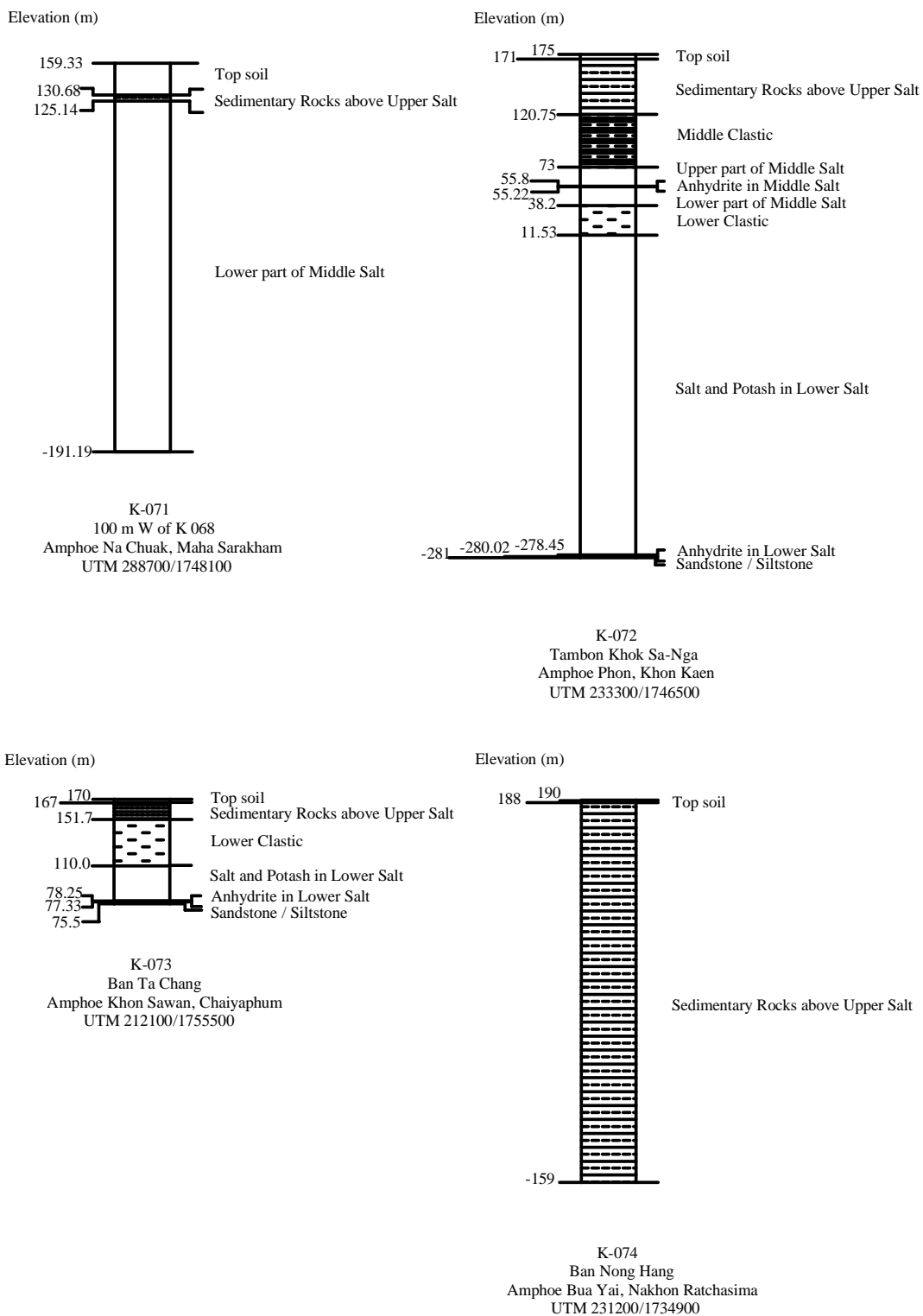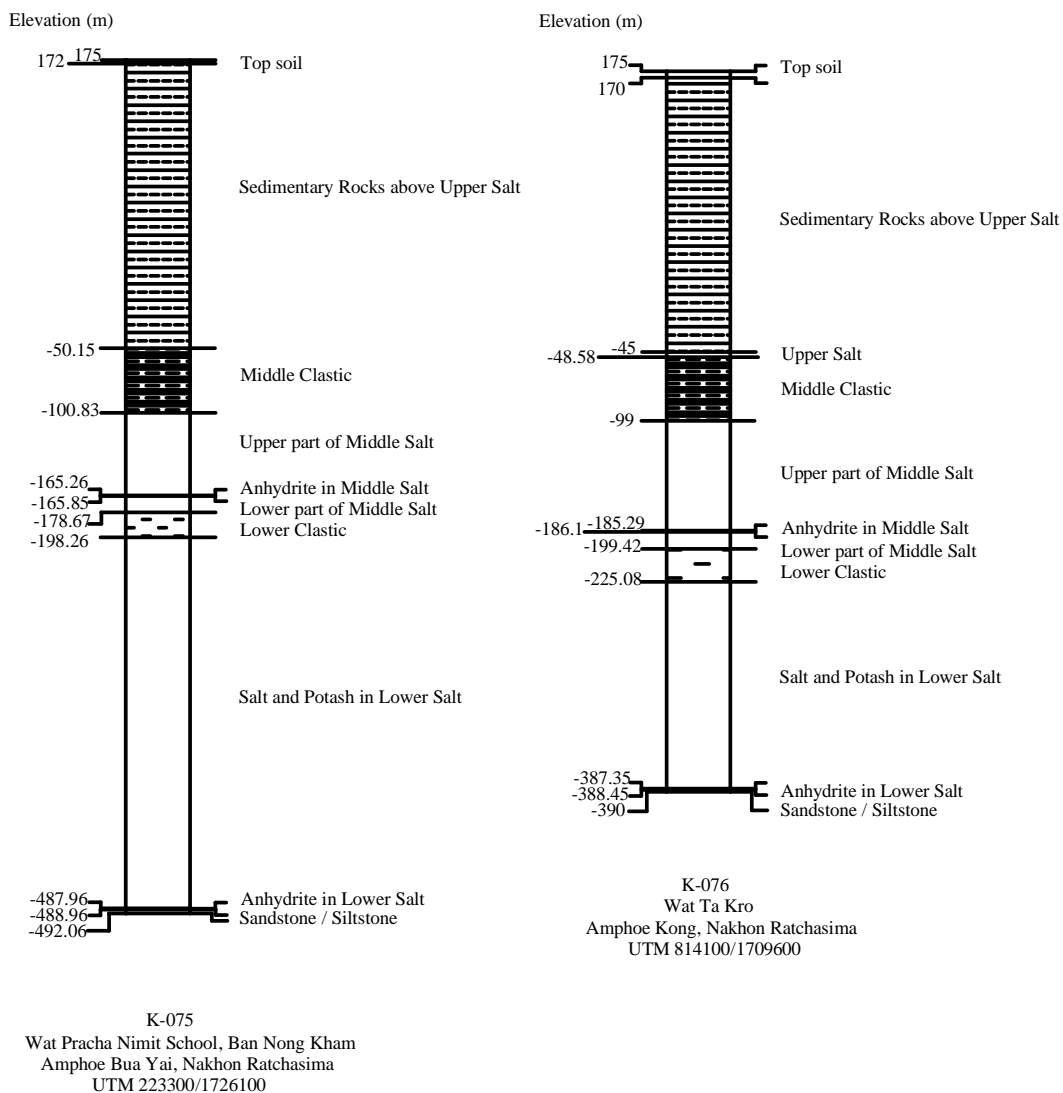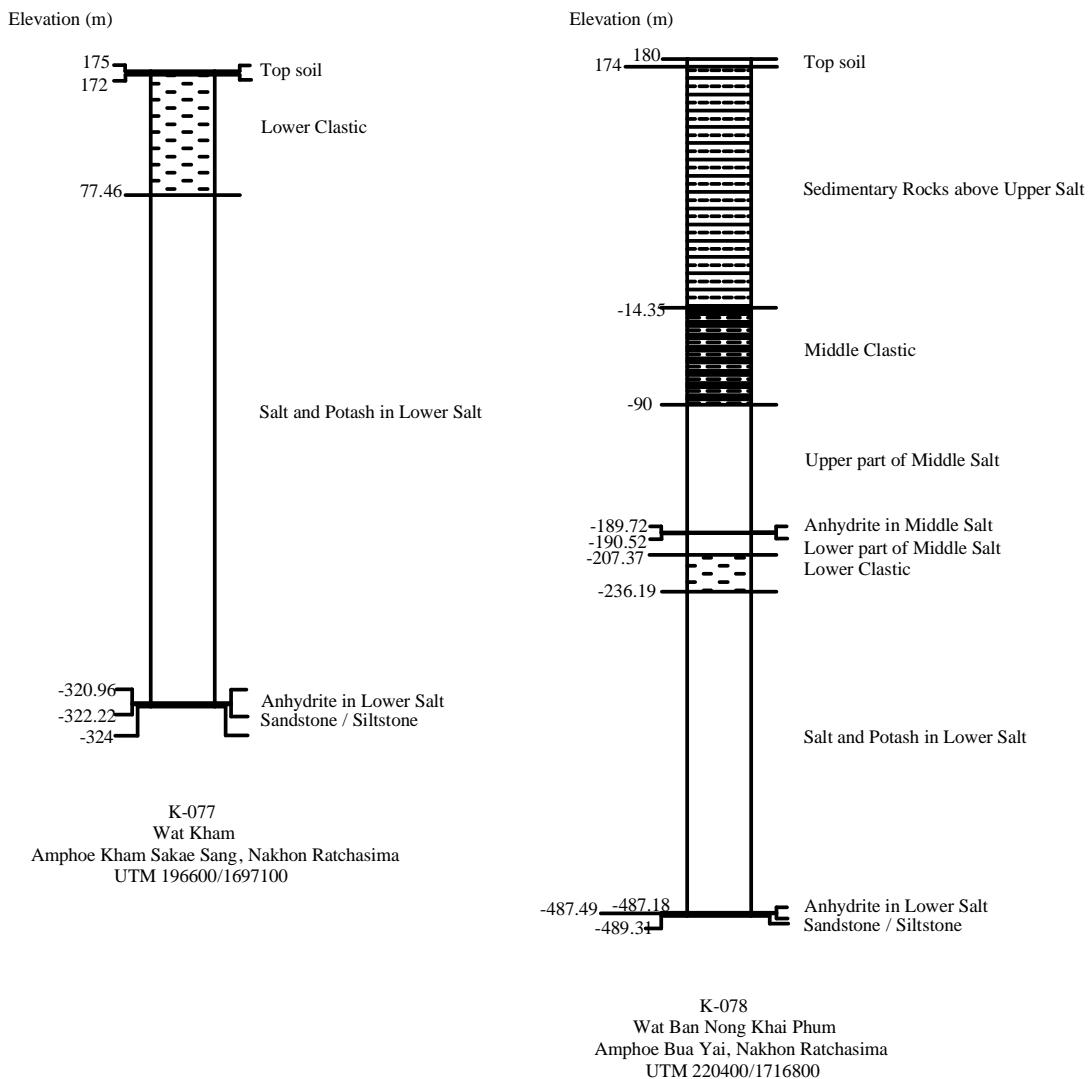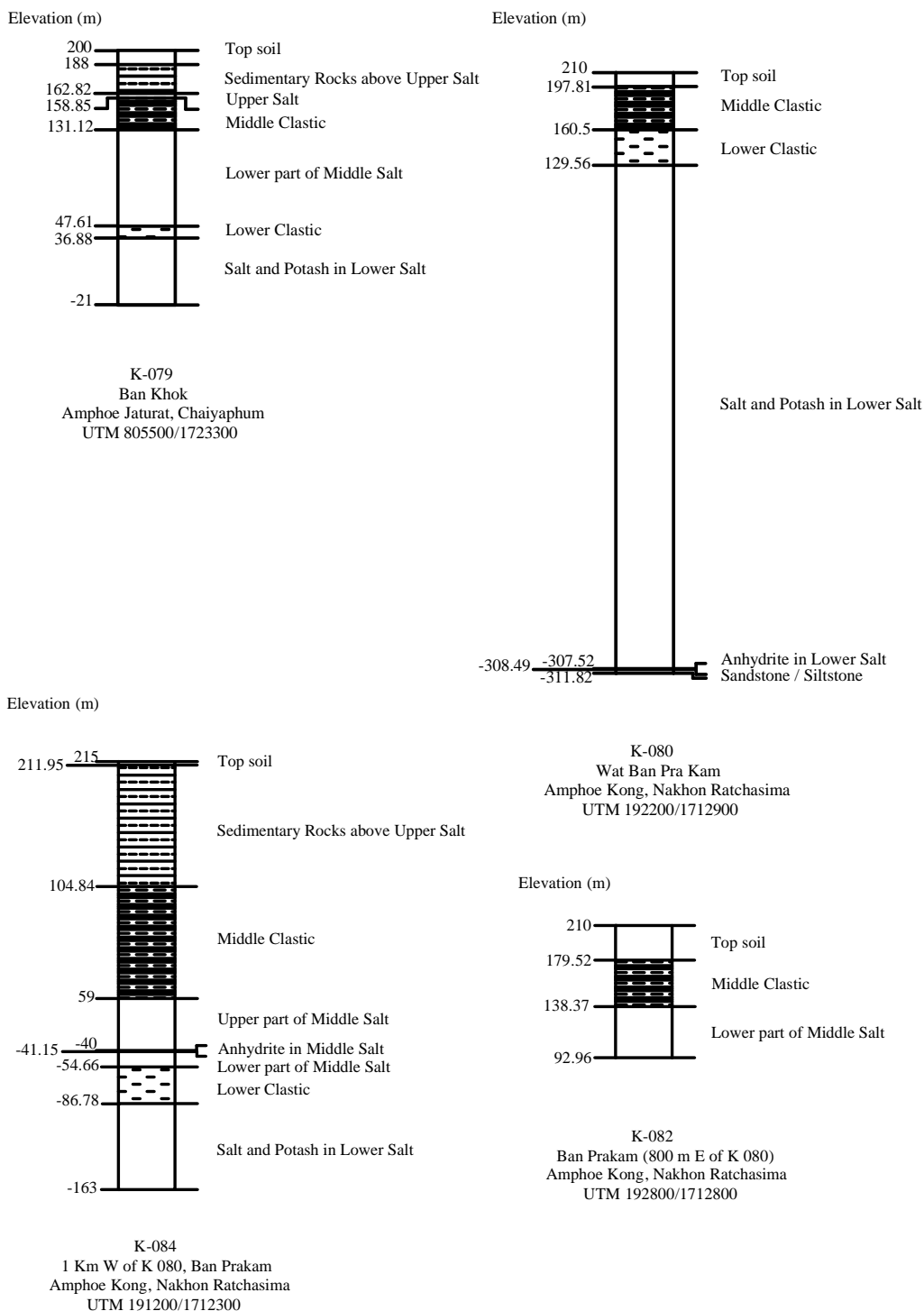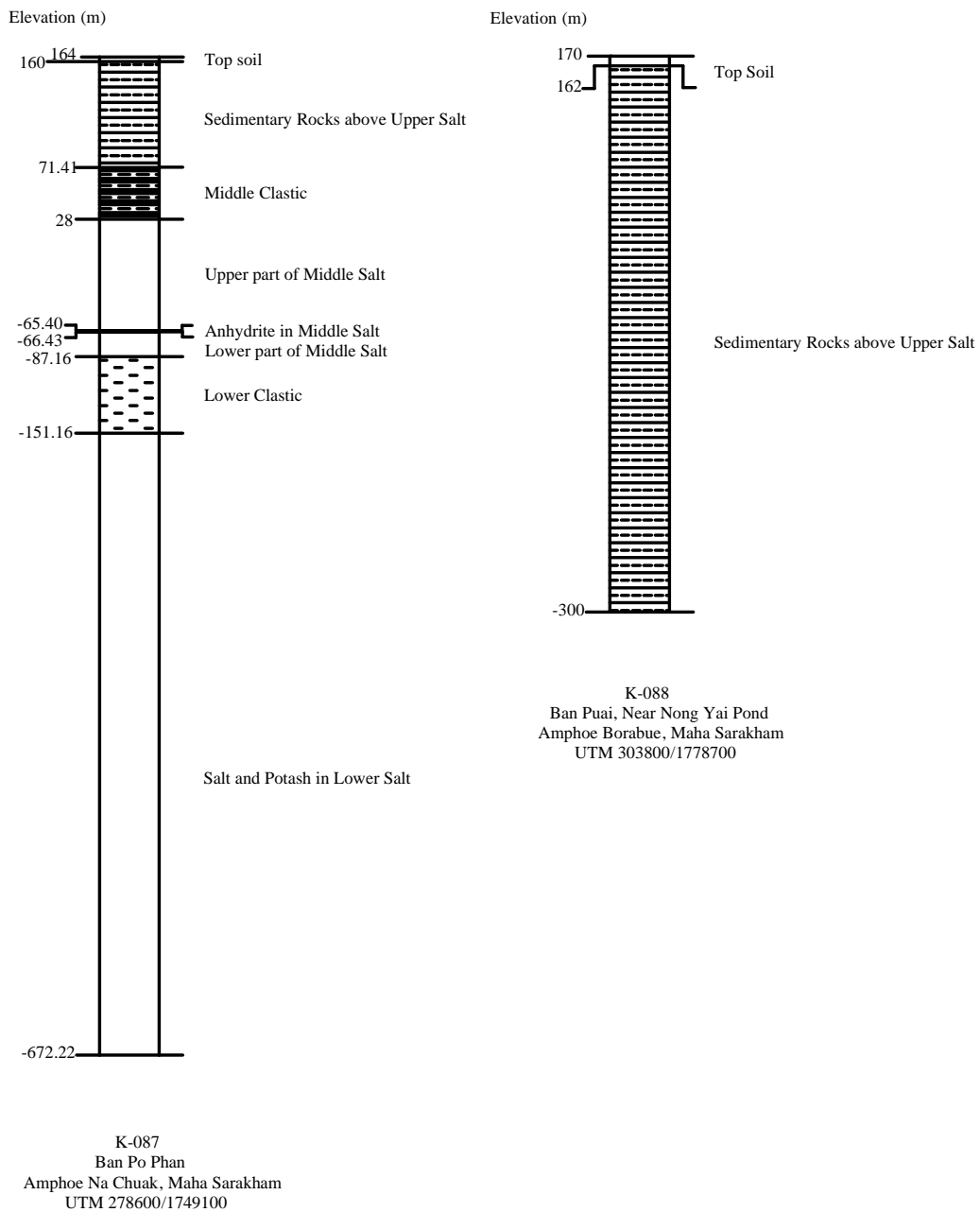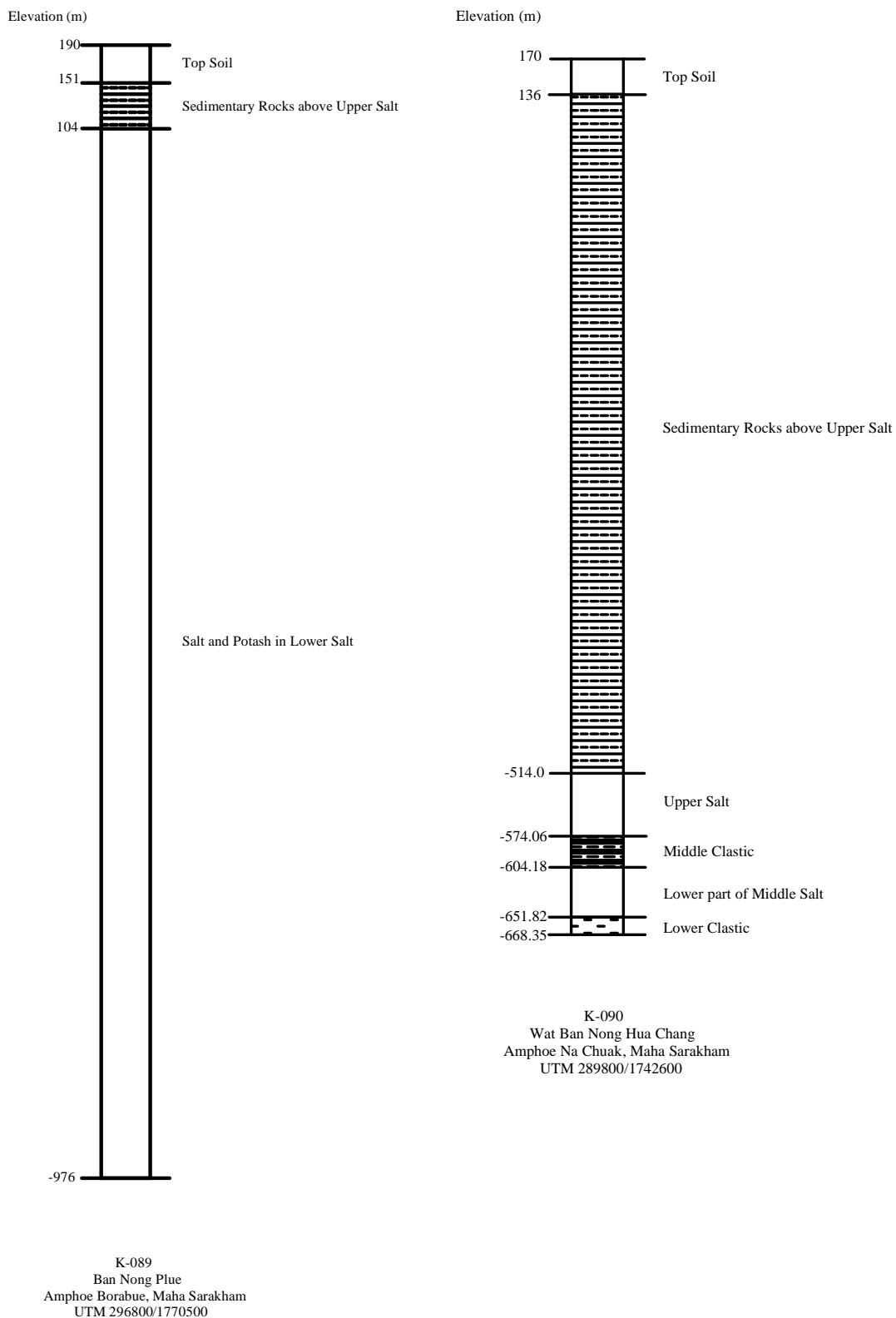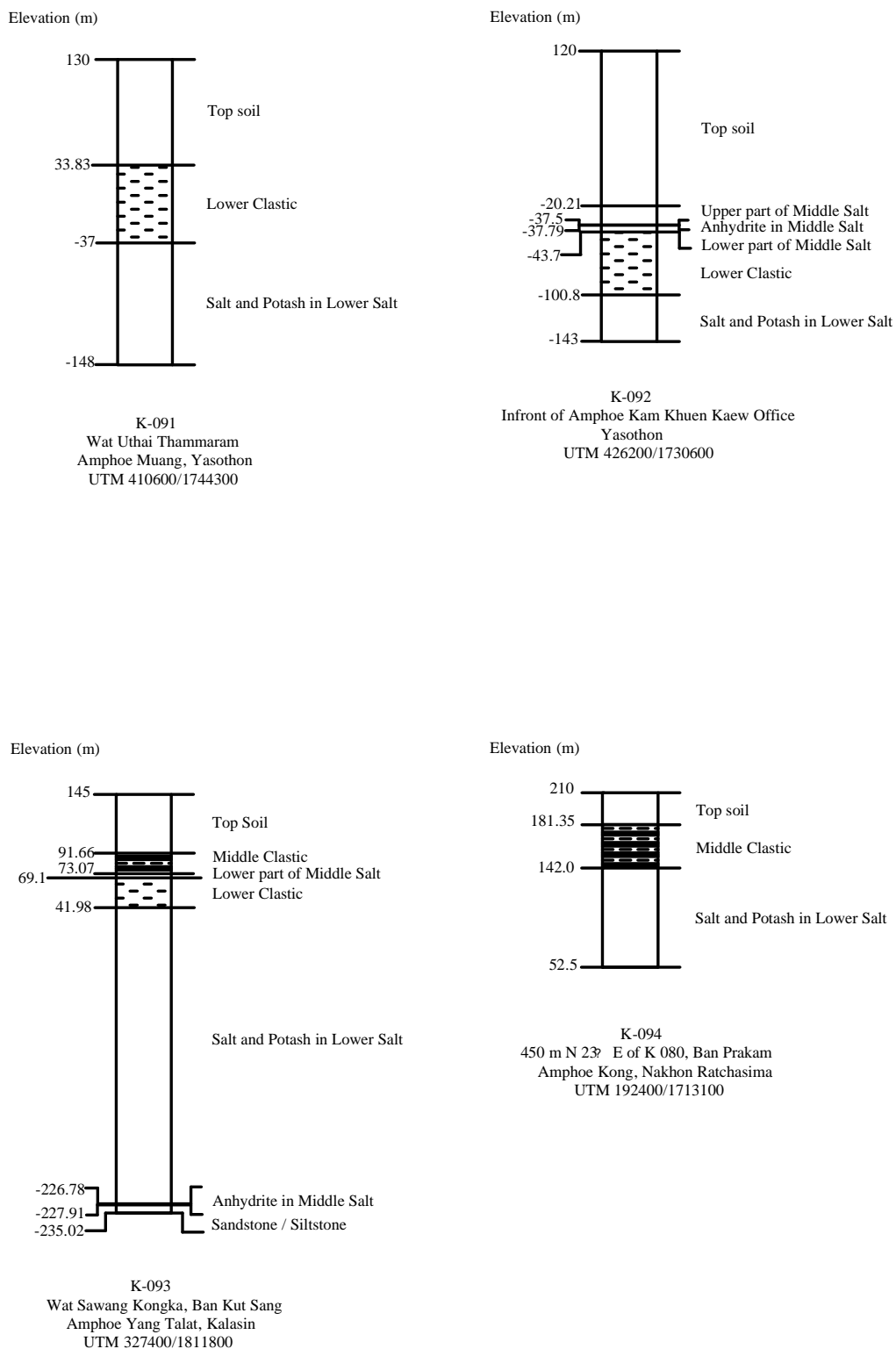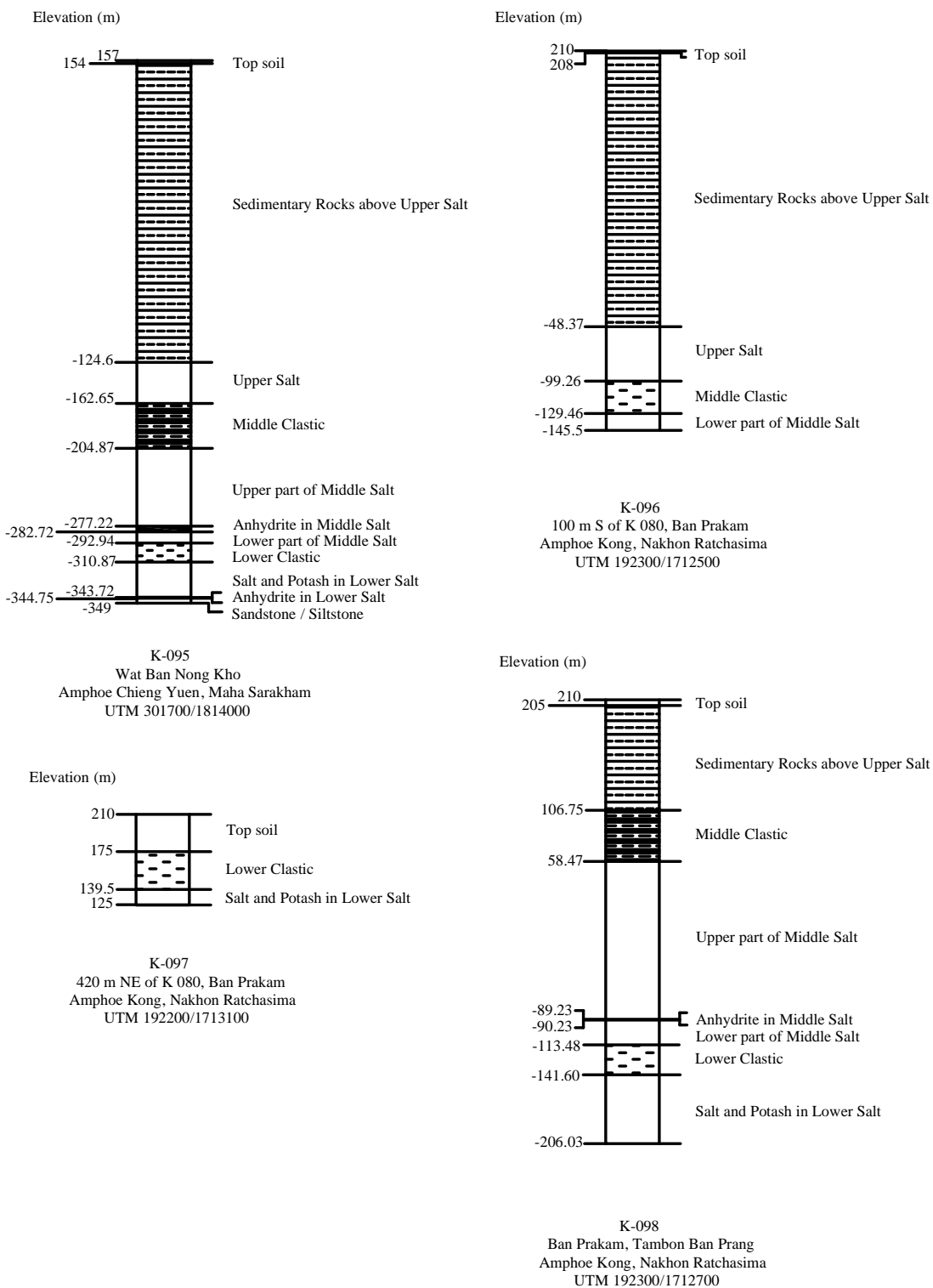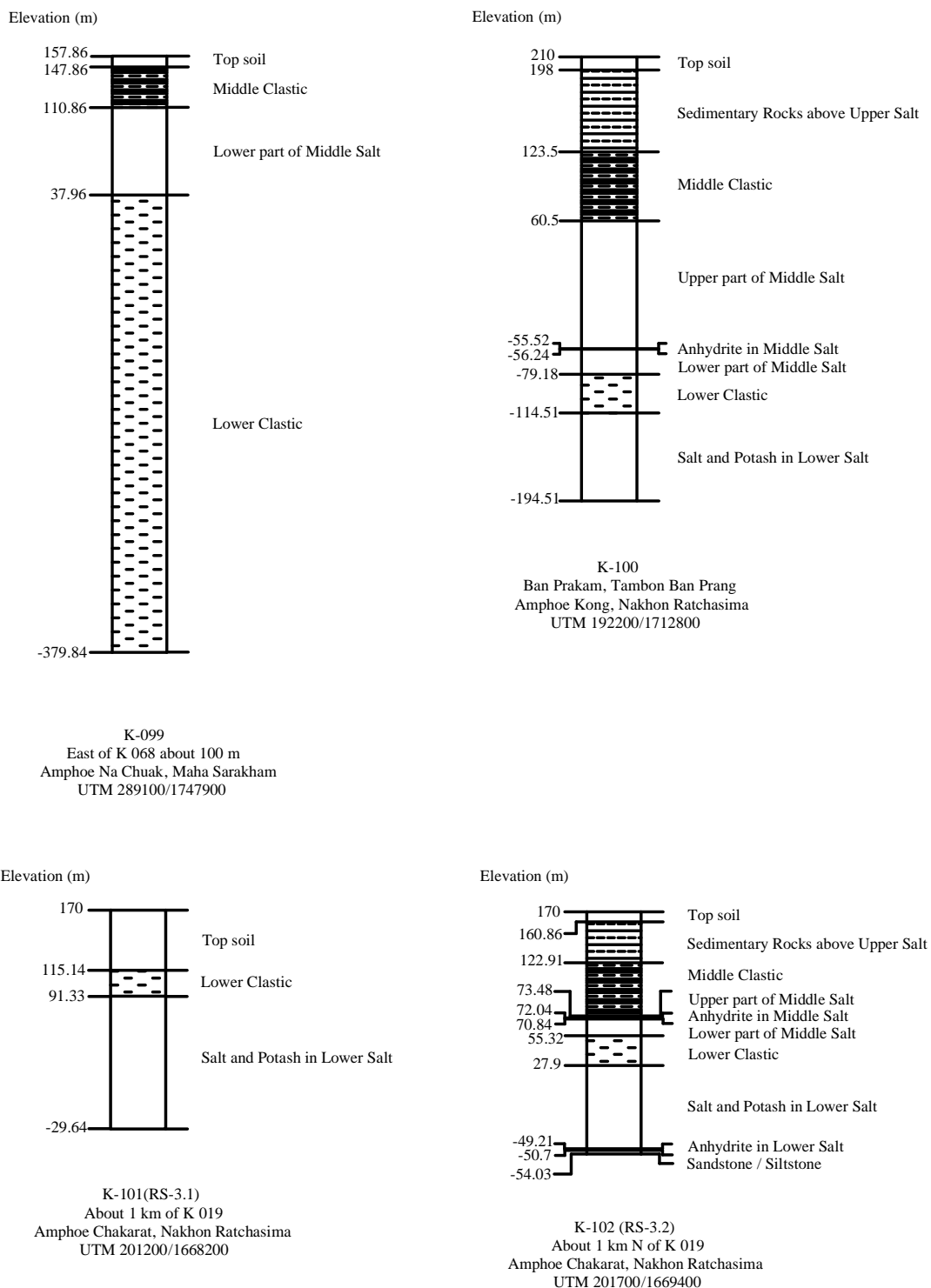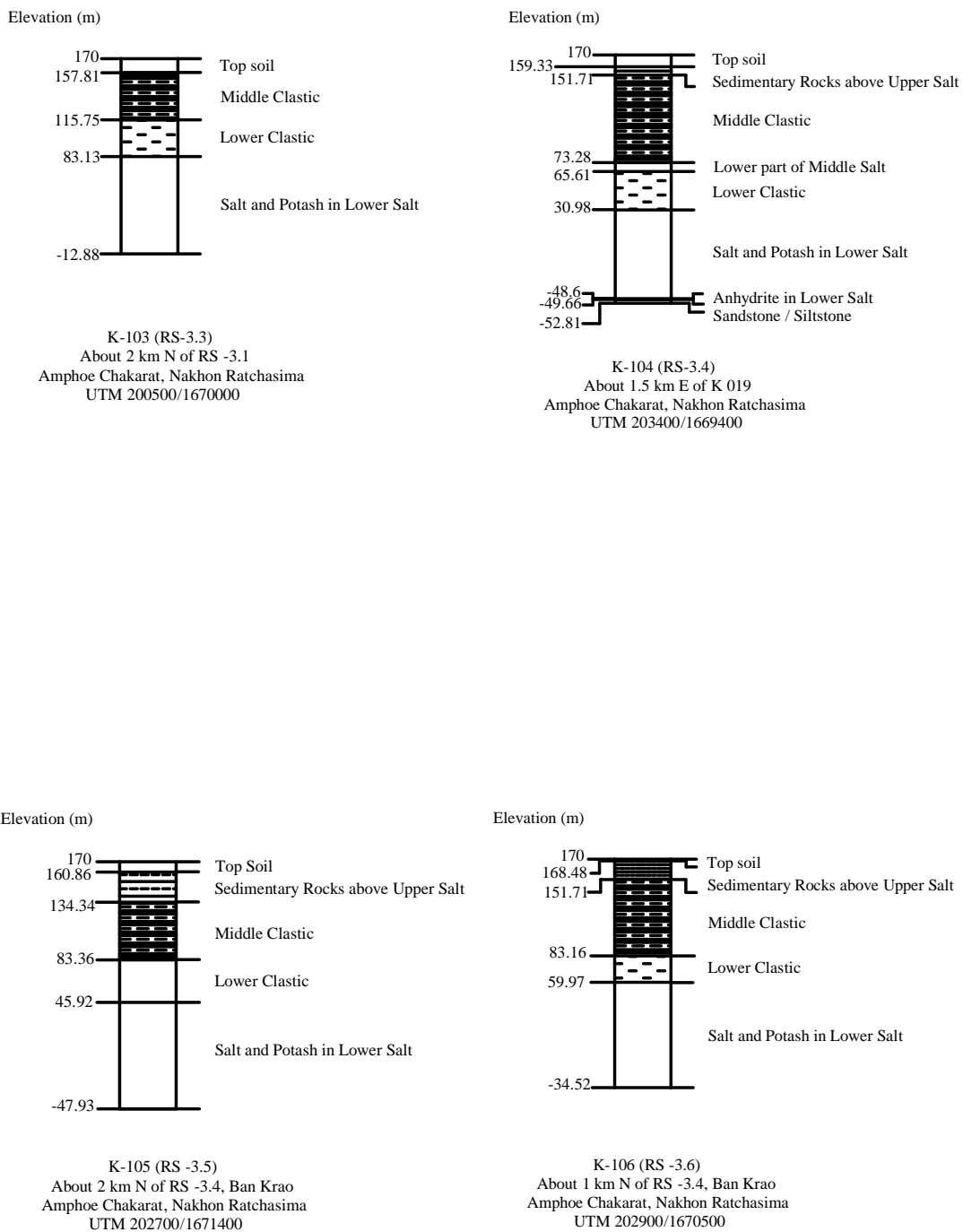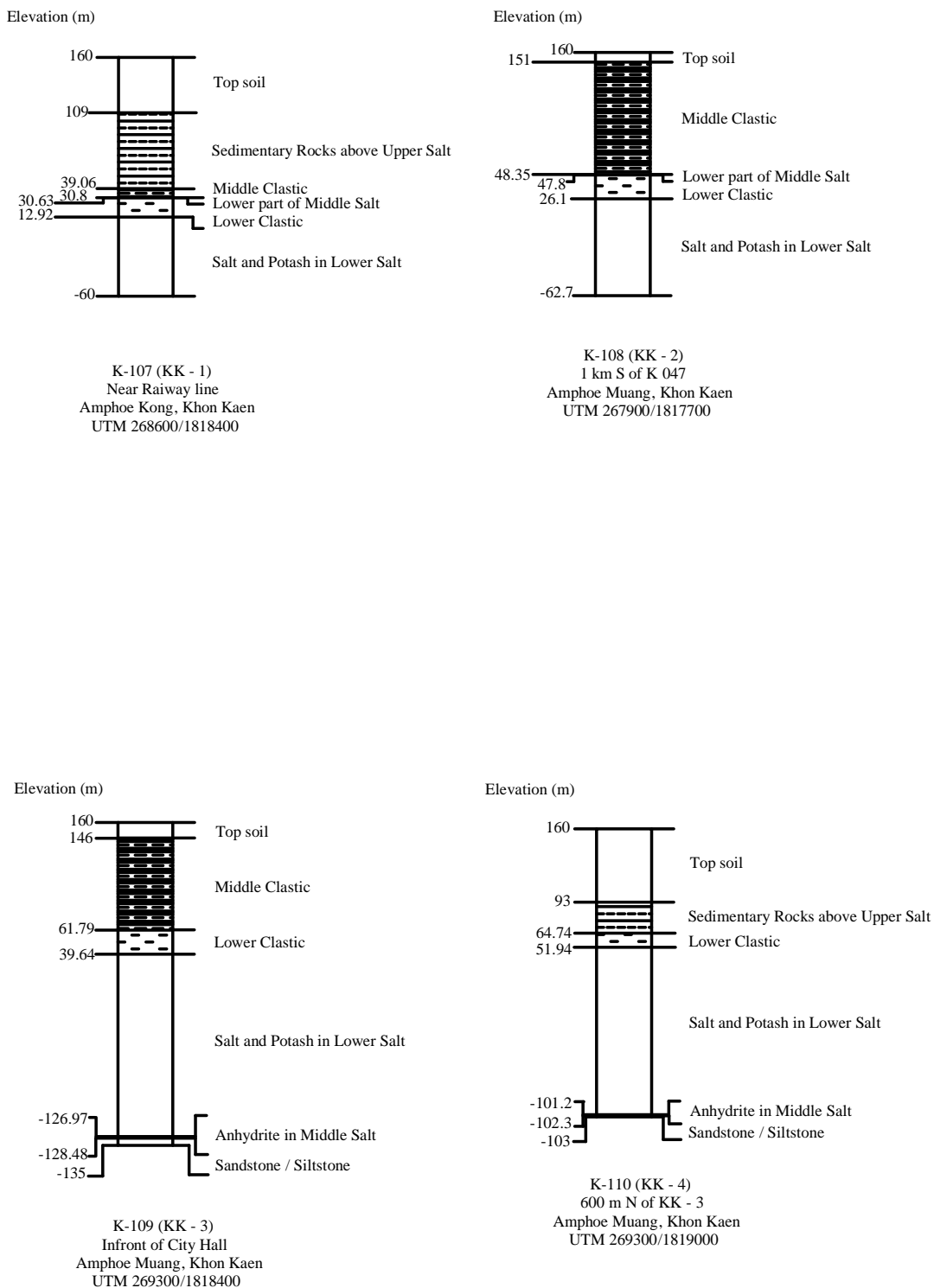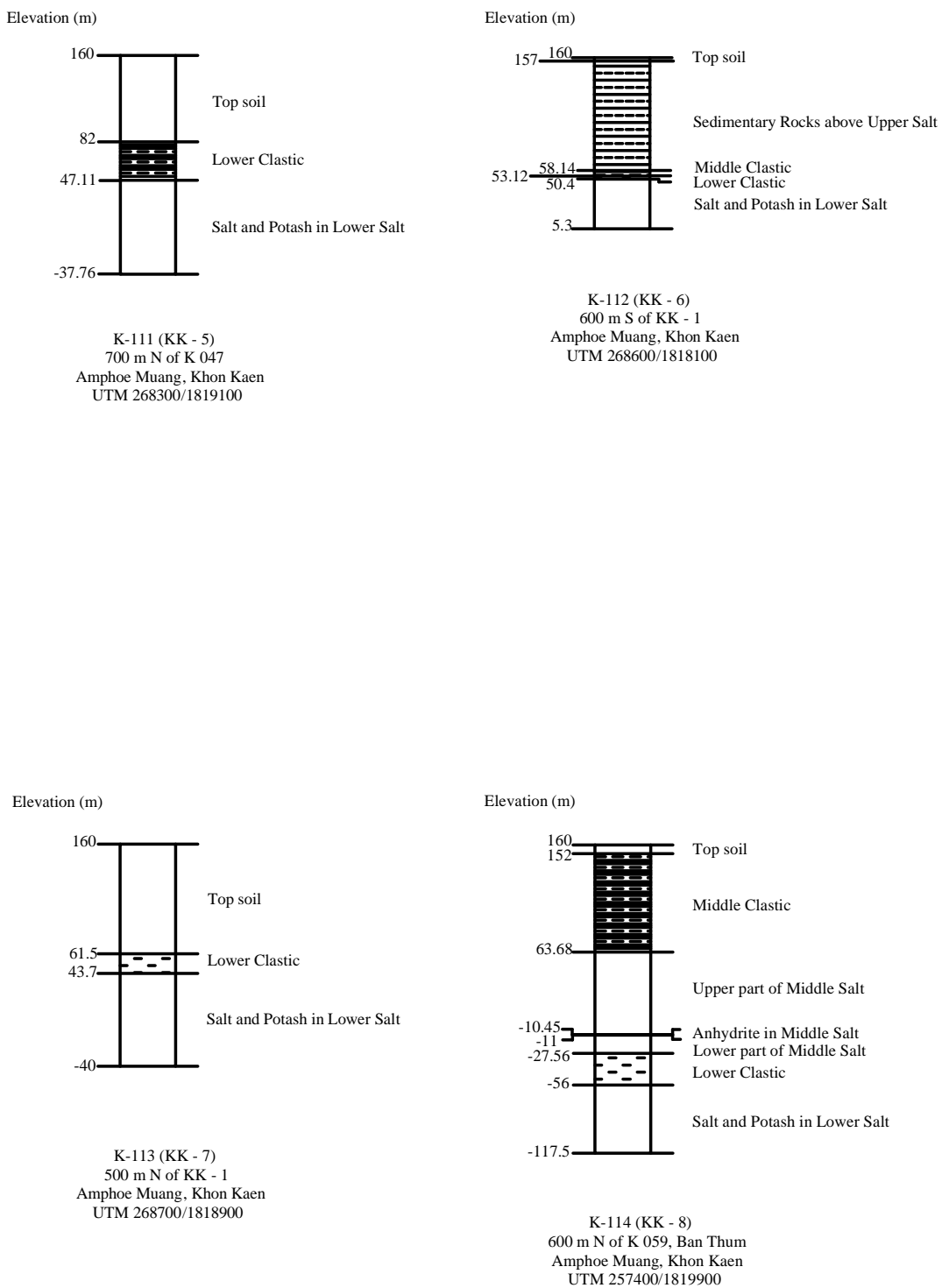**Figure A.34** Identification of stratigraphic units for borehole Nos. KB-21 to KB-24.

Elevation (m)

223.00 —	Top Soil
217.00 —	
	Sedimentary rocks above Upper Salt
90.65 —	Upper Salt
57.69 —	Middle Clastic
24.91 —	
	Upper part of Middle Salt
-45.50 —	Anhydrite in Middle Salt
-46.36 —	Lower part of Middle Salt
-56.90 —	Lower Clastic
-70.55 —	
	Salt and Potash in Lower Salt
-201.38 —	Anhydrite in Lower Salt
-202.00 —	

KB-25
Ban Nong Yai But, Amphoe
Bamnet Narong, Chaiyaphum
UTM 798000/1708000

Elevation (m)

206.00 —	Top Soil
202.00 —	Middle Clastic
148.22 —	Anhydrite in Middle Salt
148.15 —	
	Lower part of Middle Salt
96.58 —	Lower Clastic
77.74 —	
	Salt and Potash in Lower Salt
-3.45 —	

KB-26
Ban Tan, Amphoe Bamnet
Narong, Chaiyaphum
UTM 793800/1712000

Elevation (m)

205.00 —	Top Soil
176.35 —	Middle Clastic
147.20 —	Upper part of Middle Salt
110.31 —	Anhydrite in Middle Salt
109.70 —	Lower part of Middle Salt
89.01 —	Lower Clastic
66.80 —	
	Salt and Potash in Lower Salt
-13.45 —	

KB-27
South of Bamnet Narong Mine,
Ban Khok Phet, Amphoe Bamnet
Narong, Chaiyaphum
UTM 793200/1711500

Elevation (m)

205.00 —	Top Soil
196.00 —	Sedimentary rocks above Upper Salt
143.00 —	
	Upper part of Middle Salt
71.08 —	Anhydrite in Middle Salt
70.45 —	Lower part of Middle Salt
50.25 —	Lower Clastic
33.86 —	
	Salt and Potash in Lower Salt
-6.30 —	

KB-28
About 50 m SW of RS-2.1,
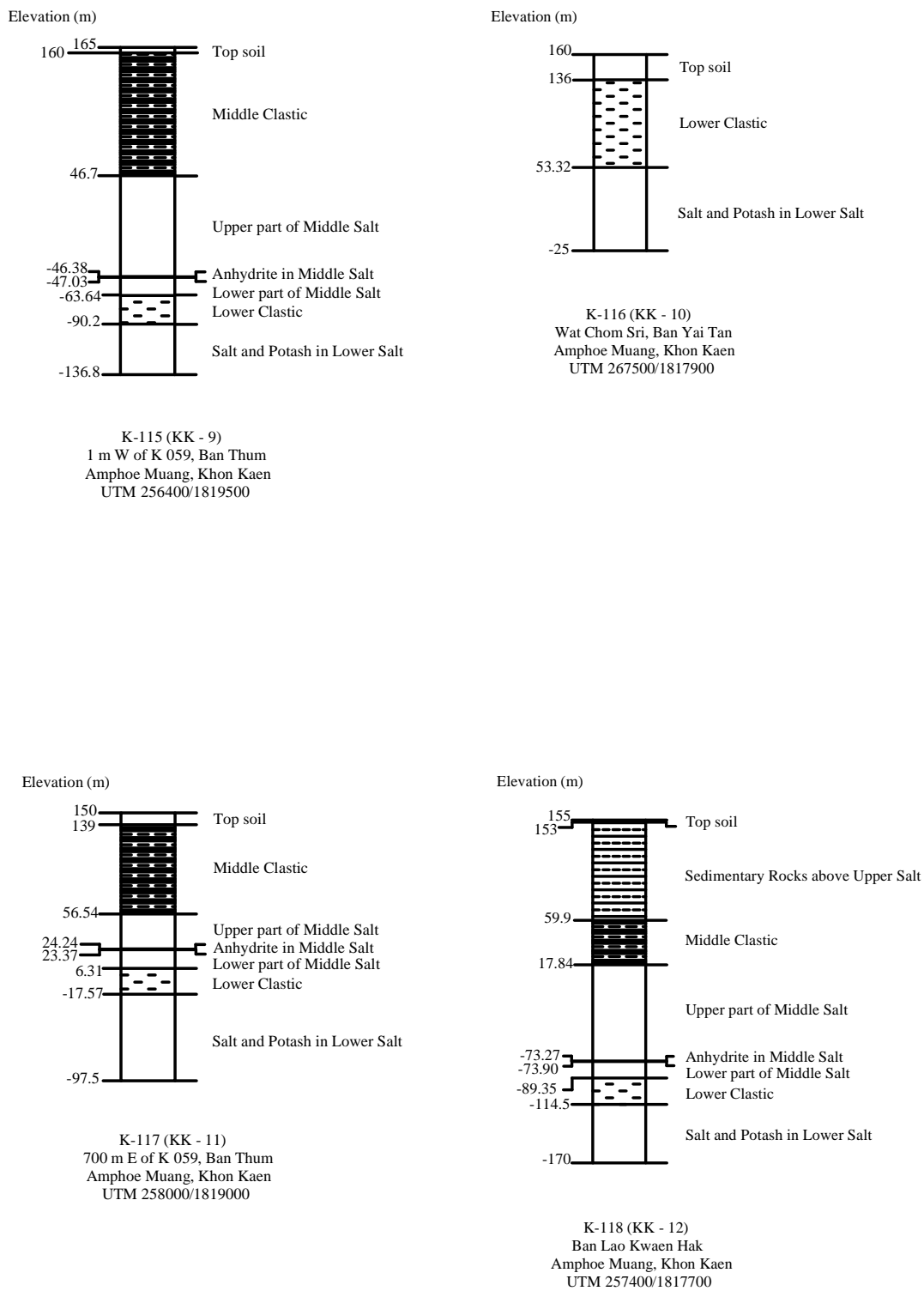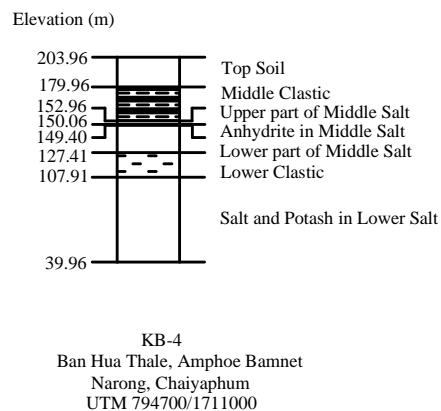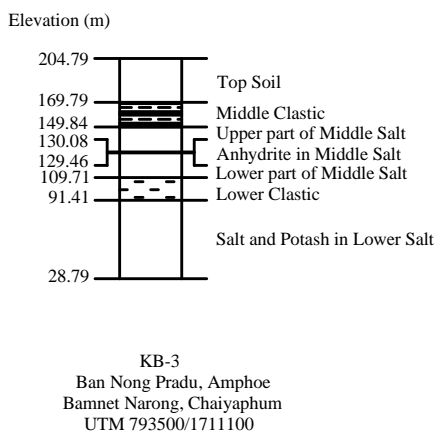Amphoe Bamnet Narong,
Chaiyaphum
UTM 794800/1711500

Figure A.35 Identification of stratigraphic units for borehole Nos. KB-25 to KB-28.

Elevation (m)

205.00 — Top Soil
177.00 — Sedimentary rocks above Upper Salt
144.65 — Lower part of Middle Salt
138.77 — Lower Clastic
123.50 —
92.00 — Salt and Potash in Lower Salt

KB-29
Ban Nong Pradu, Amphoe
Bamnet Narong, Chaiyaphum
UTM 793500/1709700

Elevation (m)

230.00 — Top Soil
227.00 —
Sedimentary rocks above Upper Salt
116.55 — Middle Clastic
79.86 —
Upper part of Middle Salt
-21.16 — Anhydrite in Middle Salt
-22.09 — Lower part of Middle Salt
-41.87 — Lower Clastic
-60.80 —
Salt and Potash in Lower Salt
-178.68 — Anhydrite in Lower Salt
-182.52 — Sandstone/Siltstone
-186.50 —

KB-30
Ban Nong Dong School, Amphoe
Bamnet Narong, Chaiyaphum
UTM 798300/1705200

Elevation (m)

202.00 — Top Soil
189.00 —
Sedimentary rocks above Upper Salt
4.50 —
Upper Salt
-45.03 — Middle Clastic
-60.73 — Lower part of Middle Salt
-82.00 —
Salt and Potash in Lower Salt
-151.43 — Anhydrite in Lower Salt
-152.65 — Sandstone/Siltstone
-157.00 —

KB-31
Tung Samian Tra School,
Amphoe Jaturat, Chaiyaphum
UTM 797100/1716100

Elevation (m)

203.96 — Top Soil
191.49 — Middle Clastic
158.14 — Lower part of Middle Salt
152.96 — Lower Clastic
135.76 —
Salt and Potash in Lower Salt
68.16 —

KB-32
South of KB-4 about 350 m, Ban
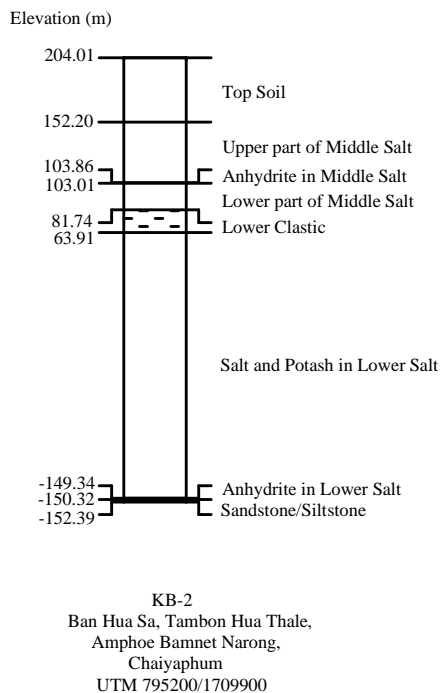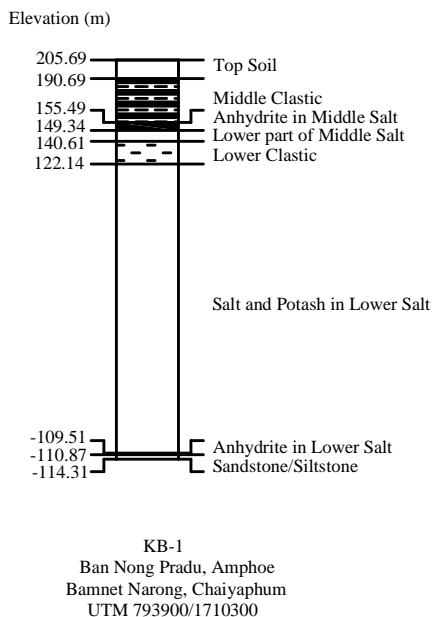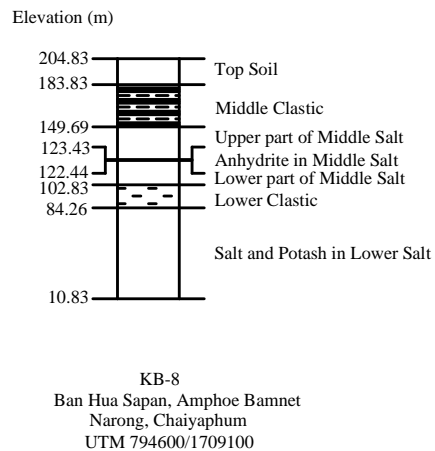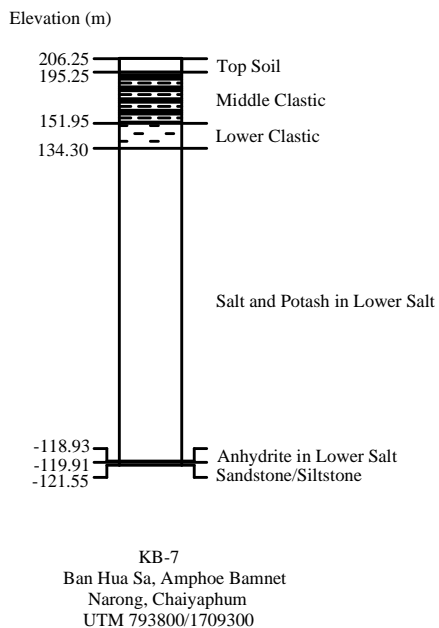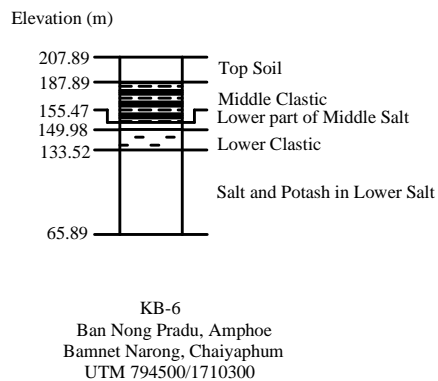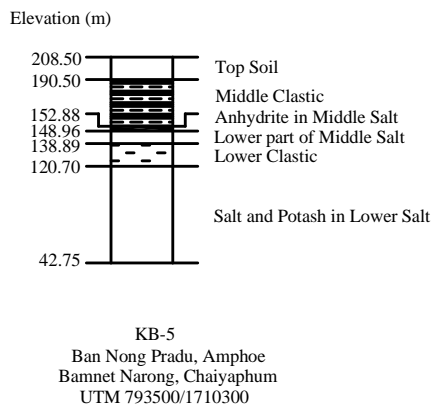Nong Pradu, Amphoe Bamnet
Narong, Chaiyaphum
UTM 794600/1710700

Figure A.36 Identification of stratigraphic units for borehole Nos. KB-29 to KB-32.

Elevation (m)

204.00 — Top Soil

168.37 — Middle Clastic

146.00 — Upper part of Middle Salt

131.06 — Anhydrite in Middle Salt
130.56 — Lower part of Middle Salt
111.05 — Lower Clastic

90.37 — Salt and Potash in Lower Salt

30.35 —

KB-33
South-West of KB-27 about 700
m, Ban Nong Pradu, Amphoe
Bamnet Narong, Chaiyaphum
UTM 796900/1711100

Elevation (m)

220.00 — Top Soil
210.80 —

Sedimentary rocks above Upper Salt

-3.82 —

Upper Salt

-56.60 — Middle Clastic

-84.37 —

Lower part of Middle Salt

-134.90 — Salt and Potash in Lower Salt

-172.00 —

KB-34
Ban Nong Dhon, Amphoe Jaturat,
Chaiyaphum
UTM 800800/1717000

Elevation (m)

220.00 — Top Soil
214.00 —

Sedimentary rocks above Upper Salt

9.08 —

Upper Salt

-35.95 — Middle Clastic

-66.39 —

Upper part of Middle Salt

-121.50 — Anhydrite in Middle Salt
-123.15 — Lower part of Middle Salt
-136.20 — Lower Clastic
-145.70 — Salt and Potash in Lower Salt

-171.00 —

KB-35
Wat Pho Lom, Tambon Nong
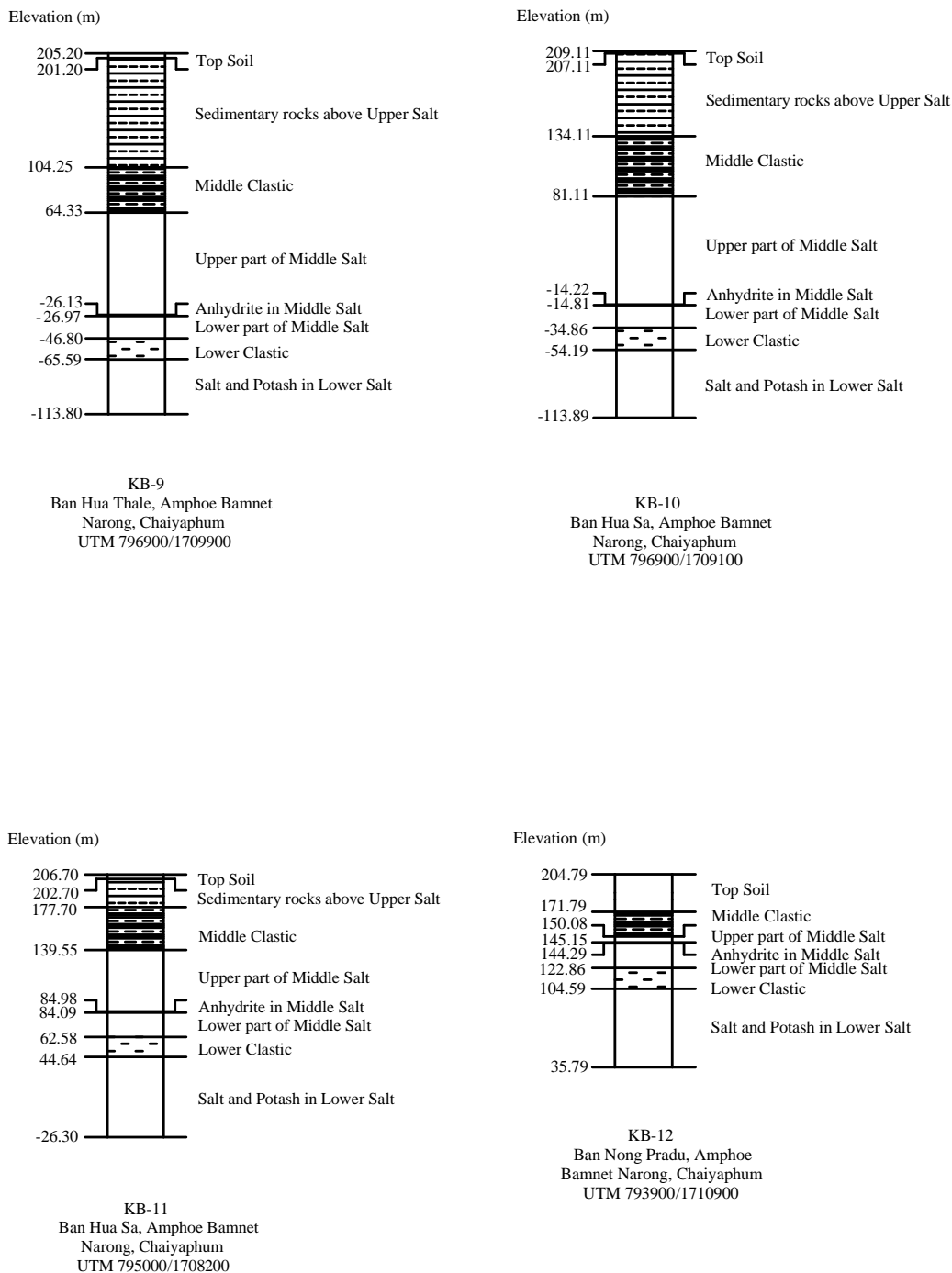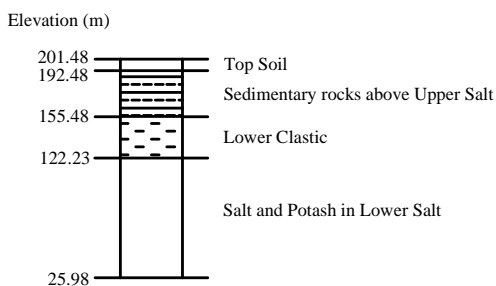Dhon, Ban Non Fai, Amphoe
Jaturat, Chaiyaphum
UTM 799500/1717000

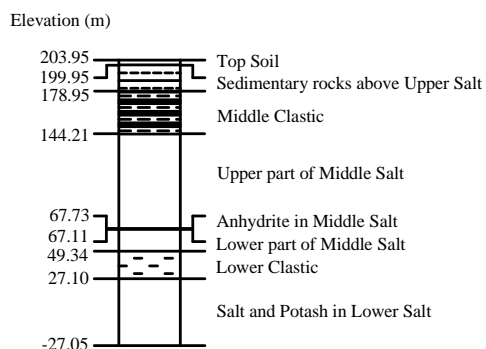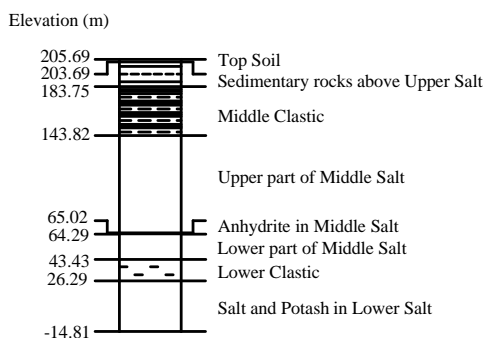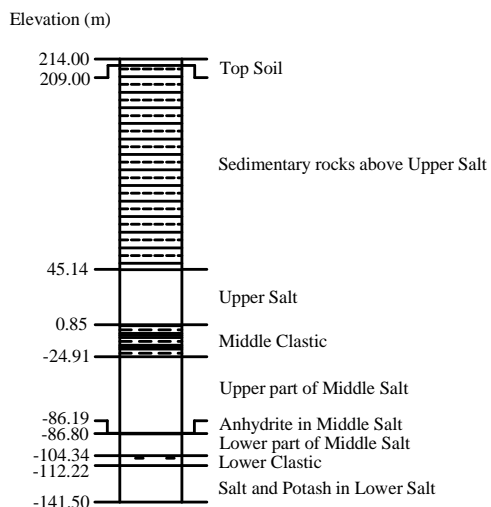**Figure A.37** Identification of stratigraphic units for borehole Nos. KB-33 to KB-35.

Elevation (m)

206.25
201.68
166.66
152.00
105.48
104.29
93.35
86.31

-7.72

Top Soil
Sedimentary rocks above Upper Salt
Middle Clastic
Upper part of Middle Salt
Anhydrite in Middle Salt
Lower part of Middle Salt
Lower Clastic

Salt and Potash in Lower Salt

PQ-1
4 m S of RS-2.0, Ban Tan,
Amphoe Bamnet Narong,
Chaiyapum
UTM 794100/1712100

Elevation (m)

204.38
188.53
160.18

-9.28

Top Soil
Middle Clastic

Salt and Potash in Lower Salt

PQ-2
Ban Tan,Amphoe Bamnet
Narong,Chaiyapum
UTM 794100/1712700

Elevation (m)

204.56
169.51
155.18
147.61

-10.32

Top Soil
Sedimentary rocks above Upper Salt
Lower Clastic

Salt and Potash in Lower Salt

PQ-3
Ban Wang Ka-Am,
Amphoe Bamnet Narong,
Chaiyapum
UTM 793900/17155000

Elevation (m)

209.44
201.64
147.44
116.48
73.24
73.11
50.94
32.20
-14.59

Top Soil
Sedimentary rocks above Upper Salt
Middle Clastic
Upper part of Middle Salt
Anhydrite in Middle Salt
Lower part of Middle Salt
Lower Clastic
Salt and Potash in Lower Salt

PQ-4
Ban Khok Phet,
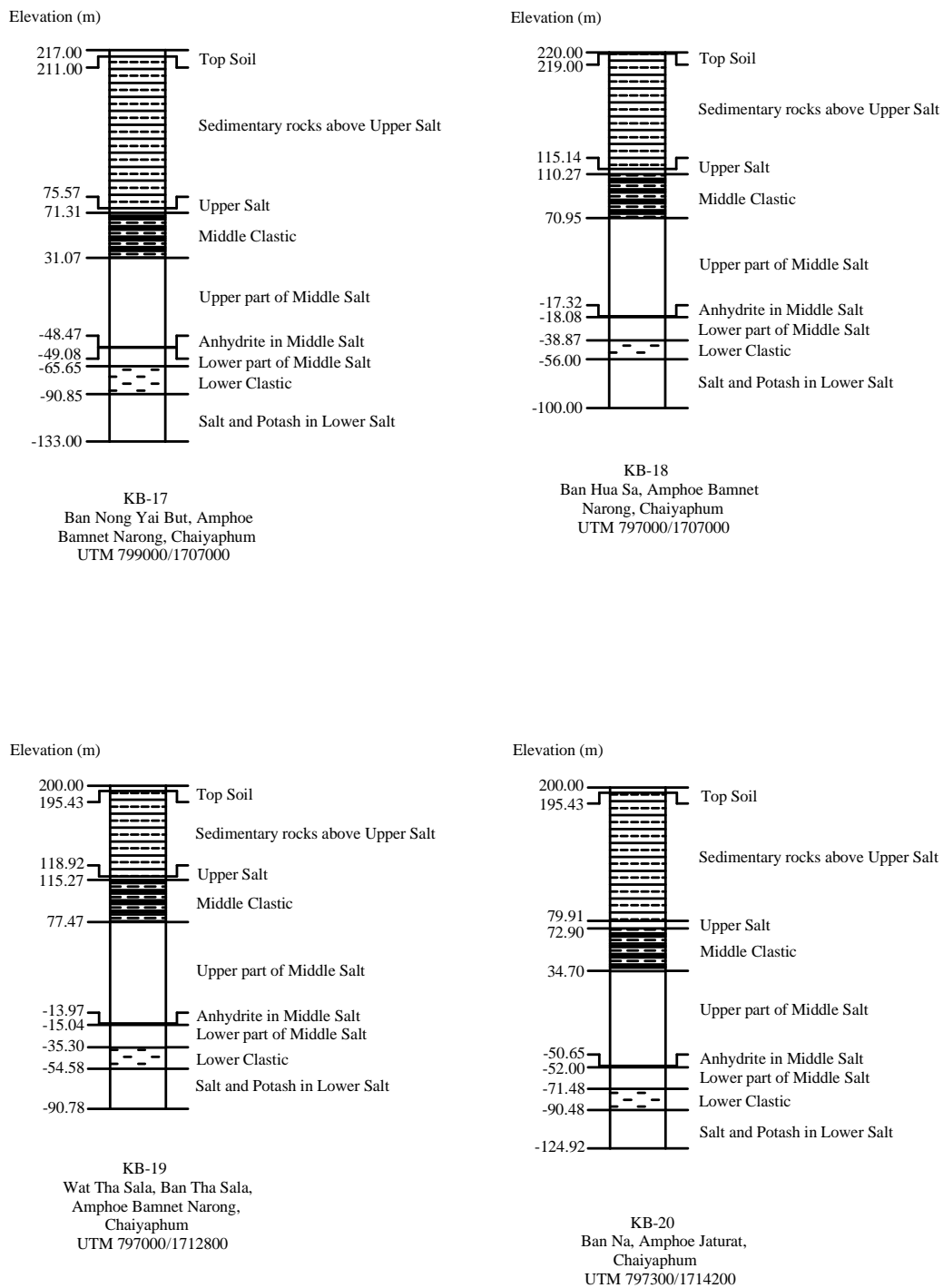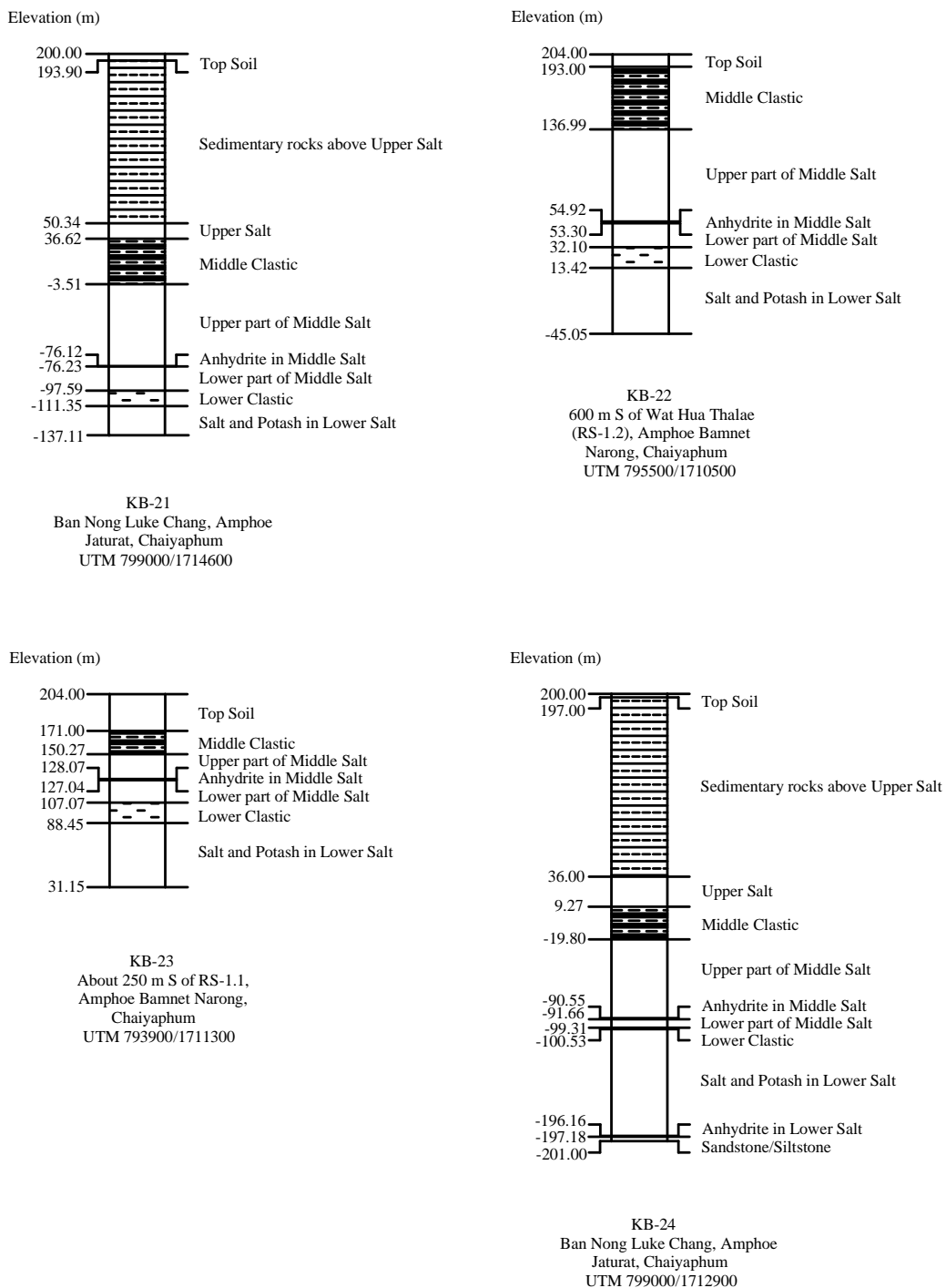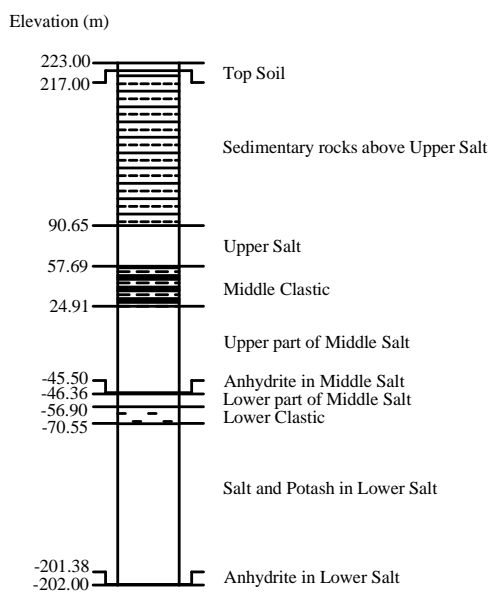Amphoe Bamnet Narong,
Chaiyapum
UTM 793300/17125000

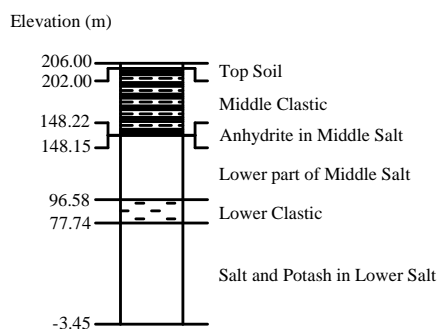**Figure A.38** Identification of stratigraphic units for borehole Nos. PQ-1 to PQ-4.

Elevation (m)

204.65 — Top Soil
182.40 — Middle Clastic
148.26 — Upper part of Middle Salt
118.24 — Anhydrite in Middle Salt
117.30 — Lower part of Middle Salt
97.21 — Lower Clastic
95.53 — Salt and Potash in Lower Salt
61.70 —

PQ-5
Ban Tan (near RS-2.7),
Amphoe Bamnet Narong,
Chaiyapum
UTM 793500/1711600

Elevation (m)

206.30 — Top Soil
198.73 — Sedimentary rocks above Upper Salt
174.37 — Lower Clastic
144.88 — Salt and Potash in Lower Salt
143.51 —

PQ-6
About 450 m north of PQ-5,
Ban Tan , Amphoe Bamnet
Narong, Chaiyapum
UTM 793500/1712000

Elevation (m)

205.25 — Top Soil
195.42 — Lower Clastic
148.56 — Salt and Potash in Lower Salt
145.51 —

PQ-7
About 300 m north of PQ-5,
Ban Tan , Amphoe Bamnet
Narong, Chaiyapum
UTM 793400/1711800

Elevation (m)

205.83 — Top Soil
198.51 — Sedimentary rocks above Upper Salt
170.47 —

PQ-8
About 100 m north of PQ-6,
Ban Tan , Amphoe Bamnet
Narong, Chaiyapum
UTM 793500/1712200

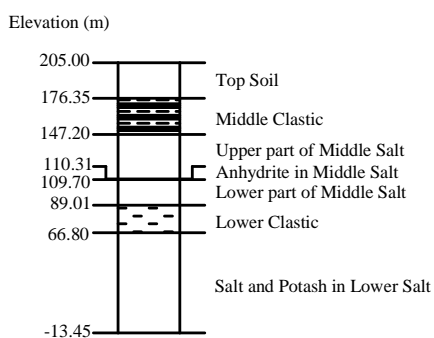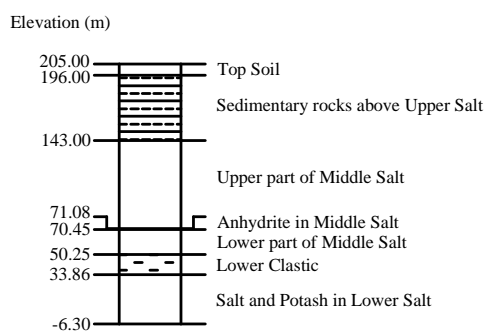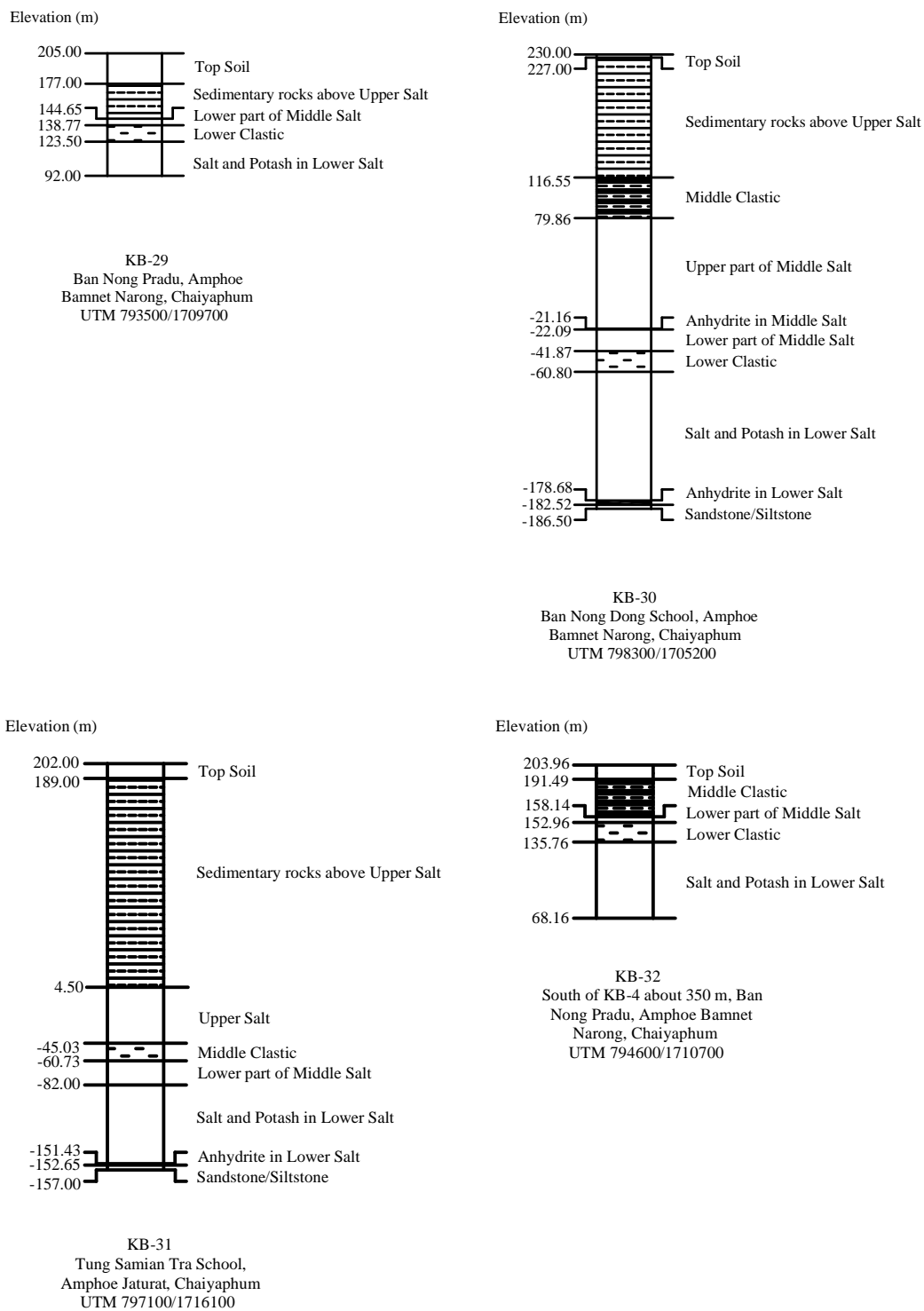**Figure A.39** Identification of stratigraphic units for borehole Nos. PQ-5 to PQ-8.

Elevation (m)

204.55 — Top Soil
178.64 —
        Middle Clastic
149.79 —
        Upper part of Middle Salt
118.37 —
117.45 — Anhydrite in Middle Salt
        Lower part of Middle Salt
97.31 —
        Lower Clastic
76.53 —
        Salt and Potash in Lower Salt
34.47 —

PQ-9
About 100 m, south of PQ-5
Ban Tan, Amphoe Bamnet
Narong, Chaiyapum
UTM 793600/1711500

Elevation (m)

205.60 — Top Soil
176.95 —
167.19 — Sedimentary rocks above Upper Salt

PQ-10
Ban Khok Phet,
Amphoe Bamnet Narong,
Chaiyapum
UTM 793300/1711500

Elevation (m)

205.44 — Top Soil
182.44 — Sedimentary rocks above Upper Salt
179.33 — Lower Clastic
148.49 —
139.60 — Salt and Potash in Lower Salt

PQ-11
150 m east of PQ-10,
Ban Khok Phet , Amphoe
Bamnet Narong, Chaiyapum
UTM 793400/1711600

Figure A.40 Identification of stratigraphic units for borehole Nos. PQ-9 to PQ-11.

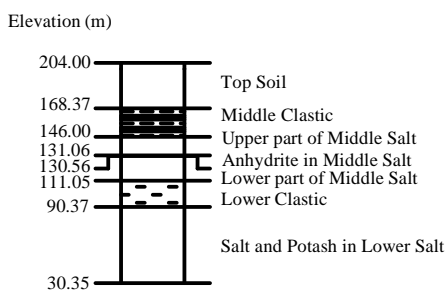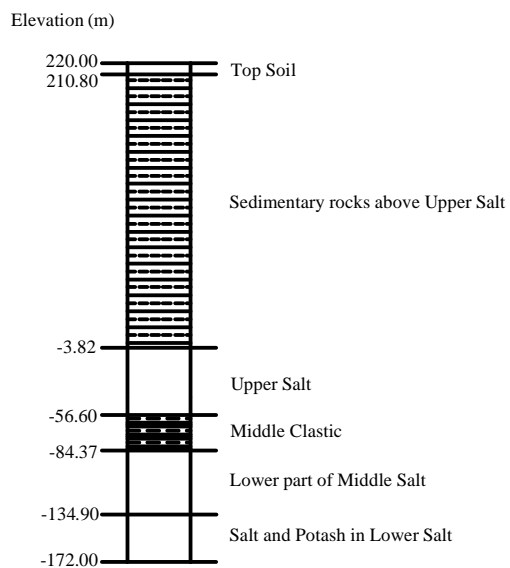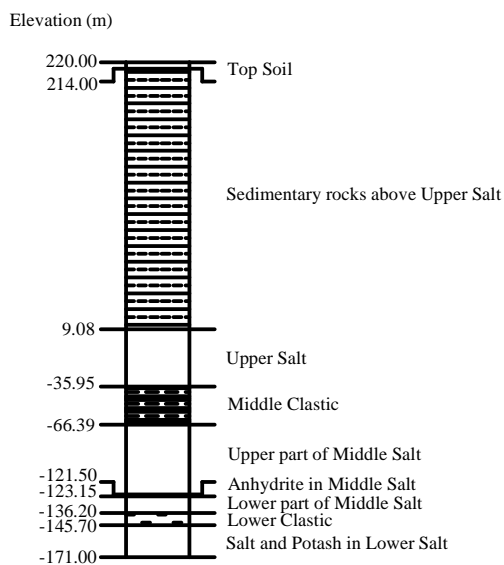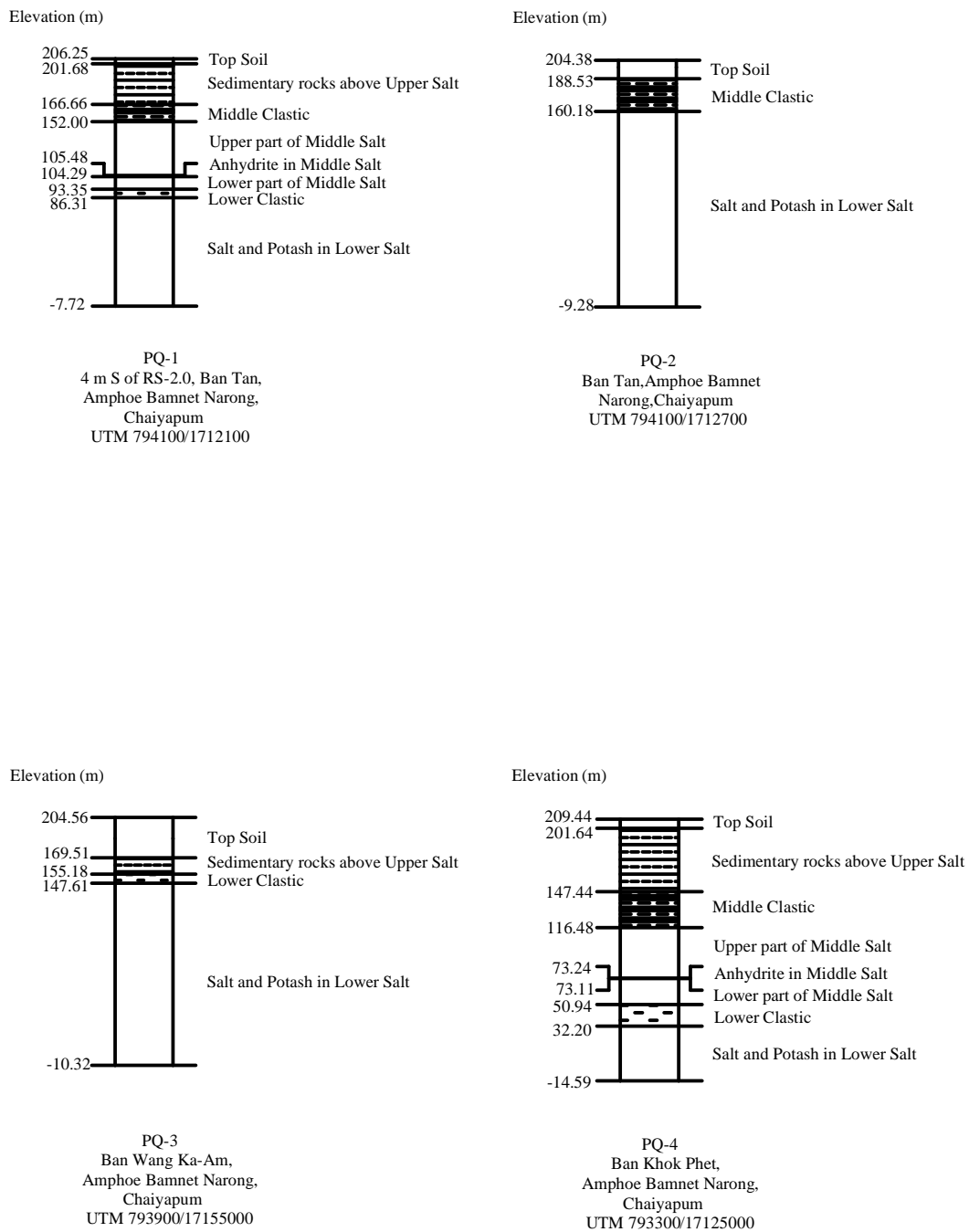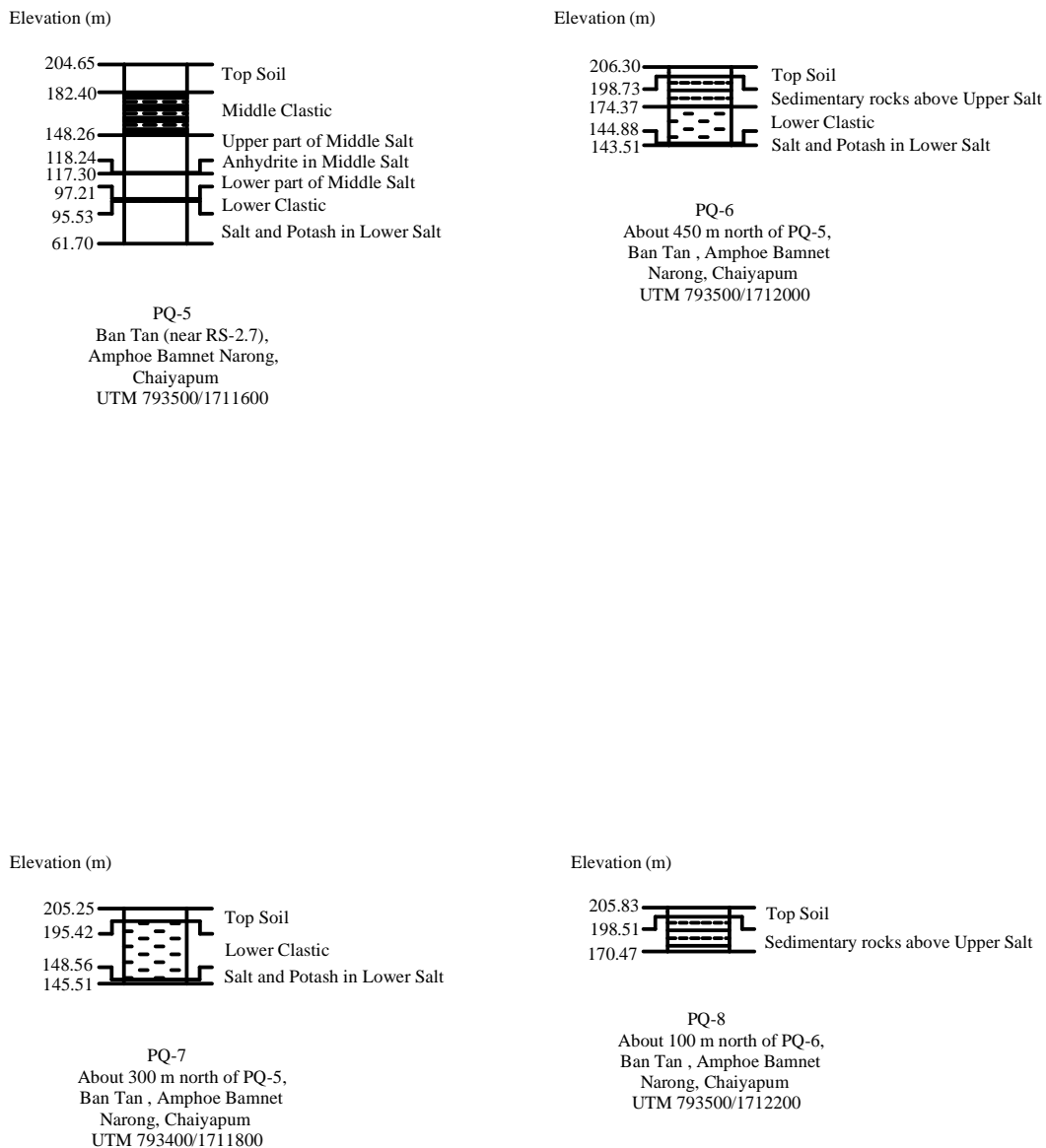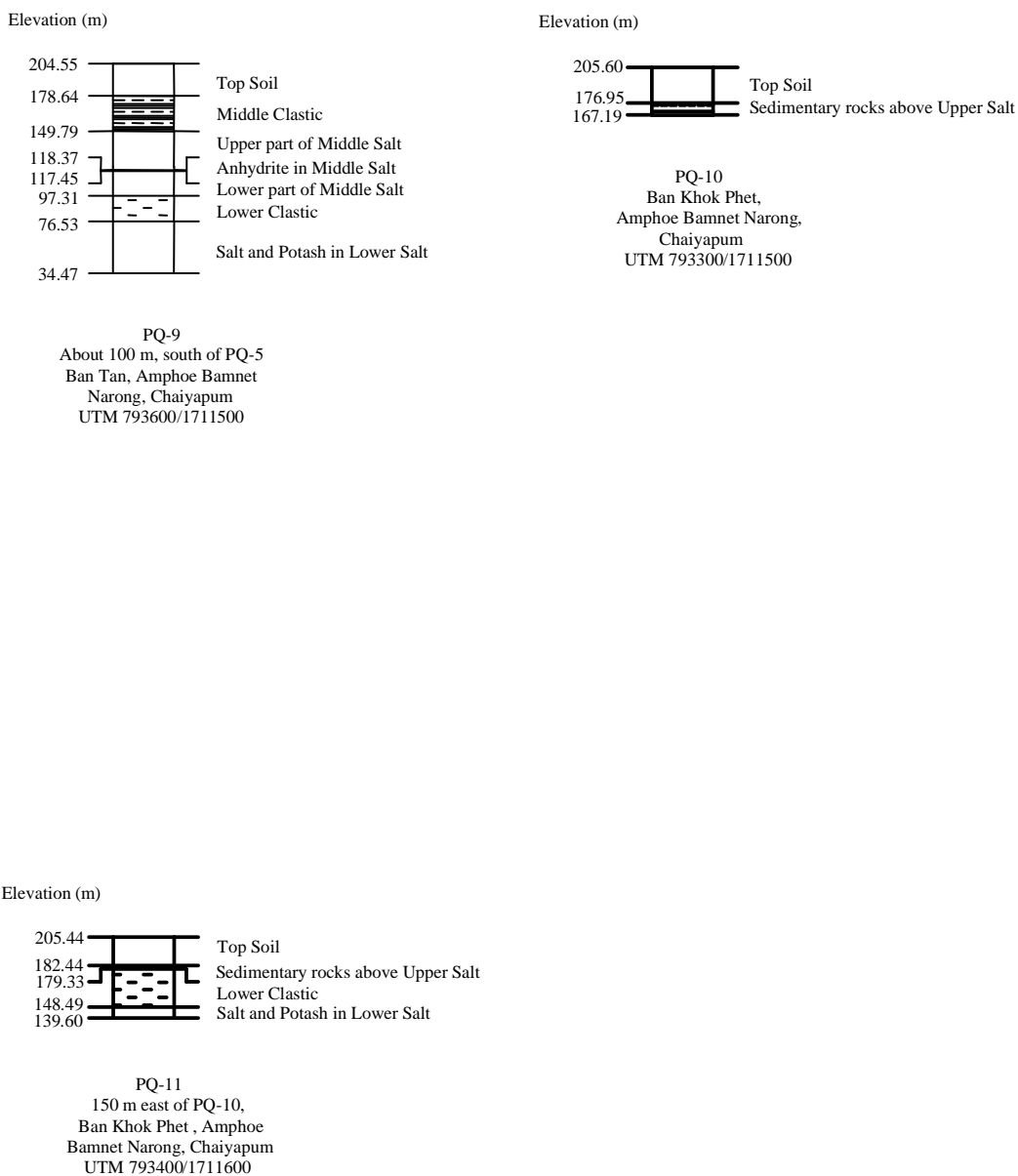**Figure A.41** Identification of stratigraphic units for borehole Nos. RS-1.2 to RS-1.4.

Elevation (m)

205.25 — Top Soil
192.45 — Sedimentary rocks above Upper Salt

163.95 — Middle Clastic

129.35 — Upper part of Middle Salt

42.13 — Anhydrite in Middle Salt
41.45 — Lower part of Middle Salt
21.63 — Lower Clastic
4.49 —

Salt and Potash in Lower Salt

-133.08 — Anhydrite in Lower Salt
-134.30 — Sandstone/Siltstone
-136.13 —

RS-1.5
Wat Pa Samakkhi Tham, Ban
Krathumphra, Amphoe Bamnet
Narong, Chaiyaphum
UTM 795600/1713800

Elevation (m)

203.10 — Top Soil
183.29 — Sedimentary rocks abover Upper Salt
172.01 — Middle Clastic
156.28 — Lower Clastic
151.22 —

Salt and Potash in Lower Salt

-79.17 — Anhydrite in Lower Salt
-80.73 —
-84.94 — Sandstone/Siltstone

RS-1.6
Wat Sarika, Ban Wang Ka-Am,
Amphoe Bamnet Narong,
Chaiyaphum
UTM 794300/1714600

Elevation (m)

206.25 — Top Soil
200.05 — Sedimentary rocks above Upper Salt

166.85 — Middle Clastic
152.66 — Upper part of Middle Salt

106.89 — Anhydrite in Middle Salt
104.85 — Lower part of Middle Salt
93.35 — Lower Clastic
87.02 —

Salt and Potash in Lower Salt

-45.21 —

RS-2.0
Ban Tan, Amphoe Bamnet
Narong, Chaiyaphum
UTM 794100/1712200

Elevation (m)

205.26 — Top Soil
202.21 — Sedimentary rocks above Upper Salt

170.67 — Middle Clastic

133.48 — Upper part of Middle Salt

50.83 — Anhydrite in Middle Salt
50.22 — Lower part of Middle Salt
30.73 — Lower Clastic
15.22 — Salt and Potash in Lower Salt
6.84 —

RS-2.1
Ban Tan, Amphoe Bamnet
Narong, Chaiyaphum
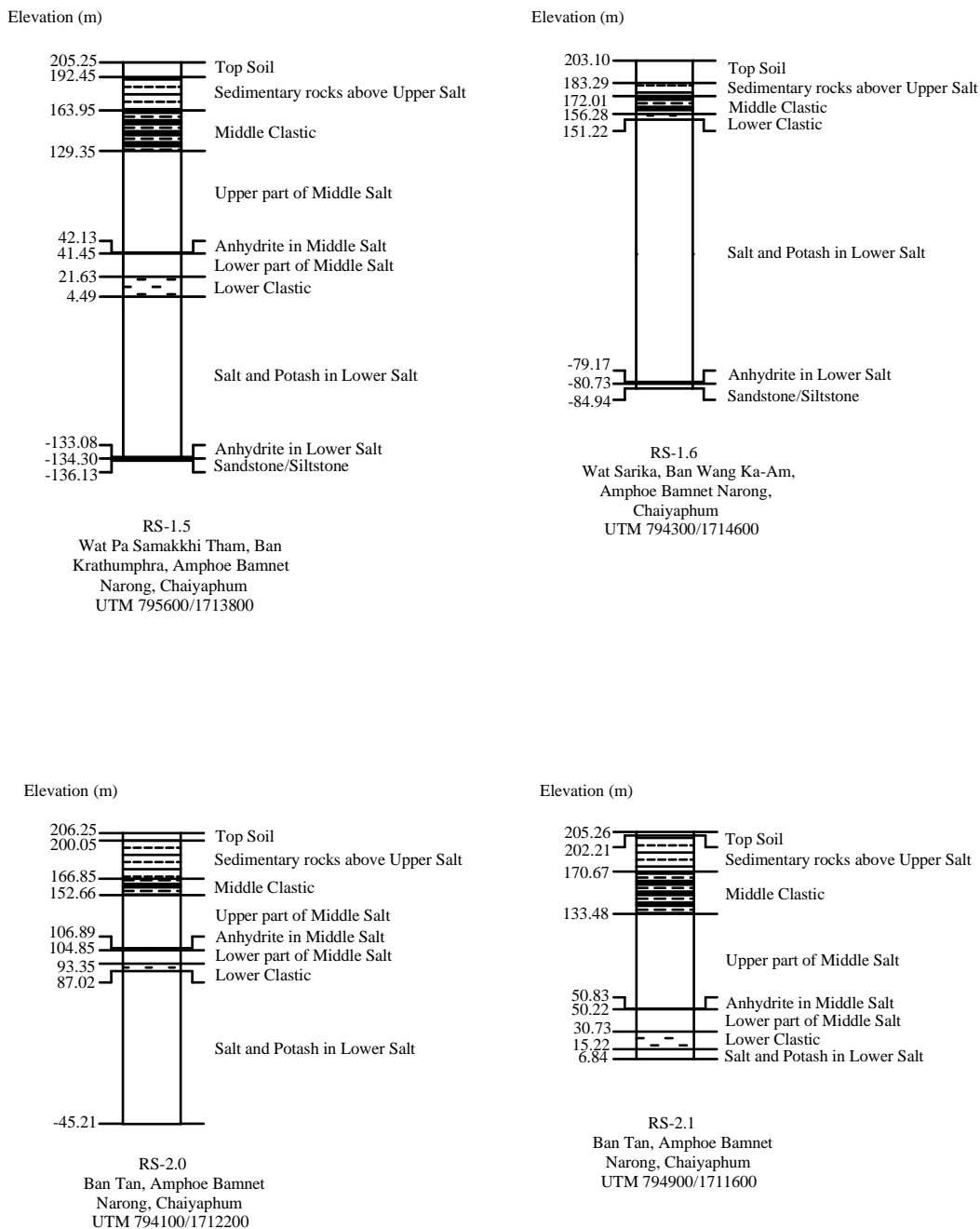UTM 794900/1711600

Figure A.42 Identification of stratigraphic units for borehole Nos. RS-1.5 to RS-1.6

and RS-2.0 to RS-2.1.

Elevation (m)

202.26 ─ Top Soil
190.80 ─ Sedimentary rocks above Upper Salt
159.66 ─ Lower Clastic
141.86 ─

Salt and Potash in Lower Salt

-143.11 ─ Anhydrite in Lower Salt
-144.25 ─ Sandstone/Siltstone
-146.74 ─

RS-2.2
Ban Hua Bung, Amphoe Bamnet
Narong, Chaiyaphum
UTM 795900/1712100

Elevation (m)

207.90 ─ Top Soil
181.90 ─ Sedimentary rocks above Upper Salt
175.90 ─ Middle Clastic
141.38 ─ Upper part of Middle Salt
105.18 ─ Anhydrite in Middle Salt
104.34 ─ Lower part of Middle Salt
83.54 ─ Lower Clastic
63.53 ─

Salt and Potash in Lower Salt

-10.06 ─ Anhydrite in Lower Salt
-11.05 ─ Sandstone/Siltstone
-14.30 ─

RS-2.3
Ban Hin Tang, Amphoe Bamnet
Narong, Chaiyaphum
UTM 792300/1714700

Elevation (m)

209.05 ─ Top Soil
190.69 ─ Sedimentary rocks above Upper Salt
161.20 ─ Middle Clastic
138.49 ─ Upper part of Middle Salt
123.71 ─ Anhydrite in Middle Salt
123.50 ─ Lower part of Middle Salt
105.88 ─ Lower Clastic
88.10 ─

Salt and Potash in Lower Salt

25.13 ─ Anhydrite in Lower Salt
23.85 ─ Sandstone/Siltstone
22.21 ─

RS-2.4
Ban Khok Faek, Amphoe Bamnet
Narong, Chaiyaphum
UTM 790300/1711600

Elevation (m)

205.45 ─ Top Soil
159.73 ─ Lower Clastic
143.63 ─

Salt and Potash in Lower Salt

-17.05 ─

RS-2.5
Ban Tan, Amphoe Bamnet
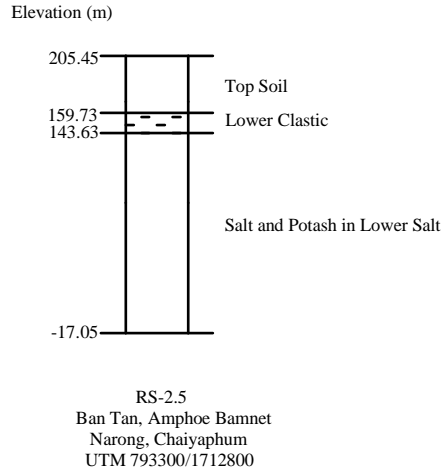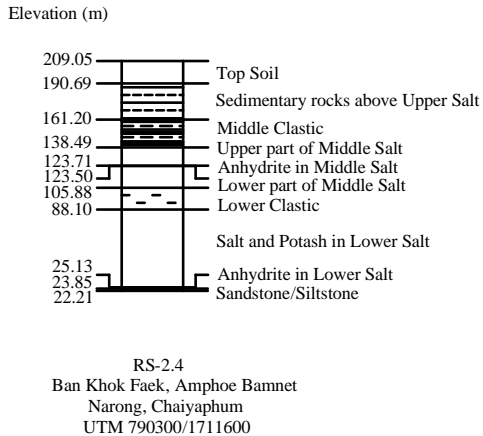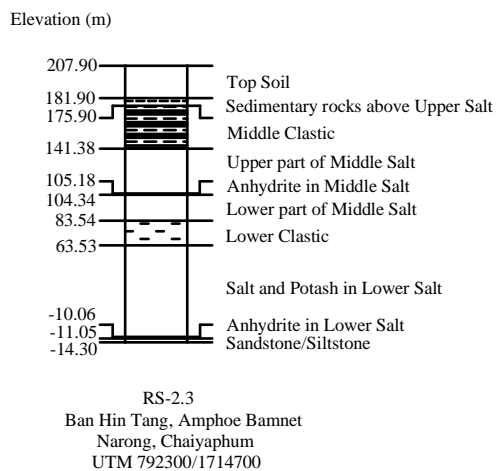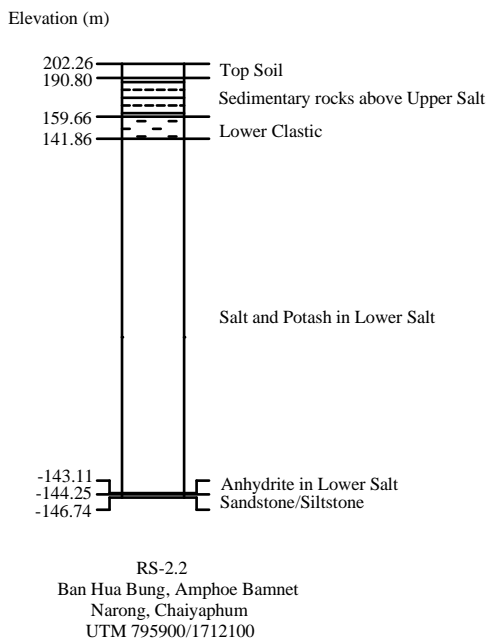Narong, Chaiyaphum
UTM 793300/1712800

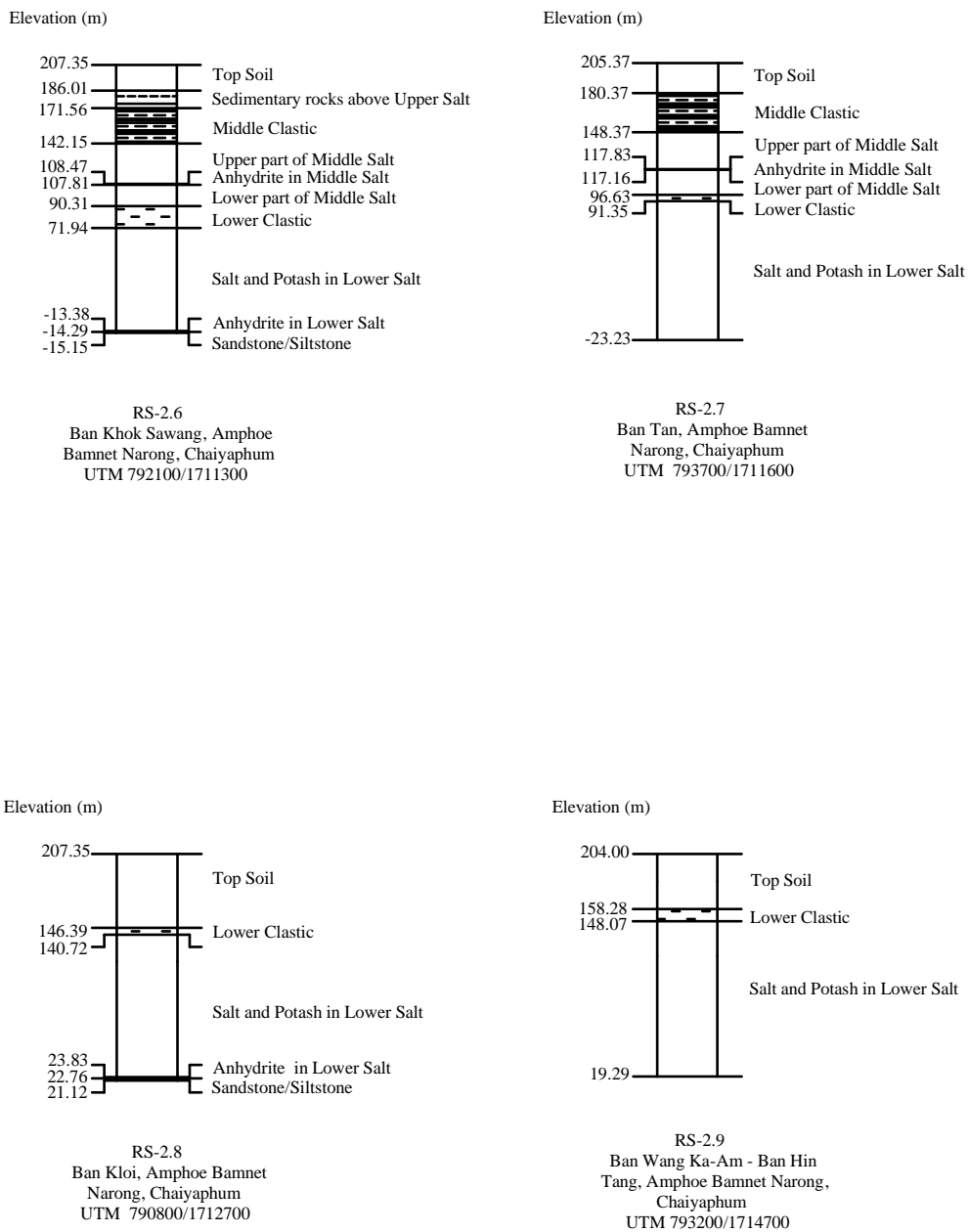**Figure A.43** Identification of stratigraphic units for borehole Nos. RS-2.2 to RS-2.5.

Figure A.44 Identification of stratigraphic units for borehole Nos. RS-2.6 to RS-2.9.
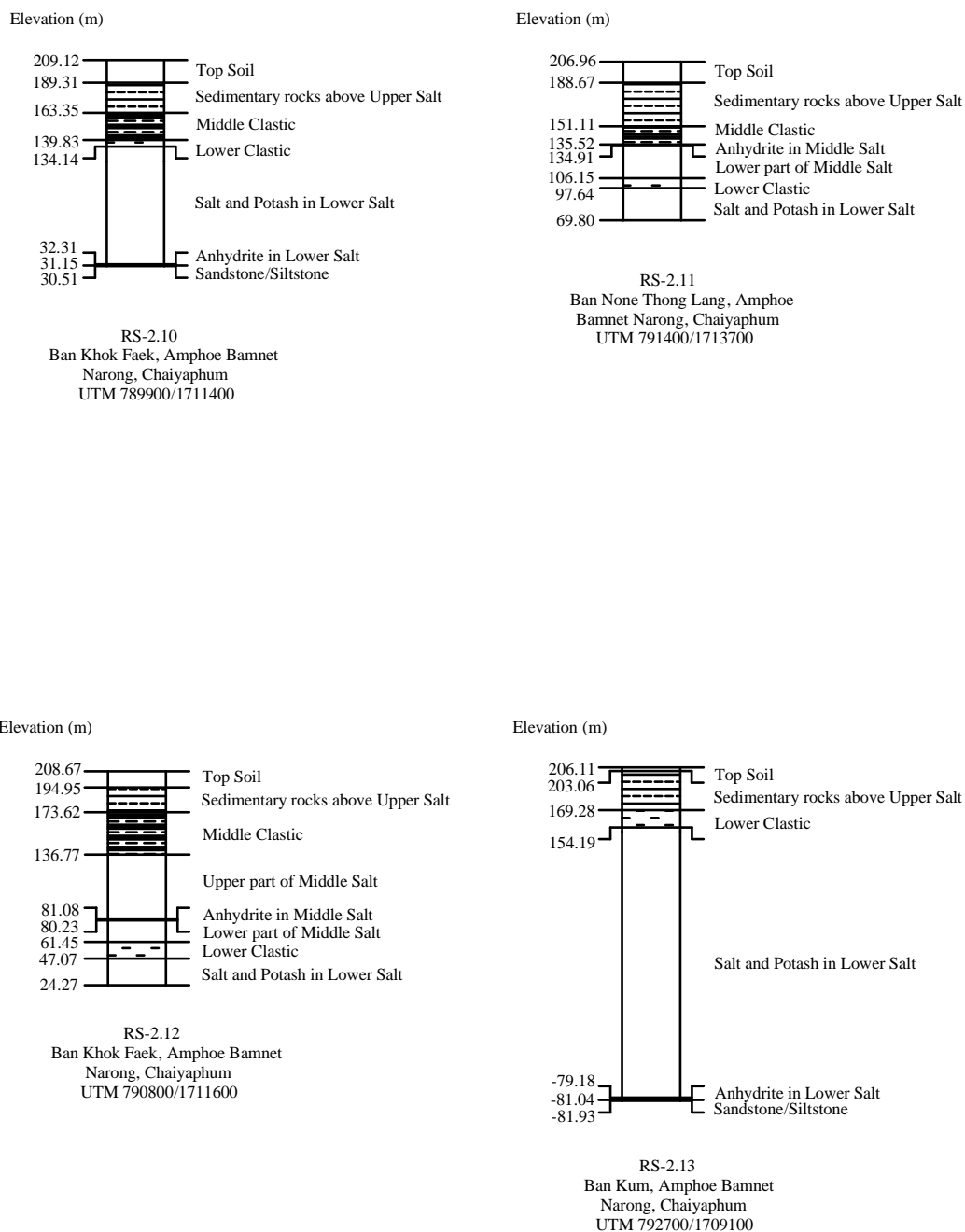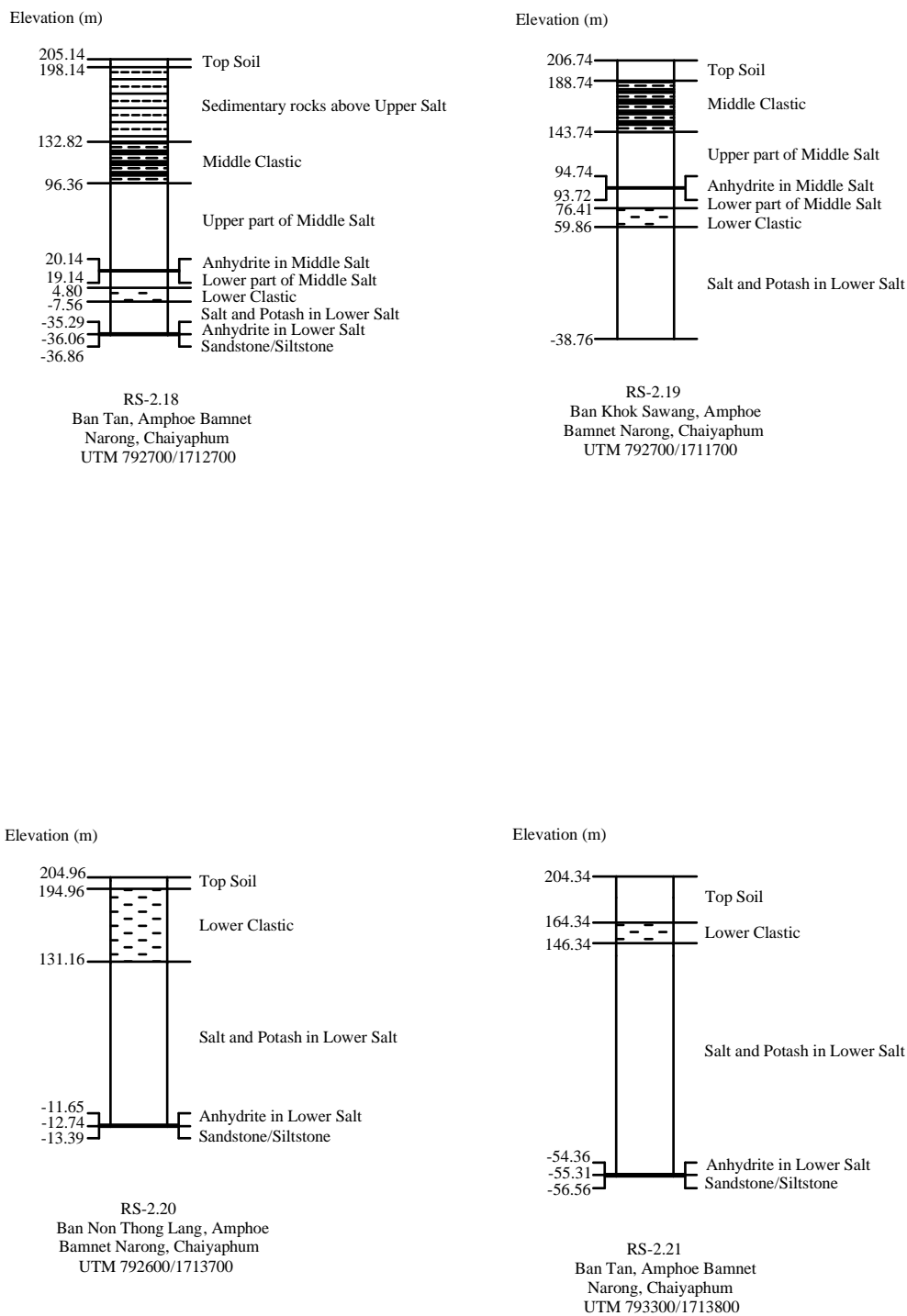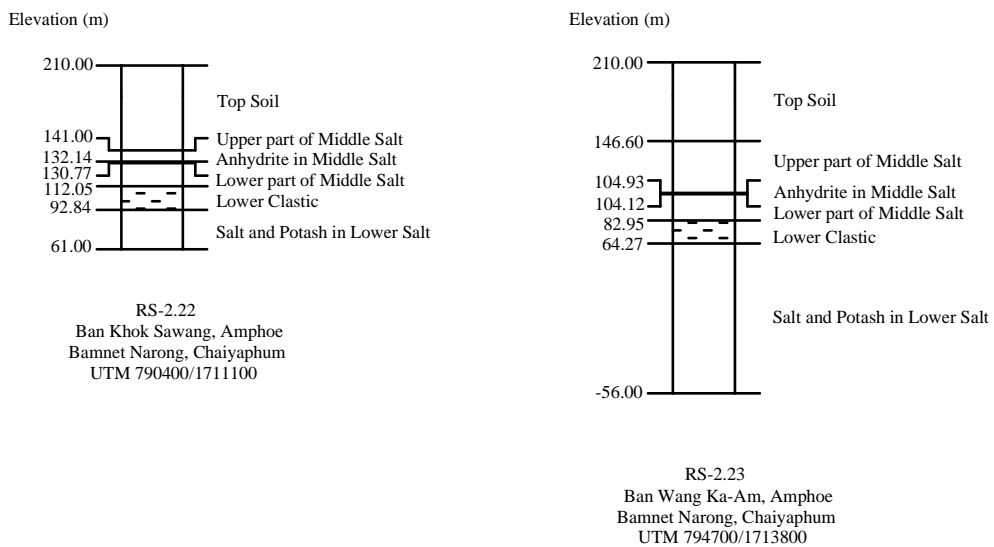
Elevation (m)

209.12 — Top Soil
189.31 — Sedimentary rocks above Upper Salt
163.35 — Middle Clastic
139.83 — Lower Clastic
134.14 —

Salt and Potash in Lower Salt

32.31 — Anhydrite in Lower Salt
31.15 —
30.51 — Sandstone/Siltstone

RS-2.10
Ban Khok Faek, Amphoe Bamnet
Narong, Chaiyaphum
UTM 789900/1711400

Elevation (m)

206.96 — Top Soil
188.67 — Sedimentary rocks above Upper Salt
151.11 — Middle Clastic
135.52 — Anhydrite in Middle Salt
134.91 — Lower part of Middle Salt
106.15 — Lower Clastic
97.64 — Salt and Potash in Lower Salt
69.80 —

RS-2.11
Ban None Thong Lang, Amphoe
Bamnet Narong, Chaiyaphum
UTM 791400/1713700

Elevation (m)

208.67 — Top Soil
194.95 — Sedimentary rocks above Upper Salt
173.62 —
Middle Clastic
136.77 —
Upper part of Middle Salt
81.08 — Anhydrite in Middle Salt
80.23 — Lower part of Middle Salt
61.45 — Lower Clastic
47.07 —
Salt and Potash in Lower Salt
24.27 —

RS-2.12
Ban Khok Faek, Amphoe Bamnet
Narong, Chaiyaphum
UTM 790800/1711600

Elevation (m)

206.11 — Top Soil
203.06 — Sedimentary rocks above Upper Salt
169.28 — Lower Clastic
154.19 —

Salt and Potash in Lower Salt

-79.18 — Anhydrite in Lower Salt
-81.04 —
-81.93 — Sandstone/Siltstone

RS-2.13
Ban Kum, Amphoe Bamnet
Narong, Chaiyaphum
UTM 792700/1709100

Figure A.45 Identification of stratigraphic units for borehole Nos. RS-2.10 to

RS-2.13.

Elevation (m)

220.00 — Top Soil
207.81 — Sedimentary rocks above Upper Salt
182.21 —
— Middle Clastic
148.58 —
— Lower Clastic
133.10 —
— Salt and Potash in Lower Salt
95.57 —
94.61 — Anhydrite in Lower Salt
93.51 — Sandstone/Siltstone

RS-2.14
Ban Kut Talad, Amphoe Bamnet
Narong, Chaiyaphum
UTM 785800/1706400

Elevation (m)

202.60 — Top Soil

166.02 —
— Middle Clastic
139.81 —
121.91 — Lower Clastic

Salt and Potash in Lower Salt

-35.57 —
-37.09 — Anhydrite in Lower Salt
-39.72 — Sandstone/Siltstone

RS-2.15
Ban Khok Sawang, Amphoe
Bamnet Narong, Chaiyaphum
UTM 791500/1710100

Elevation (m)

202.00 — Top Soil
186.76 — Sedimentary rocks above Upper Salt
158.95 —
— Lower Clastic
116.90 —

Salt and Potash in Lower Salt

-180.12 —
-181.32 — Anhydrite in Lower Salt
-183.57 — Sandstone/Siltstone

RS-2.16
Ban Nong Yai But (KM.331.8),
Amphoe Bamnet Narong,
Chaiyaphum
UTM 797600/1710900

Elevation (m)

220.00 — Top Soil
215.43 —

Sedimentary rocks above Upper Salt

-100.65 — Upper Salt
-126.05 — Middle Clastic
-135.02 — Upper part of Middle Salt
-168.32 —
-168.87 — Anhydrite in Middle Salt
— Lower part of Middle Salt
-183.56 —
-199.13 — Lower Clastic
— Salt and Potash in Lower Salt
-240.43 —
-241.80 — Anhydrite in Lower Salt
-244.82 — Sandstone/Siltstone

RS-2.17
Ban Khao Din, Amphoe Bamnet
Narong, Chaiyaphum
UTM 801100/1707800

Figure A.46 Identification of stratigraphic units for borehole Nos. RS-2.14 to

RS-2.17.

Figure A.47 Identification of stratigraphic units for borehole Nos. RS-2.18 to RS-2.21.

Elevation (m)

```
210.00 ──┐┌──           Top Soil
         ││
141.00 ─┐├┤├─           Upper part of Middle Salt
132.14 ─┤├┼┤├─          Anhydrite in Middle Salt
130.77 ─┘├┼┤├─          Lower part of Middle Salt
112.05 ──├ ─ ┤├─        Lower Clastic
 92.84 ──├ ─ ┤├─
                        Salt and Potash in Lower Salt
 61.00 ──┘└──
```

RS-2.22
Ban Khok Sawang, Amphoe
Bamnet Narong, Chaiyaphum
UTM 790400/1711100

Elevation (m)

```
210.00 ──┐┌──           Top Soil
         ││
146.60 ──├┤├─           Upper part of Middle Salt
         ││
104.93 ─┐├┤├─           Anhydrite in Middle Salt
104.12 ─┘├┤├─           Lower part of Middle Salt
 82.95 ──├ ─ ┤├─        Lower Clastic
 64.27 ──├ ─ ┤├─
         ││
                        Salt and Potash in Lower Salt
         ││
-56.00 ──┘└──
```

RS-2.23
Ban Wang Ka-Am, Amphoe
Bamnet Narong, Chaiyaphum
UTM 794700/1713800

Figure A.48 Identification of stratigraphic units for borehole Nos. RS-2.22 to

RS-2.23.

APPENDIX B

COMPUTER MODELING OF SOLUTION CAVERNS

B.1 Introduction

Before performing the computer analysis, physical and mechanical properties of rock salt are determined in order to use as constant values in the calculation. GEO software is employed for this research. The GEO mechanical behavior consists of spring, dashpot, and friction element and so-called GEO rheological components as illustrated in Figure B.1. The major and significant constant values in the models are shear modulus (G_1), retarded shear modulus (G_2), elastoviscosity (V_2), plastoviscosity (V_4), ultimate bulk modulus (K_1), retarded bulk modulus (K_2), and critical strain of failure (γ_c).
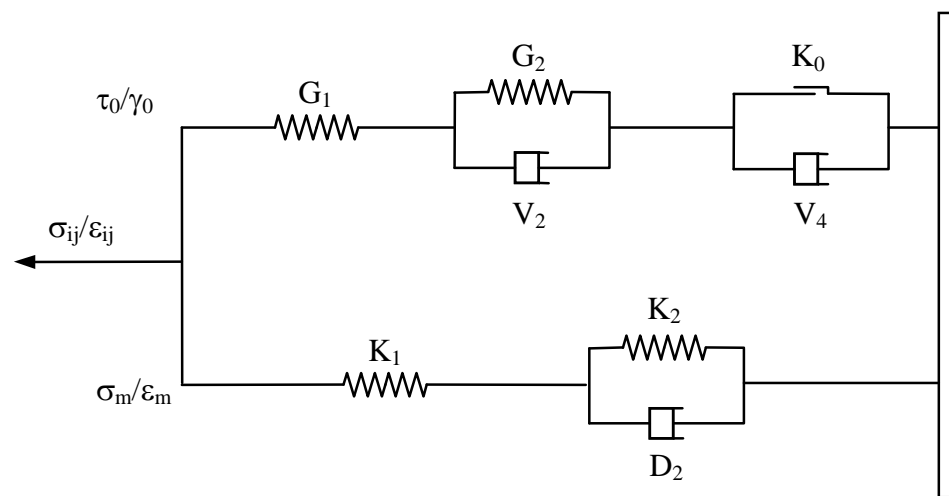
Figure B.1 GEO rheological components (modified from Serata and Fuenkajorn, 1993).

B.2 Property parameters

The coefficient of rock salt properties have been derived from calibrating the test results obtained by Wetchasat (2002), Klayvimut (2003), Jandakaew (2003), and Fuenkajorn (2006). Wetchasat (2002) and Pueakphum (2003) perform the tests on rock salt from the same sources with this research. The associated rocks include all geological formations between and above the salt formations (e.g., anhydrite, mudstone, clay, claystone, siltstone, etc.). The rock salt represents the Lower Salt bed. The Sandstone/Siltstone group represents all rock formations below the salt formation. The specified properties of those rocks are summarized in Table B.1. The properties of rock salt used in the model are explained in Table B.2. Whereas the associated rocks properties are obtained from the database of GEO software. The properties of these rocks do not change with time. They are rather constant and do not directly affect the stability of the cavern. The mechanical properties selected from the database are the most conservative.

Table B.1 Properties of rock salt and associated rocks used in the computer modeling (from Wetchasat, 2002, Pueakphum, 2003, and Klayvimut, 2003).

Properties	Symbols	Units	Associated Rocks	Rock Salt	Sandstone/ Siltstone
Shear Modulus	G_1	GPa	0.3	8.8	13.8
Retarded Shear Modulus	G_2	GPa	0.3	1.1	13.8
Elastoviscosity	V_2	GPa.day	0.3	9.1	3.4
Plastoviscosity	V_4	GPa.day	2.8	17.2	13.8
Ultimate Bulk Modulus	K_1	GPa	1.7	41.1	82.8
Retarded Bulk Modulus	K_2	GPa	1.4	4.9	82.8
Critical Strain of Failure	γ_C	10^{-3}	10	2	2
Pressure Gradient	P_{grad}	kPa/m	25	20.8	25

Table B.2 Properties of rock salt used in the computer modeling (from Wetchasat, 2002, Pueakphum, 2003, and Klayvimut, 2003).

Properties	Symbols	Units	Ranges	Used
Shear Modulus	G_1	GPa	8.7 – 9.0	8.8
Retarded Shear Modulus ($\tau_0 < K_0$)	G_2	GPa	0.2 – 2.1	1.1
Elastoviscosity ($\tau_0 < K_0$)	V_2	GPa.day	0.1 – 17.0	9.1
Plastoviscosity	V_4	GPa.day	6.9 – 27.6	17.2
Ultimate Bulk Modulus	K_1	GPa	40.6 – 42.0	41.1
Retarded Bulk Modulus	K_2	GPa	0.9 – 9.8	4.9
Critical Strain of Failure	γ_C	10^{-3}	2	2
Pressure Gradient	P_{grad}	kPa/m	20.8	20.8

B.3 Cavern models

The study assumed that hydrostatic stresses act on the cavern wall. The finite element mesh consists of nodes and elements. The mesh size is created to be small around the cavern wall because the stress and strain gradients are high on this zone. Hence, at the area far away from the cavern wall where stress and strain gradients are lower, size of elements are bigger. The vertical stress at any point in the model is calculated from the depth and density of the overburden. The internal pressure in the solution cavern is taken to be equal to the brine pressure. Top of the brine is at the ground surface. The brine pressure gradient is 0.01 MPa/m (0.42 psi/ft).

Figure B.2 shows the finite element mesh of the shallowest cavern model which the cavern ground is discretized from the ground surface to the depth of 500 meters (D200). The mesh is constructed to represent a vertical cross-section of the single cavern and designed for axisymmetric analysis using the cavern axis as a centerline. It covers a horizontal distance (radius) of 240 meters (S/D ratio = 4). No load is acted on the upper part. The left boundary represents the cavern centerline and
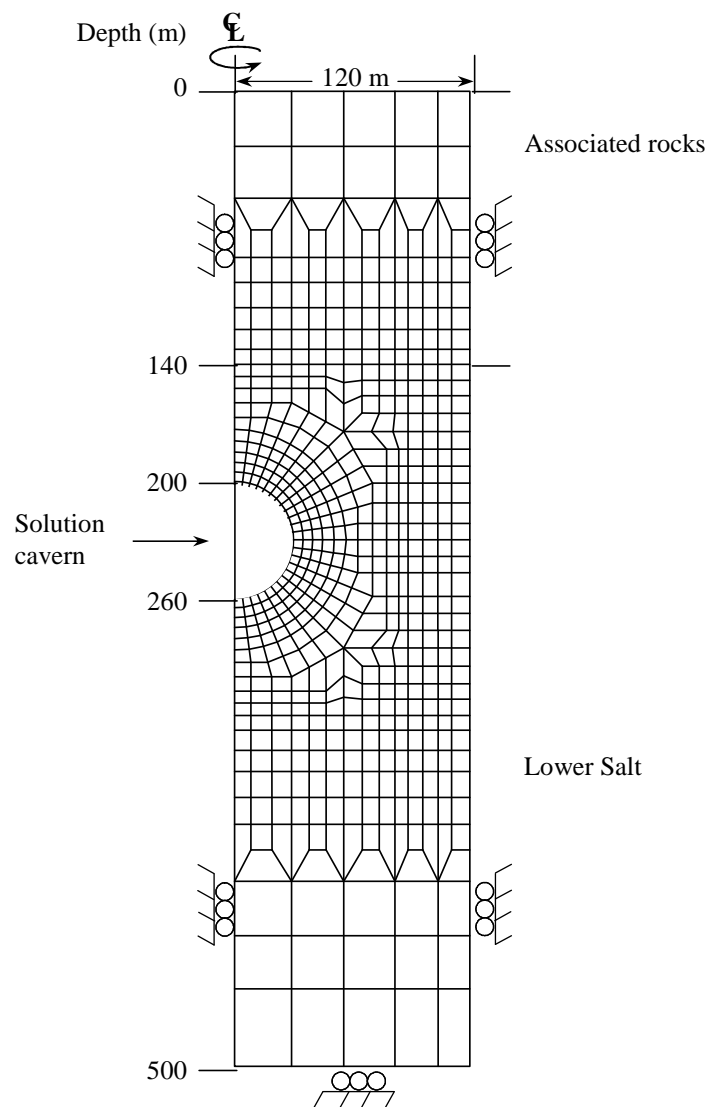
Figure B.2 Finite element mesh for solution cavern model D200.

is laterally constrained. The right boundary is subjected to pressure gradient. In order to show the cavern boundaries, the elements inside the cavern are not drawn in the Figure. The top and bottom of this shallowest cavern are located at depths of 200 meters and 260 meters. The pressure acted in the internal walls is varies according to brine pressures with any depth. The upper boundary can move freely in both x- and y-directions. The left and right boundaries which are a symmetrical axis is freed in y-direction but is fixed in x-direction. The bottom boundary is fixed in y-direction. Small elements (3 meters × 4 meters) are used adjacent to the cavern boundaries to capture the stresses and strains distribution under high gradients. Larger elements are used in the overburden (far from the cavern roof and floor as its behavior does not impact the cavern stability). The overburden is included in the analysis in order to provide the gravitational weight on the salt cavern, and to allow an assessment of the ground surface subsidence. The mesh model is composed of 589 elements and 635 nodes. The characteristics of model (the mesh construction, the analysis method, the cavern shape, and size) are similar for other depths.

Figure B.3 shows the top and bottom of the deepest cavern which are located at depth of 400 (D400). Small elements (3 meters × 4 meters) are close to the cavern boundaries. The cavern ground is discretized from the ground surface to the depth of 700 meters. The mesh model comprises 614 elements and 665 nodes.
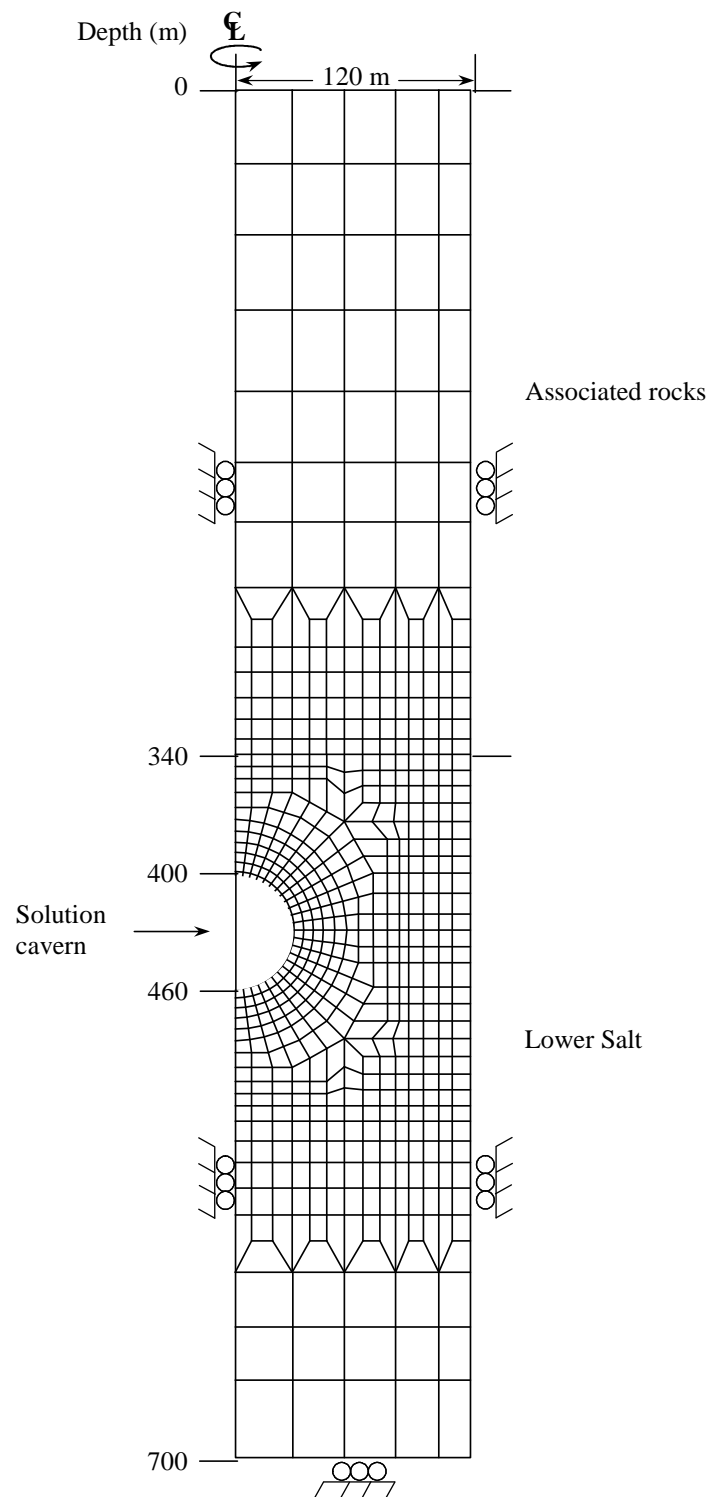
Figure B.3 Finite element mesh for solution cavern model D400.

B.4 Modeling results

The contours of octahedral shear stress near the solution caverns are shown in Figures B.4 and B.5. The shear stress concentrated near the cavern boundary. The maximum octahedral shear stress is about 775 psi (5.3 MPa). The contours of octahedralshear strain near the salt cavern are illustrated in Figures B.6 and B.7. The octahedral shear strain tends to be uniform with radial distance from the cavern boundary. The model D200 shows the lowest value of octahedral shear strain about 0.2%. The model D400 shows the maximum octahedral shear strain about 0.4%. The distributions of the stress vector are shown in Figures B.8 and B.9. The maximum stress of model D400 is 2,362 psi (19.29 MPa) and the maximum stress of model D200 is 1,573 psi (10.85 MPa). The largest stress concentrates near the cavern boundary. The distributions of the strain vector are shown in Figures B.10 and B.11. The model D400 shows the maximum strain about 0.27%. The largest strain is concentrated near the middle of the cavern boundary.

Figure B.12 shows the surface subsidence for solution cavern at various depths. The maximum surface subsidence of model D400 is approximately 6.45 centimeters. Figures B.13 and B.14 show the vertical cavern closures at the centerline of the cavern. The maximum vertical closure is about 0.67% or 20.08 centimeters. Figures B.15 and B.16 show the horizontal closure about 0.25% or 7.47 centimeters. The surface subsidence, vertical and horizontal closures rapidly increase during the first year, after operating the solution mine and remain constant through the 50 years.
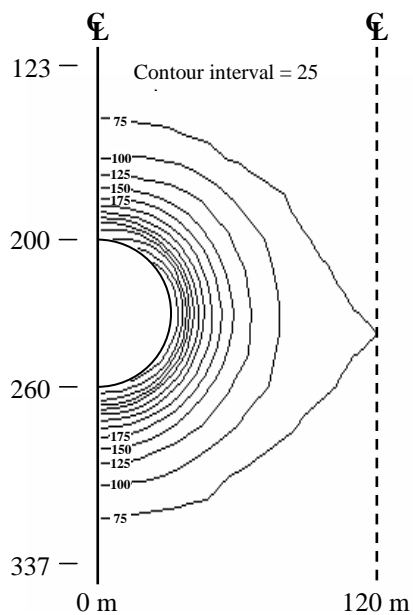
Figure B.4 Contour of octahedral shear stress around solution cavern (model D200)

at 50 years (the maximum octahedral shear stress = 375 psi).
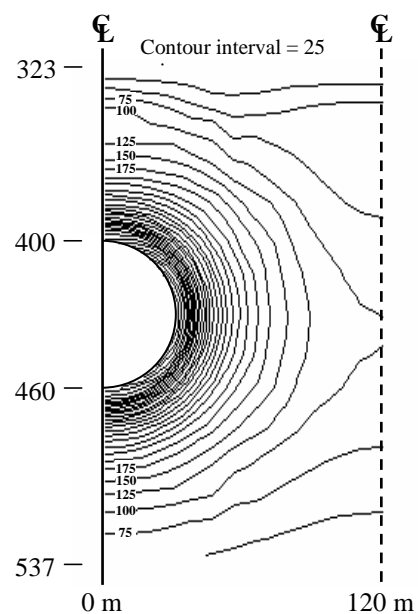
Figure B.5 Contour of octahedral shear stress around solution cavern (model D400)

at 50 years (the maximum octahedral shear stress = 775 psi).
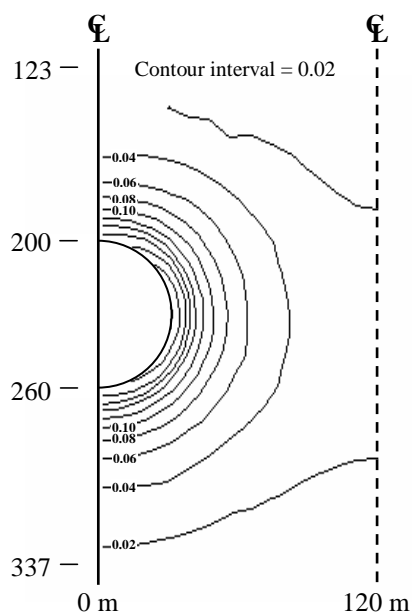
Figure B.6 Contour of octahedral shear strain around solution cavern (model D200)

at 50 years (the maximum octahedral shear strain = 0.2%).
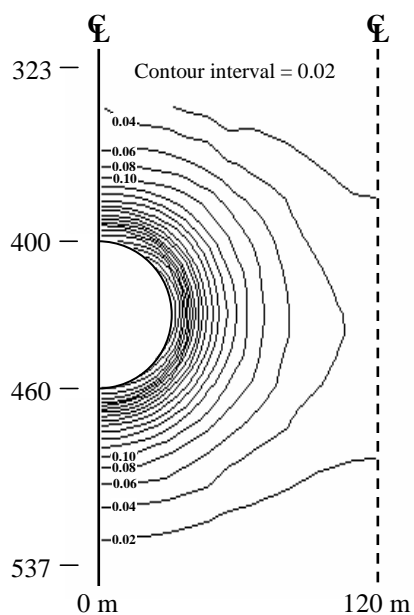
Figure B.7 Contour of octahedral shear strain around solution cavern (model D400)

at 50 years (the maximum octahedral shear strain = 0.4%).
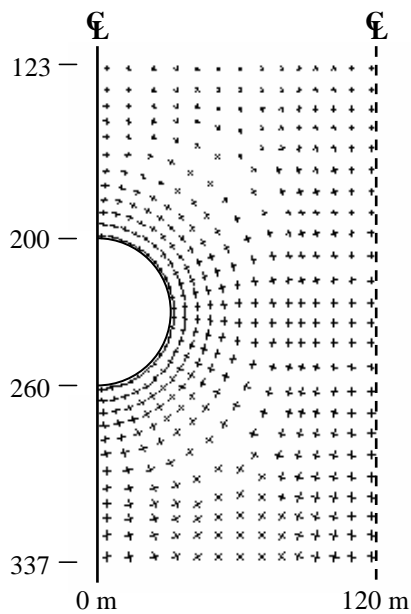
Figure B.8 Principal stress vector around solution cavern (model D200) at 50 years

(the maximum stress = 1,573 psi). Scale is 15,000 psi/inch.
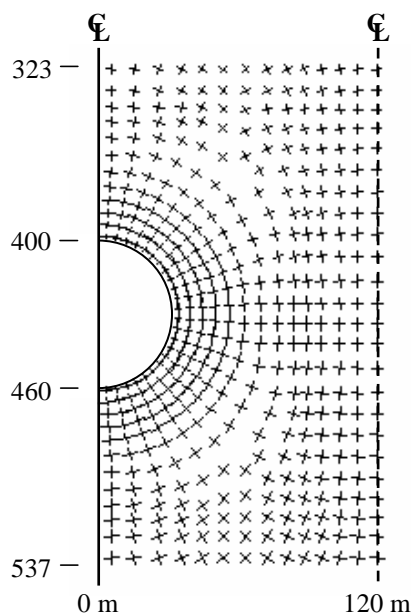
Figure B.9 Principal stress vector around solution cavern (model D400) at 50 years

(the maximum stress = 2,362 psi). Scale is 15,000 psi/inch.
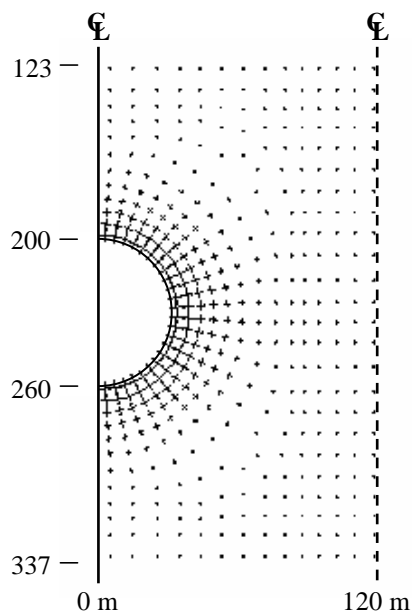
Figure B.10 Principal strain vector around solution cavern (model D200) at 50 years

(the maximum strain = 0.13%). Scale is 1.0% per inch.
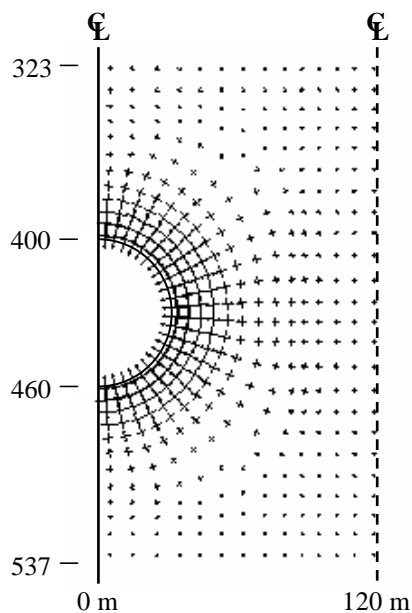
Figure B.11 Principal strain vector around solution cavern (model D400) at 50 years

(the maximum strain = 0.27%). Scale is 1.0% per inch.
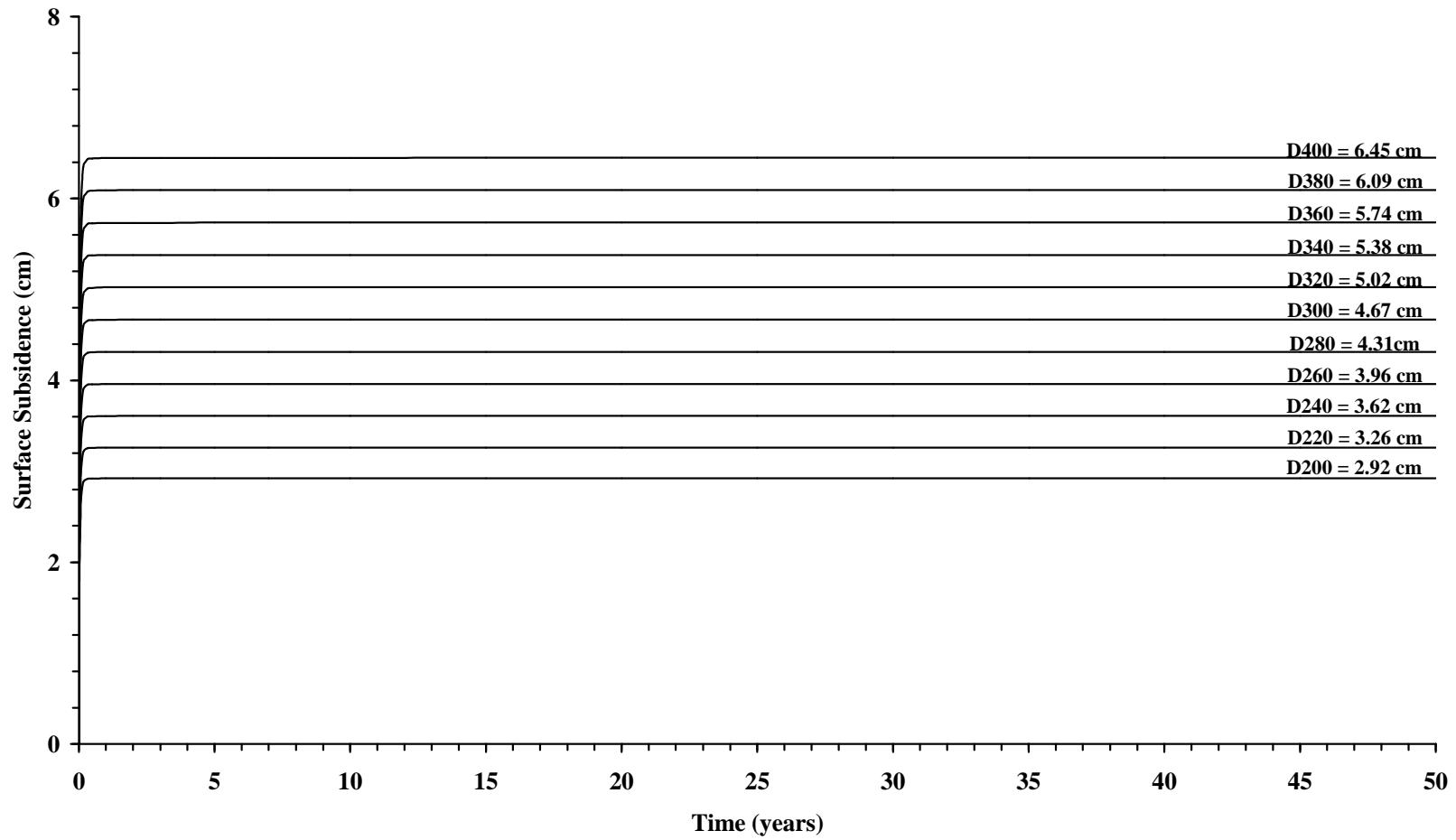
Figure B.12 Predicted surface subsidence for solution caverns.
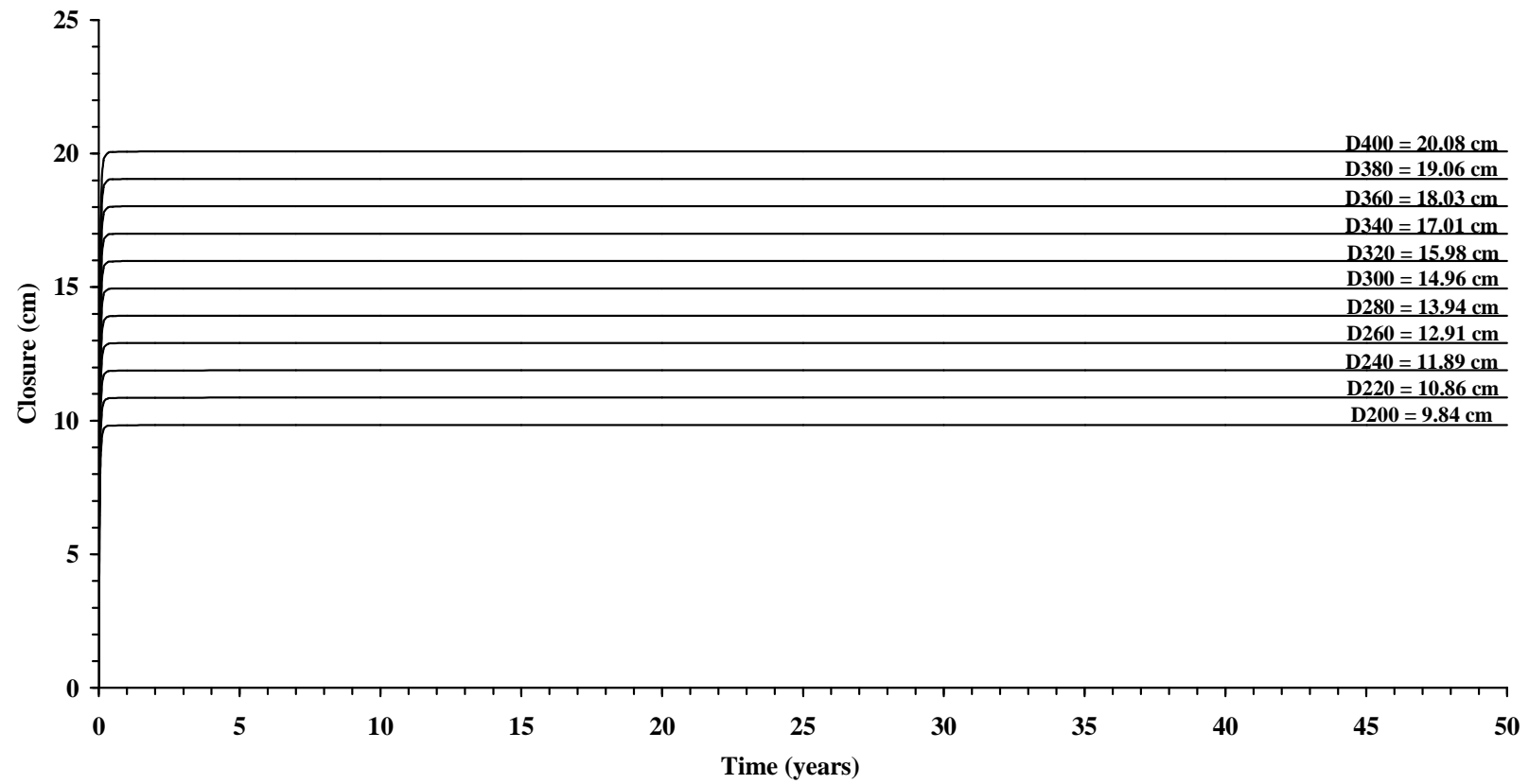
Figure B.13 Predicted vertical closure for solution caverns.
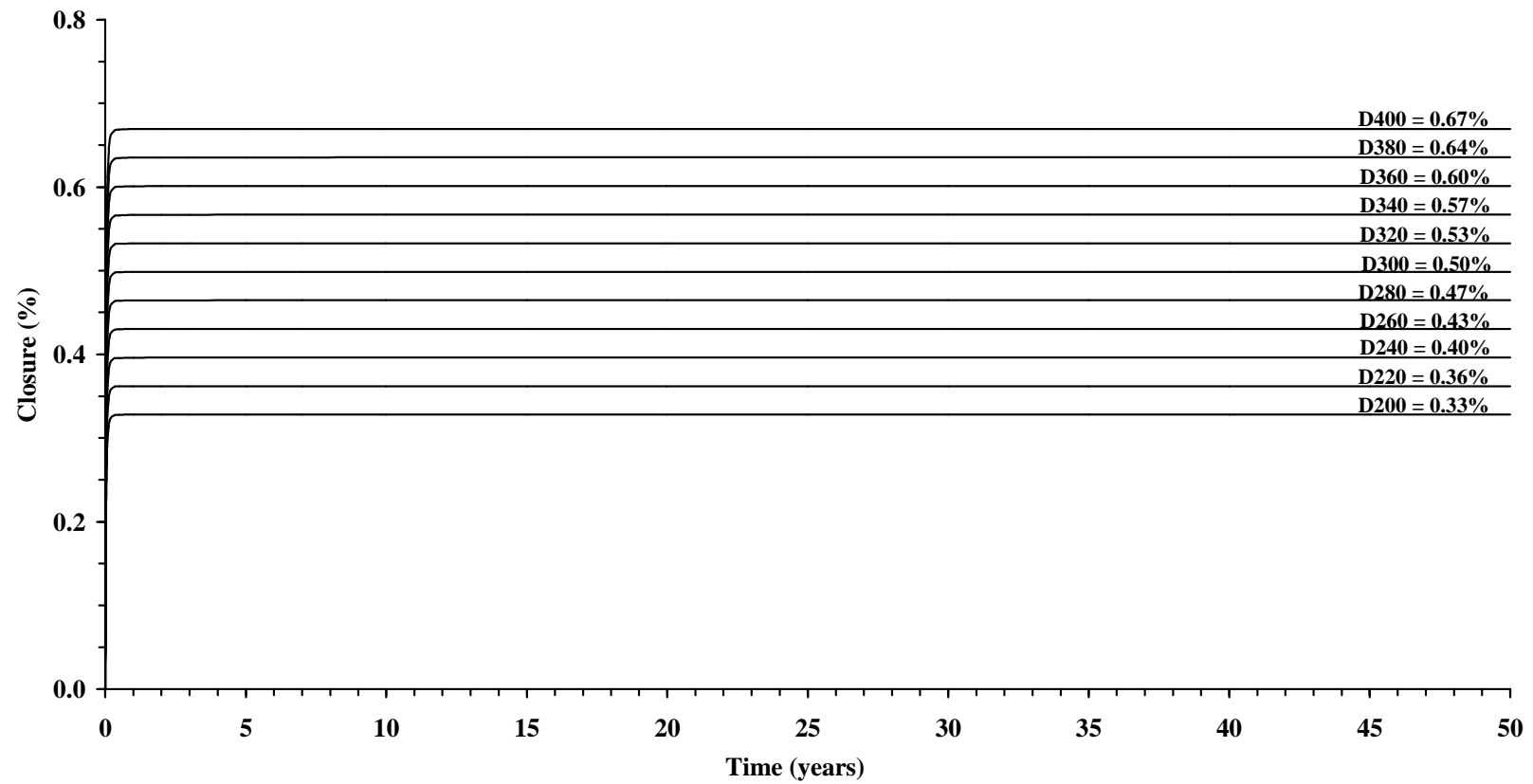
Figure B.14 Predicted percentage of vertical closure for solution caverns.
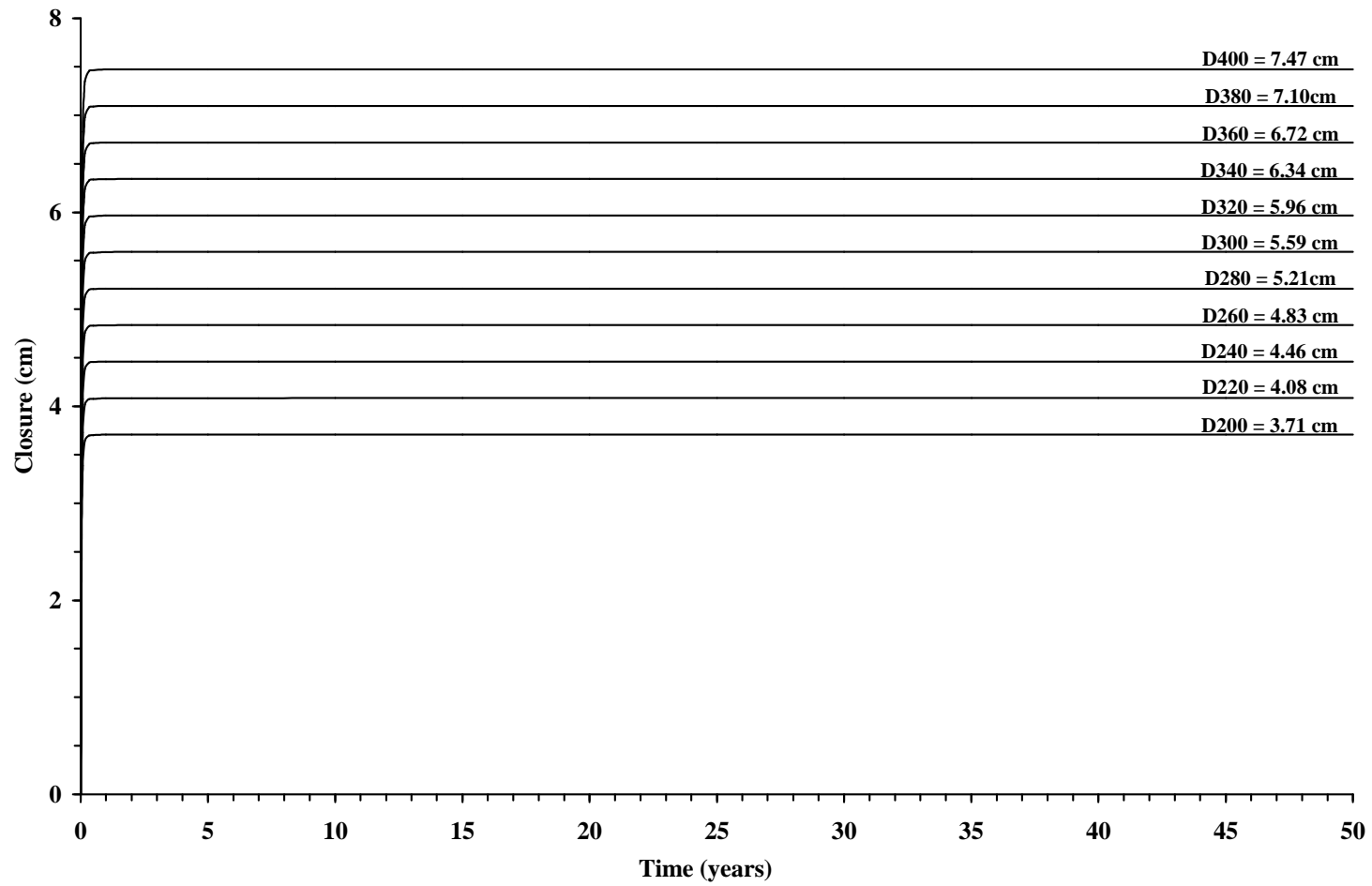
Figure B.15 Predicted horizontal closure for solution caverns.
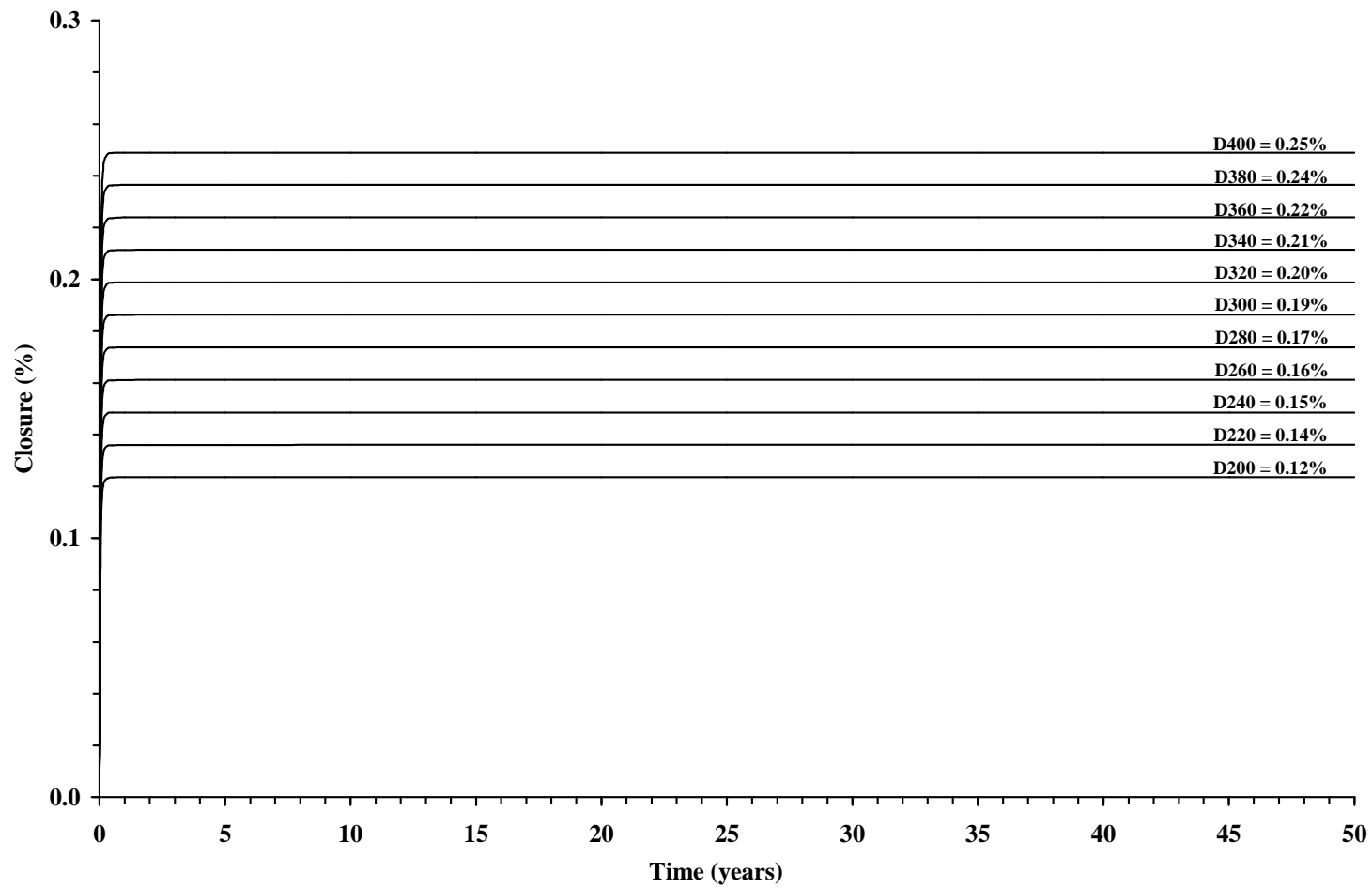
Figure B.16 Predicted percentage of horizontal closure for solution caverns.

B.5 Subsidence prediction

The distribution of surface subsidence is calculated by using a profile function (Hartman, 1992). The results are shown in Figures B.17 and B.18. To assess the effects of the surface subsidence on the engineering structures, farmland, highway etc, a set of criteria proposed by Singh (1992) is used. Table B.3 shows the results of comparison which indicates that all designed caverns will not have adverse impact on the engineering structures and natural resources. These are evidenced by the fact that the induced subsidence components are less than the limits proposed by Singh (1992).
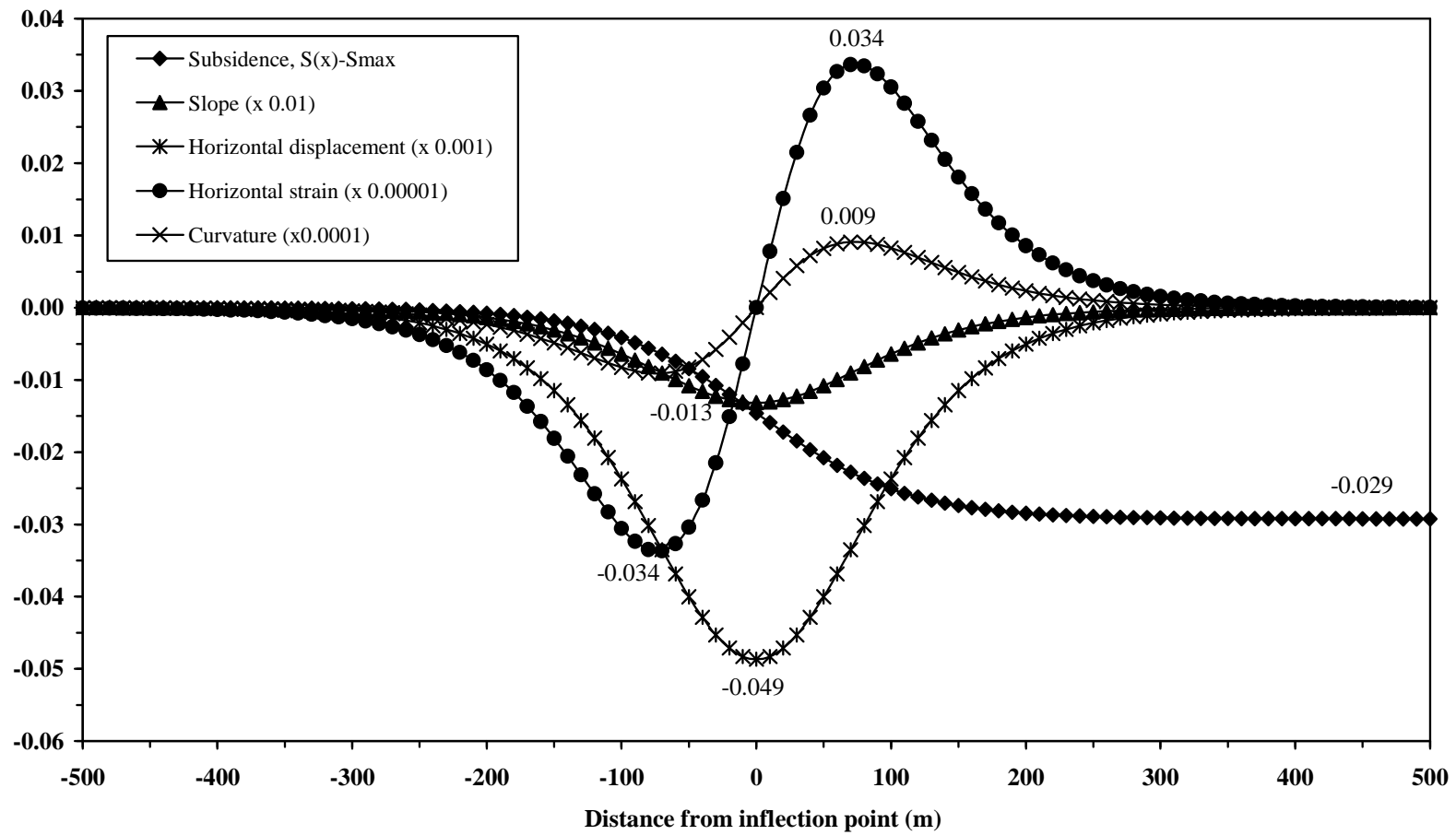
Figure B.17 Components of surface subsidence at 50 years measured from the edge of solution cavern D200.
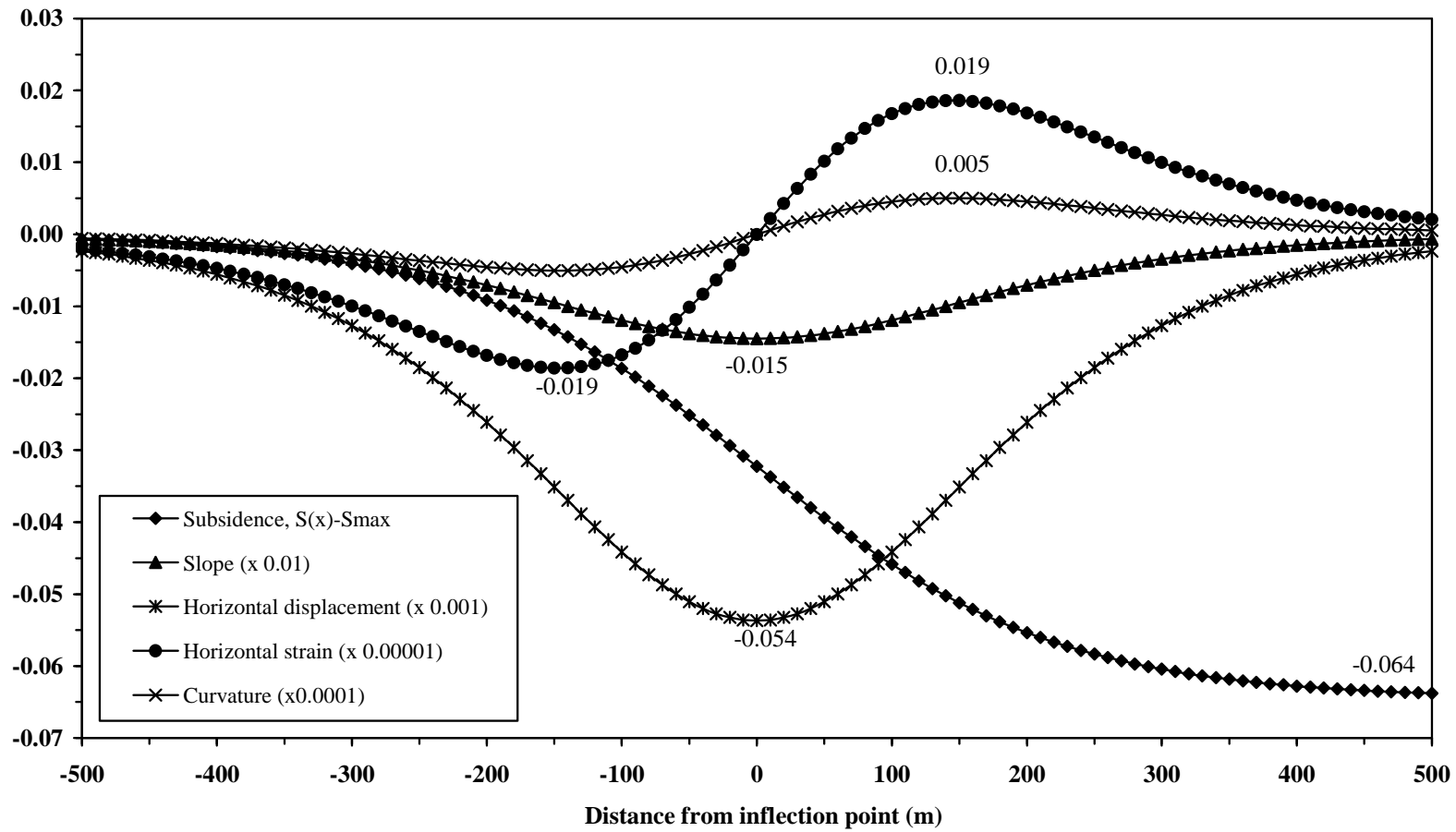
Figure B.18 Components of surface subsidence at 50 years measured from the edge of solution cavern D400.

Table B.3 Summary of subsidence components.

	Depth (cm)	Maximum Subsidence (cm)	Key Components of Subsidence		
			Slope	Horizontal Strain	Horizontal Movement (m)
Designed results	200	2.92	1.3×10^{-4}	3.4×10^{-7}	4.9×10^{-5}
	400	6.45	1.5×10^{-4}	1.9×10^{-7}	5.4×10^{-5}
Singh (1992) Suggested Limit	Buildings		--	0.5×10^{-3}	--
	Bridges		--	--	25×10^{-3}
	Railroad		10.0×10^{-3}	2.0×10^{-3}	--
	Road		10.0×10^{-3}	1.0×10^{-3}	--
	Pipeline		--	1.0×10^{-3}	--
	Farmland		$2.0\text{-}3.0 \times 10^{-3}$	2.0×10^{-3}	--
	Aquifer		--	5.0×10^{-3}	--
	Surface Water Bodies		--	5.0×10^{-3}	--

Where   D is depth to top of cavern, $\gamma = 45\,°$, $c = 1.4$ and $b = 0.37$ then $B = D \cdot \tan\gamma$

Subsidence, $S(x)$

$$S(x) = \frac{1}{2} S_{max} \left[1 - \tanh\left(\frac{cx}{B} \right) \right]$$

Slope, $G(x)$

$$G(x) = S'(x) = \frac{1}{2} S_{max} \left(\frac{c}{B} \right) \left[\sec h\left(\frac{cx}{B} \right) \right]$$

Horizontal strain, $\varepsilon(x)$

$$\varepsilon(x) = bS''(x) = bS_{max} \left(\frac{c}{B} \right)^2 \left[\sec h\left(\frac{cx}{B} \right) \right] \tanh\left[\left(\frac{cx}{B} \right) \right]$$

Horizontal movement, $u(x)$

$$u(x) = bS'(x) = \frac{1}{2} bS_{max} \left(\frac{c}{B} \right) \left[\sec h\left(\frac{cx}{B} \right) \right]$$

BIOGRAPHY

Miss Hathaichanok Vattanasak was born in Nakhon Ratchasima province. She earned her Bachelor's Degree in Geotechnology, Department of Geotechnology, Faculty of Technology, Khon Kaen Unviersity (KKU) in 1998. After graduation, she has been employed under the position of assistant research by Groundwater Research Center, Faculty of Technology, KKU. From 2002 to 2006, she studied for her Master's Degree in Geological Engineering emphasis on rock mechanics at School of Geotechnology, Institute of Engineering, Suranaree University of Technology (SUT). During graduation, 2003-2006, she was a part time worker in positions of teaching assistant at SUT, research assistant at the Department of Alternative Energy Development and Efficiency (DEDE) and research assistant at the Geomechanics Research Unit, Institute of Engineering, SUT. For her work, she is a good knowledge in geological and geomechanical of rock salt theory.
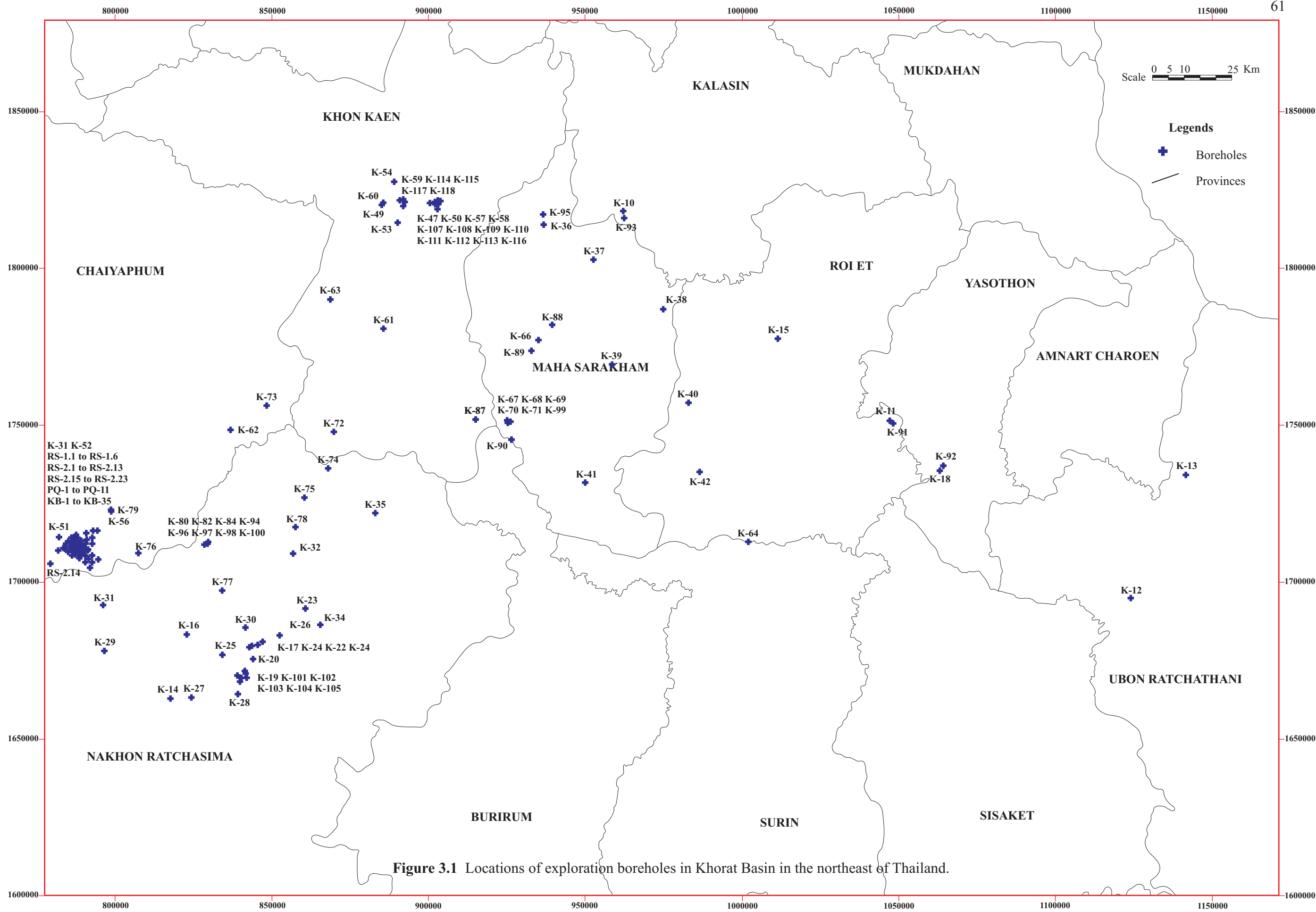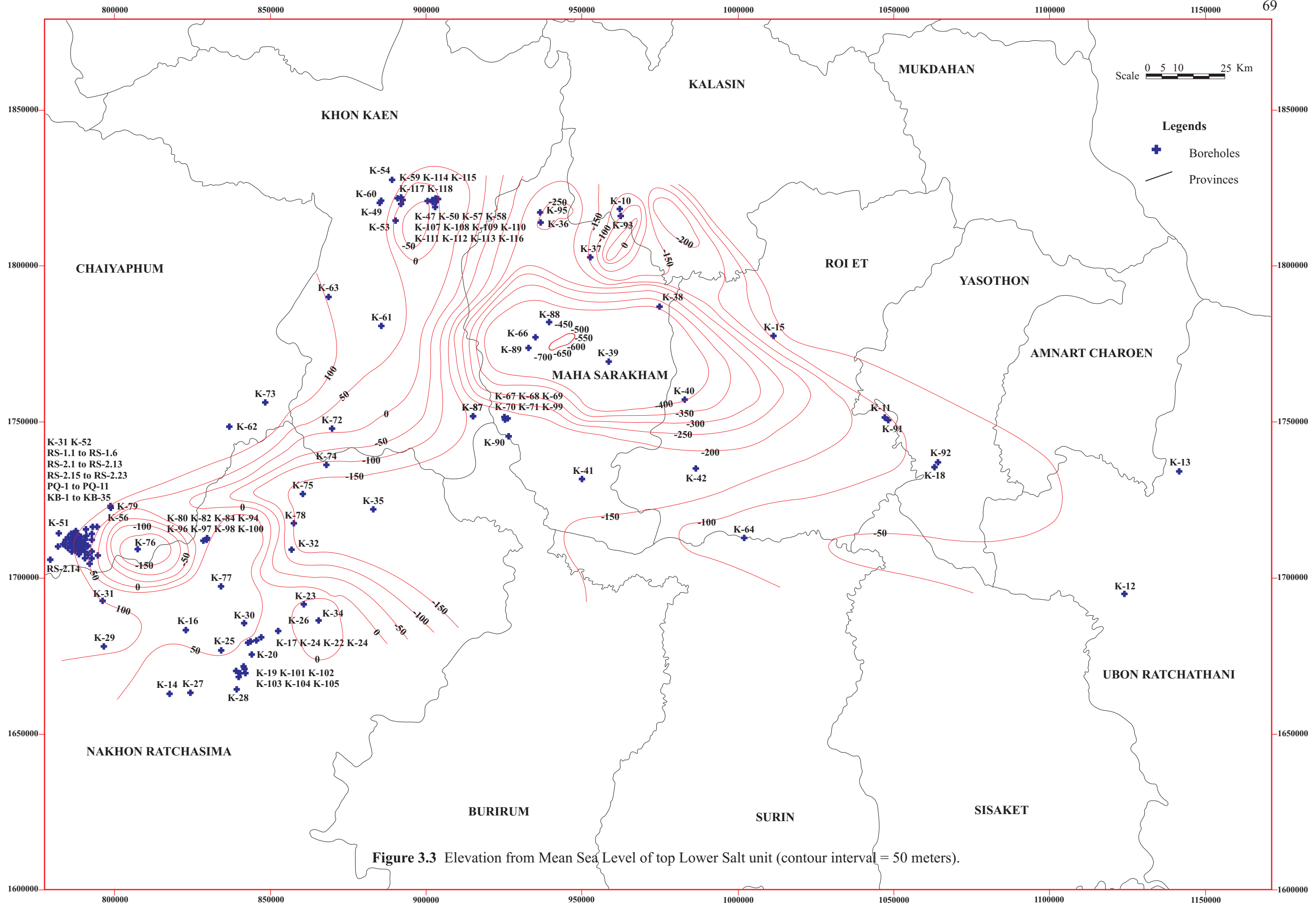
Figure 3.1 Locations of exploration boreholes in Khorat Basin in the northeast of Thailand.

Figure 3.2 Elevation from Mean Sea Level of top Khok Kurat Formation (contour interval = 50 meters).

Figure 3.3 Elevation from Mean Sea Level of top Lower Salt unit (contour interval = 50 meters).

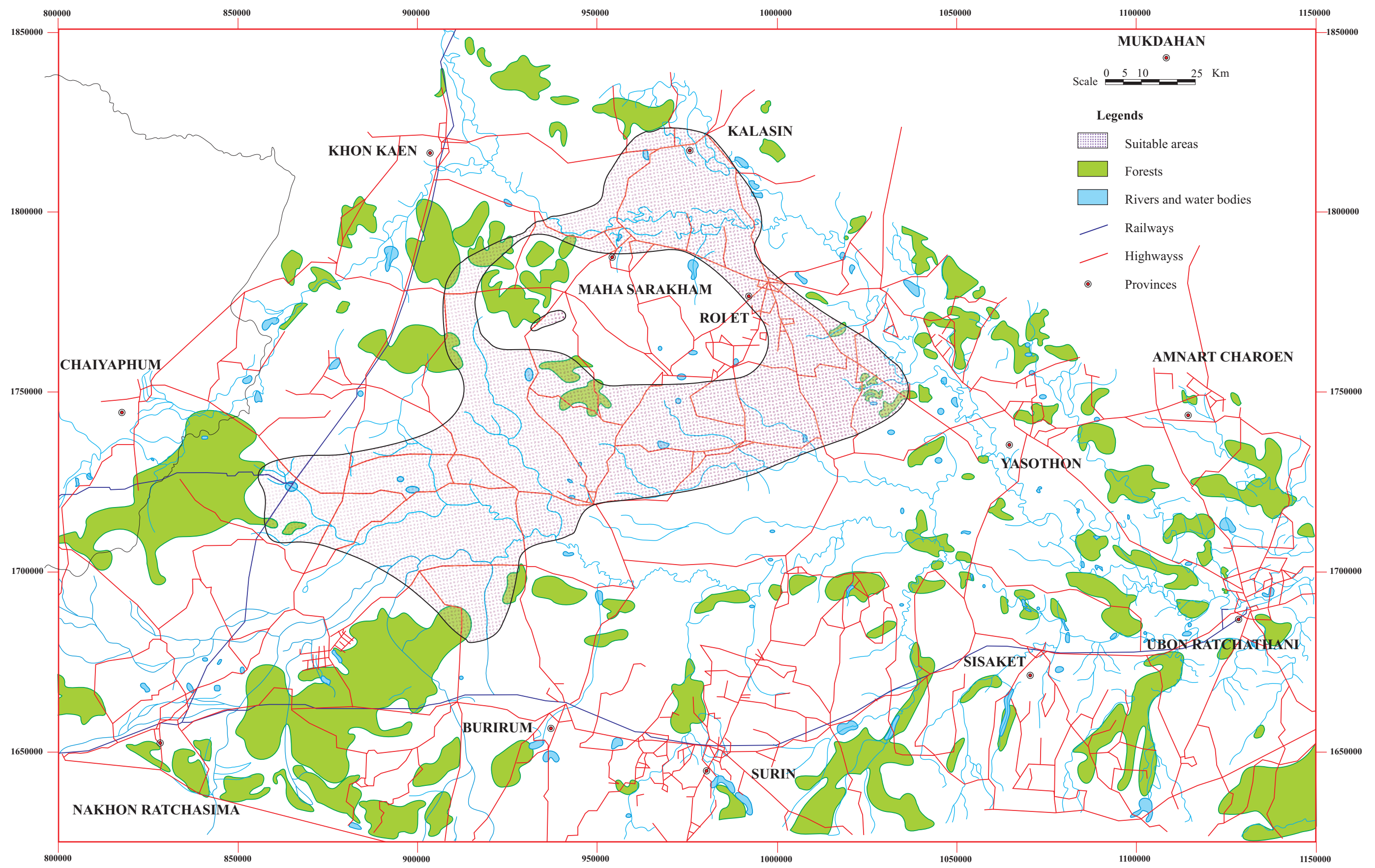**Figure 3.4** Isopach map of Lower Salt in Khorat basin (contour interval = 20 meters).

Figure 5.1 Suitable areas (shaded area of about 10,500 square kilometers) for developing solution mined caverns in terms of Lower Salt depth and thickness.
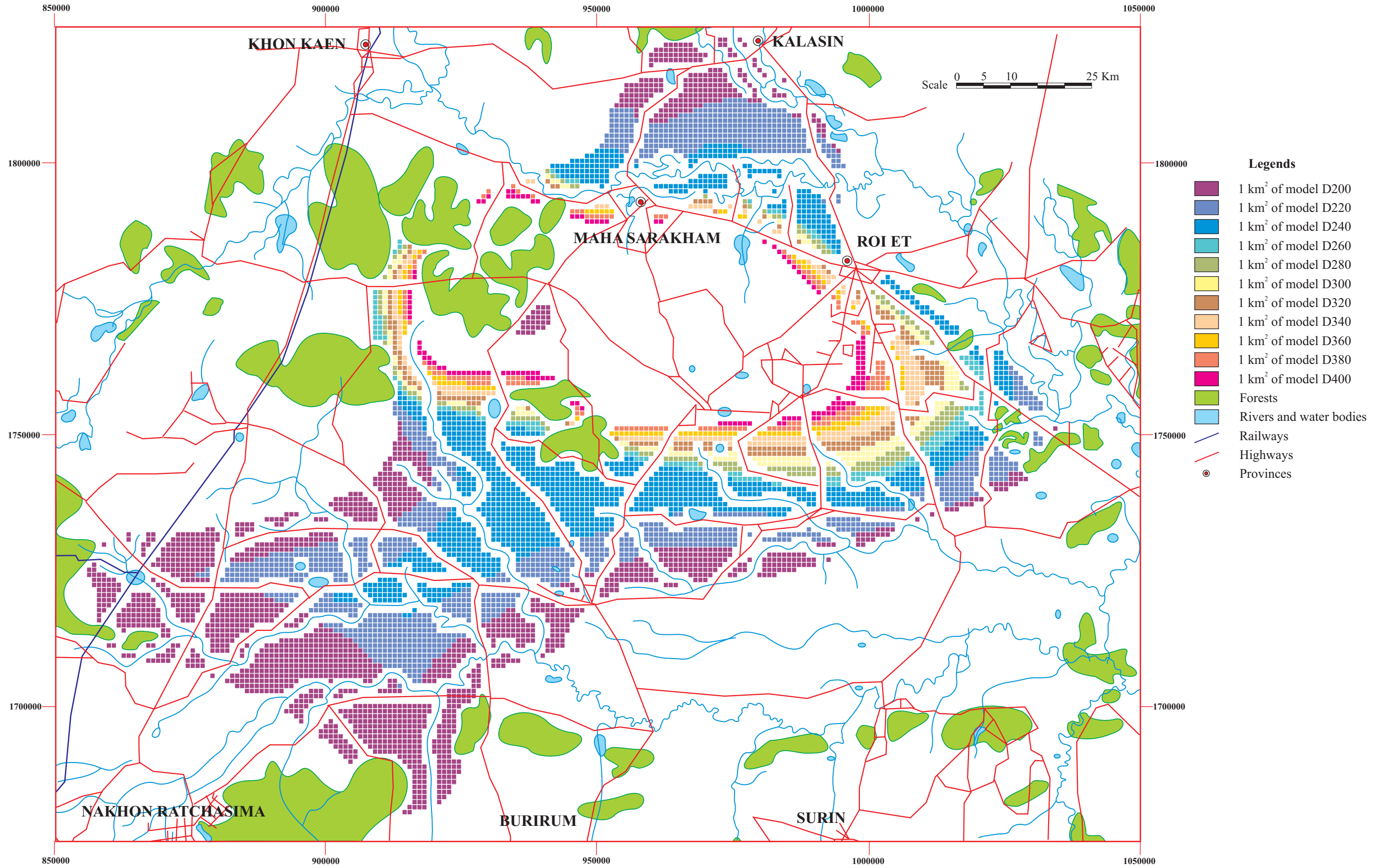
Figure 5.2 Suitable areas (colored blocks of about 5,741 square kilometers) for solution mining that exclude highways, forests, rivers, surface water bodies, railways, and main districts. Each block represents 1 square kilometers.